UNIVERSITI MALAYSIA PAHANG

SChE 2021

# ENERGY SECURITY AND CHEMICAL ENGINEERING CONGRESS 2021

## Virtual Conference
## 3 – 5 November 2021

*Sustainable Technological Solution for a Better World*

**Organizer**

Universiti Malaysia PAHANG
Engineering • Technology • Creativity

Centre for Research in Advanced Fluid and Processes
Pusat Penyelidikan Bendalir dan Proses Termaju

**In partnership with**

University of Stavanger

NGUYEN TAT THANH UNIVERSITY

TDT ĐẠI HỌC TÔN ĐỨC THẮNG TON DUC THANG UNIVERSITY

**Sponsored by**

JEOL

**ADVANCED MATERIAL**

**Paper ID: ESCE005**

# EFFECTS OF PINEAPPLE LEAF FIBRE AS REINFORCEMENT IN OIL PALM SHELL LIGHTWEIGHT CONCRETE

**S. C. Chin[1,2]*, M. L. Tang[1], Bakar N.[1], J. L. Che[3], S.I Doh[1,2]**

[1] *Centre for Research in Advanced Fluid and Processes (Fluid Centre),* [2] *Department of Civil Engineering, College of Engineering, Universiti Malaysia Pahang, 26300 Gambang, Pahang, Malaysia.*
[3] *School of Civil and Hydraulic Engineering, Ningxia University, Ningxia 750021, China.*
*Corresponding author: scchin@ump.edu.my

## Extended Abstract

Lightweight concrete is environmentally sustainable as compared to conventional concrete because it reduces the usage of cement as well as quantities of aggregates which resulted from destruction of hills causing geological and environmental imbalance [1]. Conventional concrete is relatively a brittle material where the structural cracks will be developed even before loadings are applied due to its low tensile strength, limited ductility, and little resistance towards cracking [2]. The external load will lead to further propagation of existing cracks and eventually caused spalling of concrete and the newly formed additional cracks. Hence, inclusion of reinforcement in concrete is necessary to mitigate cracks propagation [4].

Fibres are commonly used in concrete to control the propagation of micro cracks, shrinkage and to improve the strength and performance of concrete [5]. The highlight of this research is to focus on the mechanical behaviour of pineapple leaf fibre (PALF) in oil palm shell lightweight concrete in different fibre volume fraction to concrete volume 0.5%, 1%, 1.5% and 2.0% of PALF compared to plain concrete. PALF are extracted and then treated with sodium hydroxide with concentration of 10% to enhance fibres durability. In this research, the length of PALF was made constant as 40 mm based on optimum fibre length from previous investigations. The experimental testing in this work includes slump test and compressive strength test. Results showed that the fresh properties of concrete decreased with the increase fibre volume fraction as shown in Fig. 1. Fig. 2 shows the compressive strength of the PALF decreased at all curing ages of 3, 7, 14 and 28 days with an increase in PALF fibre volume fraction. Findings in this study shows that the addition of PALF is unable to improve the compressive strength of the oil palm shell lightweight concrete. This paper aims to provide knowledge and understanding of PALF as reinforcing materials when incorporated in oil palm shell lightweight concrete.

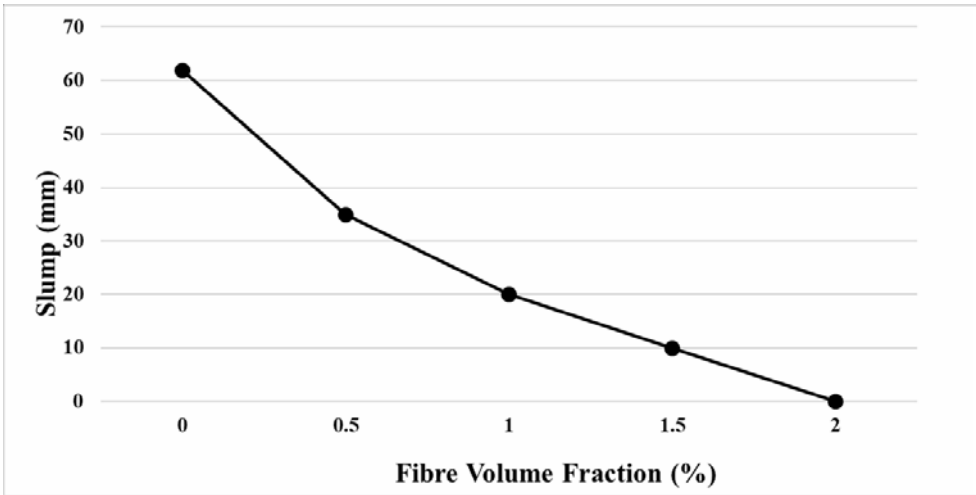


Fig. 1: Effect of PALF volume fraction on concrete slump.

**ADVANCED MATERIAL**

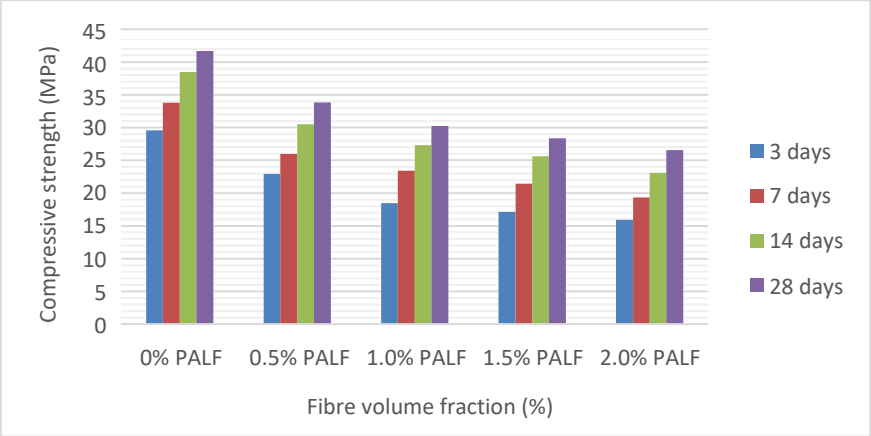


Fig. 2: Relationship of compressive strength versus fibre volume fraction.

**Keywords:** Compressive strength; Oil palm shells; Lightweight concrete; Pineapple leave fibre; Workability.

## Acknowledgment

This study was supported by UMP internal research grant PGRS200375.

## References

[1] Rout, M. D. K. and Jena, R. R. (2015) Investigation on the Development of Light Weight Concrete with Sintered Fly Ash Aggregate and Activated Fly Ash in Blended Cement, Int. J. Eng. Res. Technol 4:25-28.
[2] Khan, M. S. (2006). Control of cracking in concrete: state of the art. Transportation Research Circular, 107.
[3] Moccia, F., Ruiz, M. F., & Muttoni, A. (2021). Spalling of concrete cover induced by reinforcement. Eng. Struct., 237: 112188.
[4] Amin, A. K. A. F., Keong, C. K., & Geem-Eng, T. (2020). Mechanical behaviour of Steel fibre reinforced concrete beams: a review. In *IOP Conference Series: Materials Science and Engineering* (Vol. 920, No. 1, p. 012032). IOP Publishing.
[5] Serdar, M., Baričević, A., Jelčić Rukavina, M., Pezer, M., Bjegović, D., & Štirmer, N. (2015). Shrinkage behaviour of fibre reinforced concrete with recycled tyre polymer fibres. Int. J. of Polym. Sci., 2015:1-10.

**ADVANCED MATERIAL**

**Paper ID: ESCE006**

# SILICA POWDER SURFACE ACTIVITIES PRODUCED BY MILLING

**Tran Thi Thu Hien[1]*, Takashi Shirai[2], Masayoshi Fuji[2], Ngo Quoc Dung[1]**

[1] *Hanoi University of Science and Technology, 1st Dai Co Viet Street, Hai Ba Trung District, Ha noi, Vietnam.*
[2] *Ceramics Research Laboratory, Nagoya Institute of Technology, 3-101-1 Honmachi, Tajimi, Gifu 507-0033, Japan.*
*Corresponding author: hien.tranthithu@hust.edu.vn

## Extended Abstract

Laboratory planetary mill was used to mill the silica under air at room temperature. Raw silica powder sample was milled in a 500ml zirconia pot using zirconia balls for periods of 15, 30 and 60 minutes. Rotation speeds of 50, 100, 200 and 300 rpm were applied. Three different ball sizes; 01, 05 and 10 mm were used. For all the experiments 25g of raw powder was used with a weight ratio to the zirconia ball of 1:4. The surface activities of the raw and treated powder are evaluated by the amounts of surface OH groups and the quantitative dissolved loads of cation $Si^{4+}$ concentration. Possible links between the raw powder characteristics and the efficiency of the mechanical treatment in increasing the surface activity are discussed.

The changes in the particle size distribution (PSD), morphology, specific surface area (SSA) of the raw powder produced by milling under different conditions was investigated. By the milling treatment the original particle size of the powder could be effectively reduced. The raw powder has very large, almost uniform particle size (1290µm) but after milling at any conditions even at the lowest rotation speed and shortest time, the particle size was reduced to less than 1µm (0.6µm). At rotation speeds of 200 and 300rpm prolonged milling causes the formation of a broad range of particles of larger sizes especially for the 05 and 10mm size balls. This observation may be explained as due to the agglomeration of smaller particles. The observed particle size of the modified powder by SEM is in agreement with the particle size distribution measurements under these conditions. The raw powder contains many large agglomerated particles together with a large quantity of small spherical particles. The shape of the original particles did not change but the agglomerated particles were dispersed by the milling modifications. Particle size measurements showed that agglomerated particles could not be dispersed by ultrasound, therefore it could be stated that the milling process is a useful technique for de-agglomeration of powders. However, prolonged milling, high rotation speed and large ball size cause re-agglomeration of particles. The SSA values of all powders were obtained from 9.3 - 11.6$m^2$/g (changing of 19.8%). SSA increase hardly at rotation speed of 300rpm and milling time of 60mm. The raw powder has much larger particle size but obtained specific surface area is similar. This can be explained by agglomerated powder, SSA of agglomerated particles is sum of SSA of its contained small spherical particles. The surface activity of raw and treated powder at various conditions was measured as the amounts of dissolved $Si^{4+}$ ion into ammonia solution after 2 hours shaking time. Surface area normalized dissolved silicon ion values for raw and treated powder are shown in Figure 1. The specific surface activity increased by the mechanical treatment at every tested condition. Primary particles were de-agglomerated and generated new surface by these milling conditions, silicon ion concentration will increase. Beside that silicon ion generation during milling process of silica powders can be also generated by the braking of surface silanol (Si-OH) and siloxane (Si-O-Si) groups bonds were discussed [1]. The 05mm ball size was the most effective for 100 and 200rpm rotation speeds almost independently of the milling time. According to these results, from an economical point of view 15min milling time at 200rpm with a 05mm ball will be sufficient to considerably increase the specific surface activity of this powder.

## ADVANCED MATERIAL

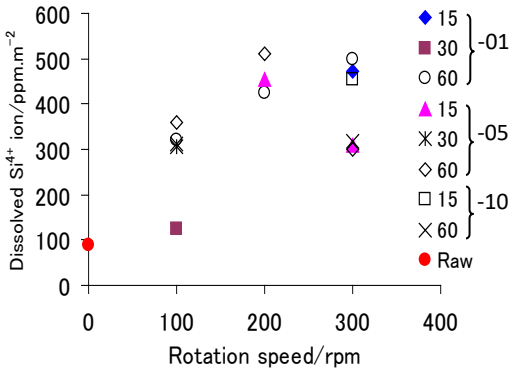


Fig. 1: Surface area normalized dissolved $Si^{4+}$ ion values for raw and treated silica powder at various milling conditions. 60, 30 and 15 indicate milling time in minutes. 01, 05 and 10 correspond to the ball size in mm.

Figure 2 shows the common scale DRIFT spectra of the raw and mechanically treated with condition 200-05-15 (M) silica powders in the SiOH (silanol) and SiH (silane) stretching band frequency regions 4000 – 2000$cm^{-1}$. The presence of OH stretching vibration is revealed by the broad band between 2800 and 3800$cm^{-1}$ (dotted arrow). Three peaks assigned to related silanol groups are considered in this region. A sharp peak at 3750$cm^{-1}$ is due to isolated SiOH groups. The highest band at 3670$cm^{-1}$ is assigned to weakly hydrogen bonded SiOH groups and adsorbed water molecules. The shoulder peak at 3440$cm^{-1}$ is due to water molecules hydrogen bonded to each other and to SiOH groups [2, 3]. The band at 2250 $cm^{-1}$ is assigned to SiH bond vibrations [4]. This band at 2250$cm^{-1}$ appears not to be affected by the DRIFT accessory and can be used as a reference for each individual spectrum. The amount of OH in raw or treated silica powder surfaces is then assessed in the form of an integrated OH/SiH band frequency absorbance ratio. The results are shown in (b). It is observed that OH surface groups could be produced by mechanical treatment and the amount of the groups increases 1.5 times compared to the as received silica powder.

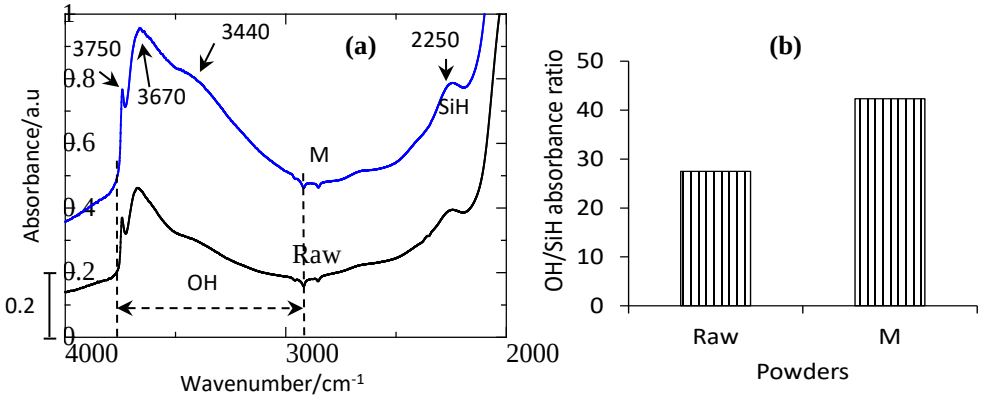


Fig. 2: (a) Common scale DRIFT spectra of the raw and milled (M) silica powders in the SiOH and SiH stretching band frequency regions. The indicated numbers are vibration frequencies of silanol and silane groups. (b) OH/SiH absorbance ratios

The present work can be summarried that the particle size, specific surface activity and amount of silanol groups of silica powder were successfully modified by milling process. The measured amounts of dissolved $Si^{4+}$ ion into ammonia solution and silanol surface groups are efficient to increase by milling. The particles morphology of the powder did not change by milling modifications.

**Keywords:** Silica powder; Surface activities; Mechanical milling.

### Acknowledgment

This study was partly supported by Hanoi University of Science and Technology with code T2018-PC-085.

## ADVANCED MATERIAL

### References

[1] T. T. T. Hien, T. Shirai and M. Fuji, J. Ceram. Soc. Jpn., 120[10], 429-435 (2012).
[2] R. S. McDonald, J. Phys. Chem. 62[10] 1168-1178 (1958).
[3] X. Y. Mei, A. Ji, H. D. Min, W. D. Mei, C. H. Ying, G. Jun and Z. Q. Min, Oil Shale 27[1], 37-48(2010).
[4] S. Watanabe, Y. Sugita, Surface Science 327, 001-008 (1995).

**ADVANCED MATERIAL**

**Paper ID: ESCE038**

# RECENT DEVELOPMENT IN METAL OXIDE-BASED CORE-SHELL MATERIAL FOR $CO_2$ CAPTURE AND UTILIZATION

**N. Mat[1], and L.P. Teh[1]***

[1] *Department of Chemical Sciences, Faculty of Science and Technology, Universiti Kebangsaan Malaysia, 43600 UKM Bangi, Selangor, Malaysia.*
*Corresponding author: lpteh@ukm.edu.my

## Extended Abstract

Carbon dioxide ($CO_2$) is the most abundant greenhouse gas in the atmosphere and causing global warming. According to the $CO_2$ Earth website [1], the rate of $CO_2$ in the atmosphere achieved 416.46 ppm that above a normal range (250-350 ppm) (updated in February 2021). Various technologies have been introduced to minimize the dissipation of $CO_2$ to the atmosphere. Nowadays, carbon capture, utilization, and storage (CCUS) systems have recently gained popularity as a viable means of reducing $CO_2$ emissions [2]. Since fossil fuels will continue to dominate the global energy structure for the foreseeable future, CCUS has been deemed the most viable solution for short-term $CO_2$ emission reduction to achieve the IEA 450 Scenario [2,3]. Utilization of $CO_2$ as a desirable renewable source to produce syngas such as can be obtained by dry reforming process [4,5]. Recently, core-shell nanomaterial (CSN) has received increased attention as a promising $CO_2$ capture and utilization material [6]. Several core-shell materials have been introduced for $CO_2$ adsorption and conversion such as carbon nanofiber [7], zeolite [8], metal oxide [9], and metal organic framework (MOF) [10,11]. Among these materials, metal oxide possesses basic property for high $CO_2$ adsorption and $CO_2$ conversion reaction. Core-shell nanoparticles also have been documented on the used in CO2 utilization including photoconversion, photoreduction, syngas reduction and reforming, as well as hydrogenation reactions. Consequently, metal oxide-based core shell material is highly potential in the CO2 capture and CO2 application. To the best of our knowledge, there is scarcity report in this aspect. The present review focused on the latest development of the metal oxide-based core-shell material in CO2 adsorption and utilization.

**Keywords:** $CO_2$ Adsorption and Conversion; Core-Shell; Metal Oxide.

### Acknowledgment

This study was supported by Ministry of Higher Education, Malaysia through Fundamental Research Grant Scheme (FRGS/1/2019/STG01/UKM/02/6).

### References

[1] CO2 Earth website (2021): CO2-Earth are we stabilizing yet? https://www.co2.earth/ (accessed 31.03.21)
[2] Ding J., Yu C., Lu J., Wei X., Wang W., & Pan G. (2020) Enhanced CO2 Adsorption of MgO With Alkali Metal Nitrates and Carbonates. Applied Energy, 263:114681.
[3] Guo Y., Tan C., Sun J., Li W., Zhao C., Zhang J., & Lu P. (2018) Nanostructured MgO Sorbents Derived from Organometallic Magnesium Precursors for Post-Combustion CO2 Capture. Energy & Fuels, 32:6910-6917.
[4] Rahmat N., Yaakob Z., Rahman N. A., & Jahaya S. S. (2020) Renewable Hydrogen-Rich Syngas from CO2 Reforming of CH4 with Steam Over Ni/Mgal2o4 And Its Process Optimization. International Journal of Environmental Science and Technology, 17:843-856.
[5] Lu Y., Guo D., Ruan Y., Zhao Y., Wang S., & Ma X. (2018) Facile One-Pot Synthesis of Ni@ HSS As A Novel Yolk-Shell Structure Catalyst for Dry Reforming of Methane. Journal of CO2 Utilization, 24:190-199.
[6] Nakano K., Hoshino Y., Numata K., & Tanaka K. (2021) CO2: Capture Of, Utilization Of, And Degradation Into. Polymer Journal, 53:1-2.
[7] Ma S., Wang Y., Liu Z., Huang M., Yang H., & Xu Z. L. (2019) Preparation of Carbon Nanofiber with Multilevel Gradient Porous Structure for Supercapacitor and CO2 Adsorption. Chemical Engineering Science, 205:181-189.
[8] Miyamoto M., Ono S., Kusukami K., Oumi Y., & Uemiya S. (2018). High Water Tolerance of a Core–Shell-StructuredZeolite for CO2 Adsorptive Separation Under Wet Conditions. ChemSusChem, 11:1756-1760.
[9] Yuan L., Han C., Pagliaro M., & Xu Y. J. (2016). Origin of Enhancing the Photocatalytic Performance of TiO2 For

Artificial Photoreduction of CO2 Through a SiO2 Coating Strategy. The Journal of Physical Chemistry C, 120:265-273.
[10] Li Q., Guo J., Zhu H., & Yan F. (2019). Space-Confined Synthesis of ZIF-67 Nanoparticles in Hollow Carbon Nanospheres for CO2 Adsorption. Small, 15:1804874.
[11] Mu X., Liu S., Chen Y., Cheang U. K., George M. W., & Wu T. (2020). Mechanistic and Experimental Study of the Formation of MoS2/HKUST-1 Core–Shell Composites on MoS2 Quantum Dots with an Enhanced CO2 Adsorption Capacity. Industrial & Engineering Chemistry Research, 59:5808-5817.

**ADVANCED MATERIAL**

**Paper ID: ESCE039**

# REVIEW ON $CO_2$ ADSORPTION AND CONVERSION STUDIES USING METAL ORGANIC FRAMEWORK BASED MATERIAL

**Z. I. Zulkifli[1], L. P. Teh[1]***

[1] *Department of Chemical Sciences, Faculty of Science and Technology, Universiti Kebangsaan Malaysia, 43600 UKM Bangi, Selangor, Malaysia.*
*Corresponding author: lpteh@ukm.edu.my

## Extended Abstract

The frequent usage of humans on fossil fuels as primary source of energy has led to atmospheric gradually increase of greenhouse gas $CO_2$ through the process of combustion and it is believed to contribute immensely to climate changes on a global scale. Sustaining the atmosphere and protecting the global climate are recognized as the main concerns of the planet [1]. So far, several $CO_2$ capture and sequestration (CCS) techniques have been developed to address this issue [2]. Besides, the captured $CO_2$ can be potentially used for many applications such as polymers, fertilizer, refrigerants, chemicals, and cosmetics. Moreover, it also becomes an important precursor in the petroleum industry, especially in enhancing the oil recovery [3]. There are various types of $CO_2$ capture technologies that are presently available including absorption (chemical and physical absorptions), adsorption, and membrane technologies [1]. The chemical absorption of amine scrubbing has been found to be a common technique used, especially power plants in industrial settings [4]. But this method has disadvantages with a large quantity of absorbent requirements, high energy consumption, and corrosiveness [1]. Solid adsorption processes have been recommended to overcome these inherent problems. So far, significant classes of porous material have been studied and introduced as adsorbents such as activated carbon, aluminophosphates, zeolite, carbon nanotubes, metal-oxide molecular-sieves, activated alumina, silica gel, inorganic and polymeric resins, as well as porous metal-organic framework [5]. Among the mentioned materials, zeolites and activated carbons have been extensively studied, being found to be more efficient for the $CO_2$ capture [6]. Nevertheless, they suffered from the instability in the presence of water (zeolite-based adsorbents) as well as some limitations such as low $CO_2$ adsorption capacity at high temperatures. $CO_2$ molecules interaction in the activated carbon is very weak and thus making this adsorbent sensitive to temperature changes although it is acknowledged that activated carbon has a greater $CO_2$ adsorption capacity than zeolites. To overcome this issue, metal-organic frameworks (MOFs) are considered as the newest and most promising $CO_2$ adsorption and conversion material. These novel hybrid materials are formed by the combination of metal ions and organic ligands, which are connected via coordination bonding. Due to their unique properties such as high surface area, large pore volume, and robust 3D structures, MOFs has shown a significant potential for gas separation technologies, particularly for $CO_2$ adsorption and $CO_2$ conversion [7]. Therefore, the present review attempts to provide current understanding of the $CO_2$ adsorption and conversion performance over MOFs based material.

**Keywords:** $CO_2$ Adsorption; Metal-Organic Framework; Metal; Organic Ligands; $CO_2$ Conversion.

### Acknowledgment

This study was supported by Ministry of Higher Education, Malaysia through Fundamental Research Grant Scheme (FRGS/1/2019/STG01/UKM/02/6).

### References

[1] Yu C.H. (2012) A Review of $CO_2$ Capture by Absorption and Adsorption. Aerosol Air Qual Res. 12:745-769.
[2] Gibbins J. & Chalmers H. (2008) Carbon Capture and Storage. Energy Policy 36:4317-4322.
[3] Ghanbari T., Abnisa F. & Daud W.M.A.W (2020) A Review on Production of Metal Organic Frameworks (MOF) for $CO_2$ Adsorption. Sci. Total Environ. 707:135090.
[4] Rochelle G.T. (2009) Amine Scrubbing for $CO_2$ Capture. Science 325:1652-1654.
[5] Li Z. Q., Qiu L. G., Xu T., Wu Y., Wang W., Wu Z. Y., & Jiang, X. (2009) Ultrasonic Synthesis of The Microporous

Metal–Organic Framework Cu3-(BTC)2 at Ambient Temperature and Pressure: An Efficient and Environmentally Friendly Method. Mater. Lett. 63:78-80.

[6] Zhang X., Zhang X., Song L., Hou F., Yang Y., Wang Y., & Liu N. (2018) Enhanced Catalytic Performance for CO Oxidation and Preferential CO Oxidation Over CuO/CeO2 Catalysts Synthesized from Metal Organic Framework: Effects of Preparation Methods. Int. J. Hydrog. Energy 43:18279-18288.

[7] Millward A.R. & Yaghi O.M. (2005) Metal-Organic Frameworks with Exceptionally High Capacity for Storage of Carbon Dioxide and Room Temperature. J Am Chem Soc. 127:17998-17999.

**ADVANCED MATERIAL**

**Paper ID: ESCE042**

# SYNTHESIS OF CARBOXYMETHYL CELLULOSE (CMC) FROM COCOA POD HUSK

**N. Hafiz[1], M. Rajin[1]*, S. E. How[2], S. Saalah[1]**

[1] *Faculty of Engineering,* [2] *Faculty of Sciences & Natural Resources, Universiti Malaysia Sabah, 88400 Kota Kinabalu, Sabah, Malaysia.*
*Corresponding author: mariani@ums.edu.my

## Extended Abstract

Most of the Southeast Asian countries have agro-based economies. The major constraint on the plantation is waste disposal. One of attempts to overcome the constraint is by utilizing crops rich in cellulose. Cellulose is commonly found in cell wall of plant [1]. It is a common natural polymer with a linear molecular structure that is biodegradable [2]. It has strong intramolecular and intermolecular hydrogen bonds [3]. Therefore, cellulose is neither melts nor dissolves and converted into its derivates before being utilized for other applications. A common derivative of cellulose is carboxymethyl cellulose (CMC) [4]. CMC is a primary source of biopolymer with a straight chain of polysaccharide [5]. Numerous hydroxyl and carboxyl functional groups present in the structure induce its binding and absorbing abilities [6]. CMC is synthesized from cellulose by its monochloroacetic acid or sodium salt with a surplus of organic solvent such as isopropanol and ethanol. In the synthesis of CMC, carboxymethyl groups typically substitute hydroxyl groups in cellulose [7]. CMC is biocompatible since it is soluble in water. Due to its wide range of applications, especially in biodegradable polymer due to its degradable properties, CMC has been synthesized from different cellulose sources including agricultural waste. Previous studies have shown successful CMC synthesis from agricultural wastes such as wheat, soy, sago, and durian [6]. In this study, CMC was produced from the cellulose of cocoa pod husk. In Malaysia, cocoa (*Theobroma cacao L.*) is one of the important commodities due to its economic value [8]. Thus, this study was conducted to extract CMC from the cellulose of agricultural waste, cocoa pod husk.

The synthesis of CMC followed the procedure described by Hutomo [1]. Then the samples were characterized for yield percentage following method by Mondal [2]. For degree of substitution (DS), it was characterized for its absolute and relative. The absolute degree of substitution ($DS_{abs}$) of samples was conducted through back-titration in accordance with ASTM D1439 [2]. In contrast, the relative degree of substitution ($DS_{rel}$) values was obtained from infrared radiation (IR). For FTIR analysis, Fourier Transform Infrared (FTIR) spectrophotometer (INVENIO FT-IR Spectrometer-Bruker) was used. The transmission was measured at a wavenumber of 400- 4000 $cm^{-1}$.

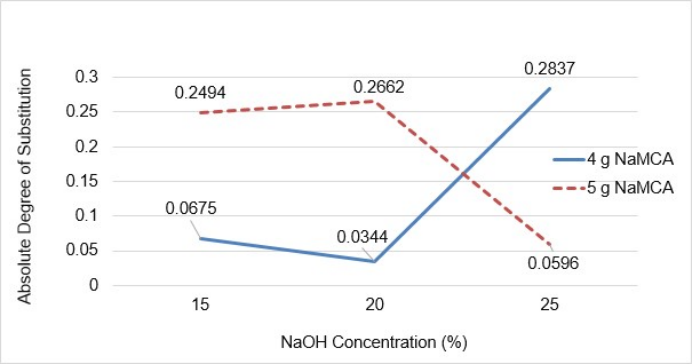


Fig. 1: Effect of NaOH concentration on DS for 4 and 5 g of NaOH.

The degree substitutions of the samples were in the range of 0.0212-0.3724 (Fig.1). The result trend demonstrated that higher amounts of sodium monochloacetate (NaMCA) would lead to higher DS values. $DS_{abs}$ was obtained at the highest NaOH concentration (25%) with 4 g of NaMCA. While the lowest DS was obtained from 20% NaOH concentration with the same NaMCA amount.

**ADVANCED MATERIAL**

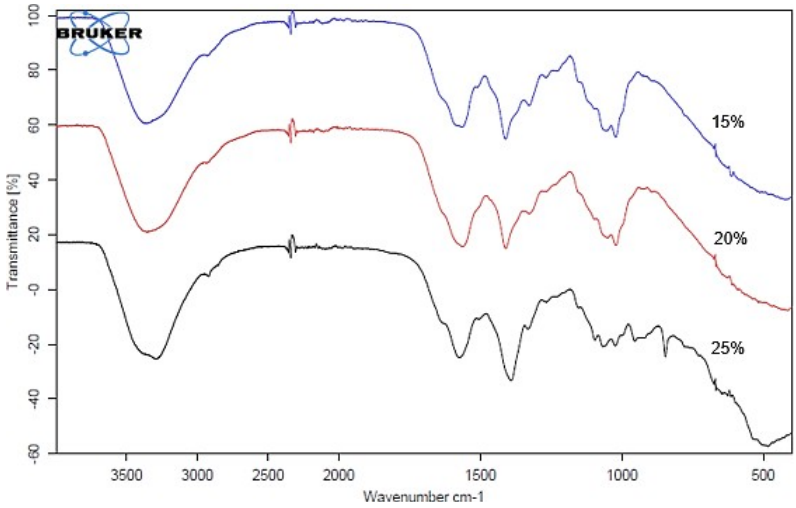


Fig. 2: FTIR spectra of CMC samples for 4 g of NaMCA with various NaOH concentrations.

The presence of the carboxyl group and its salts in the CMC spectra was confirmed with the existence of two-peak wavelengths around 1400-1450 $cm^{-1}$ and 1600-1640 $cm^{-1}$ as shown in the FTIR spectra (Fig. 2). Thesepeaks indicate the presence of carboxymethyl substituents [9] in the sample. The infrared spectra of the CMC samples synthesized using different NaOH concentrations and NaMCA amounts exhibited similar patterns. The presence of peaks in the spectra confirmed the functional groups of the CMC samples.

In conclusion, CMC was successfully synthesized from the cellulose of cocoa pod using various NaOH concentrations with different amounts of NaMCA. The FTIR analysis confirmed the presence of functional groups of CMCs.

**Keywords:** Agricultural waste; Cocoa pod husk; Cellulose; Carboxymethyl cellulose.

## Acknowledgment

This project is financially aided by Skim Dana Nic (SDN0068-2019) from Universiti Malaysia Sabah (UMS). The authors would like to thank Faculty of Engineering and Faculty of Science and Natural Resources of UMS for supporting this study.

## References

[1] Hutomo G. S., Marseno D. W., Anggrahini S. (2012) Synthesis and characterization of sodium carboxymethylcellulose from pod husk of Cacao (Theobroma cacao L.), African Journal of Food Science, (6) 6, 180-185. DOI: 10.5897/ajfs12.020.
[2] Mondal M. I. H., Yeasmin M. S., Rahman M. S. (2015) Preparation of food grade carboxymethyl cellulose from corn husk agrowaste, International Journal of Biological Macromolecules, 79, 144-150. DOI: 101016/j.ojbiomac.2015.04.061.
[3] Gilbert R. D., Kadla J. F. (2000) Cellulose Modification, Plastic Engineering, 60, 21-66.
[4] Alizadeh S. A., Mousavi M, Labbafi M. (2017) Synthesis and characterization of carboxymethyl cellulosefrom sugarcane bagasse, Journal of Food Processing and Technology, 8 (8). DOI: 10.4172/2157-7110.1000687.
[5] Rodsamran P., Sothornvit R. (2017) Rice stubble as a new biopolymer source to produce carboxymethylcellulose-blended films, Carbohydrate polymers, 171, 94-101. DOI: 10.1016/j.carb.pol.2017.05.003.
[6] Huang C. M., Chia P., Lim C. S., Nai J., Ding D. Y., Seow P., Chan E. W. (2017) Synthesis and characterisation ofcarboxymethyl cellulose from various agricultural wastes. Cellul. Chem. Technol., 51 (7-8), 665-672.
[7] Adinugraha M. P., Marseno D. W. (2005) Synthesis and characterization of sodium carboxymethylcellulosefrom cavendish banana pseudo stem (Musa cavendishii LAMBERT), Carbohydrate Polymers, 62 (2), 164-169. DOI: 10.1016/j.carbpol.2005.07.019.
[8] Daud Z., Sari A., Kassim M., Aripin A. M., Awang H., Hatta Z. M. (2013) Chemical composition and morphological of cocoa pod husk and cassava peels for pulp and paper production, Australian Journal of Basic and Applied Sciences, 7 (9), 406-411.
[9] Ge M., Chen M. (2013) Preparation and characterization of magadiite, Kuei Suan Jen Hsueh Pao/Journal of the Chinese Ceramic Society, (12), 1704–1708.

**ADVANCED MATERIAL**

**Paper ID: ESCE092**

# PREPARATION AND CHARACTERIZATION OF INVERSE VULCANIZED COPOLYMERS USING TARAMIRA OIL

**Ali Shaan Manzoor Ghumman[1], Rashid Shamsuddin[2]*, Mohamed Mahmoud Nasef[3], Wan Zaireen Nisa Yahya[1] and Amin Abbasi[1]**

[1] *Chemical Engineering Department,* [2] *HICoE, Centre for Biofuel and Biochemical Research (CBBR), Institute of Self-Sustainable Building, Universiti Teknologi PETRONAS, 32610, Seri Iskandar, Perak, Malaysia.*
[3] *Department of Chemical and Environmental Engineering, Malaysia Japan International Institute of Technology, Universiti Teknologi Malaysia, Jalan Sultan Yahya Petra, Kuala Lumpur 54100, Malaysia.*
*Corresponding author: mrashids@utp.edu.my

## Extended Abstract

Synthetic polymers from petro-based monomers are ubiquitous to humans and are among the most largely produced materials on the earth [1-5]. However, the declining abundance of such monomers and environmental problem associated with them are important to consider. Therefore, a rigorous research is needed to identify green, sustainable, and cheap monomers from agriculture, biomass, and industrial waste [6,7].

Inverse vulcanization is a facile, solvent free and atom economic method to produce sustainable copolymers recently invented by Pyun and his collaborators [6]. This method utilizes sulfur (a petroleum industry waste, which accumulated in open large piles due to its underutilization in market making it a cheap readily available raw material) as initiator and monomer to produce sulfur enriched copolymers [6-8].

Inverse vulcanization reaction has been previously utilized in diverse range of studies however, those studies used petroleum derived, terpenes and edible vegetable oils as monomers for this reaction. The depleting abundance, high synthesis and purification cost and high food market make them less sustainable feedstocks [6,7]. Herein, we reported the synthesis of the inverse vulcanized copolymers utilizing abundantly available non-edible oil as alternative monomer. The properties of the obtained copolymers were evaluated using FTIR (Fourier Transform Infrared Spectroscopy), SEM (Scanning Electron Microscopy) and p-XRD (Powdered X-ray Diffractogram). FTIR confirmed the formation of the copolymer and composite morphology of the copolymers was revealed by SEM images and confirmed by p-XRD.

Pristine taramira oil showed cis-alkene characters (3009cm$^{-1}$) in the FTIR spectrum, absence of these signals from spectra of all obtained copolymers confirmed the formation of the copolymers. These copolymers possess significant amount of the unreacted sulfur which was revealed by the appearance of the cystalline signals in the diffractogram of all obtained copolymer resembling with β-$S_8$[9-15]. Due to the presence of the unreacted sulfur these copolymers possess composite morphology, containing smooth surface representing copolymer formed and some isolated crystal particles representing unreacted sulfur. Above observations are preceeded by previous utilization edible vegetable oil, which shows that non-edible oil can successfully replace the edible as monomers [16-21]. Above observations are consistent with reported literatures on successful monomer synthesis using edible vegetable oils which highlights the potential of nonedible taramira oil as an alternative precursor material [22-24].

**Keywords:** Inverse vulcanization; Sulfur-based polymers; Non-edible oil; Value adding product.

### Acknowledgment

This research work is supported by collaborative research grant (015ME0-197) from UP-UTP. Authors would also like to acknowledge the facilities provided by Unversiti Teknologi PETRONAS.

### References

[1] R. Geyer, J.R. Jambeck, K.L. Law, Production, use, and fate of all plastics ever made, Sci. Adv. 3 (2017) 25–29. https://doi.org/10.1126/sciadv.1700782.

## ADVANCED MATERIAL

[2] Global Plastic Production, (n.d.). https://www.statista.com/statistics/282732/global-production-of-plastics-since-1950/.
[3] P. Anastas, N. Eghbali, Green chemistry: Principles and practice, Chem. Soc. Rev. 39 (2010) 301–312. https://doi.org/10.1039/b918763b.
[4] Y. Zhu, C. Romain, C.K. Williams, Sustainable polymers from renewable resources, Nature. 540 (2016) 354–362. https://doi.org/10.1038/nature21001.
[5] U. Minerals Information Team, U.S. Geological Survey, Mineral Commodity Summaries, February 2019, (2006) 2018–2019. https://minerals.usgs.gov/minerals/pubs/commodity/sulfur/sulfumcs06.pdf?fbclid=IwAR3RxFoolmxI2xzqF6om-O8vAEZEZEQOvPBh8Y6noMQ3oAGhcDmk4sCS3is.
[6] A. Abbasi, M. Mahmoud, W. Zaireen, N. Yahya, Copolymerization of vegetable oils and bio-based monomers with elemental sulfur : A new promising route for bio-based polymers, Sustain. Chem. Pharm. 13 (2019) 100158. https://doi.org/10.1016/j.scp.2019.100158.
[7] A.S.M. Ghumman, M.M. Nasef, M.R. Shamsuddin, A. Abbasi, Evaluation of properties of sulfur-based polymers obtained by inverse vulcanization: Techniques and challenges, Polym. Polym. Compos. (2020). https://doi.org/10.1177/0967391120954072.
[8] C.R. Arza, P. Froimowicz, H. Ishida, Triggering effect caused by elemental sulfur as a mean to reduce the polymerization temperature of benzoxazine monomers, RSC Adv. 6 (2016) 35144–35151. https://doi.org/10.1039/C6RA04420D.
[9] A. Abbasi, M.M. Nasef, W.Z.N. Yahya, Sulfur Based Polymers by Inverse Vulcanization: a Novel Path to Foster Green Chemistry, Green Mater. (2020) 1–8. https://doi.org/10.1680/jgrma.19.00053.
[10] S. Diez, A. Hoefling, P. Theato, W. Pauer, Mechanical and electrical properties of sulfur-containing polymeric materials prepared via inverse vulcanization, Polymers (Basel). 9 (2017) 1–16. https://doi.org/10.3390/polym9020059.
[11] W.J. Chung, J.J. Griebel, E.T. Kim, H. Yoon, A.G. Simmonds, H.J. Ji, P.T. Dirlam, R.S. Glass, J.J. Wie, N.A. Nguyen, B.W. Guralnick, P. Theato, M.E. Mackay, Y. Sung, J. Park, The use of elemental sulfur as an alternative feedstock for polymeric materials, 5 (2013). https://doi.org/10.1038/NCHEM.1624.
[12] J.M. Chalker, M.J.H. Worthington, N.A. Lundquist, L.J. Esdaile, Synthesis and Applications of Polymers Made by Inverse Vulcanization, Top. Curr. Chem. 377 (2019) 1–27. https://doi.org/10.1007/s41061-019-0242-7.
[13] A. Abbasi, M.M. Nasef, W.Z.N. Yahya, M. Moniruzzaman, A.S.M. Ghumman, Preparation and characterization of sulfur-vinylbenzyl chloride polymer under optimized reaction conditions using inverse vulcanization, Eur. Polym. J. 143 (2021) 110202. https://doi.org/10.1016/j.eurpolymj.2020.110202.
[14] A.S.M. Ghumman, M.R. Shamsuddin, M.M. Nasef, W.Z.N. Yahya, M. Ayoub, B. Cheah, A. Abbasi, Synthesis and Characterization of Sustainable Inverse Vulcanized Copolymers from Non-Edible Oil, ChemistrySelect. 6 (2021) 1180–1190. https://doi.org/https://doi.org/10.1002/slct.202004554.
[15] A.S.M. Ghumman, R. Shamsuddin, M.M. Nasef, W.Z. Nisa Yahya, A. Abbasi, Optimization of synthesis of inverse vulcanized copolymers from rubber seed oil using response surface methodology, Polymer (Guildf). 219 (2021) 123553. https://doi.org/10.1016/j.polymer.2021.123553.
[16] A. Abbasi, M.M. Nasef, W.Z.N. Yahya, M. Moniruzzaman, A.S. Ghumman, Preparation and characterization of green polymer by copolymerization of corn oil and sulphur at molten state, Polym. Polym. Compos. (2020). https://doi.org/10.1177/0967391120959536.
[17] A. Hoefling, Y.J. Lee, P. Theato, Sulfur-Based Polymer Composites from Vegetable Oils and Elemental Sulfur: A Sustainable Active Material for Li-S Batteries, Macromol. Chem. Phys. 218 (2017) 1600303. https://doi.org/10.1002/macp.201600303.
[18] S. Oishi, K. Oi, J. Kuwabara, R. Omoda, Y. Aihara, T. Fukuda, T. Takahashi, J.-C. Choi, M. Watanabe, T. Kanbara, Synthesis and Characterization of Sulfur-Based Polymers from Elemental Sulfur and Algae Oil, ACS Appl. Polym. Mater. 1 (2019) 1195–1202. https://doi.org/10.1021/acsapm.9b00197.
[19] M.J.H. Worthington, R.L. Kucera, I.S. Albuquerque, C.T. Gibson, A. Sibley, A.D. Slattery, J.A. Campbell, S.F.K. Alboaiji, K.A. Muller, J. Young, N. Adamson, J.R. Gascooke, D. Jampaiah, Y.M. Sabri, S.K. Bhargava, S.J. Ippolito, D.A. Lewis, J.S. Quinton, A. V. Ellis, A. Johs, G.J.L. Bernardes, J.M. Chalker, Laying Waste to Mercury: Inexpensive Sorbents Made from Sulfur and Recycled Cooking Oils, Chem. - A Eur. J. 23 (2017) 16219–16230. https://doi.org/10.1002/chem.201702871.
[20] S.F. Valle, A.S. Giroto, R. Klaic, G.G.F. Guimar, Sulfur fertilizer based on inverse vulcanization process with soybean oil, Polym. Degrad. Stab. 162 (2019) 102–105. https://doi.org/10.1016/j.polymdegradstab.2019.02.011.
[21] J.C. Bear, W.J. Peveler, P.D. McNaughter, I.P. Parkin, P. O'Brien, C.W. Dunnill, Nanoparticle–sulphur "inverse vulcanisation" polymer composites, Chem. Commun. 51 (2015) 10467–10470. https://doi.org/10.1039/C5CC03419A.
[22] A. Hoefling, D.T. Nguyen, Y.J. Lee, S.-W. Song, P. Theato, A sulfur–eugenol allyl ether copolymer: a material synthesized via inverse vulcanization from renewable resources and its application in Li–S batteries, Mater. Chem. Front. 1 (2017) 1818–1822. https://doi.org/10.1039/C7QM00083A.
[23] A.N. Sankaran, M. Swaminathan, A.B. Exptl, & The Composition of Seed and Seed Oils of Taramira ( Eruca sativa ), 62 (1985) 1134–1135.
[24] E. Sastry, Taramira (Eruca sativa) and its improvement – A review, Agric. Rev. 24 (2003) 235–249.

**ADVANCED MATERIAL**

**Paper ID: ESCE129**

# INTUMESCENT FLAME RETARDANT BASED ON SEPIOLITE FILLED RIGID POLYURETHANE FOAM

**Abdulwasiu Muhammed Raji[1,2] *, Zurina Binti Mohamad[1]*, Azman Hassan[1]**

[1] *Enhanced Polymer Research Group, School of Chemical and Energy Engineering, Faculty of Engineering, Universiti Teknologi Malaysia, 81310 Johor Bahru, Malaysia.*
[2] *Department of Polymer and Textile Technology, Yaba College of Technology, P.M.B. 2011, Lagos, Nigeria.*
*Corresponding author: r.abdulwasiu@graduate.utm.my and r-zurina@utm.my

## Extended Abstract

The global market for rigid polyurethane foam (RPUF) consumes around 50% of all polyurethane foam supply (Sonnenschein, 2015; Akindoyo *et al.*, 2016). RPUF is a highly cross-linked polymer with a closed-cell structure. It has low density, and moisture permeability, high strength to weight ratio, and specifically, its low thermal conductivity have made it a formidable synthetic material globally (AbiSaleh *et al*., 2003; Banik and Sain, 2008). The rapid growth in the use of RPUFs after their launch in the 1950s have been credited to their improved water resistance (both liquid and vapour) and low thermal conductivity (Eaves, 2001). However, RPUF is highly flammable with a low limiting oxygen index value near 18 % (Li *et al.*, 2018). Consequently, in the event of a fire outbreak it burns quickly with rapid flame spread due to low thermal inertia, large surface area, high carbon and hydrogen content and porous structure. Due to this, poisonous gases like hydrogen cyanide (HCN) and carbon monoxide (CO) are released as the foam easily collapse during burning. The released gas when inhaled is a threat to human health during combustion (Zhou *et al.*, 2020; Baguian *et al.*, 2021). Hence, it is mandatory to protect RPUF with flame retardants (FR) to boost their fire retardancy and smoke suppressing property (Cao *et al.*, 2017). RPUF's famous FR's are halogen-based compounds such as pentabromodiphenyl ether (Wilkie, 2009), chloroethyl phosphate (C. Wang *et al.*, 2018), polybrominated diphenyl ethers (Chattopadhyay and Webster, 2009), and decabromodiphenyl ether (Wang *et al.*, 2014). All this popular FR's can provide excellent flame retardation to RPUF; however, they are environment unfriendly. Necessitating the continuous demand for FR additives with high flame retardance efficiency and that seldom pollute the environment (Chen *et al.*, 2012). More so, due to strict regulations and in some countries, outright ban on the use of halogenated FRs, the demand for halogen-free FRs has increased rapidly (Covaci *et al.*, 2020). These has led to a new generation of halogen-free FRs such as intumescent flame retardants (IFR) (Bhoyate *et al.*, 2018). IFRs are popularly used to make flame retarded polymeric materials, as they offer less smoke, lower toxicity, excellent fire protection and anti-dripping properties. As a result, this research developed an intumescent flame-retardant system based on ammonium polyphosphate, sepiolite, and melamine, which was then applied to rigid polyurethane foam. Sepiolite stands out as one of the elements in our IFR system because, to the best of our knowledge, it has never been used as a carbonizing agent in a polyurethane or other polymer matrix. The intumescent flame-retardant RPUF was characterized by Underwriter's Laboratories' (UL94) vertical test and limiting oxygen index flammability test.

The LOI test was performed using the LOI apparatus from Rheometer Scientific, United Kingdom, according to ASTM D2863-2013 standard method. The test was conducted by preparing five samples from each formulation with dimensions of 100 × 10 × 10mm$^3$, length, width, and thickness, respectively. The test was repeated under different oxygen and nitrogen ($O_2/N_2$) atmosphere. This was vital to identify the approximate amount of $O_2/N_2$ required for burning 5cm of the sample in 3 minutes. The average LOI value from each formulation was recorded from five samples' burning. These data were used as an indication of the flammability of the samples. Underwriters Laboratories (UL-94) test, UL-94 measures sample response to a removed fire threat and the time required to self-extinguish. This test was conducted on a manually set UL-94 chamber as shown in (Wilkie and Morgan, 2010) according to ASTM D3801. Five samples with dimensions of 130 ×13 ×3mm$^3$ (length, width, and thickness), respectively, were prepared. The burning ratings was used to classify the UL-94 test results into HB, V- 0, V-1, or V-2 (Li *et al.*, 2018). Observations were recorded according to; time until the flame extinguishes itself, distance the burn propagates through the sample, and lastly whether the flame burns through the sample or flame drops from the sample.

**ADVANCED MATERIAL**

RPUF were satisfactorily modified with IFR of ammonium polyphosphate, sepiolite, and melamine. The LOI residue images (Figure 1) showed that embedded IFRs has protected the underneath matrix and enhances the reaction to flame of RPUF foams. Additionally, RPUF/IFR composites showed the lowest after flame times and achieved V-0 rating in comparison with pristine RPUF, that failed the UL-94 analysis. A display of inferior flame retardant performance for the reference sample. This outcome is represented in Figure 2. The improved flame retardancy of the IFR modified RPUF was achieved with a 16phr of IFR ingredients compared with prior studies at above 25phr. Also, sepiolite as a novel carbonizing agent in intumescent systems is quite cost effective in comparison to popular carbonizing agents such as pentaerythritol, methylol melamine, and phenol formaldehyde. Sepiolite is an inorganic carbon source contributing to release of nontoxic smoke during combustion.


Fig. 1: LOI test images showing the reaction of the pristine RPUF and modified RPUF to $O_2/N_2$ mixture in a controlled atmosphere.

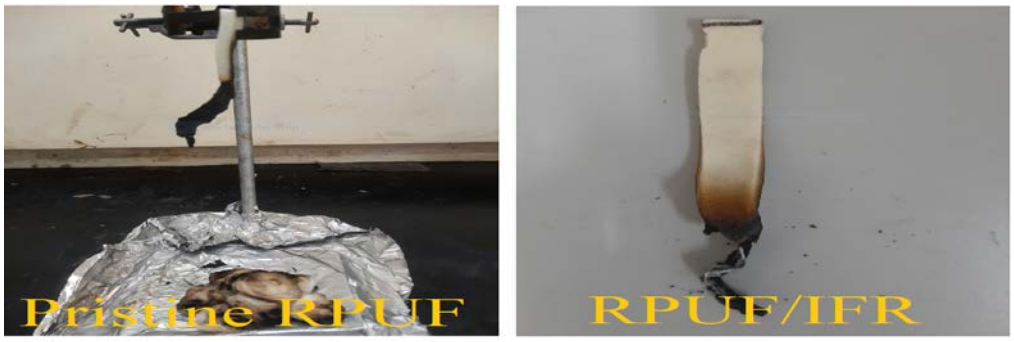


Fig. 2: Digital pictures of UL-94 test of RPUF and its composite.

**Keywords:** Intumescent flame retardant; Sepiolite; Rigid polyurethane foam; Flame retardancy.

**Acknowledgment**

Special thanks to Tertiary Education Trust Fund (TETFUND), Nigeria and Universiti Teknologi Malaysia for providing financial support for this study.

**References**

[1] Sonnenschein, M.F., (2015) *POLYURETHANES - Science, Technology, Markets, and Trends* Nwabunma, R.F.G.D., (ed.), Wiley, New Jersey.
[2] Akindoyo, J.O. et al., (2016) Polyurethane types, synthesis and applications-a review. *RSC Advances*, 6(115), pp.114453–114482.
[3] T. AbiSaleh, M. Anderson, M. Barker, G. Biesmans, J. Bosman, D.D., (2003) Introduction to Polyurethanes. In: S., D.R. and and Lee, (eds.) *The Polyurethanes Book*. Wiley, New York, pp. 1–8.
[4] Banik, I. and Sain, M.M., (2008) Water Blown Soy Polyol-Based Polyurethane Foams of Different Rigidities. *J. Reinforced Plastics and Composites*, 27(4), pp.357–373.
[5] Li, J. et al., (2018) Influence of expandable graphite particle size on the synergy flame retardant property between expandable graphite and ammonium polyphosphate in semi-rigid polyurethane foam. *Polym Bulletin*, 75(11), pp.5287–5304.
[6] Eaves, D. (2001) *Polymer Foams - Trends in Use and Technology.*, Rapra Technology Ltd, Shropshire.
[7] Zhou, F. et al., (2020) Synthesis of a novel liquid phosphorus-containing flame retardant for flexible polyurethane foam: Combustion behaviors and thermal properties. *Polym Degrad and Stab*, 173, pp.1–11.

## ADVANCED MATERIAL

[8] Baguian, A.F. et al., (2021) Influence of density on foam collapse under burning. *Polymers*, 23(1), pp.1–17.
[9] Wang, C. et al., (2018) Flame-retardant rigid polyurethane foam with a phosphorus-nitrogen single intumescent flame retardant. *Polym for Advanced Tech*, 29(1), pp.668–676.
[10] Chattopadhyay, D.K. and Webster, D.C., (2009) Thermal stability and flame retardancy of polyurethanes. *Prog in Polym Sci (Oxford)*, 34(10), pp.1068–1133.
[11] Wang, F. et al., (2014) Effect of modified sepiolite nanofibers and hollow glass microspheres on performance of rigid polyurethane foams composite materials. Nanosci and Nanotech Letters, 6(6), pp 524-531.
[12] Chen, M.-J., Shao, Z.-B., et al., (2012) Halogen-free flame-retardant flexible polyurethane foam with a novel nitrogen-phosphorus flame retardant. *Industrial and Eng Chem Research*, 51(29), pp.9769–9776.
[13] Covaci, A. et al., 2020. Novel brominated fl ame retardants: A review of their analysis, environmental fate and behaviour. *Environment International*, 37(2), pp.532–556.
[14] Bhoyate, S., Ionescu, M., Kahol, P.K. and Gupta, R.K., (2018) Sustainable flame-retardant polyurethanes using renewable resources. *Industrial Crops and Products*, 123(July), pp.480–488.

2ND ENERGY SECURITY AND CHEMICAL ENGINEERING CONGRESS 2021
*"Sustainable Technological Solution for a Better World"*
VIRTUAL CONFERENCE | 3-5 NOVEMBER 2021

**ADVANCED MATERIAL**

**Paper ID: ESCE136**

# RECENT ADVANCES ON THE ENHANCED THERMAL CONDUCTIVITY OF GRAPHENE NANOPLATELETS COMPOSITES: A SHORT REVIEW

**W. H. Danial[1]*, Z. Abdul Majid[2]**

[1] *Department of Chemistry, Kulliyyah of Science, International Islamic University Malaysia, 25200 Kuantan, Pahang, Malaysia.*
[2] *Department of Chemistry, Faculty of Science, Universiti Teknologi Malaysia, 81310 UTM Johor Bahru, Johor, Malaysia.*
*Corresponding author: whazman@iium.edu.my

## Extended Abstract

Graphene nanoplatelets (GNPs) have attracted significant attention in the field of thermal management materials due to their unique morphology and remarkable thermal conductive properties. In addition, their impressive thermal properties make them interesting nanofillers for producing multifunctional composite materials with a multitude range of applications. This work specifically reviews the recent advances of the application of GNPs as nanofillers for the development of enhanced thermal conductivity of various materials or composites. In this review, the insight on the improved thermal conductivity of the composites bestowed by the GNPs with comprehensive comparison are briefly discussed. This review might unlock windows of opportunities and paves the way towards the production of enhanced materials for thermal applications including electronics, aerospace devices, batteries, and structural reinforcement.

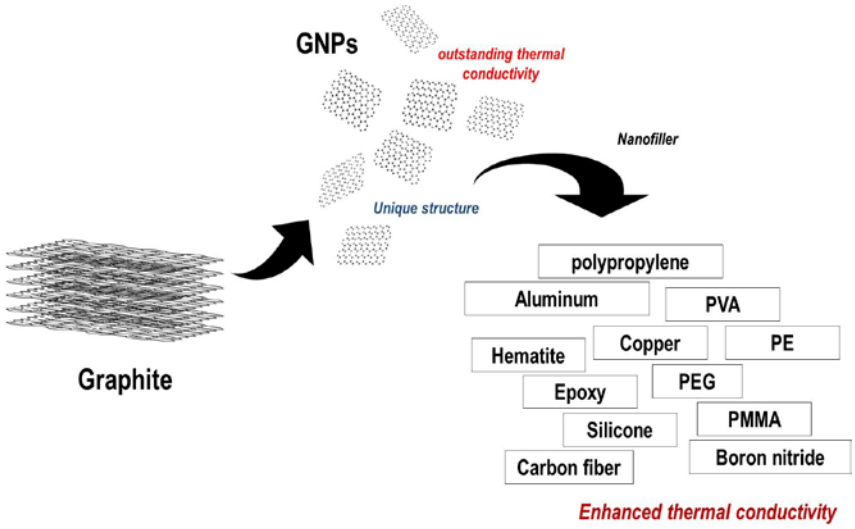


Fig. 1: Schematic representation of the development of enhanced thermal conductivity of various materials using graphene nanoplatelets as nanofiller.

**Keywords:** Graphene nanoplatelets; GNPs; Composites; Nanofiller; Thermal conductivity.

**Acknowledgment**

This work was supported by the Fundamental Research Grant Scheme (FRGS19- 015-0623), Ministry of Higher Education (MOHE), Malaysia.

## ADVANCED MATERIAL

### References

[1] Medellín-Banda, D. I., Navarro-Rodríguez, D., Fernández-Tavizón, S., Ávila-Orta, C. A., Cadenas-Pliego, G., & Comparán-Padilla, V. E. (2019). Enhancement of the thermal conductivity of polypropylene with low loadings of CuAg alloy nanoparticles and graphene nanoplatelets. Materials Today Communications, 21, 100695.

[2] Wang, C., Su, Y., Ouyang, Q., & Zhang, D. (2020). Enhanced through-plane thermal conductivity and mechanical properties of vertically aligned graphene nanoplatelet@graphite flakes reinforced aluminum composites. Diamond and Related Materials, 108, 107929.

[3] Liu, Y., Wu, K., Luo, F., Lu, M., Xiao, F., Du, X., Zhang, S., Liang, L., & Lu, M. (2019). Significantly enhanced thermal conductivity in polyvinyl alcohol composites enabled by dopamine modified graphene nanoplatelets. Composites Part A: Applied Science and Manufacturing, 117, 134–143.

2ND ENERGY SECURITY AND CHEMICAL ENGINEERING CONGRESS 2021
*"Sustainable Technological Solution for a Better World"*
VIRTUAL CONFERENCE | 3-5 NOVEMBER 2021

**ADVANCED MATERIAL**

**Paper ID: ESCE141**

# NUTRIENTS RELEASE EVALUATION ON THE NPK FERTILIZER COATED BY CARBON MICROSPHERES SUPERABSORBENT POLYMER

**N. Che Ani[1], S. Ghazali[1], C. T. Ahmed Khan[2], H.-J. Kim[2], S.S. Jamari[1]***

[1] *Faculty of Chemical and Process Engineering Technology, College of Engineering Technology, Universiti Malaysia Pahang, 26300, Kuantan, Pahang, Malaysia.*
[2] *Lab. of Adhesion & Bio-Composites, Program in Environmental Materials Science, Research Institute of Agriculture and Life Sciences, Seoul National University, Seoul 151-921, Republic of Korea.*
*Corresponding author: sshima@ump.edu.my

## Extended Abstract

Nowadays, agricultural sector is moving towards good agricultural practices (GAP) to ensure high quality and sustainable production to meet market demands [1]. In agricultural activities, fertilizer and water are essential input materials to boost crop production, resulted in a more sustainable food supply. The implementation of slow release fertilizer in agriculture is quite well known. Among the advantages of slow release fertilizer are that it could develop plant growth and enhance the water retention capacity in soils [2]. These properties can reduce the dewatering system and improve the efficiency of the soil condition so that a higher product yield can be obtained, particularly in arid regions. Slow release fertilizer can reduce the watering cycles, nutrient release capacity, and improve the soil environment [3]. The objective of this work is to evaluate the nutrient released and diffusion behavior of the NPK fertilizer which were coated by carbon microspheres superabsorbent polymer (SCC). The morphology, and chemical structure of the SCC, water absorbency, release behavior and its kinetic parameters in soil were discussed. The works started by synthesizing the carbonaceous microsphere from the natural kenaf fibers using hydrothermal carbonization process. Then, producing the superabsorbent carbonaceous microsphere (SCC) using graft polymerization and then coated the SCC with NPK fertilizer. Finally, the SCC coated NPK fertilizer behavior in terms of the nutrient release and diffusion properties was investigated.

Figure 1 shows the water absorbency data for the SAP and different amount of carbonaceous filler. The maximum water absorbency of ~290 g/g was observed at 2 wt% of carbon microspheres in the polymer. Basically, this vinyl group enhances the crosslinking density, thereby allowing water absorption during the gelation process [4]. At this point, the networks in the SAP were becoming very loosely crosslinked leading to an increase in the porous formation with a flexible structure. This can give a high facility for water molecules to attract to the polymers. As a result, a highly swollen SAP was formed compared to the other samples. The released rate of NPK coated superabsorbent polymer (SAP) was 12% slower than uncoated NPK fertilizer but 24% faster as compared to the NPK coated by SCC. It was also observed that the NPK coated by SCC fitted well with the Korsmeyer-Peppas model as compared to the NPK coated by SAP. In conclusion, the addition of carbon microspheres enhanced the functionality of the superabsorbent polymer and release behavior of the fertilizer solutions.

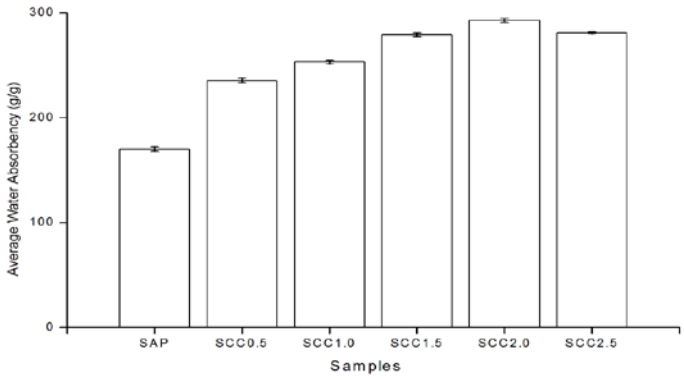


Fig. 1: Effect of water absorbency at different amounts of carbonaceous filler.

**Keywords:** Fertilizer; Water absorbency; Superabsorbent polymer; Carbon microspheres; Release kinetic.

## Acknowledgment

This work was supported by the Ministry of Higher Education Malaysia under the Fundamental Research Grant Scheme [FRGS/1/2014/TK04/UMP/02/7]. Thank also to the Universiti Malaysia Pahang [lab facilities] and National Kenaf and Tobacco Board [raw material].

## References

[1] Leong W-H, Teh S-Y, Hossain M.M., Nadarajaw T., Zabidi-Hussin Z., Chin S.-Y., Lai K.-S., Lim S.-H. E. (2020). Application, monitoring and adverse effects in pesticide use: The importance of reinforcement of Good Agricultural Practices (GAPs), J. Environ. Manage., 260: 109987.

[2] Wu Q., Wang Y.-H., Ding Y.-F., Tao W.-K., Gao S., Li Q.-X., Li W.-W., Liu Z.-H., Li G.-H. (2021). Effects of different types of slow- and controlled-release fertilizers on rice yield, Journal of Integrative Agriculture, 20 (6); 1503-1514.

[3] Salimi M., Motamedi E., Motesharezedeh B., Hosseini H.M., Alikhani H.A. (2020). Starch-g-poly (acrylic acid-co-acrylamide) composites reinforced with natural char nanoparticles toward environmentally benign slow-release urea fertilizers, J. Environ. Chem. Eng., 8 (3); 103765.

[4] Nasution H., Tantra A., and Arista T.P. (2016) the effect of filler content and particle size on the impact strength and water absorption of epoxy/cockleshell powder (*Anadora Granosa*) composite, JEAS. 11:7.

2ND ENERGY SECURITY AND CHEMICAL ENGINEERING CONGRESS 2021
*"Sustainable Technological Solution for a Better World"*
VIRTUAL CONFERENCE | 3-5 NOVEMBER 2021

**ADVANCED MATERIAL**

**Paper ID: ESCE149**

# *Chlorella vulgaris* BLENDING INDUCE THE PERFORMANCE OF CARRAGEENAN BIO-FILMS

**N. A. Othman[1], N. H. Mat Yasin[1], F. Adam[1,2]***

[1] *Faculty of Chemical & Process Engineering Technology,* [2] *Centre of Research in Advanced Fluid & Processes (Fluid Centre), Universiti Malaysia Pahang, 26300 Gambang, Pahang, Malaysia.*
*Corresponding author: fatmawati@ump.edu.my

## Extended Abstract

Microalgae are multicellular species that exist individually or in groups which typically found in freshwater and marine systems and a good and highly potential source to produce bio-films. Bio-films with carrageenan possessed several drawbacks that needed to be encounter including highly hydrophilicity. In this study, *Chlorella vulgaris* (*C. vulgaris*) microalgae was used as another compound to produce bio-films. The purpose of the blending of microalgae in the matrix of carrageenan bio-films was to observe the number of microalgae cell influenced the performance of the bio-film obtained where the higher number of cell produce higher lipid influence higher hydrophobicity of the bio-film. Cultivation of free cell *C. vulgaris* microalgae was conducted in Bold's Basal Medium (BBM) for 16 days. Growth curve of the *C.vulgaris* was observed and lipid extraction was conducted on the alternate days of cultivation. 3 mL of *C. vulgaris* microalgae was added into the formulation of carrageenan at the alternate days of cultivation which is 0, 4, 8, 12, 16 days. Carra-*vulgaris* bio-film was characterized by examining the hydrocolloid properties, tensile strength, thermal properties, moisture content and water contact angle to observe the hydrophobicity of the film. Results shows that, at day 16 of cultivation, the number of cell and percentage oil yield of *C. vulgaris* is the highest hence affect the tensile strength of the bio-film and the solution viscosity with 36.26 Mpa and 245.29 mpa/s, respectively. It also shows the lowest value of moisture content which increases the EAB of the biofilm with 10.99% moisture and 50.24% elasticity. With the high number of cell shows the film has the highest value of water contact angle with 107.11°. This can be concluded that the higher the number of cell and percentage oil yield, the higher the contact angle value, the better surface solid hydrophobicity of the bio-films obtained.

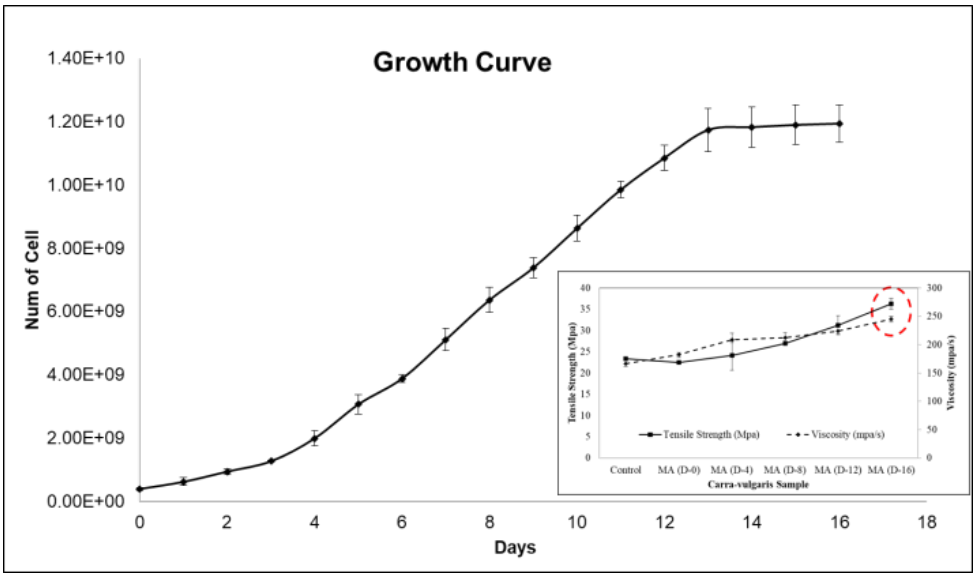


Fig. 1: The growth of the cell number of *C. vulgaris* microalgae influence the tensile strength of the bio-film and the viscosity of the bio-film solution.

**Keywords:** Microalgae Bio-film; Carrageenan; Growth curve; Thermal stability; Hydrophobicity.

**ADVANCED MATERIAL**

## Acknowledgment

This study was supported by Universiti Malaysia Pahang under PGRS scheme (PGRS200353).

## References

[1] Cooler A. S. (1999) Binary Flow Systems. J. Fluid Mech 999:999-996.
[2] Icer D.F., Adams J.A. (1977) Mathematical Elements for Computer Simulation. McGraw Hill, NY.
[3] Nygus, G. (1983) Numerical Analysis Using Finite Element Method. PhD Thesis, NTU Mech. Eng. Dept., Lagos.
[4] Cancer Research UK (2003). Cancer statistics reports for the UK. http://www.cancerresearchuk.org/aboutcancer/statistics/cancerstatsreport/ (accessed 13.03.03).

**ADVANCED MATERIAL**

**Paper ID: ESCE157**

# SYNTHESIS OF GRAPHITE-BASED IMPRINTED POLYMER FOR SELECTIVE REMOVAL OF NITRATE ION FROM AQUEOUS SOLUTION

**Anis Syahirah Ismail[1], Noorhidayah Ishak[1]*, Qasrina Kamarudin[1], Vivian Ewe Shin Hui[1], Nur Bahijah Mustapa[1], Azalina Mohamed Nasir[1]**

[1] *Faculty of Chemical Engineering Technology, University Malaysia Perlis, 02100 Padang Besar, Perlis, Malaysia.*
*Corresponding author: noorhidayah@unimap.edu.my

## Extended Abstract

This study highlighted on the synthesis and characterization of graphite ion imprinted polymer (G-IIP) and its preliminary application through solid phase extraction (SPE) in paddy field wastewater. G-IIP has been developed for selective adsorption with high stability, good selectivity and sensitivity [1] towards target ion at low cost. Surface imprinting technique (SIT) was applied to overcome the drawbacks suffered in the conventional method preparation of molecular imprinted polymer as such bulk polymerization that requires grinding and sieving process to obtain desired particle. This method can destroy the cavity sites thus resulting low binding performance. The combination of ion imprinted polymer (IIP) and modified graphite (G) using SIT gives high selective binding performance and low mass transfer resistance. The binding sites are created near or on the surface of IIP, giving complete removal of template ion [2]. Firstly, graphite was 24unctionalized with silane coupling reagent, 3-methacryloxypropyl trimethoxyilane (MPS) by introducing vinyl group onto the surface of the graphite to obtain vinyl-functionalised graphite (G-MPS). The G-IIP was fabricated using allylthiourea (AT) as a functional monomer, sodium nitrate ($NaNO_3$) as a template molecule, dimethylsulfoxide (DMSO) and acetonitrile (CAN) as the solvents, ethylene glycol dimethacrylate (EGDMA) and 2,2'-azobisisobutyronitrile (AIBN) as the crosslinker and initiator, respectively. A non-imprinted polymer (G-NIP) as a control was synthesized under similar conditions in absence of template molecule. The influence of concentration of G-MPS, functional monomer, Ph, contact time and initial concentration of nitrate ion were analysed. The obtained adsorbent was further characterized using thermogravimetric analysis (TGA), Fourier-transform infrared spectroscopy (FT-IR) and field emission scanning electron microscopy (FESEM). The result shows that the thermal stability of G-IIP was slightly higher than G-NIP. The FTIR was used to study the properties and structure of the adsorbent, verifying that the polymers were successfully formed and the graphite was successfully grafted with the imprinted layer which has the specific affinity for nitrate ions. The G-IIP gives good recognition ability with high adsorption capacity with 252.86 mg/g compared to G-NIP (145.71 mg/g). The adsorption capacity of G-IIP also higher than G-NIP, owning to the tailored specific recognition sites on the G-IIP surface that complementary to the geometry of the target ions. The adsorption kinetic and isotherm model is used to evaluate the efficiency and the mechanism of the adsorption. The adsorption of G-IIP and G-NIP followed pseudo-second order and Freundlich model indicating that chemisorption may be the rate of controlling step and multi-layer adsorption process [3]. The sorption capacity of G-IIP and G-NIP towards nitrate ion also much higher compared to the IIP and NIP in the previous study [4]. A preliminary evaluation of elution step in SPE analysis was performed and resulted ammonia as the suitable eluent. The percent recoveries for nitrate ion removal from paddy field wastewater was 85%. From results above suggested that the fabricated polymer is a potential adsorbent to be applied for the wastewater treatment.

**ADVANCED MATERIAL**

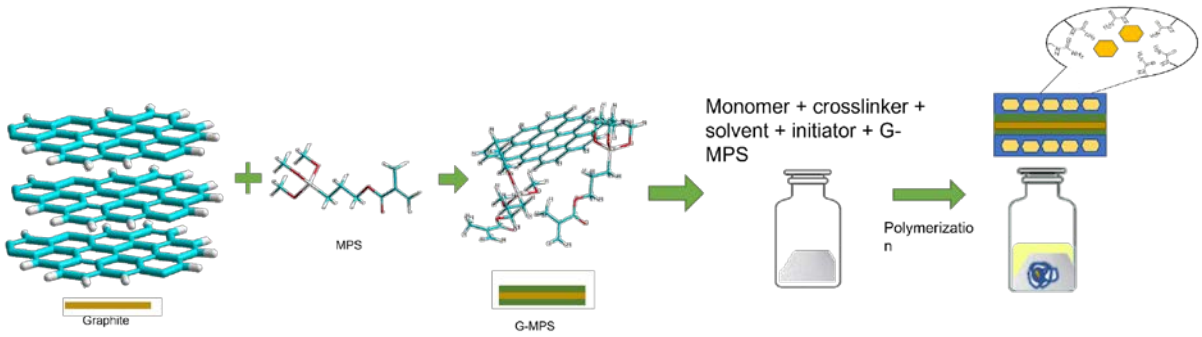


Fig. 1: Schematic diagram of preparation G-IIP.

**Keywords:** Nitrate ion; Ion imprinted polymer; Selective adsorption; Surface imprinting technique.

**Acknowledgment**

The author would like to express gratitude to Faculty of Chemical Engineering Technology, University Malaysia Perlis. Financial support from the Fundamental Research Grant Scheme (FRGS) (FRGS/1/2019/TK05/UNIMAP/03/2) is gratefully acknowledged.

**References**

[1] Branger C., Meouche W., and Margaillan A. (2013) Recent advances on ion-imprinted polymers. Reactive and Functional Polymers 73: 859-875.
[2] Liu Y., Meng X., Liu Z., Meng M., Jiang F., Luo M., Ni L., Qiu J., Liu F., and Zhong G. (2015) Preparation of a Two-Dimensional Ion-Imprinted Polymer Based on a Graphene Oxide/SiO2 Composite for the Selective Adsorption of Nickel Ions. Langmuir 31: 8841-8851.
[3] Kong D., Qiao N., Liu H., Du J., Wang N., Zhou Z., and Ren Z. (2017) Fast and efficient removal of copper using sandwich-like graphene oxide composite imprinted materials. Chemical Engineering Journal 326: 141-150.
[4] Ishak N., Ahmad M., Nasir A., Kamarudin S. F., Islam A. K. M., and Ariffin M. (2017) Theoretical and experimental studies of ion imprinted polymer for nitrate detection. Polymer Science, Series A 59: 649-659.

**ADVANCED MATERIAL**

**Paper ID: ESCE162**

# EFFECT OF RICE HUSK ASH GEL ON THE PROPERTIES OF INTERGRAL MEMBRANE FROM A BLEND OF POLYSULFONE/CHITOSAN/ POLYVINYL ALCOHOL

**N. S. I. Chik[1], N. Z. K. Shaari[1]***

[1] *School of Chemical Engineering, College of Engineering, Universiti Teknologi MARA, 40450 Shah Alam, Selangor, Malaysia.*
*Corresponding author: norinzamiah@uitm.edu.my

## Extended Abstract

Rice Husk Ash (RHA) can produce 85-95% of amorphous silica with burning temperature of 350-750˚C, while crystalline silica is produced when burning temperature is above 800˚C. Due to high content of silica, RHA is utilized in many applications as adsorbents, fillers for membrane and activated carbon. In this research silica gel was extracted from RHA by using acid-leaching process and it was used as cross-linking agent for integral membrane of PSF/CS/PVA. The silica gel was dried and characterized using X-Ray Diffractometer (XRD) and X-Ray Fluorescence (XRF). The silica gel was added at various concentration (0wt%, 0.05wt% and 0.1wt%) into the membrane formulations. The membrane was characterized using Fourier Transform Infrared Spectroscopy (FTIR) the performance was measured through pure water flux (PWF) performance. The result from XRD and XRF showed that 76.85% of silica presence in the gel. The cross linking of membrane was occurred as displayed through the detected Si-O-C bond around 1107cm$^{-1}$ from FTIR analysis. Furthermore, lower water flux portrayed by membrane with RHA gel (MA and MB) as compared to membrane from pure polymer blend showed that membrane has attained the integral stability through the cross-linking process. The concentration of RHA silica gel added also effect the performance of the pure water flux, as MA with 0.1wt% of RHA silica gel showing lower flux compared to MB with 0.05wt% silica gel. Therefore, results showed the potential of silica gel from RHA to be incorporated into membrane formulation to increase the physical properties and performance of the membrane for effective filtration process. This finding shown that the performance of membrane can be further studied with higher silica gel concentration and evaluated for water-oil separation process.

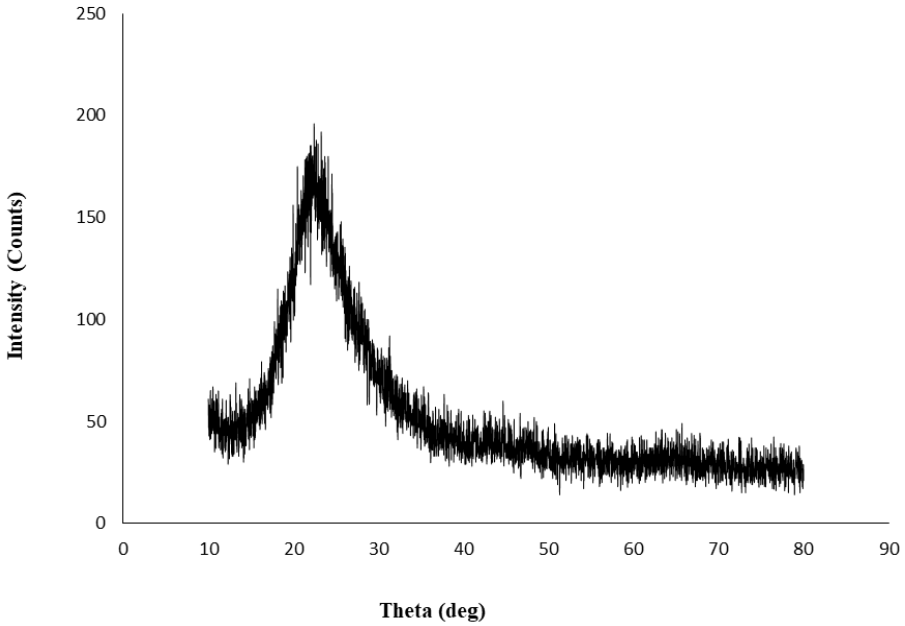


Fig. 1: X-ray Diffraction of silica gel.

**ADVANCED MATERIAL**

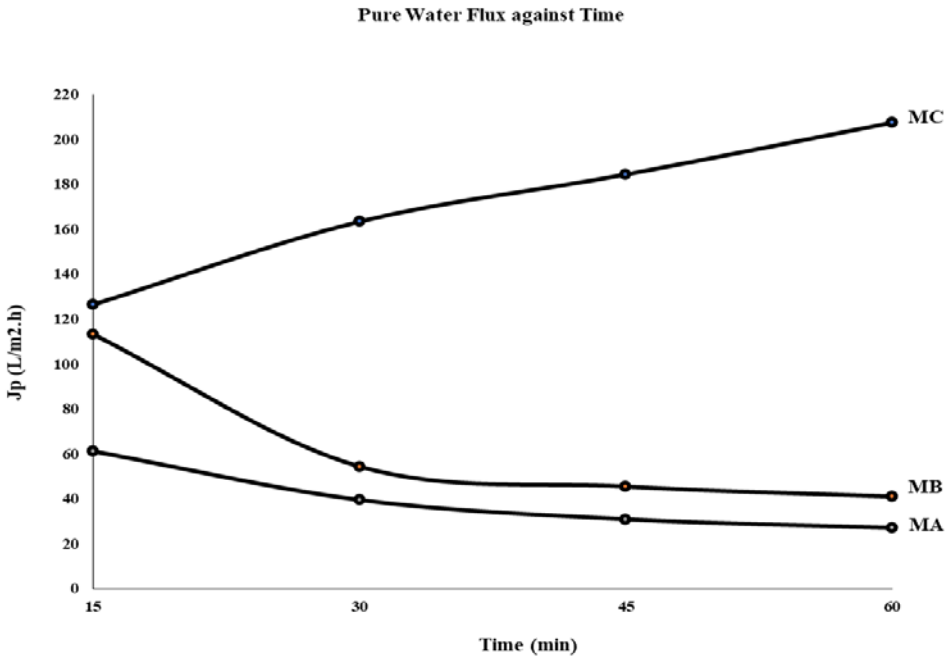


Fig. 2: Pure water flux performance analysis
(MA – 0.1wt% silica gel; MB – 0.05wt% silica gel; MC – 0wt% silica gel).

**Keywords:** Cross-linking; Integral Membrane; Pure Water Flux; Rice Husk Ash; Silica Gel.

## Acknowledgment

The study was supported by Universiti Teknologi MARA (UiTM) through grant with file number 600-RMC/GPK 5/3 (119/2020).

## References

[1] M. Sarangi, S. Bhattacharyya, R. C. Behera. Effect of temperature on morphology and phase transformations of nano-crystalline silica obtained from rice husk. Phase Transitions **82**(5), pp. 377-86 (2009).
[2] V. P. Della, I. Kühn, D. Hotza. Rice husk ash as an alternate source for active silica production. Materials Letters **57**(4), pp. 818-21 (2002).
[3] B. I. Rasoul, F. K. Günzel, M. I. Rafiq. Effect of Rice Husk Ash Properties on the Early Age and Long Term Strength of Mortar. In: Hordijk D., Luković M. (eds) High Tech Concrete: Where Technology and Engineering Meet pp. 207-14 (2018).
[4] S. K. S. Hossain, L. Mathur, A. Bhardwaj, P. K. Roy. A facile route for the preparation of silica foams using rice husk ash. Int J Appl Ceram Technol **16**(3), pp. 1069-77 (2019).

2ND ENERGY SECURITY AND CHEMICAL ENGINEERING CONGRESS 2021
*"Sustainable Technological Solution for a Better World"*
VIRTUAL CONFERENCE | 3-5 NOVEMBER 2021

**ADVANCED MATERIAL**

**Paper ID: ESCE180**

# SYNTHESIS OF MIXED-PHASE MESOPOROUS TITANIA NANOPARTICLES USING DIFFERENT SURFACTANTS FOR PHOTOCATALYTIC DEGRADATION OF 2-CHLOROPHENOL

**N. A. Marfur[1], N. F. Jaafar[1]*, J. Matmin[2]**

[1] *School of Chemical Sciences, Universiti Sains Malaysia, 11800 USM Penang, Malaysia.*
[2] *Department of Chemistry, Faculty of Science, Universiti Teknologi Malaysia, Johor Bahru, Johor, Malaysia.*
*Corresponding author: nurfarhana@usm.my

## Extended Abstract

In this study, mesoporous titania nanoparticles (MTN) were successfully synthesised using different type of surfactants namely cationic (MTN-C), anionic (MTN-A), and nonionic (MTN-NI) via microwave-assisted method. The catalysts were characterised by FTIR, BET, XRD, PL, UV-Vis DRS, TEM, FESEM and XPS. The characterisation outcomes showed that different surfactants influenced the formation of $TiO_2$ phase, surface area, pore sizes, particles size and amount of site defects. Photoactivity of these catalysts were tested upon 2-chlorophenol (2-CP) under visible light irradiation. MTN-A showed the best performance with 85% degradation compared to MTN-C, MTN-NI and pretreated commercial $TiO_2$, Degussa P25 (P25) with 77%, 18% and 62% degradation, respectively. MTN-A showed a remarkable performance due to the presence of anatase and rutile which aided the charge migration. MTN-A also had numerous $Ti^{3+}$ site defects (TSD) and oxygen vacancies (OV) because of its $TiO_2$ mixed-phase structures which could improve the visible light activities. The synergistic effect between the $TiO_2$ mixed-phase, TSD and OV have enhanced the electronic band structure, eased the electron transfer and lowered the electron-hole recombination rate thus boosted the photoactivity of MTN-A. The photocatalytic degradation of 2-CP over MTN-A followed a pseudo-first order kinetics. MTN-A still worked efficiently even at fifth cycle of reaction which determined its stability besides it could degrade other chlorophenol derivatives.

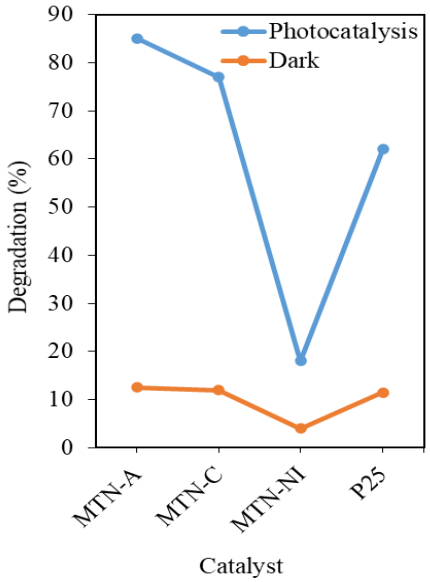


Fig. 1: Photocatalytic performance of MTN-A, MTN-C, MTN-NI and P25 ($C_{2\text{-}CP}$ =70 mg $L^{-1}$, pH=5, W=0.375 g $L^{-1}$, *t*=8 h, T=303 K).

**Keywords:** Surfactant; Mesoporous titania nanoparticles; Microwave-assisted method; Mixed phase; Site defects.

## Acknowledgment

The authors are thankful for the financial support by Ministry of Education Malaysia for Fundamental Research Grant (203.PKIMIA.6711607) and Universiti Sains Malaysia (USM) for Short Term Grant (304/PKIMIA/6315055).

## References

[1] Yuenyongsuwana J., Nithiyakorna N., Sabkirda P., O'Rearc E.A., Pongprayoon T. (2018) Surfactant effect on phase-controlled synthesis and photocatalyst property of $TiO_2$ nanoparticles. Mater. Chem. Phys. 214: 330-336.
[2] Li W., Wu Z., Wang J., Elzatahry A.A., Zhao D. (2014) A perspective on mesoporous $TiO_2$ materials. J. Chem. Mater. 26: 287-298.
[3] Padmanabhan N.T., Jayaraj M.K., John H. (2018) Mechanistic insights into CTAB assisted $TiO_2$ crystal growth with largely exposed high energy crystal facets. J. Environ. Chem. Eng. 6: 5510-5519.
[4] Darkins R., Sushko M.L., Liu J., Duffy D.M. (2013) Adhesion of sodium dodecyl sulfate surfactant monolayers with $TiO_2$ (rutile and anatase) surfaces. Langmuir 29: 11609-11614.
[5] Zhang D., Dong S. (2019) Challenges in band alignment between semiconducting materials: A case of rutile and anatase $TiO_2$, Prog. Nat. Sci.: Mater. Int. 29: 277-284.
[6] Huang C.W., Sin W.C., Nguyen V.H., Wu Y.C., Chen W.Y., Chien A.C. (2020) Solvothermal synthesis of mesoporous $TiO_2$ using sodium dodecyl sulfate for photocatalytic degradation of methylene blue, Top. Catal. 11: 1-10.
[7] Wang X., Li Y., Liu X., Gao S., Huang B., Dai Y. (2015) Preparation of $Ti^{3+}$ self-doped $TiO_2$ nanoparticles and their visible light photocatalytic activity. Chin. J. Catal. 36: 389-399.
[8] Deskins N.R., Rouseau R., Dupuis M. (2011) Distribution of $Ti^{3+}$ surface sites in reduced $TiO_2$. J. Phys. Chem. C 115: 7562-7572.

**ENVIRONMENTAL ENGINEERING**

**Paper ID: ESCE001**

# ANALYZING THE VIABILITY OF CARBON CAPTURE AND STORAGE TECHNOLOGY VIA SWOT-PESTEL ANALYSIS: CASE STUDY IN MALAYSIA

**H. Mohamed Haniffa[1], W. M. B. Wan Muzaffar[1], D. Kemala[1], F. F. N. Ismail[1], W. M. R. Wan Mohd Hanizam[1], N. Abdul Manaf[1]***

[1] *Department of Chemical and Environmental Engineering, Malaysia-Japan International Institute of Technology (MJIIT).*
*Corresponding author: norhuda.kl@utm.my

## Extended Abstract

Malaysia is one of the highest energy-related $CO_2$ emitters among the South-East Asian countries, with the biggest contribution comes from the energy sector. It is predicted that the coal demand would increase more than triple by 2040 consequently overtaking both oil and gas as the premier fuel in Malaysian's energy mix [1-4]. At present, coal and gas contribute approximately 51% and 45% from the total power generation mix in Malaysia while the rest is from hydro [5]. Whereby, coal demand was monopolized by energy generator approximately at 70% while the remaining was utilized by difference types of heavy industries for example steel and cement [6]. This scenario features plausible elevation of fossil fuel-based electricity demand due to the rapid industrialization as well as the population growth.

As the fastest developing country, Malaysia plays significant role in promoting clean energy despite its heavy reliance on conventional fossil-fuel power plant (e.g. coal). Essentially, carbon capture and storage (CCS) technology has been proven to be able in transforming dirty-to-clean energy via integration into the existing coal power plant. This integrated plant is able to reduce coal-power plant emission up to 50-90% [7,8]. Many studies have been conducted to investigate the relevancy and viability of CCS technology for coal-power sector. This includes technical assessment [8-10], economic evaluations [9-10] and policy analyses [10,11]. Their studies indicated positive outcome with regards to the commercial scale-up of CCS retrofitted into coal plant. Nevertheless, quantitative techno-economy-policy studies may not be able to holistically reflect the viability of CCS thus require supported qualitative measurement to predict CCS technology penetration especially in Malaysia. Thus, this work is performed to analyze the viability of CCS technology by conducting SWOT and PESTLE analysis. Subsequently, underpinning the existing techno-economic-policies results by highlighting the aspect of social acceptance and market trends. To the best of author knowledge, there is no systematic SWOT and PESTLE analyses have been conducted pertains to CCS diffusion in Malaysia. While, few was available from other countries such as in Italy [12] and China [13].

SWOT analysis is identified by strengths (S), weaknesses (W), opportunities (O) and threats (T). While, PESTEL analysis reflects by politic (P), economic (E), social (S), technological (T), economic (E) and legal (L). Both analyses are used to assess the viability of CCS deployment specifically in Sarawak, Malaysia. Sarawak is chosen as a case study because of the newly built 600 MW coal power plant located in Mukah. This coal power plant was designed to utilize local coal resources and to provide sustainable source of inexpensive electricity for the community. Therefore, it is of significant to consider the deployment of CCS technology in this area. The SWOT-PESTEL analysis performed in this work will provide descriptive outputs via review of academic and grey literatures. Multiple search engines including Science Direct (Elsevier), Scopus and Wiley Online Library (Wiley) are used to obtain the peer-review literature (academic literature). Whereas, grey literature is attained from the online platform of government/non-government agencies, business and industries.

Tables 1 and 2 shows the outcomes from the SWOT-PESTEL analysis conducted in this study. Through the SWOT analysis, Sarawak's Government is able to prepare strategic options, maximize the strong points and prepare solutions to risks and issues that may arise from the deployment of CCS technology. On the other hand, PESTEL analysis exhibits that it is important to outline information for detailed research and investigation before the CCS operation. Moreover, close collaboration between the stakeholders are needed to build a more sustainable future

of CCS technology in Mukah area.

Table 1: SWOT analysis of CCS plan proposed in Mukah, Sarawak.

| **Strengths** | **Weaknesses** |
|---|---|
| Introduced in 2009, Green Technology Financing Scheme (GTFS) with RM1.5billion funding was provided to support industries in Malaysia to adopt green technologies | High energy penalty which lowers efficiency |
| **Opportunities** | **Threats** |
| Participate in CDM for carbon trading | Perceived risks from community |

Table 2: PESTEL analysis of CCS plan proposed in Mukah, Sarawak.

| *POLITICAL (P)* | *ENVIRONMENT (E)* | *SOCIAL (S)* | *TECHNOLOGICAL (T)* | *ECONOMIC (E)* | *LEGAL (L)* |
|---|---|---|---|---|---|
| • Towards Sarawak Energy Excellence by 2020.<br>• Major support by state government of Sarawak.<br>• Government establish potential sale of electricity to Indonesia.<br>• Lacking policies related to coal mining in Malaysia.<br>• Coal mining industry could generate jobs, reduce dependence on fuel and coal import and increase stimulate the local economy of Sarawak state.<br>• New coal fired plant may cause damaging social ills for the Iban community due to mining activity.<br>• Sarawak Corridor of Renewable Energy (SCORE) was developed to achieve bulk-energy industries and to support Sarawak's digital economy initiatives. | • $CO_2$ capture technology can be reduced gas emission released to the atmosphere.<br>• Land availability and geological suitability are needed to store compressed carbon.<br>• Additional of post combustion capture technology could lead to the increasing of water use.<br>• Post combustion carbon capture may impacts on ozone and cause depreciate on natural resource availability<br>• The implementation of carbon capture technology would potentially effects for long term on environment such as groundwater quality, soil and flora | • Safety aspects where carbon captures new technology could risk human health in long term period.<br>• Increasing awareness of climate change issue in Malaysia<br>• Public acceptance on carbon capture project<br>• Consumer's perception toward implementation of CCS on power plant and new technologies in Malaysia.<br>• The presence of post combustion capture could improve quality of life by providing a job opportunities and new research in this industry. | • The development of CCS technology was starting accepted globally and in Malaysia.<br>• CCS is essential technologies to help achieve the ambition of net zero anthropogenic greenhouse gas emissions by 2050.<br>• Technological development will be a key element of driving future cost reductions in CCS possible for some hard-to abate sectors such as cement, steel and direct air $CO_2$ capture.<br>• CCS can reduce emissions across most industry sectors as a retrofit technology or for existing industrial. | • Coal power plant and mining industry in Mukah, Sarawak provides job creation and sales for Sarawak state.<br>• Encourage and increase an economic activity in the state.<br>• Adopt carbon and climate change policy in term of carbon tax.<br>• Attract more investor in energy supply sector.<br>• Cost of CCS is economies of scale. Higher rates of production will drive lower unit costs.<br>• Additional incentives for CCS technologies such as to have an emissions intensity below a legal limit.<br>• The cost of CCS requires significant energy to regenerate CO2 capture media and to achieve a suitable phase for transport and geological storage. | • Mining and quarrying activities are regulated under the Sarawak Mining Ordinance, 1965, and Natural Resources and Environment Ordinance, 1956<br>• Legal requirement consuming transport and storage of capture $CO_2$.<br>• Guidelines for conducting EIA is needed<br>• Environmental Quality Act Definition for Pollution that could potentially apply to carbon.<br>• Regulatory regime related to storage and transportation under Ministry of Natural Resources and Environment (MNRE).<br>• Strong policy is required to remove barriers and incentivise private sector investment in CCS. |

**Keywords:** SWOT; PESTLE; CCS; Malaysia.

**Acknowledgment**

This study was supported by Ministry of Education (MOE) through Fundamental Research Grant Scheme (FRGS), project no. FRGS/1/2018/TK02/UTM/02/27, vot no. 4F996 and Tier 2, Universiti Teknologi Malaysia, project no. Q.K130000.2643.15J77.

**References**

[1] Green Technology Master Plan Malaysia 2017-2030 (2017). Ministry of Energy Green Technology and Water.
[2] International Energy Agency (2015). Southeast Asia Energy Outlook. World Energy Outlook Special Report.
[3] Oh, T. H. (2010). Carbon capture and storage potential in coal-fired plant in Malaysia—A review. Renewable and Sustainable Energy Reviews, 14(9), 2697-2709.
[4] Amy, T. L. C., (2018). Security of Energy Supply. http://www.parlimen.gov.my (accessed on 07.01.21).
[5] Yee L. H., (2017). Rising cost of electricity generation. https://www.thestar.com.my (accessed on 07.01.21).
[6] Oh, T. H., Pang, S. Y., & Chua, S. C. (2010). Energy policy and alternative energy in Malaysia: issues and challenges for sustainable growth. Renewable and Sustainable Energy Reviews, 14(4), 1241-1252.

## ENVIRONMENTAL ENGINEERING

[7] Garg, B., Haque, N., Cousins, A., Pearson, P., Verheyen, T. V., & Feron, P. H. (2020). Techno-economic evaluation of amine-reclamation technologies and combined CO2/SO2 capture for Australian coal-fired plants. International Journal of Greenhouse Gas Control, 98, 103065.

[8] Manaf, N. A., Qadir, A., & Abbas, A. (2016). Temporal multiscalar decision support framework for flexible operation of carbon capture plants targeting low-carbon management of power plant emissions. Applied Energy, 169, 912-926.

[9] Lee, M. Y., & Hashim, H. (2014). Modelling and optimization of CO2 abatement strategies. Journal of cleaner production, 71, 40-47.

[10] Manaf, N. A. & Abbas, A. (2019). Economic and environmental sustainability of low-carbon power generation: relevancy in the Malaysia Green Technology Master Plan (GTMP). Journal of Chemical Technology & Biotechnology, 94(5), 1425-1432.

[11] Chen, H., Wang, C., & Ye, M. (2016). An uncertainty analysis of subsidy for carbon capture and storage (CCS) retrofitting investment in China's coal power plants using a real-options approach. Journal of Cleaner Production, 137, 200-212.

[12] Fichera, A., Pagano, A., Volpe, R., & Cammarata, L. (2019, December). Understanding the status of the carbon capture and storage technology in Italy: A discussion based on a SWOT analysis. In AIP Conference Proceedings (Vol. 2191, No. 1, p. 020072). AIP Publishing LLC.

[13] Fozer, D., Sziraky, F. Z., Racz, L., Nagy, T., Tarjani, A. J., Toth, A. J., … & Mizsey, P. (2017). Life cycle, PESTLE, and multi-criteria decision analysis of CCS process alternatives. Journal of cleaner production, 147, 75-85.

**ENVIRONMENTAL ENGINEERING**

**Paper ID: ESCE071**

# DESIGN OF A WATER QUALITY MONITORING SYSTEM UTILIZING IOT PLATFORM FOR HYDROPONICS APPLICATION

**H. N. Ang[1], M. W. Lim[1]*, W. S. Chua[2]**

[1] *Centre for Water Research, Faculty of Engineering, Built Environment and Information Technology, SEGi University, 47810 Kota Damansara, Selangor Darul Ehsan, Malaysia.*
[2] *Malaysian Smart Factory 4.0, Selangor Human Resource Development Centre (SHRDC), 40100 Shah Alam, Selangor Darul Ehsan, Malaysia.*
*Corresponding author: limmeewei@segi.edu.my

## Extended Abstract

Hydroponics is defined as the soil-less farming method, that grows plants with the roots suspended in nutrients solution. Since hydroponics cultivation of the plant is through the aqueous nutrient solution, the overall growth efficiency of hydroponic plants is highly dependent on the quality of the water. The water quality of the nutrient solution is mainly determined by the parameters such as potential of Hydrogen (pH), water temperature, and dissolved oxygen [1]. It is crucial to ensure all the water quality parameters are within the optimal range in order to meet the growth requirements of the plant. The water temperature can greatly affect the growth atmosphere for hydroponics system due to the fact that temperature can affect the concentration of dissolved oxygen in the solution. For leafy plant, the optimal temperature is normally controlled at 24 $^{o}$C [2]. On the other hand, the pH of the nutrient solution can greatly affect the nutrient uptake rate by the plant. Hence, it is suggested to maintain the pH in between pH 5 to pH 7 [3]. As for the dissolved oxygen (DO) concentration, Suyantohadi et al (2010) suggested to maintain the DO concentration at 7 – 8 ppm while Goto (1996) suggested that the minimum requirement for DO concentration for leafy plant was 2.1 ppm [4,5].

In order to monitor the parameters mentioned above, conventional monitoring technique is often adopted by farmer. This method however, is inefficient and labour intensive as these parameters must be manually measured periodically to ensure the values are in optimum range. In order to simplify this process, it is important to introduce an IoT based water quality monitoring system in hydroponics system, which would be able to analyse the data continuously, remotely and instant alert users to change in the system. This enables the ease of use and allowing easy access to real time data in one place via Internet. By tracking the real time monitoring data, the trends of the water parameters can be analysed, revealed and predicted. Thus, IoT sensors-based water quality monitoring system can be implemented improve the efficiency of the hydroponics cultivation. However, the implementation of smart hydroponics is challenging due to the lack of knowledge in the application of technology in agriculture. One of the challenges is to build a suitable architecture of the IoT for hydroponics application to measure the properties of the nutrient solution to monitor the growth efficiency of the plant. In this architecture, the processing and storing large quantity of collected data by the sensors has become another challenge as the collected data will become a big data which requires a lot of memory in the computer. Another potential challenge after the design of the water quality monitoring system is to ensure the accuracy of the data in real-time that is not influenced by other external factors such as vibration and electrical noise. Thus, it is important to ensure the sensors are able to closely measure the parameters as well as able to repeat the same readings many times with little variation between values [6,7].

The concept of hydroponics is investigated by using a smart water quality monitoring system to produce lettuce in a controlled environment, free of bugs and other stresses. The primary aim is to design a water quality monitoring system utilizing IoT platform for hydroponics application for the cultivation of *Lactuca sativa*. A smart water quality monitoring system was designed by connecting the desired parameter sensors: water temperature, water pH and water DO concentration sensors to the Arduino, and then the Arduino will send the collected data to the Raspberry Pi 3. The application of Arduino UNO for the interfacing of sensors is due to its effectiveness at reading the sensors data with high rates. On the other hand, the function of the Raspberry Pi 3 is to be used as a data logger and data processor. To facilitate the data processing, the Raspberry Pi 3 is combined with Node-RED programming language to enhance visualization for real time analytics. By using Node-RED, the

**ENVIRONMENTAL ENGINEERING**

collected data would be stored in an InfluxDB database and would be able to be displayed as time-series plot for visualization and analysis purposes using Grafana dashboard. The conceptual visualization of the whole system is summarized in Fig. 1.

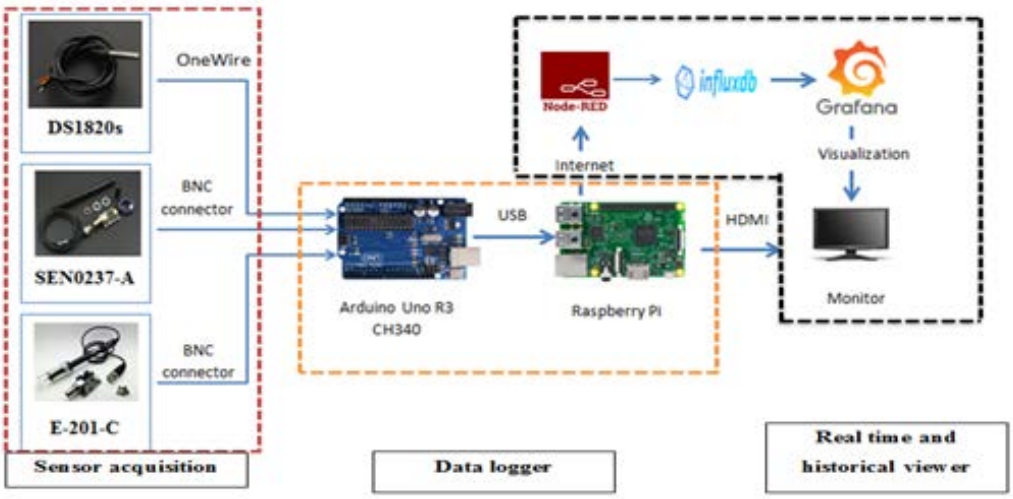


Fig. 1: Schematic diagram of the IOT-based monitoring system.

The water quality monitoring system was applied in a deep-water culture (DWC) hydroponics system for the cultivation of loose leaf lettuce (*Lactuca sativa*). This method ensured that the lettuce was able to grow in a controlled root-zone condition in order to achieve the maximum lettuce growth rate. The DWC system was set up with an air pump to increase the amount of dissolved oxygen in the nutrient water. The container which is used to build to DWC system is 75L. The plants were left to grow uninterrupted continuously for 28 days. During the growth periods, the sampling time of the water temperature, pH and DO were collecting the water parameters was every 5s. These water parameters were monitored remotely through IoT sensors, and the outcome of the data collected averaged per day are presented as per Fig. 2.

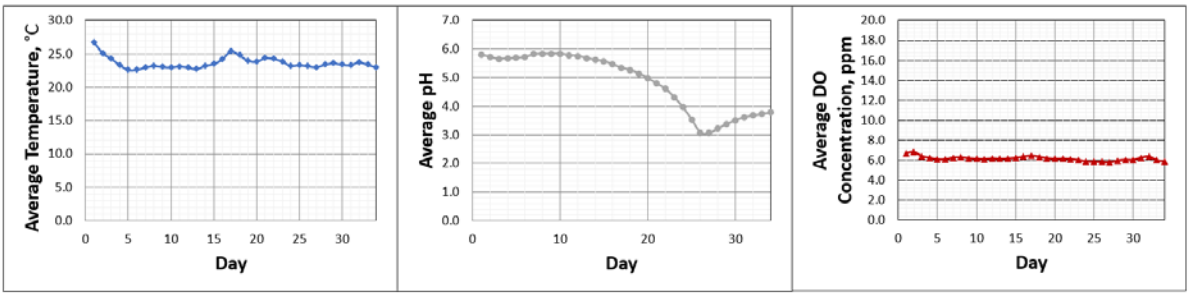


Fig. 2: Water parameters versus time.

Based on the lettuce growth throughout the 28 days, it was found that the water temperature and dissolved oxygen concentration was generally uniform throughout the cultivation of lettuce. In contrast, the pH value significantly decrease from Day 14 onwards below the optimal range to an acidity value of pH 3.0. This could be attributed to the maximum rate of lettuce growth between Day 14 – Day 21 which increases the adsorption of water from the lettuces, resulting in a reduction in the water volume leading to an overall increase in the nutrient concentration. From Day 21 onwards, the rate of growth of the lettuce started to slow down, due to the low pH of the nutrient solution that is detrimental for the nutrient uptake for plant growth. From Day 25 onwards, an upward trend of pH was observed from pH 3 to pH 4. This was attributed to the algae bloom in the nutrient solution which causes the increase in algae respiratory activity and photosynthesis activity. This increased the carbon dioxide released by the algae due to respiration activity, forming carbonic acid when it dissolves in the nutrient solution. At the same time, the photosynthesis activity of the algae will consume carbon dioxide. When the rate of photosynthesis is greater than the rate of respiration, the pH of the solution starts to increase [8].

The outcome from the work above suggests that by monitoring the water quality parameters of the hydroponics system, the trend of the hydroponics cultivation could be observed throughout the plant growth. By being able to detect the minute changes in the water parameters, these would be able to assist the farmers to make corrective action in order to enhance the overall growth efficiency of the plant. Therefore, it can be concluded that the water quality monitoring system utilizing IOT platform for hydroponics application was successfully designed and developed. The system was able to visualize all the historical and real-time data involving three water parameters which are dissolved oxygen concentration, pH as well as temperature remotely without the need for human intervention. This would enable the future development of smart agriculture technologies for increased productivity and efficiency.

**Keywords:** Water quality monitoring; Hydroponics; Internet-of-Things; Precision agriculture; Smart farming.

## Acknowledgment

The authors gratefully acknowledge the support of SEGi University, Malaysia (SEGiIRF/2021-03/FOEBEIT-04/109) and Malaysian Smart Factory 4.0 at Selangor Human Resource Development Centre for providing the research facilities.

## References

[1] Sharma, N., Acharya, S., Kumar, K., Singh, N., & Chaurasia, O. P. (2018). Hydroponics as an advanced technique for vegetable production: An overview. J. Soil Water Conserv. 17: 364-371.
[2] Gent, M. P. N. (2017). Factors affecting relative growth rate of lettuce and spinach in hydroponics in a greenhouse. HortScience 52: 1742–1747.
[3] Roosta, H. R., & Rezaei, I. (2014). Effect of nutrient solution pH on the vegetative and reproductive growth and physiological characteristics of rose cv. 'grand gala' in hydroponic system. J. Plant Nutr 37: 2179–2194.
[4] Suyantohadi, A., Kyoren, T., Hariadi, M., Purnomo, M. H., & Morimoto, T. (2010). Effect of high consentrated dissolved oxygen on the plant growth in a deep hydroponic culture under a low temperature. IFAC Proceedings Volumes (IFAC-PapersOnline), 3 (PART 1).
[5] Goto, E., Both A.J., Albright L.D., Langhans R.W., & Leed A.R. (1996). Effect of Dissolved Oxygen Concentration on Lettuce Growth in Floating Hydroponics. Acta Hort. 440: 205-210.
[6] Mohd Pu'Ad, M. F., Sidek, K. A., & Mel, M. (2019). Portable water quality monitoring system for aquaponics using we MOS. Int. J. Inn. Tech. Exp. Eng 9: 4181–4184.
[7] Ibarra, J. B. G., Caya, M. V. C., Andal, Angelica, J., Soc, M. C. L., Ralph, V. K., Vincent, V. S., & Sauli, Z. (2018). Water quality monitoring system using 3g network. J. Telecommun. Electron. Comput. Eng 10: 15–18.
[8] Wurts, W.A., & Durborow, R.M. (1992). Interactions of pH, Carbon Dioxide, Alkalinity and Hardness in Fish Ponds. Southern Regional Aquaculture Center 464:1–4.

**ENVIRONMENTAL ENGINEERING**

**Paper ID: ESCE077**

# SYNTHESIS AND CHARACTERIZATION OF N-DOPED GRAPHENE OXIDE QUANTUM DOTS/Fe-BDC COMPOSITE FOR METHYLENE BLUE DECOMPOSITION

**Tran Hong Minh[1], Nguyen Xuan Truong[1], Nguyen Ngoc Tue[1], Nguyen Duc Trung[1], Giang Thi Phuong Ly[1], Tran Thuong Quang[1]***

[1] *School of Chemical Engineering, Hanoi University of Science and Technology, 1 Dai Co Viet, Hanoi, Vietnam.*
*Corresponding author: quang.tranthuong@hust.edu.vn

## Extended Abstract

In this paper, we have synthesized a series of NGQ-doped Fe-MOF samples by a facile in situ solvothermal method and investigated the photocatalytic activity of the as-prepared samples. NGQ was prepared via microwave method from Huang *et al* research combined with a methanol washing stage to separate small particles [1]. Pristine *FeBDC* catalyst was prepared by solvothermal method, reported in our previous paper with some modifications [2]. Characteristic features of all as-prepared materials were examined by FTIR, XRD, UV– Vis DRS, $N_2$ adsorption–desorption isotherm, SEM, and TEM. The MB degradation reactions under visible light was conducted to test photocatalytic activity of all samples. The light source was from an OSRAM Mercury lamp 250W through a UV-cutoff filter (420 nm). Dye concentration was investigated by Hatch UV–vis spectrophotometer model DR 3900 with a 1 cm quartz cell.

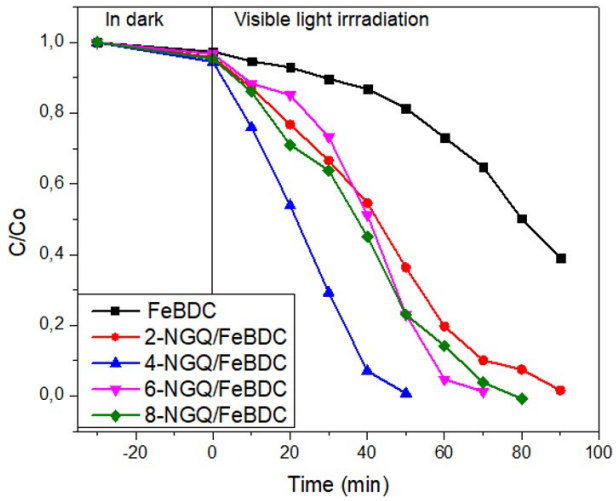


Fig. 1: The effect of NGQ loading amount on MB degradation activity in different conditions (Experimental conditions: MB, 10mg $L^{-1}$; $H_2O_2$, 5 mM; pH 7 and catalyst, 0.2 g $L^{-1}$).

The catalytic performance of pristine *FeBDC* and NGQ/FeBDC samples was evaluated by degradation MB in catalyst-$H_2O_2$-visible light system, and the results were shown in Figure 1. The optimal catalyst was *4-NGQ/FeBDC*, with the doping content of NGQ in NGQ/FeBDC composite was 4%wt. of the precursors. The sample named *4-NGQ/FeBDC* was able to completely decompose MB within 50 minutes, while pristine *FeBDC* could only degrade about 60% of MB. Besides, the results of UV-vis DRS, $N_2$ adsorption–desorption isotherm also indicated that *4-NGQ/FeBDC* have superior optical, band gap energy, and porous properties than the single catalyst *FeBDC*. Finally, 4-NGQ/FeBDC could produce •OH and h+ which played as the contributors to the MB photocatalytic processing.

**ENVIRONMENTAL ENGINEERING**

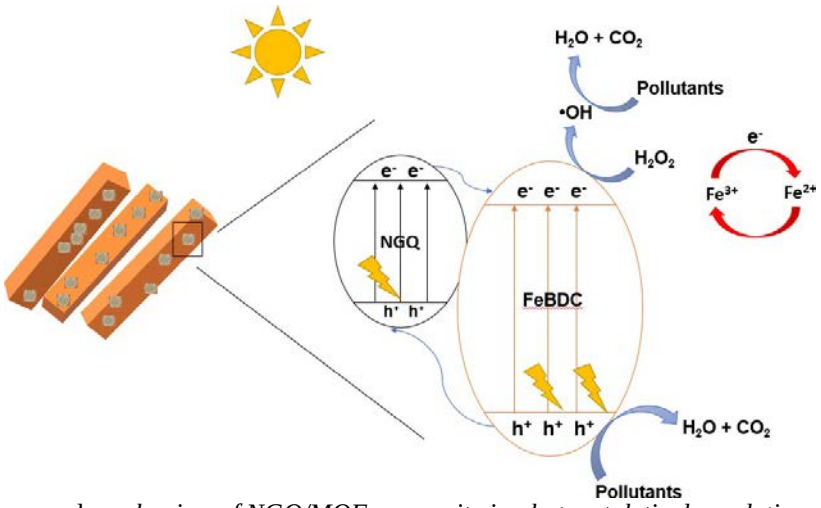


Scheme 1: Proposed m*echanism of NGQ/MOF composite in photocatalytic degradation of pollutants.*

**Keywords:** Graphene quantum dots; Metal organic frameworks; Dye degradation; Fenton reaction.

## Acknowledgment

This study was supported by the International Technology Center Pacific (ITC-PAC)'s program (US-ARMY). This work and paper were made with Government support under Contract No. FA520920P0139 awarded by the International Technology Center Pacific (ITC-PAC).

## References

[1] J. J. Huang, M. Z. Rong, and M. Q. Zhang, "Preparation of graphene oxide and polymer-like quantum dots and their one- and two-photon induced fluorescence properties," *Phys Chem Chem Phys*, vol. 18, no. 6, pp. 4800-6, Feb 14, 2016.
[2] T. T. Quang, N. X. Truong, T. H. Minh, N. N. Tue, and G. T. P. Ly, "Enhanced Photocatalytic Degradation of MB Under Visible Light Using the Modified MIL-53(Fe)," *Topics in Catalysis*, vol. 63, no. 11-14, pp. 1227-1239, 2020.

**ENVIRONMENTAL ENGINEERING**

**Paper ID: ESCE100**

# SYNTHESIS AND STRUCTURAL ELUCIDATION OF CORE-SHELL STRUCTURED BLACK TITANIUM DIOXIDE

**R Nawaz[1,2]*, Y C Ho[3], F K Chong[1,2], M H Isa[4], W H Lim[5]**

[1] *Department of Fundamental and Applied Sciences,* [2] *Centre of Innovative Nanostructures and Nanodevices, Institute of Autonomous system,* [3] *Department of Civil and Environmental Engineering, Universiti Teknologi PETRONAS, 32610 Seri Iskandar, Perak, Malaysia.*
[4] *Department of Civil Engineering, Faculty of Engineering, Universiti Teknologi Brunei, Jalan Tungku Link, Gadong BE1410, Brunei Darussalam.*
[5] *Advanced Oleochemical Technology Division, Malaysia Palm Oil Board, Bandar Baru Bangi, Kajang, Selangor, Malaysia.*
*Corresponding author: rab_17000005@ump.edu.my

## Extended Abstract

CS B-$TiO_2$ is believed to overcome the drawback of $TiO_2$ and drastically enhance photocatalytic performance [1-4]. For instance, Hu et al. [5] reported 81% of methylene blue removal within 150 min of visible light irradiation by CS B-$TiO_2$ synthesized via hydrogen treatment at 500°C. However, the existing methods for the synthesis of CS B-$TiO_2$ use complex procedures, expensive and toxic chemicals, and harsh synthesis condition such as high temperature and pressure [6]. It is desirable to devise a simple and sustainable synthesis method and eliminate the use of toxic, hazardous, and expensive solvents during the production of CS B-$TiO_2$. Moreover, the structure formation has been elucidated for rutile phase of the $TiO_2$ [7] whereas the formation of anatase phase CS B-$TiO_2$ remained under explored. In most cases highly sophisticated analytical instruments have been used to explain the structure of CS B-$TiO_2$. In the current study, the CS B-$TiO_2$ was synthesized by hydrolysis of titanium tetrachloride ($TiCl_4$) in aqueous glycerol and post calcination at a convenient temperature of 300°C for 1h. The properties of the CS B-$TiO_2$ were determined using readily available characterization techniques such as x-ray diffraction (XRD), high resolution transmission electron microscopy (HRTEM) coupled with Fast Fourier Transform (FFT) and 3-dimension (3D) view plots, field emission scanning electron microscopy (FESEM), and photoluminescence spectroscopy (PL). Since, in most cases the performance of the CS B-$TiO_2$ has been investigated for the removal of model organic compounds from synthetic wastewater. Thus, it is also very important to investigate the performance of the CS B-$TiO_2$ for the removal of high concentration of pollutants from real environmental matrices. The photocatalytic activity of the CS B-$TiO_2$ was evaluated for the removal of phenolic compounds from real wastewater matrix. The results demonstrated anatase phase, particle size of 14.30 nm and an amorphous shell with a thickness of 1.5 nm surrounding the crystalline core of the CS B-$TiO_2$.

Interestingly, the Black-$TiO_2$ exhibits an amorphous shell as highlighted in pink colored solid line surrounding the crystalline core at the bottom of 1(a). The amorphous nature of the shell and crystalline nature of the core was confirmed by the Fast Furrier Transform (FFT) amplitude of the HRTEM images as shown in 1(a(i)) and (a(ii)), respectively. The bright dots in the FFT image in Figure 1(a(i)) taken from the inner region of Black-$TiO_2$ as highlighted by a solid red colored rectangular line confirms the crystalline nature of the core. On the other hand, the concentric circle in the FFT image taken from the outer region and highlighted in yellow colored dashed rectangular line shown in 1(a(ii)) indicate the amorphous nature of shell and agrees well with previous works [8]. Compared to Black-$TiO_2$, the bright dots were observed in the FFT images for both inner [Figure 1(b(ii))] and outer region [Figure 1 (b(i))] of White-$TiO_2$ confirms the crystalline nature of the particles. The results suggest that the core-shell structure was induced in the synthesize Black-$TiO_2$ by only the addition of glycerol in the synthesis medium. The nature of the White-$TiO_2$ and Black-$TiO_2$ were further investigated by constructing the 3D view surface plots as shown in Figure 1. The 3D surface plots generated from inner region and outer region of White-$TiO_2$ as shown in Figure 1(b(iv)) and (b(iii)), respectively indicated a well order structure and atomic arrangement in the samples. On the other hand, the 3D surface plots generated from the inner region of Black-$TiO_2$ as displayed in Figure 1(a(iii)) indicated crystalline nature of the core and is consistent with FFT results. The 3D plots constructed from the outer region of Black-$TiO_2$ as shown in 1(a(iv)) revealed the amorphous and disordered nature of the outermost shell of the sample. The incessant loss of interstitial Ti atoms from the $TiO_2$

**ENVIRONMENTAL ENGINEERING**

lattice create the possibility of disrupting the long-range atomic order and forming an amorphous structure. Analyzing the 3D surface plots demonstrated that an amorphous shell and crystalline core framework was synthesized successfully an aqueous glycerol followed by calcination at 300°C.

Most importantly, the electron-hole pair recombination was considerably suppressed in CS B-$TiO_2$ which led to enhanced photocatalytic performance indicated by the 48.17% removal of the initial 224.85 mg/L phenolic compounds within 180 min of visible light irradiation. The study successfully elucidated the structure of anatase phase Black-$TiO_2$ which will help understand its photocatalytic properties for further enhancing visible light photocatalytic activity of the said material for environmental application.

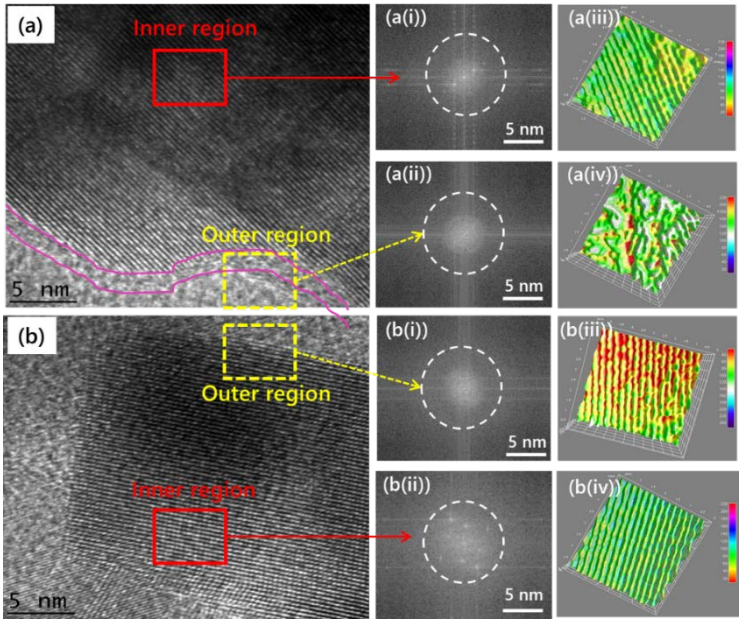


Fig. 1: HRTEM images of (a) Black-$TiO_2$, (b) White-$TiO_2$; FFT images of Black-$TiO_2$ (a(i)) inner region and (a(ii)) outer region; FFT images of White-$TiO_2$ (b(i)) outer region and (b(ii)) inner region; 3D images of Black-$TiO_2$ (a(iii)) inner region and (a(iv)) outer region; and 3D images of White-$TiO_2$ (b(iii)) outer region and (b(iv)) inner region.

**Keywords:** Black-$TiO_2$; Core-shell structure; HRTEM analysis; Phenolic compounds degradation.

## Acknowledgment

The authors would like to thank the Centre of Innovative Nanostructures and Nanodevices (COINN), and Photocatalyst Laboratory at Catalyst Research (CARE) Laboratory in Universiti Teknologi PETRONAS for providing the facilities. Financial support from the Ministry of Higher Education Malaysia (FRGS/1/2020/STG05/UTP/02/2) and from Yayasan Universiti Teknologi PETRONAS (YUTP 015LC0-276) are greatly acknowledged.

## References

[1] H. Hu, Y. Lin and Y. H. Hu, Chemical Engineering Journal **375**, 122029 (2019).
[2] S. Kim, Y. Cho, R. Rhee and J. H. Park, Carbon Energy (2020).
[3] R. Nawaz, C. F. Kait, H. Y. Chia, M. H. Isa and L. W. Huei, Environmental Technology & Innovation, 101007 (2020).
[4] S. J. Babu, V. N. Rao, D. H. K. Murthy, M. Shastri, M. M, M. Shetty, K. S. A. Raju, P. D. Shivaramu, C. S. A. Kumar, M. V. Shankar and D. Rangappa, Ceramics International **47** (10, Part B), 14821-14828 (2021).
[5] H. Hu, Y. Lin and Y. H. Hu, Catalysis Today **341**, 90-95 (2020).
[6] L. Andronic and A. Enesca, Frontiers in Chemistry **8** (2020).
[7] M. Tian, M. Mahjouri-Samani, G. Eres, R. Sachan, M. Yoon, M. F. Chisholm, K. Wang, A. A. Puretzky, C. M. Rouleau and D. B. Geohegan, ACS Nano **9** (10), 10482-10488 (2015).
[8] S. G. Ullattil and P. Periyat, Journal of Materials Chemistry A **4** (16), 5854-5858 (2016).

**ENVIRONMENTAL ENGINEERING**

**Paper ID: ESCE109**

# PARAMETRIC STUDIES ON RADIATION GRAFTING OF TRIPROPYLENE GLYCOL DIACRYLATE ONTO WASTE TIRE DUST

**S. S. M. Shirajuddin[1,2]*, C. T. Ratnam[1], M. M. A. B. Abdullah[2]**

[1] *Radiation Processing Technology, Malaysian Nuclear Agency, Bangi, 43000 Kajang, Selangor, Malaysia.*
[2] *Faculty of Chemical Engineering Technology, Universiti Malaysia Perlis, 01000 Kangar, Perlis, Malaysia.*
*Corresponding author: sitisalwa@nm.gov.my

## Extended Abstract

In recent years, the rate of waste tire disposal has increased dramatically, jeopardizing world ecological equilibrium. Since waste tire dust (WTD) have a crosslinked network structure, its compatibility with most matrices is limited and unsatisfactory. In this study, a surface modification of WTD activated and modified via an electron beam to graft with tripropylene glycol diacrylate (TPGDA) monomer was investigated. This process was carried in conjunction with reaction parameters namely, monomer concentration, absorbed dose, grafting temperature and grafting time on the effect of grafting yield (GY). It was found that GY increased with the increase of absorbed dose, TPGDA monomer concentration, and the grafting temperature. However, a further increase in the grafting reaction time would not affect the GY. The radiation-induced grafting technique used in this study was successful with the maximum GY of 930.06% at an optimum grafting parameter of; 5 w/v% TPGDA concentration, 60 kGy irradiation dose, 3 hours reaction time and 60 ºC reaction temperature. Fourier Transform Infrared Spectroscopy (FTIR) and Scanning Electron Microscopy (SEM) were used to provide evidence for the formation of graft copolymers in the grafting systems. The results of the present study show that radiation-induced grafting (RIG) techniques can be used to prepared grafted WTD successfully.

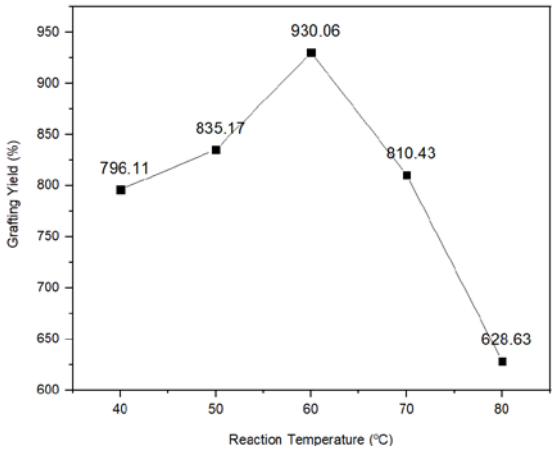


Fig. 1: Effect of reaction temperature on GY
(Absorbed radiation dose: 60 kGy, Monomer concentration: 5 w/v%, Reaction time: 3 hours).

**Keywords**: Waste tire dust; Radiation grafting; Grafting yield; FTIR quantification; Surface modification.

### Acknowledgment

This study was supported by Malaysian Nuclear Agency and Universiti Malaysia Perlis.

### References

[1] Adesina, A. Y., Zainelabdeen, I. H., Dalhat, M. A., Mohammed, A. S., Sorour, A. A., & Al-Badou, F. A. (2020). Influence of micronized waste tire rubber on the mechanical and tribological properties of epoxy composite coatings. Tribology International, 146(January). https://doi.org/10.1016/j.triboint.2020.106244.

## ENVIRONMENTAL ENGINEERING

[2] Alkadi, F., Lee, J., Seok, J., Seok, Y., Hwang, H., & Won, J. (2019). 3D Printing of Ground Tire Rubber Composites. International Journal of Precision Engineering and Manufacturing-Green Technology. https://doi.org/10.1007/s40684-019-00023-6.

[3] Aly, A. M., El-Feky, M. S., Kohail, M., & Nasr, E. S. A. R. (2019). Performance of geopolymer concrete containing recycled rubber. Construction and Building Materials, 207, 136–144. https://doi.org/10.1016/j.conbuildmat.2019.02.121.

[4] Barsbay, M., & Güven, O. (2019). Surface modification of cellulose via conventional and controlled radiation-induced grafting. Radiation Physics and Chemistry, 160(March), 1–8. https://doi.org/10.1016/j.radphyschem.2019.03.002.

2ND ENERGY SECURITY AND CHEMICAL ENGINEERING CONGRESS 2021
*"Sustainable Technological Solution for a Better World"*
VIRTUAL CONFERENCE | 3-5 NOVEMBER 2021

**ENVIRONMENTAL ENGINEERING**

**Paper ID: ESCE153**

# ADSORPTION OF NITRATE IONS TOWARDS CELLULOSE POWDER

**M. M. Chong[1], L. S. Tan[1]*, N. W. C. Jusoh[1], M. Goto[1], T. Tsuji[1], S. Sethupathi[2]**

[1] *Department of Chemical and Environmental Engineering, Malaysia-Japan International Institute Technology, Universiti Teknologi Malaysia, 54000 Kuala Lumpur, Kuala Lumpur, Malaysia.*
[2] *Department of Environmental Engineering, Faculty of Engineering and Green Technology, University Tunku Abdul Rahman, Jalan University, Bandar Barat, 31900 Kampar, Perak, Malaysia.*
*Corresponding author: liansee.tan@utm.my

## Extended Abstract

Nitrate is one of the main ions that contributes to eutrophication condition, which is currently an ongoing issue in the aquaculture industry. If the concentration of nitrate ions exceeds its threshold, it can lead to overproduction of algae and plankton and subsequently lowers the dissolve oxygen and causes eutrophication condition to occur [1]. Adsorption using cellulose has been known to be a suitable option due to the abundance, low cost, and feasibility [2], [3]. To date, the use of cellulose as adsorbent had been well-established in many adsorption field to remove dyes, heavy metals, and ions either individually or mixtures. Most of which reported none to low adsorption occurred during the use of cellulose without any form of modification. In a previous study conducted [4], adsorption of nitrate ions were observed using pure cellulose (i.e. no form of modification). The adsorption of nitrate ions onto cellulose were suspected to be due to the pH of nitrate ion solution and the pH of point of zero charge (pHpzc) of cellulose adsorbent. Here, the pH of point of zero charge refers to the value of pH where the surface of the adsorbent achieved an equivalent amount of negative and positive charges [5]. Therefore, at pHpzc of adsorbent, no adsorption would occur naturally due to the balance charges around the surface. If the pH of solution is lower than the pHpzc of adsorbent, adsorption of anionic would occur whilst pH of solution higher than pHpzc of adsorbent, adsorption of cationic would occur [5]. Nitrate is categorized as anion due to its negative charge, thus, it is desirable to have a pHpzc cellulose which is higher than the nitrate ion solution so that the positively charged cellulose surface can serve as a driving force for the attraction of nitrate anion that leads to the adsorption occurance. In this study, the pHpzc of cellulose would be determined via salt addition method, and the adsorption of nitrate ions is observed. The determination of pHpzc of cellulose was conducted using salt addition method which was slightly altered from Bakatula *et.al* [5]. A weight of 0.15g of cellulose powder was mixed into a 250mL conical flask containing 50mL of 0.01M sodium chloride and stirred continuously for 48 hours in a incubator shaker at 160rpm. The pH of each sample was adjusted from pH 2.0 to 12.0 with an interval of pH 2.0. After 48 hours, the samples were collected and final pH reading of the samples were measured and recorded. The experiment was repeated trice. Batch adsorption experiment was conducted by altering the initial concentration of nitrate anion from 5.0mg/L to 30.0mg/L with 5.0mg/L intervals and the adsorption capacity is calculated. The adsorbent dosage was fixed at 0.3g, temperature at 25°C, and contact time of 30 minutes. The samples were then centrifuged at 4000 rpm for an hour and the concentration of nitrate anion were determined using ultraviolet-visible spectrometry. The batch adsorption experiment was repeated trice. Based on Figure 1, the pHpzc of cellulose adsorbent was detected at pH 6.11±0.16. The adsorption capacity of the nitrate ion towards cellulose increases with increasing initial concentration, which serves as the driving force for the attraction to occur. The highest adsorption capacity obtained was calculated at 3.536mg/g at initial concentration of 30.0mg/L. Hence, this study proves that the adsorption of nitrate ion towards cellulose adsorbent can occur without any form of modification needed, as long as the pH of the nitrate ion solution remains lower than the pHpzc of cellulose adsorbent.

**ENVIRONMENTAL ENGINEERING**

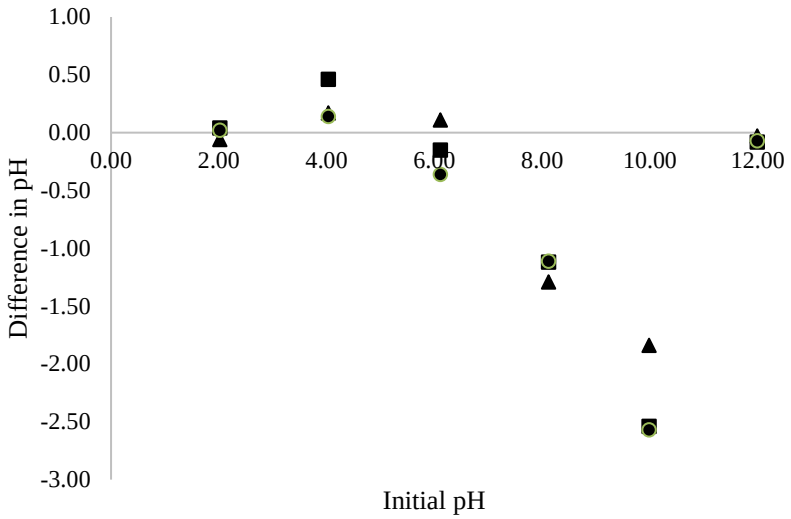


Fig. 1: pH of point of zero charge of cellulose adsorbent using salt addition method. Symbols represent: (■) first experimental run, (▲) second experimental run and (♦) third experimental run.

**Keywords:** Nitrate; Cellulose; Adsorption; pH of point of zero charge.

## Acknowledgment

This study was supported by Long Term Research Grant Scheme (LRGS/1/2018/USM/01/1/2) (UTAR/ 4411-S01) (UTM Ref. No. PY/2020/03532), which is supported by the Ministry of Higher Education Malaysia.

## References

[1] Sulaiman R., Ismail Z., Othman S. Z., Ramli A. H., and Shirazi S. M. (2014) "A comparative study of trends of nitrate, chloride and phosphate concentration levels in selected urban rivers," *Meas. J. Int. Meas. Confed.*, *55*, 74–81, https://doi.org/10.1016/j.measurement.2014.04.035.

[2] Kalaruban M., Loganathan P., Shim W. G., Kandasamy J., Ngo H. H., and Vigneswaran S. (2016) "Enhanced removal of nitrate from water using amine-grafted agricultural wastes," *Sci. Total Environ.*, *565*, 503–510, https://doi.org/10.1016/j.scitotenv.2016.04.194.

[3] Hokkanen S., Repo E., Westholm L. J., Lou S., Sainio T., and Sillanpää M. (2014) "Adsorption of Ni2+, Cd2+, PO43- and NO3- from aqueous solutions by nanostructured microfibrillated cellulose modified with carbonated hydroxyapatite," *Chem. Eng. J.*, *252*, 64–74, https://doi.org/10.1016/j.cej.2014.04.101.

[4] Chong M. M., Tan L. S., Jusoh N. W. C., Goto M., and Tsuji T. (2021) "Natural Cellulosic Adsorbent for Recovery of Nitrate from Aquaculture Effluent," in *IOP Conference Series: Materials Science and Engineering*, *1051*, Article 012063, https://doi.org/10.1088/1757-899x/1051/1/012063.

[5] Bakatula E. N., Richard D., Neculita C. M., and Zagury G. J. (2018) "Determination of point of zero charge of natural organic materials," *Environ. Sci. Pollut. Res.*, *25* (8), 7823–7833, https://doi.org/10.1007/s11356-017-1115-7.

2ND ENERGY SECURITY AND CHEMICAL ENGINEERING CONGRESS 2021
*"Sustainable Technological Solution for a Better World"*
VIRTUAL CONFERENCE | 3-5 NOVEMBER 2021

**ENVIRONMENTAL ENGINEERING**

**Paper ID: ESCE165**

# MICROBIAL TREATMENT OF WATER IN TUBE WELLS FOR IMPROVED WATER QUALITY

**N. A. Husain[1], D. N. A. Zaidel[2]*, A. A. Rahim[3], A. S. M. Kassim[4]**

[1] *School of Chemical & Energy Engineering, Faculty of Engineering,* [2] *Institute of Bioproduct Development, Universiti Teknologi Malaysia, 81310 Johor Bahru, Johor, Malaysia.*
[3] *Faculty of Bioengineering & Technology, Universiti Malaysia Kelantan, 17600 Jeli, Kelantan, Malaysia.*
[4] *Faculty of Engineering Technology, Universiti Tun Hussein Onn Malaysia, 84500 Pagoh, Johor, Malaysia.*
*Corresponding author: dnorulfairuz@utm.my

## Extended Abstract

Groundwater is water found below the earth's surface in spaces between rock and soil. Groundwater supplies water to wells and springs and is an important source of water for public water systems and private wells. Groundwater sometimes contains naturally present germs and harmful chemicals from the environment, such as arsenic and radon [1]. There are many factors that can contaminate the quality of groundwater for instance human activities including incorrect use of fertilizers and pesticides, poorly situated or maintained septic systems, improper removal or storage of wastes and many more. This contamination may lead to outbreak of disease. Several methods such as chlorination and filtration have been introduced for water treatment in the tube wells. However, these methods can be a very dangerous and contains toxic substances such as chlorine which can cause throat swelling and water filling in the lungs. Microbial treatment (MT) is a biological treatment that is produced by fermentation process using banana peel, milk, rice water, rice bran and red soil. The main natural source of agricultural residue is banana peel in production of microbial treatment due to the banana peels contain of nitrogen atoms, sulfur and organic matter such as carboxylic acids [2], which can bind the metals in water. Banana also contained several biochemical components, including cellulose, hemicellulose, chlorophyll pigment and pectin that contains galacturonic acid, arabinose, galactose and rhamnose. These components are good as water purifier. Galacturonic acid is a functional group of carboxyl sugars that bind metal ion in water. Cellulose also has the ability to bind the heavy metals in water [3]. MT is produced in solid form that is suitable to put at the bottom of tube well and it will act slowly from the bottom of the water to break down organic molecules such as waste, mud, heavy metals and so on. MT can treat water to produce high quality of water. It can block and kill the bad bacteria in water, increase dissolved oxygen (DO), stabilize pH, reduce flies and smell disorders, reduce biological oxygen demand (BOD) readings, reduce gas of hydrogen sulphate and reduce the level of organic matter in water.

This study aimed to investigate the effectiveness of using microbial treatment (MT) in improving water quality in tube wells for allowing more clean water to be supplied to the communities. The location of tube well resources for this study was located at Kampung Jeli, Kelantan and the water samples from the tube wells were taken to the laboratory for treatment and the quality level was analyzed for the turbidity, total dissolve solid (TDS), pH, presence of *Escherichia coli* and total coliform.

Fermentation of banana peels with rice water, milk and brown sugar at different ratios was performed to obtain three different microbe solutions (MS1, MS2 and MS3). Two solutions of microbial treatment (MT2 and MT3) were produced at different composition of MS1, MS2 and MS3. The presence of lactic acid bacteria in the MT2 and MT3 was analyzed using morphological test and gram staining method. Water samples from three tube wells, designated as station 1, station 2, and station 3 were taken to the laboratory for treatment using two microbial treatments (MT2 and MT3). Quality of the untreated samples and treated water were analyzed for the turbidity, total dissolve solid (TDS), pH, presence *E. coli* and total coliform.

The quality of untreated water was analyzed where turbidity value for the untreated water from all three stations exceeded the drinking water quality standard of 5 NTU. The turbidity value at station 1 was 5.65 NTU, station 2 was 5.32 NTU, and 6.96 NTU at station 3. pH level for the untreated water of all three stations was in the range of drinking water quality standards between 6.5-9.0. TDS levels of untreated water at the stations vary from 33.42mg/L to 40.31mg/L, which were below the level for drinking water quality standards. *E. coli* and total

coliform were also detected in the all the untreated samples. Results in Table 1 shows the effect of different treatment (MT2 and MT3) on the water samples from the three tube wells. After the treatment with MT2 and MT3, the values of pH, turbidity and TDS were reduced for the treated water samples. While the presence of *E. coli* and total coliform were also reduced (not detected) in most samples. It can be seen that the results of treated water were within the appropriate range for drinking water standards, with the exception of water sample from Station 1, where turbidity for treated water by MT2 exceeded the standard drinking water. It could be concluded that MT3 was effective in reducing turbidity, TDS, *E. coli*, total coliform. MT3 is more successful in enhancing water quality than MT2 because MT3 contains more lactic acid bacteria (Fig. 1). The total amount of lactic acid in microbe treatment are significant indicators for improving water quality. This microbial treatment method is economical, safe, environmental friendly and costs savings that is worthwhile to use as water treatment in the tube wells.

Table 1: Result of water quality from three tube wells after treatment with MT2 and MT3.

| **STATION 1** | | | | | | | | | | |
|---|---|---|---|---|---|---|---|---|---|---|
| | MT2 | | | | | MT3 | | | | |
| No. of sample | pH | Turbidity | TDS | *E. coli* | Total coliform | pH | Turbidity | TDS | *E. coli* | Total coliform |
| 1 | 7.61 | 5.32 | 35.40 | ND | Detected | 7.30 | 4.93 | 35.41 | ND | ND |
| 2 | 7.75 | 5.21 | 36.71 | Detected | ND | 7.42 | 4.91 | 36.04 | Detected | Detected |
| 3 | 7.50 | 5.11 | 35.91 | ND | Detected | 7.16 | 5.01 | 34.91 | ND | ND |
| 4 | 7.62 | 5.07 | 36.11 | ND | Detected | 7.52 | 4.87 | 36.22 | ND | ND |
| Mean | 7.62 | 5.18 | 36.03 | - | - | 7.35 | 4.93 | 35.65 | - | - |
| **STATION 2** | | | | | | | | | | |
| 1 | 6.65 | 3.05 | 37.40 | ND | Detected | 7.30 | 2.04 | 31.20 | ND | ND |
| 2 | 6.73 | 3.13 | 38.62 | Detected | ND | 7.21 | 2.32 | 30.11 | ND | Detected |
| 3 | 6.51 | 3.15 | 37.20 | ND | ND | 7.30 | 2.06 | 31.15 | ND | ND |
| 4 | 6.82 | 3.25 | 37.55 | ND | ND | 7.25 | 2.15 | 31.85 | ND | ND |
| Mean | 6.68 | 3.15 | 37.70 | - | - | 7.27 | 2.14 | 31.11 | - | - |
| **STATION 3** | | | | | | | | | | |
| 1 | 7.29 | 3.26 | 26.00 | ND | Detected | 7.07 | 3.06 | 26.00 | ND | Detected |
| 2 | 7.15 | 3.25 | 26.71 | Detected | ND | 7.12 | 3.10 | 26.50 | ND | ND |
| 3 | 7.24 | 3.31 | 26.52 | ND | ND | 7.01 | 3.01 | 26.00 | ND | Detected |
| 4 | 7.02 | 3.22 | 26.41 | ND | Detected | 7.05 | 2.98 | 26.41 | Detected | ND |
| Mean | 7.18 | 3.26 | 26.41 | - | - | 7.06 | 3.04 | 26.22 | - | - |

Note: ND = not detected

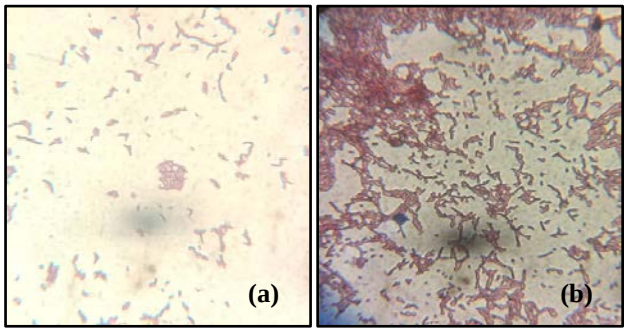


Fig 1: Presence of lactic acid bacteria in (a) MT2 and (b) MT3 from morphological analysis

**Keywords:** Microbial treatment; Water quality; Groundwater; Tube well.

**Acknowledgment**

This study was supported by Fundamental Research Grant Scheme (R.J130000.7851.4F993).

**ENVIRONMENTAL ENGINEERING**

## References

[1] Shankar, S., Shanker, U., Shikha. (2014). Arsenic contamination of groundwater: A review of sources, prevalence, health risks and strategies for mitigation. Scientific World J., Article 304524.
[2] Padam, B. S., Tin, H. S., Chye, F. Y., Abdullah, M. I. (2014). Banana by-products: an under-utilized renewable food biomass with great potential. J. Food Sci. Technol., 51(12), 3527-3545.
[3] Redondo-Gómez, C., Rodríguez Quesada, M., Vallejo Astúa, S., Murillo Zamora, J. P., Lopretti, M., & Vega-Baudrit, J. R. (2020). Biorefinery of Biomass of Agro-Industrial Banana Waste to Obtain High-Value Biopolymers. Molecules, 25(17), 3829.

2ND ENERGY SECURITY AND CHEMICAL ENGINEERING CONGRESS 2021
*"Sustainable Technological Solution for a Better World"*
VIRTUAL CONFERENCE | 3-5 NOVEMBER 2021

**ENVIRONMENTAL ENGINEERING**

**Paper ID: ESCE186**

# INFLUENCE OF PH AND BENZO[A]PYRENE CONCENTRATION ON GROWTH OF BACTERIA - FUNGUS

**N. A. Ismail[1], N. Kasmuri[1]*, N. Hamzah[1], M. F. Miskon[2], and N. H. Ramli[3]**

[1] *School of Civil Engineering, College of Engineering, Universiti Teknologi MARA, 40450, Selangor, Malaysia.*
[2] *Institute of Oceanography and Maritime Studies (INOCEM), Kulliyyah of Science, International Islamic University Malaysia, Bandar Indera Mahkota, 25200 Kuantan, Pahang Malaysia.*
[3] *Fakulti Teknologi Kejuruteraan Kimia dan Proses, Universiti Malaysia, 26300 Kuantan, Pahang, Malaysia.*
*Corresponding author: norhafezahkasmuri@uitm.edu.my

## Extended Abstract

The bioremediation method has been widely used in wastewater treatment. The fungi and bacteria have been recognized as useful bioremediation agents. It has been noticed that polycyclic aromatic hydrocarbons (PAHs) have been detected in the wastewater. Thus, removing these pollutants needs to be performed to reduce the damage to the surrounding environment. The benzo [a]pyrene, one of the most carcinogenic PAHs, was used in this study, degraded by *Sphingobacterium spiritovorum* and *Aspergillus brasiliensis*. Here, the batch culture experiment has been executed to evaluate the optimum pH and benzo [a]pyrene concentration towards the bacteria and fungus growth. Later, the statistical method of response surface methodology (RSM) was performed to fit the experimental results with the study's parameters. From the experimental results, the optimum conditions were at pH 6 and 40 ppm benzo[a]pyrene concentration, which yields the maximum growth of 4.37E+07 CFU/ml bacteria and 0.254 g/l fungi growth, respectively. The percentage removal of benzo[a]pyrene on the batch experiment has been obtained as 38.98% under bacteria consumption and 44.14% removal by fungi bioremediation process. In comparing with RSM, the optimum conditions evaluated from the model were found to be at pH 6.5 and 38 ppm benzo[a]pyrene concentration. It showed a minor gap between the experimental and model analysis for the optimization result. Therefore, it has been denoted that the results for the experimental and statistical models were parallel and can be acceptable. Moreover, the ANOVA for all the models obtained was significant, which showed the reliability of the results. It also can be deduced that the fungi exhibited a better removal percentage of benzo [a]pyrene compared to the bacteria in the wastewater.

**Keywords:** *Aspergillus brasiliensis*; Benzo[a]pyrene; Bioremediation; *Sphingobacterium spiritovorum*; Wastewater.

### INTRODUCTION

Bioremediation is one of the most useful techniques for pollutants removal. Therefore, the investigation on bacteria and fungi remediation has been significant in eliminating the polycyclic aromatic hydrocarbon (PAH). The PAHs have been categorized into two types: high molecular weight (HMW) and low molecular weight (LMW) of PAH. Thus, this research focused on the HMW PAH, which is benzo [a]pyrene. However, it can be presumed that bacteria and fungi in bioremediation would be affected by many environmental factors. These factors can be classified as abiotic and biotic factors (Mohd Kami et al., 2020). All these factors are vital in the bioremediation method as they may lead to the retardation of the process. Thus, the optimization studies to these factors need to be performed to obtain the optimum condition for maximum PAH degradation. Hence, this analysis aims to determine the abiotic factors: the optimum pH and pollutant concentration, which is benzo [a]pyrene (Abatenh et al., 2017). Following the experimental results, the interaction on bacteria–fungi growth on the selected parameters have been interpreted in response surface methodology (RSM) by Design Expert 7.0 software. Therefore, ANOVA analysis has significantly evaluated the optimum condition and the influence of the parameters regarding the pH and initial concentration of benzo [a]pyrene.

### METHODS

*Sphingobacterium spiritovorum* has been chosen as the bacteria strain for this research study. This strain was isolated from municipal sludge (Othman et al., 2009). The bacterium was sub-cultured to obtain the active bacteria for a further experiment (Ismail et al. 2020). A single colony of bacteria was taken and put into a centrifuge tube

with 25 ml nutrient broth (NB, OXOID Thermo Fisher Scientific). This centrifuge tube was placed in the mechanical shaker with a temperature of 30ºC and 150 rpm agitation for two days. Later, the bacteria were centrifuged, and the pellet was then suspended in the wastewater. After that, the bacteria can be used for the following experiments. In addition, the fungus used in this analysis was purchased from BioFocus (M) Sdn Bhd, *Aspergillus brasiliensis* ATCC 16404. Concurrently, the fungal spores from the potato dextrose agar (PDA) medium (OXOID Thermo Fisher Scientific) were scraped and put into the 10 ml phosphate-buffered saline. After that, the petri dish containing PDA medium was prepared and autoclave (Black, 2020). Later, the 6ul of the spore suspension was streaked onto the middle of the petri dish containing the PDA medium for the growth development of the fungi (Ismail et al., 2020). This streak plate was placed in the oven at a temperature of 30ºC (Al- Dossary et al., 2020). The fungal mycelium was then formed from the observation, and this part of mycelium was used for further experiment. For the optimization experiments, the flasks with 50 ml wastewater were prepared, and the pH was controlled by adding the 0.1 M hydrochloric acid (HCl) and 0.1 M sodium hydroxide solution (NaOH) (Vural et al., 2019). The pH used were 4, 6 and 8. Then, the benzo[a]pyrene initial concentrations were added according to the concentration set, which was 10ppm, 20ppm and 40ppm. For the bacteria growth, the plate count method was used to obtain the growth curve of the bacteria after the experiments (Sanders, 2012). The colonies formed on the agar plates were counted and expressed as colony-forming units per mL of culture (CFU/ml) (Mohd-Kami, 2020). Meanwhile, the fungus growth was obtained by filtering and weighing the mycelium fungus to establish the fungus growth trend (Lappa et al., 2015). Furthermore, for the degradation result of PAH, the samples were extracted using liquid-liquid extraction (LLE) to obtain the benzo[a]pyrene concentration after seven days of incubations (Haneef et al., 2020). The sample was placed into the vials following the extraction method to evaluate the percentage removal using high-performance liquid chromatography (HPLC) (Beyene et al., 2019). The results were obtained by assessing the peak area of HPLC results. Next, statistical analysis of RSM was used to interpret the relationship between the bacteria - fungi growth and selected variables of pH and benzo [a]pyrene concentration.

## RESULT AND DISCUSSION

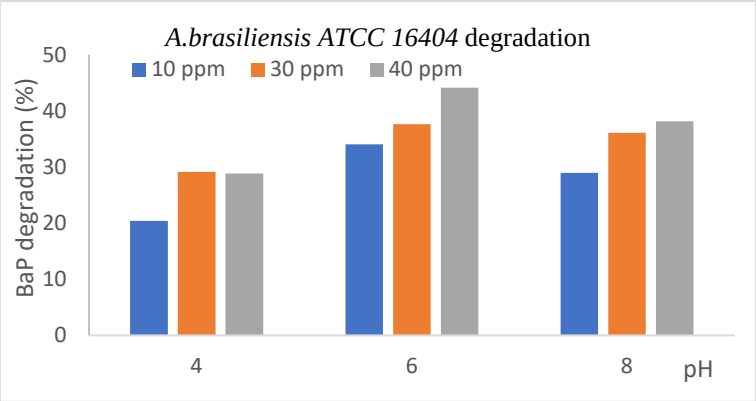


Fig. 1: The effect of pH and benzo [a]pyrene concentration to the benzo [a]pyrene degradation.

Figure 1 showed the pH and benzo [a]pyrene concentration on the benzo[a]pyrene percentage removal by the *Aspergillus brasiliensis*. Based on Figure 1, the maximum degradation of benzo (a)pyrene was found to be at pH 6 with 40 ppm benzo[a]pyrene concentration with a 44.14% removal rate. From the previous study of Agrawal et al. (2018), the maximum degradation of phenanthrene and pyrene at pH 6 was 99.65% and 99.58% percentage removal, respectively. Ganoderma lucidum fungi utilized the degradation of phenanthrene and pyrene. The increase of phenanthrene and pyrene removal was due to the high biomass concentration in both media. In addition, the study done by Agrawal and Shahi (2017) degraded the pyrene using C*oriolopsis byrsina* fungi. It can be observed that the optimum pH for pyrene degradation was at pH 6. It is parallel with this research study which showed that variable types of fungi produced the same preferable condition for the growth development.

**Acknowledgment**

This study was supported by Universiti Teknologi Mara (UiTM) for the IIUM-UMP-UiTM Sustainable Research Collaboration Grant (600-RMC/SRC/5/3 (051/2020)) and Fundamental Research Grant Scheme (FRGS) (600-IRMI/FRGS 5/3 (334/2019)) under Ministry of Higher Education (MOHE) for financially supporting this study and providing the resources.

## ENVIRONMENTAL ENGINEERING

### References

[1] Mohd Kami, N.A.F., Tao, W., Hamzah, N. (2020). Establishing the order of importance factor based on optimization of conditions in PAHs biodegradation. Polycyclic Aromatic Compounds.
[2] Abatenh, E., Gizaw, B., Tsegaye, Z., Wassie, M. (2017). The Role of Microorganisms in Bioremediation- A Review. Open J Environ Biol 2(1): 038-046.
[3] Othman, N., Tun, U., Onn, H., Hussain, N., Karim, A.A., Tun, U., Onn, H. (2009).
[4] Ismail, N.A., Hamzah, N., Kasmuri, N., Jaafar, J., Ali, M.F., Khalil, K.A., Singhal, N. (2020). Optimization and interaction analysis of bacterial and fungal growth in the presence of benzo (a)pyrene in wastewater. IOP Conf. Series: Earth and Environ. Sci.
[5] Black W.D. (2020). A comparison of several media types and basic techniques used to assess outdoor airborne fungi in Melbourne, Australia. PLoS ONE 15(12): e0238901.
[6] Al-Dossary M.A., Abood S.A., Al-Saad H.T. (2020). Factors affecting polycyclic aromatic hydrocarbon biodegradation by *Aspergillus flavus*. Remediation.
[7] Vural C., Vural C., Ozdemir G. (2019). Monitoring of the degradation of aromatic hydrocarbons by bio augmented activated sludge. J Chem Technol Biotechnol.
[8] Sanders E.R. (2012). Aseptic laboratory techniques: plating methods. Journal of visualized experiments: JoVE, (63), e3064.
[9] Lappa I., Kizis D., Natskoulis P., Panagou E. (2015). Comparative study of growth responses and screening of inter-specific OTA production kinetics by *A. carbonarius* isolated from grapes. Front Microbiol.
[10] Haneef, T., Ul Mustafa, M.R., Wan Yusof, K., Isa, M.H., Bashir, M.J.K., Ahmad, M., Zafar, M. (2020). Removal of polycyclic aromatic hydrocarbons (PAHs) from produced water by ferrate (VI) oxidation. Water.
[11] Beyene A.M., Du X., Schrunk D.E., Ensley S., Rumbeiha W.K. (2015). High-performance liquid chromatography and Enzyme-Linked Immunosorbent Assay techniques for detection and quantification of aflatoxin B1 in feed samples: a comparative study. BMC Res Notes 12, 492.
[12] Agrawal, N., Verma, P., Shahi, S.K. (2018). Degradation of polycyclic aromatic hydrocarbons (phenanthrene and pyrene) by the ligninolytic fungi *Ganoderma lucidum* isolated from the hardwood stump. Bioresour Bioprocess.
[13] Agrawal, N., Shahi, S.K. (2017). Degradation of polycyclic aromatic hydrocarbon (pyrene) using novel fungal strain *Coriolopsis byrsina* strain APC5. Int Biodeter Biodegr.

**ENVIRONMENTAL ENGINEERING**

**Paper ID: ESCE198**

# THE EFFECTS OF ADDITIVES TOWARDS THE PARTICULATE SIZE DISTRIBUTION FROM PALM FIBER AND SHELL COMBUSTION

**M. Afiq Daniel Azmi[1]*, Z. Zahiruddin[1], S. Shahidana[1], J. NorRuwaida[1], Abd Halim Md Ali[1], M. Dewika[2], M. P. Khairunnisa[1], M. Rashid[1], M. R. Ammar[3]**

[1] *Air Resources Laboratory, Malaysia-Japan International Institute of Technology, 54100 UTM Kuala Lumpur, Malaysia.*
[2] *Centre of American Education, Sunway University, Bandar Sunway, 47500 Selangor, Malaysia.*
[3] *AMR Environmental Sdn Bhd, Taman Sri Pulai Perdana, 81110 Johor Bahru, Malaysia.*
*Corresponding author: madaniel2@graduate.utm.my

## Extended Abstract

Palm oil mill industries in Malaysia utilized their waste such as palm fiber and shell (F&S) as fuel in the boiler to generate energy and electricity. The combustion facility is equipped with air pollution control system to control the particulate emission, but it is proven that the efficiency is low in term of capturing fine particulate emission. The combustion process contributed to the release of various types of elements that tends to react with each other and cause operational and environmental problems. In addition, the formation of particulate matter (PM) released into the ambient air could harm human health and the environment [2][3].

In this regard, this study investigates the effect of additive, which are Kaolin and PreKot$^{TM}$ towards the particulate size distribution from palm F&S combustion. The characteristics of the palm F&S and the additive was evaluated using the proximate and ultimate analysis. Four (4) types of samples with different mixing ratio between the fuel and the additive was used in this study. The ratio was selected based on previous study and also the ratio of palm F&S used in the industry. Each sample consists of 40g of fuel and 8% of the additive. The combustion operating temperature was constantly maintained 800$^{o}$C for 45 minutes. The operating air flow rate and the moist content of the fuel are, 1.24 L/min and below 15%, respectively. After the combustion was completed, the ash generated was collected at the sampling point and the particulate size of the ash was determined using the Particle Size Analyzer (MALVERN, Mastersizer 2000).

Table 1: Indicator for the types of samples used in the experiment.

| **Types of sample** | **Indicators** |
|---|---|
| PFKS | Palm F&S |
| PFKS with 8% of Kaolin | Palm F&S (Kaolin) |
| PFKS with 8% of PreKot$^{TM}$ | Palm F&S (PreKot) |
| PFKS with 4% of Kaolin and 4% PreKot$^{TM}$ | Palm F&S (PreKot & Kaolin) |

The particle size distribution of the ashes from the combustion of palm F&S with the addition of PreKot$^{TM}$ was compared with the addition of a commonly used additive, which is kaolin, an alumina-silica-based additive. Based on Figure 1, the size range of the particulate for the combustion of palm F&S is between 0 to 390µm with the major fraction in between 130 to 190µm. It is also can be depicted that the particulate size distributions graph was shifted to the left when the additives were mixed with the palm F&S. Overall, the particulate size was reduced when the additives were mixed with the palm F&S. The particulate size was greatly reduced with the addition of PreKot$^{TM}$ and kaolin with the highest fraction range in between 35 to 45µm.

Figure 2 depicted the cumulative particulate size distribution of the different samples which shows that mean particulate size at 50µm is varies for all samples. The smallest mean particulate size obtained from the combustion of palm F&S with kaolin (30µm) followed by palm F&S with Prekot$^{TM}$ and kaolin (32µm), palm F&S with Prekot$^{TM}$ (55µm) and palm F&S (70µm). Kaolin is an alumina-silicate-based additive which have a large surface area. In this regard, the sorption of alkali metals can be increases with the presence of kaolin as additive by forming high-temperature stabile compounds. It was proven that it is also helps to reduce the particulate emission release from the combustion process [5]. However, finer particulate size from the combustion will gives impact towards

the collection efficiency of the air pollution arrestor. Further investigation is needed to evaluate the elemental composition of the ashes generated from the combustion of palm F&S with additives.

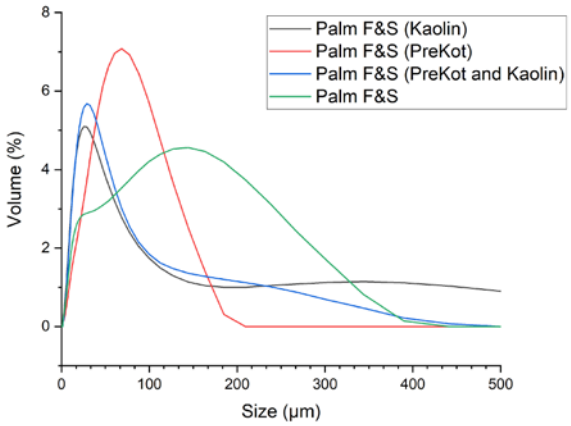


Fig. 1: Particle size distribution of different samples.

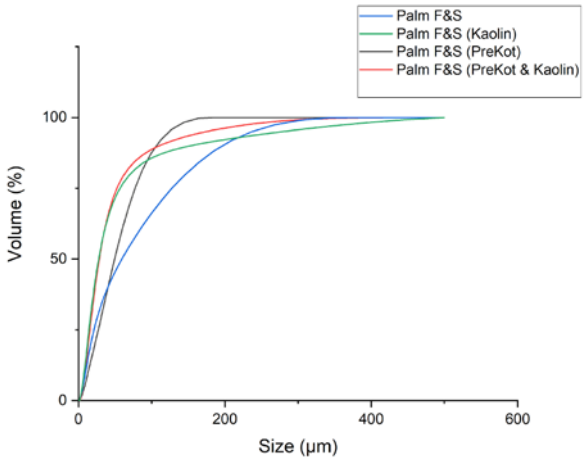


Fig. 2: Cumulative Particle Size Distribution of different samples.

**Keywords:** Palm fiber; Palm shell; Kaolin; PreKot™; Particulate matter.

## Acknowledgment

This research was funded by AUN/SEED-Net-SPRAC (grant number R.K130000.7343.4B614) and JICA grant. The author gratefully acknowledges the financial support from Malaysia - Japan International Institute of Technology (MJIIT), Universiti Teknologi Malaysia for sponsoring his master studies.

## References

[1] C. Gollmer, I. Höfer, and M. Kaltschmitt (2019) "Additives as a fuel-oriented measure to mitigate inorganic particulate matter (PM) emissions during small-scale combustion of solid biofuels," *Biomass Conversion and Biorefinery*, vol. 9, no. 1, pp. 3–20, doi: 10.1007/s13399-018-0352-4.

[2] A. Demirbas, (2004) "Combustion characteristics of different biomass fuels," *Progress in Energy and Combustion Science*, vol. 30, no. 2, pp. 219–230, doi: 10.1016/j.pecs.2003.10.004.

[3] R. Saidur, E. A. Abdelaziz, A. Demirbas, M. S. Hossain, and S. Mekhilef (2011) "A review on biomass as a fuel for boilers," *Renewable and Sustainable Energy Reviews*, vol. 15, no. 5, pp. 2262–2289, doi: 10.1016/j.rser.2011.02.015.

[4] M. Obaidullah, S. Bram, V. K. Verma, and J. de Ruyck, (2012) "A review on particle emissions from small scale biomass combustion," *International Journal of Renewable Energy Research*, vol. 2, no. 1, pp. 147–159, doi: 10.20508/ijrer.15633.

[5] Dragutinovi´c, N.; Höfer, I.; Kaltschmitt, M. Fuel Improvement Measures for Particulate Matter Emission Reduction during Corn Cob Combustion. Energies 2021, 14, 4548. https://doi.org/10.3390/en14154548.

**FINITE ELEMENT ANALYSIS**

**Paper ID: ESCE093**

# FINITE ELEMENT ANALYSIS OF 1-DIMENSION, 2-DIMENSION AXISYMMETRIC AND 3-DIMENSION TRANSIENT REDOX SIMULATION ON A SINGLE ELECTRODE MICRODISK

**H. R. Ramji[1,2*], N. Glandut[2], J. Absi[2], S. F. Lim[1] and A. A. Khan[3]**

[1] *Universiti Malaysia Sarawak (UNIMAS), 94300, Kota Samarahan, Sarawak, Malaysia.*
[2] *Institute for Research on Ceramics (IRCER), UMR 7315, CNRS, University of Limoges, European Ceramics Center, 12 Rue Atlantis, 87068, Limoges, France.*
[3] *School of Chemical & Materials Engineering (SCME), National University of Sciences & Technology (NUST), H-12, Islamabad, Pakistan.*
*Corresponding author: rhrejan@unimas.my

## Extended Abstract

Numerous kinds of literature presented works utilizing FEM in electrochemistry via COMSOL Multiphysics® as a platform. Cutress et al. [1] and Dickinson et al. [2] reported a general overview of the software's capacity to perform numerical work in electrochemistry. There are no shorts of literature presenting works on 3D simulations [3,4]. The software is often used to visualize physical phenomena and justify experimental findings. Few correlations are made on to 1D or 2D models problems or vice-versa. This paper presented a finite element method (FEM) analysis for a transient redox reaction on a single electrode microdisk via commercial software COMSOL Multiphysics®. The developed model is for cyclic voltammetry under semi-infinite spherical diffusion. Mesh refinement with its consequent number of elements (*noe*), computation time ($t_{com}$), and current, $I_{(t)}$ was compared on the 1-dimension (1D), 2-dimension (2D) axisymmetric, and 3-dimension (3D) model. Figure 1 shows the difference between cyclic voltammetry of linear diffusion on 1D and non-linear diffusion on 2D axisymmetric and 3D that were obtained from the simulation. This paper proved the software's consistency to produce less than 3% error between simulation and analytical results across all dimensions. 1D simulation took around 3 minutes to complete, giving less than 0.1% error. While the 2D axisymmetric simulation completed around 10 minutes with 0.5% error. On very fine mesh using a 3D model can yield a simulation with an error of 2.5%. It has the drawback of taking significantly longer $t_{com}$ to complete. A slight discrepancy between 2D axisymmetric and 3D simulation results on finest meshing recorded to have less than 3% difference and that is due to CPU memory limit. This was also proven by Cutress et al. [2] on the general precision of the software on a 3D microdisk model with an error of 18.54%. This was claimed as limitations due to available CPU memory that become a hindrance to achieving desirable granularity. A summary of the highest accuracy results obtained from the simulation are shown in Table 1. Further investigations on complex electrochemistry using this platform are justified and highly recommended.

Table 1: Summary of meshes on $I_p$ and $t_{com}$ for 1D, 2D axisymmetric, and 3D simulation.

| Geometry | Mesh | Max element size (m) | *noe* | $I_p$ (mA) | Percentage error, % | $t_{com}$ (s) |
|---|---|---|---|---|---|---|
| 1D | Extra Fine | 5.37 x 10-5 | 50 | -6.668 | -0.073 | 167 |
| 2D ax | Custom | 3.18 x 10-6 | 2635 | -7.924 | 0.558 | 633 |
| 3D | Custom | 1.27 x 10-5 | 97474 | -8.081 | 2.538 | 225906 |

**FINITE ELEMENT ANALYSIS**

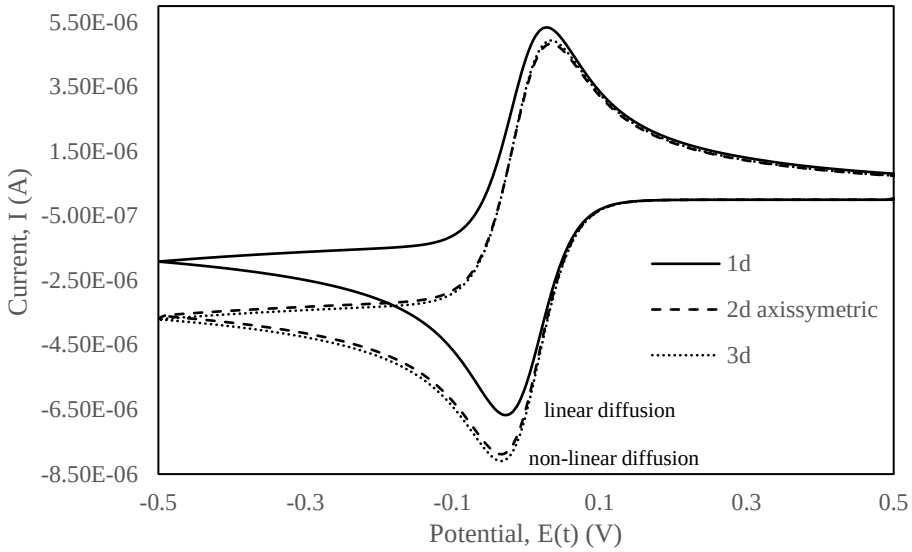


Fig 1: Comparison of current, $I_{(t)}$ vs. potential $E_{(t)}$ of the 1D, 2D axisymmetric, and 3D model on recommended meshing.

References of the article should be included in the extended abstract and numbered consecutively using Arabic numerals in square brackets. The reference list should be in 9 point of Times New Roman, using the format given and justified (see References).

**Keywords:** Finite element method; COMSOL Multiphysics®; Cyclic voltammetry; Mesh refinement.

**Acknowledgment**

This project was funded by Universiti Malaysia Sarawak (UNIMAS) under Postgraduate Student Research Grant (F02/PGRG/1953/2020). The first author would also like to thank the French Ministry for their initial support in this joint program.

**References**

[1] Cutress, I. J., Dickinson, E. J., & Compton, R. G. (2010). Analysis of commercial general engineering finiteelement software in electrochemical simulations. Journal of Electroanalytical Chemistry, 638(1), 76-83.
[2] Dickinson, E. J., Ekström, H., & Fontes, E. (2014). COMSOL Multiphysics®: Finite element software for electrochemical analysis. A mini-review. Electrochemistry Communications, 40, 71-74. 16.
[3] Lakshmi, R. B., Harikrishnan, N. P., & Juliet, A. V. (2017). Comparative analysis of 2D and 3D models of a PEMFC in COMSOL. Applied Surface Science, 418, 99-102.
[4] Li, M. S., Filice, F. P., & Ding, Z. (2016). Determining live-cell topography by scanning electrochemical microscopy. Journal of Electroanalytical Chemistry, 779, 176-186.

**FLUID FLOW**

**Paper ID: ESCE174**

# EXTRUDED AND OVERLAPPED GEOMETRIES OF FEED SPACERS FOR SOLUTION MIXING IN ELECTROCHEMICAL REACTORS AND ELECTRODIALYSIS-RELATED PROCESSES

**S. K. A. Al-Amshawee[1]*, M. S. B. Husain[1], M. Y. B. M. Yunus[1], N. F. M. Azmin[2], O. T. Lekan[3]**

[1] *Faculty of Chemical and Process Engineering Technology,* [2] *Earth Resource and Sustainability Centre (ERAS), Universiti Malaysia Pahang, 26300 Pahang, Malaysia.*
[3] *Department of Biotechnology Engineering, Kulliyyah of Engineering, International Islamic University Malaysia, 53100 Kuala Lumpur, Malaysia.*
[4] *Mechanical Engineering Department, Faculty of Engineering, Universiti Teknologi Petronas, 32610 Perak, Malaysia.*
*Corresponding author: sajjad.hillawi@hotmail.com

## Extended Abstract

Typical stacks of electrically-driven membrane operations are composed of repetitive units that are bonded together, such as electrodialysis-related processes or electrochemical reactors. Permeate spacers, which act as static mixers, are sandwiched at regular intervals between each pair of ion exchange membranes to keep membranes separated, reinforce membranes against feed pressure, and increase flow turbulence. However, inefficient geometry of feed spacers may reduce cell active area, and increase boundary layer effects near the membranes. The purpose of the present research is to discuss the designs of extruded and overlapped channel spacers. The current study is significant because it reveals the fundamental mechanisms that have a considerable impact on spacer-filled channel flow hydrodynamics. Flow behavior within extruded and overlapped spacer-filled channel passages differs depending on spacer geometry. The addition of more transverse spacer filaments with respect to the main flow direction enhances solution flow disturbance and lowers concentration polarization. An attack angle greater than 45° results in a lower pressure drop associated with a lower rate of wakes and flow disturbance because when filaments become nearly longitudinal to the flow direction, the poorer their influence. New spacer designs must demonstrate a favorable flow pattern of velocity vectors and mass transfer in spacer-filled channels, which could aid in improving membrane performance and cross-flow power consumption.

**Keywords:** Feed Spacer Geometry; Extruded Spacers; Overlapped Spacers; Attack Angle; Filaments.

### Acknowledgment

This research work is financially supported by the Fundamental Research Grant Scheme (FRGS/UMP.05/25.12/04/01/1) with the RDU number RDU190160 which is awarded by the Ministry of Higher Education Malaysia (MOHE) via Research and Innovation Department, Universiti Malaysia Pahang (UMP) Malaysia. Sajjad Khudhur Abbas Al-Amshawee is the recipient of UMP Post-Doctoral Fellowship in Research.

### References

[1] Lee S.Y., Jeong Y.J., Chae S.R., Yeon K.H., Lee Y., Kim C.S., Jeong N.J., Park J.S. (2016) Porous carbon-coated graphite electrodes for energy production from salinity gradient using reverse electrodialysis. J. Phys. Chem. Solids. 91. 34–40. https://doi.org/10.1016/j.jpcs.2015.12.006.
[2] Zoungrana A., Türk O. K., Çakmakci, M. (2020) Energy coverage of ataköy-ambarlı municipal wastewater treatment plants by salinity gradient power. J. of Water Process Engineering. 38. https://doi.org/10.1016/j.jwpe.2020.101552.

**FLUID FLOW**

**Paper ID: ESCE197**

# STUDY THE EFFECTS OF AIR INJECTION PORT DIAMETER OF AIR-BLAST ATOMIZER ON THE SPRAY CHARACTERISTICS

**Kriwitch Yasamorn[1]*, Pisit Yongyingsakthavorn[1]**

[1] *Department of Mechanical and Aerospace Engineering, Faculty of Engineering, King Mongkut's University of Technology North Bangkok, 1518 Pracharat 1 Road,Wongsawang, Bangsue, Bangkok 10800 Thailand.*
*Corresponding author: kriwitch12@gmail.com

## Extended Abstract

An air-blast atomizer employs the kinetic energy of a flowing airstream to shatter the liquid jet or sheet into ligaments and then drops. This atomizer can be designed in various configurations for many applications. The objective of this work is to investigate the effects of air-injection port diameter on the spray characteristics, which are single-phase airstream velocity and spray drop size in order to develop the household atomizer well replacing in the commercial fogging sprayer. The atomizers with three different sizes of air-injection port are constructed in this study. By experiment, drop size distribution are measured by the Malvern Spraytec drop-size analyzer. For airstream velocity field, the numerical simulation has been conducted. The results are, finally, compared and discussed.

**Keywords:** Air-Blast Atomizer; Drop-Size Distribution; Air-Jet Velocity Profile; Malvern Spraytec.

### References

[1] H.M. Gad, et al (2018). "Experimental study of diesel fuel atomization performance of air blast atomizer." Experimental Thermal and Fluid Science Vol.99: 211-218.
[2] Y. Levy, et al (2009). "Experimental CFD Study of Miniature Air-Blast Atomizers." Turbo and Jet Engines Vol.169.
[3] Rui Ma, et al (2015). "An experimental study on the spray characteristics of the air-blast atomizer." Applied Thermal engineering Vol.88: 149-156.
[4] Ibrahim I.A., et al (2020). "Experimental study of spray combustion characteristics of air-blast atomizer." Energy Report Vol.6: 209-215.
[5] Franz X. Tanner, et al (2016). "Modeling and simulation of air-assist atomizers with applications to food sprays." Applied Mathematical Modelling Vol.40: 6121-6133.
[6] Hai-Feng Liu, et al (2006). "Effect of liquid jet diameter on performance of coaxial two-fluid air-blast atomizers." Chemical Engineering and Processing Vol.45: 240-245.
[7] M. Roudini and G. Wozniak (2018). "Experimental Investigation of Spray Characteristics of Pre-filming Air-blast Atomizers." Applied Fluid Mechanics Vol.11: 1455-1469.
[8] Jakkaphan Seedam, et al (2018). "Design and Construction Testing Apparatus for Air Blast Atomizer." Department of Mechanical and Aerospace Engineering Faculty of Engineering King Mongkut's University of Technology North Bangkok.

**FOOD SCIENCE AND TECHNOLOGY**

**Paper ID: ESCE016**

# DRYING KINETICS AND ENERGY CONSUMPTION IN HOT-AIR AND MICROWAVE DRYING OF *POLYSCIAS FRUTICOSA* (L.) HARMS LEAVES

**Tran-Thi Nhu-Trang[1], Thi-Kim-Thanh Phan[1], Thi-My-Trinh Lam[1], Phuoc-Bao-Duy Nguyen[2], Thi-Van-Linh Nguyen[1]***

[1] *Faculty of Enviromental and Food Engineering, Nguyen Tat Thanh University, 700000, Ho Chi Minh city, Vietnam.*
[2] *Faculty of Electrical and Electronics Engineering, Vietnam National University Ho Chi Minh city (VNU-HCM), 700000, Ho Chi Minh city, Vietnam.*
*Corresponding author: ntvlinh@ntt.edu.vn

## Extended Abstract

*Polyscias fruticosa* (L.) Harms belongs to the *Araliaceae* family [1] that is popularly distributed in moist tropical climates like India, Malaysia, Indonesia, Laos, Cambodia, Vietnam, etc. Due to the rich source of bioactive compounds with high antioxidant activity such as chlorophyll, total polyphenol, especially flavonoid compound, etc. [2], *P. fruticosa* leaves could be used as herbal tea or food ingredients; however, *P. fruticosa* leaves have been still underutilized. *P. fruticosa* leaves contain high moisture content (an approximation of 80%), so they are classified into perishable products. The drying method is the most common technique to preserve food products by removing water [3] for enhancing their stability and extending their shelf-life. Also, it would bring more convenience in packaging, shipping, and distribution. Therefore, the aims of this research work were (1) to characterize drying behavior, (2) to determine effective diffusivity coefficients, (3) to calculate the activation energy, (4) and to analyze consumed energy for hot air and microwave drying of *P. fruticosa* leaves. From the results of this study, the suitable drying method with minimum energy and time was recommended to dry *P. fruticosa* leaves.

The experiments were conducted at different air-drying temperatures (45, 50, 55, and 60 °C) for hot air drying and microwave power (150, 300, 450, and 600 W) for microwave drying to compare drying kinetics and energy consumption for drying *Polyscias fruticosa* (L.) leaves.

The drying process occurred in the falling period except for hot air drying at 45 °C. Both Midilli and Weibull models showed that are the best characterization of drying behavior.

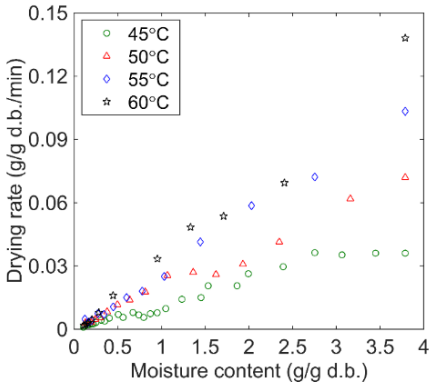


Fig. 1: Drying rate versus moisture content during HAD of PFL.

**FOOD SCIENCE AND TECHNOLOGY**

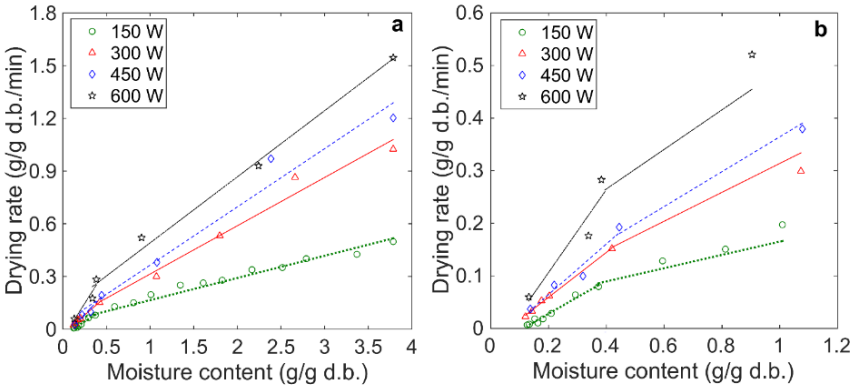


Fig. 2: Drying rate versus moisture content during MWD of PFL.

The effective diffusivity was ranged from $2.557\times10^{-11}$ to $10.550\times10^{-10}$ $m^2/s$ for hot air drying and from $3.574\times10^{-10}$ $m^2/s$ to $10.550\times10^{-10}$ $m^2/s$ for microwave drying. Thus, microwave showed an impressive ability in removing moisture from *P. fruticose* leaves more 5.41 to 41.26 times than hot-air drying. The activation energy was found at 54.34 kJ/mol in hot air drying and 8.605 W/g in microwave drying. The composition, type, and characteristics of the drying material strongly affected activation energy values.

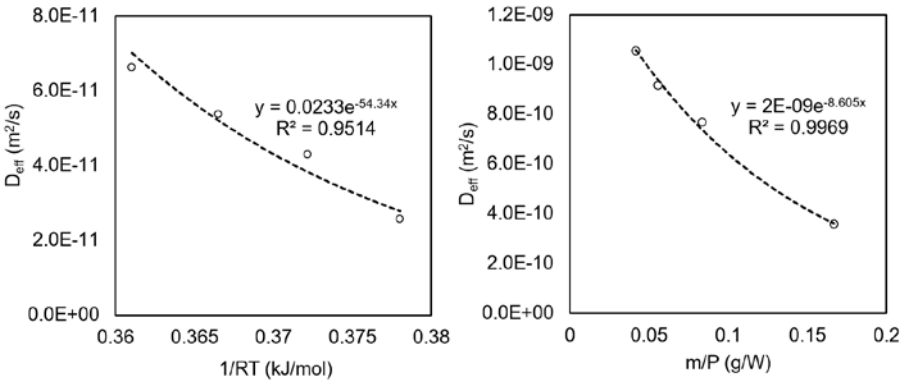


Fig. 3: The change of effective diffusivities versus 1/(RT) in HAD (a) and different ratios of initial mass and MW power in MWD (b)

Besides, microwave consumed energy less 50 times than hot-air drying. It clears that microwave drying showed as a suitable drying method for dehydrating *P. fruticosa* leaves in view of energy consumption and time. However, besides energy and time, the quality of dried products, such as optical properties, rehydration properties, nutrients characteristics, etc., after drying was also a significant criterion. Therefore, these responses should be investigated to get the overall efficiency of the drying process.

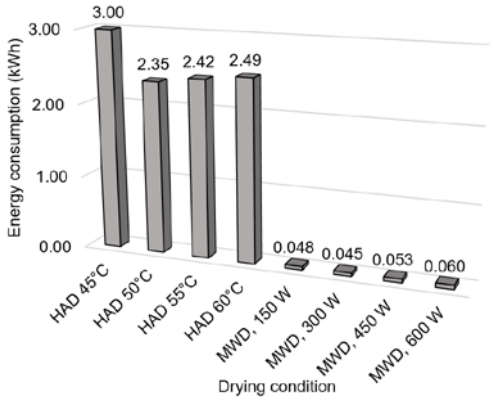


Fig. 4: Total energy consumed in the HAD and MWD of PFL.

**FOOD SCIENCE AND TECHNOLOGY**

**Keywords:** Drying kinetics; Energy; Hot air drying; Microwave drying; *Polyscias fruticosa* (L.) leaves.

## Acknowledgment

This study was funded by NTTU (Nguyen Tat Thanh University) Foundation for Science and Technology Development under the grant 2019.01.29.

## References

[1] Brophy JJ, Lassak EV, Suksamrarn A. (1990) Constituents of the volatile leaf oils of *Polyscias fruticosa* (L.) Harms. Fla vour and Fragrance Journal 5:179–182.
[2] Bernard BM, Pakianathan N, Venkataswamy R, Divakar MC. (1998) A pharmacognostic report on the leaf and root of *Polyscias fruticosa* (L.) Harms. Ancient Science of Life 18:165.
[3] Ratti C. (2001) Hot air and freeze-drying of high-value foods : a review. Food Engineering 49:311–319.

2ND ENERGY SECURITY AND CHEMICAL ENGINEERING CONGRESS 2021
*"Sustainable Technological Solution for a Better World"*
VIRTUAL CONFERENCE | 3-5 NOVEMBER 2021

**FOOD SCIENCE AND TECHNOLOGY**

**Paper ID: ESCE019**

# EFFECTS OF BLANCHING ON SOME QUALITY CHARACTERISTICS OF SPROUTED-DRIED PEANUTS

**Duong-My-Chi Truong[1], Phong-Binh Nguyen[1], Quoc-Duy Nguyen[1], Thi-Van-Linh Nguyen[1], Thi-Thuy-Dung Nguyen[1]***

[1] *Faculty of Environmental and Food Engineering, Nguyen Tat Thanh University, 700000, Ho Chi Minh City, Vietnam.*
*Corresponding author: dungntt@ntt.edu.vn

## Extended Abstract

Sprouted peanuts are rich in antioxidant activity that can be used to produce a wide variety of food products. The study was conducted to evaluate the effect of blanching on some quality characteristics of the sprouted peanut seeds. Specifically, peanuts were germinated for three days, then used as materials. In this study, two blanching methods, including steam blanching and hot water blanching, were investigated with time blanching as a factor. The one-factor-at-a-time was used to design the experiment in which four-level blanching time was conducted at 0, 2, 4, and 6 minutes. After each blanching condition, the sample was dried at 60 °C by hot air drying until the moisture content reached 0.03 g/g of sample on the dry basis (d.b). Then, the dried sample was analyzed to determine some quality characteristics, including the color parameter (by the CIE Lab), the total polyphenol (by the colorimetric method using gallic acid as standard), the flavonoid content (by the colorimetric method using quecertin as standard), and antioxidant activity (by DPPH radical scavenging assay).

The results showed that for the steam blanching, the increase of time blanching had no effect on time drying but significantly decreased the quality of the product. Specifically, the polyphenol content decreased from 3.56 ± 0.06 to 3.21 ± 0.02 mg GAE/g d.b., the flavonoid content decreased from 0.82 ± 0.01 to 0.43 ± 0.01 mg QE/g d.b., antioxidant activity decreased from 1.39 ± 0.03 to 1.04 ± 0.02 mg TE/ g d.b., but the L* values increased when the time blanching changed from 0 to 6 minutes. The drying time was prolonged significantly for the water blanching when the blanching time changed from 4 to 6 minutes. Besides, the biological activity of blanched products such as total polyphenol, flavonoid, antioxidant activity also is significantly decreased. However, the brighter color of the dried sprouted peanuts was, the longer the blanching time was. Finally, it was found that the sprouted peanuts dried without blanching retained the highest quality of the product. Further studies were required to determine the impact of the drying process on the quality of the product in order to maintain the health benefits in the production of functional nutritional food from sprouted peanuts.

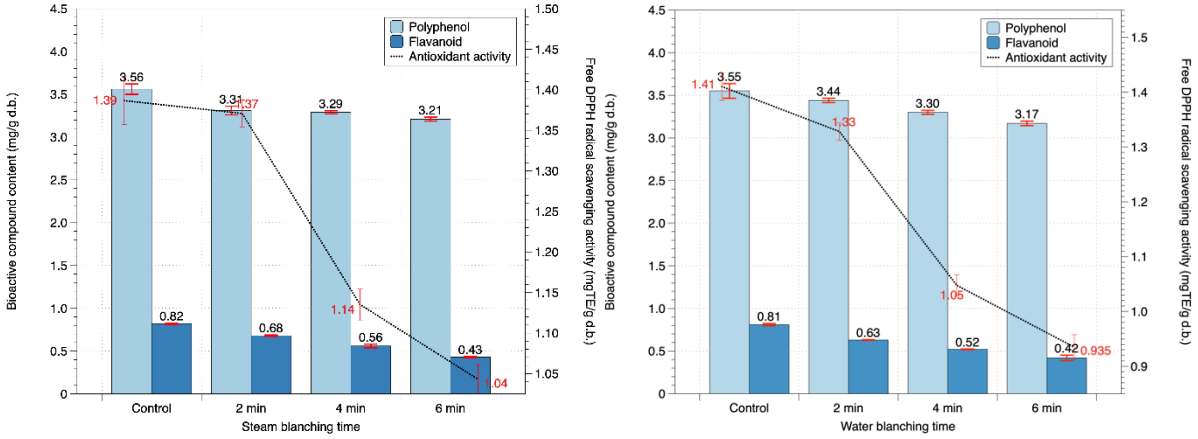


Fig. 1: Effect of blanching time on bioactive compounds of sprouted peanut seeds
(a) Steam blanching (b) Water blanching at 85 °C

Table 1: Effect of blanching time on L* values of sprouted peanut seeds.

| | Control | 2 min | 4 min | 6 min |
|---|---|---|---|---|
| Steam blanching | 63.84±0.45[a] | 74.01±0.67[b] | 75.85±0.72 [b] | 76.46±0.38 [b] |
| Water blanching | 64.04±0.32 [a] | 75.11±0.67 [b] | 76.88±0.47 [b] | 77.66±0.84 [b] |

*Values with the same letter are not significantly different (P < 0.05)*

**Keywords:** Blanching; DPPH; Flavonoid; Peanut sprouts; Polyphenol.

**Acknowledgment**

This study was funded by NTTU (Nguyen Tat Thanh University) Foundation for Science and Technology Development under the grant 2020.01.055.

**References**

[1] R.-Y. Gan et al. (2017) Bioactive compounds and bioactivities of germinated edible seeds and sprouts: An updated review. Trends Food Sci. Technol., 59:1–14.
[2] H. M. Saleh, A. A. Hassan, E. H. Mansour, H. A. Fahmy, and A. E. F. A. El-Bedawey. (2019) Melatonin, phenolics content and antioxidant activity of germinated selected legumes and their fractions. J. Saudi Soc. Agric. Sci., 18:3:294–301.
[3] R. Y. Gan et al. (2017) Antioxidant activity, total phenolic, and resveratrol content in five cultivars of peanut sprouts. Elsevier Ltd., 59:34.
[4] H.-J. Kim, K.-J. Park, and J.-H. Lim. (2011) Metabolomic analysis of phenolic compounds in buckwheat (Fagopyrum esculentum M.) sprouts treated with methyl jasmonate. J. Agric. Food Chem., 59:10:5707–5713.
[5] A. Limmongkon et al. (2017) Antioxidant activity, total phenolic, and resveratrol content in five cultivars of peanut sprouts. Asian Pac. J. Trop. Biomed., 7:4:332–338.
[6] V. Nyau, S. Prakash, J. Rodrigues, and J. Farrant. (2017) Profiling of phenolic compounds in sprouted common beans and bambara groundnuts," J. Food Res., 6:6:74–82.
[7] Z. Wu, L. Song, and D. Huang. (2011) Food grade fungal stress on germinating peanut seeds induced phytoalexins and enhanced polyphenolic antioxidants," J. Agric. Food Chem., 59:11:5993–6003.
[8] E. Ramírez-Moreno, D. Córdoba-Díaz, M. de Cortes Sánchez-Mata, C. Díez-Marqués, and I. Goñi. (2013) Effect of boiling on nutritional, antioxidant and physicochemical characteristics in cladodes (Opuntia ficus indica). LWT - Food Sci. Technol.,51:1:296–302.
[9] R. P. C. Powers, Joseph R, Jose´I.ReyesDeCorcuera. (2004) Blanching of Foods. Encycl. Agric, Food, Biol. Eng., 1–5.
[10] H. H. Nurhuda, M. Y. Maskat, S. Mamot, J. Afiq, and A. Aminah. (2013) Effect of blanching on enzyme and antioxidant activities of rambutan (nephelium lappaceum) peel. Int. Food Res. J., 20: 4:1725–1730.
[11] L.-Z. Deng et al. (2019) High-humidity hot air impingement blanching (HHAIB) enhances drying quality of apricots by inactivating the enzymes, reducing drying time and altering cellular structure. Food Control, 96:104–111.
[12] L. Priecina, D. Karklina, and T. Kince. (2018) The impact of steam-blanching and dehydration on phenolic, organic acid composition, and total carotenoids in celery roots. Innov. Food Sci. Emerg. Technol., 49:192–201.
[13] H. Kessy, Z. Hu, L. Zhao, and M. Zhou (2016) Effect of Steam Blanching and Drying on Phenolic Compounds of Litchi Pericarp. Molecules, 21:729.
[14] S. Gupta, S. Cox, and N. Abu-Ghannam. (2011) Effect of different drying temperatures on the moisture and phytochemical constituents of edible Irish brown seaweed. LWT - Food Sci. Technol., 44:5:1266–1272.

**FOOD SCIENCE AND TECHNOLOGY**

**Paper ID: ESCE028**

# A SIMPLE ELECTROCHEMICAL METHOD FOR DETERMINATION OF ROSUVASTATIN CALCIUM IN CHOLESTEROL-LOWERING MEDICAL PRODUCTS

**Tran-Thi Nhu-Trang[1], Hoang-Nguyen Nguyen (Miss.)[2], Thi-Xong Thach[2], Hoang-Nguyen Nguyen (Mr.)[2], Cong-Hau Nguyen[1], Minh Huy Do[1]***

[1] *Faculty of Environmental and Food Engineering, Nguyen Tat Thanh University (NTTU), 700000 Ho Chi Minh, Vietnam.*
[2] *Department of Analytical Chemistry, Faculty of Chemistry, University of Science, Vietnam National University – Ho Chi Minh City, 700000 Ho Chi Minh, Vietnam.*
* Corresponding author: dmhuy@ntt.edu.vn

## Extended Abstract

Rosuvastatin (RSV) is internationally known as (3*R*,5*S*,6*E*)-7-[4-(4-Fluorophenyl)-2-*N* methyl (methylsulfonyl) amino-6-propan-2-ylpyrimidin-5-yl]-3,5-dihydroxyhept-6-enoic acid [1]. On the market, RSV is sold under name Crestor, a compound of the statin medicine group [1]. In August 2003, RSV was approved for the health sector by the US Food and Drug Administration (US FDA), which had the function of decreasing "bad" cholesterol, fat (such as LDL, triglyceride) in liver and increasing "good" cholesterol (HDL) in blood, thereby minimizing the risk of cardiovascular disease, preventing strokes and heart disease [2]. The chemical formula of RSV is shown in Fig. 1. In addition, RSV has a highly selective effect on the liver, and is now widely and most commonly used to support the treatment of cardiovascular disease [3, 4].

Although pharmacological RSV is considered the most effective in the group of current statin drugs, overdose can cause adverse side effects, especially for older individuals with a history of liver disease, kidney failure, or hypothyroidism [3, 4]. The more incidence of cardiovascular disease increases, the more statin medicine group is produced. Therefore, in order to serve medical needs, monitor, and control RSV levels in the industrial medicine production process, analytical methods should be accurately developed to determine the RSV content in pharmaceutical products.

Electrochemical methods have high potential applications in controlling RSV levels during the production process and even in commercial drug tablets, which are available in many drugstores, because they offer rapid analytical performance and relatively low price. In this research study, the method of cleaning and activating the surface of the glassy carbon electrode in acidic and basic media was investigated to ensure the operational stability and electron exchange capability of the working electrode surface. Cyclic voltammetry in sulfuric acid medium was the chosen procedure to proceed to the establishment of the electrochemical method to determine rosuvastatin. The electrolyte solutions investigated were: $H_2SO_4$, $Na_2SO_4$, acetate buffer, phosphoric buffer, and Britton Robinson buffer. The results showed that the medium 0.1 M $Na_2SO_4$ (pH = 2) (Fig. 2) was the most suitable; the immersion time of the electrode in solutions containing RSV was 12 minutes. The linear range of RSV-calcium was from 0.15 mg $L^{-1}$ to 2.5 mg $L^{-1}$. LOD and LOQ were estimated to be 0.035 mg $L^{-1}$ and 0.12 mg $L^{-1}$, respectively. The difference in the content of RSV in commercial drug samples between the analytical results obtained by this electrochemical method and the published values of the manufacturer was 0.10 % ÷ 1.10 %, and the recovery varied from 98.6 % to 101.1 %. This method was then compared to HPLC-UV as an arbitration method, and our results showed a difference of 0.10 % ÷ 1.10 % in the amount of RSV.

**FOOD SCIENCE AND TECHNOLOGY**

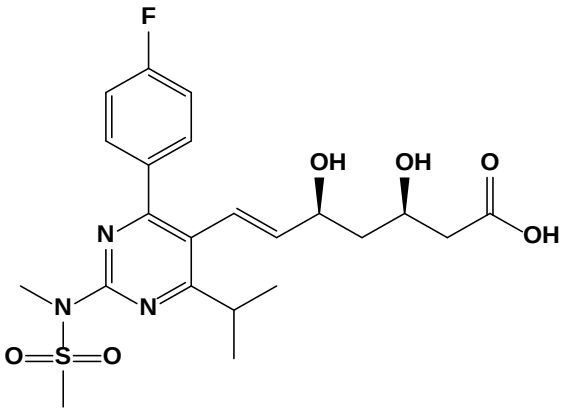


Fig. 1: The chemical formula of rosuvastatin.

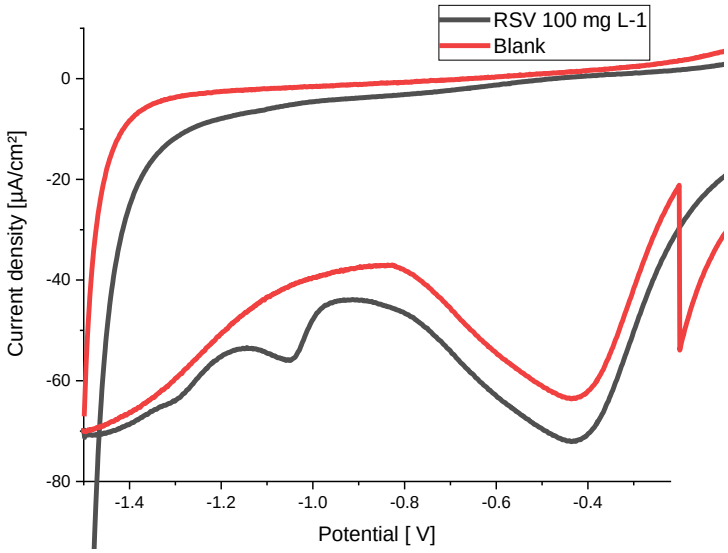


Fig.2: Cyclic voltammogram of 100 mg $L^{-1}$ RSV and blank (0.1 M $Na_2SO_4$, pH 2.048) in the potential range of -1.5 V ÷ +2.0 V, scan rate 100 mV $s^{-1}$.

**Keywords:** Rosuvastatin; Glassy carbon electrode; Medicine; Electrochemical sensor.

## Acknowledgment

This work was supported by The World Academy of Sciences (TWAS) – UNESCO. The authors would like to express our thanks and appreciation to Nguyen Tat Thanh University for the assistance and support during this study. This research is funded by Nguyen Tat Thanh University, Ho Chi Minh city, Vietnam, under grant number 2021.01.24/HĐ-KHCN.

## References

[1] Wani, T. A.; Samad, A.; Tandon, M.; Saini, G. S.; Sharma, P. L.; Pillai, K. K., The Effects of Rosuvastatin on the Serum Cortisol, Serum Lipid, and Serum Mevalonic Acid Levels in the Healthy Indian Male Population. AAPS PharmSciTech 2010, 11 (1), 425-432.
[2] J. Quirk; M. Thornton; P. Kirkpatrick, Rosuvastatin Calcium, Nature Reviews Drug Discovery 2003, 2, 769.
[3] R. Plakogiannis; H. Cohen, Optimal Low-Density Lipoprotein Cholesterol Lowering--Morning Versus Evening Statin Administration, The Annals of pharmacotherapy 2007, 41(1), 106-10.
[4] M. D. Abdulbari Bener, Lolwa Barakat, Abdulla O.A.A. Al-Hamaq, Comparison of Ef Cacy, Safety, and Cost-Effectiveness of Various Statins in Dyslipidemic Diabetic Patients, 2014.

**FOOD SCIENCE AND TECHNOLOGY**

**Paper ID: ESCE047**

# ANALYSIS OF WATER CONTENT IN ESTERIFICATION OF ISOAMYL ACETATE BY USING GAS CHROMATOGRAPHY – THERMAL CONDUCTIVITY DETECTOR (GC-TCD) WITH WATERCOL 1910 COLUMN

**N. A. Ahmad[1], N. Mansor[1], N. Yusoff Azudin[1], S. R. Abd Shukor[1]***

[1] *School of Chemical Engineering, Engineering Campus, Universiti Sains Malaysia, Seri Ampangan, 14300 Nibong Tebal, S.P.S., Pulau Pinang, Malaysia.*
*Corresponding author: chsyamrizal@usm.my

## Extended Abstract

Determination of water content in esterification products is significantly important since the presence of water leads to low production, reduce product quality, phase separation problem, limit the chemical equilibrium, challenging in product purification [1,2]. Esterification reaction is a reaction between alcohol and acid to produce ester that contains a functional group of carbonyl group (-COO-). Among the esters, isoamyl acetate is highly demand in food, cosmetic, pharmaceutical and chemical industries due to its banana like flavour. In production of isoamyl acetate, Isoamyl alcohol and acetic acid are frequently used as the main reactants. The esterification reaction of isoamyl acetate as shown below. Acetic anhydride is used to double up the production of isoamyl acetate as acyl donor instead of acetic acid as the acetic anhydride stoichiometrically yield two mole of isoamyl acetate during the reaction [3, 4].

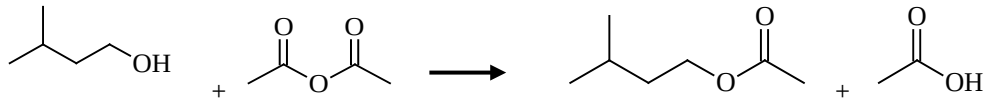

Isoamyl alcohol + Acetic anhydride → Isoamyl acetate + Acetic acid (1)

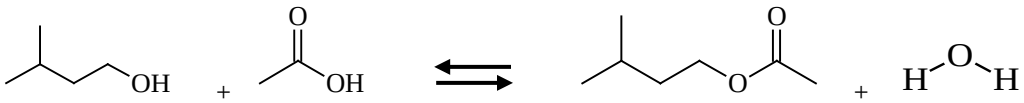

Isoamyl alcohol + Acetic acid ⇌ Isoamyl acetate + Water (2)

Water as the side product in the second esterification reaction significantly disturbed the chemical equilibrium by promoting the backward reaction hence reduce the isoamyl acetate production [5, 6]. Accumulation of water reduces the reaction rate and prevents the complete conversion of the acid and alcohol in the esterification reaction [7]. The most widely used methods for water content determination in liquid sample were; Karl Fisher (KF) titration, infrared spectroscopy (FTIR), gas chromatography (GC), and quantitative nuclear magnetic resonance ( qNMR). Among these methods, GC is considered an effective and alternative analytical approach to detect volatile compounds with boiling point of $\leq$ 300 $^{o}$C in a sample either in gas or liquid state [8]. Watercol capillary GC column by Sigma Aldrich provides an alternative column to determine water with ease and effective [9, 10]. The application of ionic-liquid (IL) as the stationary phase inside the GC capillary columns shows good selectivity, h igh stability and compatibility to water as analyte compared to traditional commercial columns [11]. In this study, GC- TCD with Watercol GC column was used to perform water analysis in the product of isoamyl acetate esterification. Among the GC parameters setting, gas flow rate and split ratio were studied in this work to determine an appropriate method for sample analysis. Meanwhile, the real samples from the isoamyl acetate esterification reaction in microreactor at 80 $^{o}$C for different reaction times were directly used to validate the method and analyse the water content. Higher carrier gas flow rate caused shorter chromatograph peaks (reduced analysis sensitivity) and shorter analysis duration. Split ratio more than 2:1 unable to detect the presence of acetic anhydride in the sample. Carrier gas flow rate of 2.5856 mL/min and 1:1 split ratio were set to analyse the samples from the esterification reactions. All the samples from esterification reactions showed the presence of water and other compounds as shown in Figure 1. The presence of water in all sample indicated that second reaction of the

esterification reaction between acetic acid and isoamyl alcohol took place. The presence of water slightly affected the reaction equilibrium, promoted the hydrolysis of isoamyl acetate and reduced the formation of isoamyl acetate from 2.7 mol/L to 2.2 mol/L when esterification reaction time extended from 60 to 90 minutes.

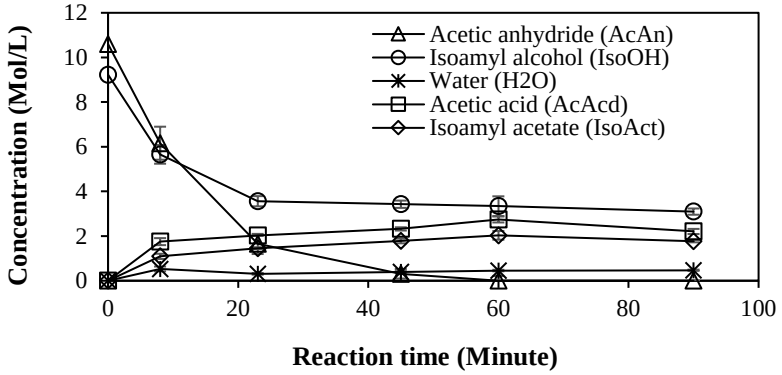


Fig. 1: Concentration of every component in the product after esterification at 80 °C at different reaction time (Minutes).

**Keywords:** Water; Gas chromatography; Split ratio; Carrier gas flow; Isoamyl acetate.

## Acknowledgment

This work was supported by Ministry of Higher Education Malaysia for providing financial support via FRGS Grant (203. PJKIMIA 6071387) and MyBrain15. Also USM Post-Doctoral Research Fellow Scheme 2020-2021.

## References

[1] Gómez-García, M. Á., Dobrosz-Gómez, I., and Osorio Viana, W. (2017) Experimental assessment and simulation of isoamyl acetate production using a batch pervaporation membrane reactor. Chem. Eng. Process. Process Intensification 122: 155-160.
[2] Kirdi, R., Ben Akacha, N., Messaoudi, Y., and Gargouri, M. (2017) Enhanced synthesis of isoamyl acetate using liquid-gas biphasic system by the transesterification reaction of isoamyl alcohol obtained from fusel oil. Biotechnol Bioproc. Eng. 22(4): 413-422.
[3] Hari Krishna, S., Divakar, S., Prapulla, S. G., and Karanth, N. G. (2001) Enzymatic synthesis of isoamyl acetate using immobilized lipase from Rhizomucor miehei. J. Biotechnol. 87(3): 193-201.
[4] Novak, U., and Žnidaršič-Plazl, P. (2013) Integrated lipase-catalyzed isoamyl acetate synthesis in a miniaturized system with enzyme and ionic liquid recycle. Green Processing and Synthesis: 561.
[5] Yusoff Azudin, N., Sangaran, S., and Abd Shukor, S. R. (2019) Non-enzymatic synthesis route for production of isoamyl acetate in a solvent-free system using miniaturized intensified reactor. J. Env. Chem. Eng.: 103186.
[6] Osorio-Viana, W., Duque-Bernal, M., Quintero-Arias, J. D., Dobrosz-Gómez, I., Fontalvo, J., and Gómez-García, M. Á. (2013) Activity model and consistent thermodynamic features for acetic acid–isoamyl alcohol–isoamyl acetate–water reactive system. Fluid Phase Equilibr. 345: 68-80.
[7] Kruis, A. J., Bohnenkamp, A. C., Patinios, C., van Nuland, Y. M., Levisson, M., Mars, A. E., van den Berg, C., Kengen, S. W. M., and Weusthuis, R. A. (2019) Microbial production of short and medium chain esters: Enzymes, pathways, and applications. Biotechnol. Adv. 37(7): 107407.
[8] Choi, Y. S., Johnston, P. A., Brown, R. C., Shanks, B. H., and Lee, K.-H. (2014) Detailed characterization of red oak-derived pyrolysis oil: Integrated use of GC, HPLC, IC, GPC and Karl-Fischer. J. Anal. Appl. Pyrolysis 110: 147-154.
[9] Frink, L. A., and Armstrong, D. W. (2016) Using headspace gas chromatography for the measurement of water in sugar and sugar-free sweeteners and products *Advance in food and beverage analysis* October 2016, 6-13.
[10] Price, F. (2018) Revolutionary wew gc columns bring magic to water analysis. March, 22, 2018 Ed., SelectScience, Bath, UK.
[11] Ying Zhang, C. W., Daniel W. Armstrong, Ross M. Woods, Dilani A. Jayawardhana. (2011) Rapid, Efficient Quantification of Water in Solvents and Solvents in Water Using an Ionic Liquid-based GC Column. LCGC North Am. 30(2): 142-158.

**FOOD SCIENCE AND TECHNOLOGY**

**Paper ID: ESCE063**

# INHIBITION OF FUNGI GROWTH AND SHELF-LIFE EXTENSION OF BREAD BY SORBIC ACID BASED ANTIMICROBIAL PACKAGING

**S. Nor Azwin[1,2]*, W. Mat Uzir[1], G. Zulkafli[1,2], F.O. Nor Azillah[2], F.H. Farah[1], A.K. Zulhairun[1]**

[1] *School of Chemical and Energy Engineering, Faculty of Engineering, Universiti Teknologi Malaysia, 81310, UTM Johor Bahru, Johor, Malaysia.*
[2] *Malaysian Nuclear Agency, Radiation Processing Technology Division, Bangi, 43000, Kajang,Selangor, Malaysia.*
*Corresponding author: azwin@nuclearmalaysia.gov.my

## Extended Abstract

New packaging technologies are continually being challenged to provide improved quality and to protect the foods with extended shelf-life. Due to potential impact on shelf-life performance as well as additional maintenance of product to ensure quality and human wellbeing, active packaging has been accepted by the food industries. Packaging is referred as active when it can perform some active role in food preservation rather than just being passive protection from external environment. It permits to alter the condition of packaged food to increase its shelf life or to boost safety and sensory properties, while keeping up its quality [1]. Active packaging system maybe in the form of oxygen scavenging [2-5], ethylene emitter [6], antioxidant [7], release agents such as antimicrobials or additives. Between the active packaging systems, antimicrobial packaging is getting more attention of researchers because of its critical role in prolonged shelf life and enhancing microbial security of the food product. It has been seen as an alternative packaging to overcome unwanted spoilage microorganism on food. The use of antimicrobial packaging provides a biological protection against spoilage microorganism and subsequently extend its shelf life while maintaining its quality [1]. Most of antimicrobial active packaging so far has been based on LDPE film where the antimicrobial agent immobilized with the polymer structure or incorporated in plastic resin. However, to our knowledge, the incorporation of sorbic acid onto polyethylene film via radiation induced grafting (RIG) is still scarce in the scientific literature. Thus, the performance of sorbic acid (SA) grafted film using radiation-induced grafting was studied to investigate the effect of SA on shelf life extension of sliced bread. By switching to RIG method, amount of preservatives can be reduced and focus the function of preservatives more precisely where microbial growth and spoilage may occur. Thus, instead of mixing antimicrobial as food additive directly with food, incorporating them in films via radiation induced grafting may allow the functional effect at the food surface, where the microbial growth is mostly found. Then, by contacting the antimicrobial packaging material with the food product, significantly shelf life extension can thus be achieved. Therefore, the objective of this study is to develop antimicrobial active packaging film based on sorbic acid via radiation-induced grafting. The successful preparation of grafted film was confirmed by the grazing-angle fourier transfromed infra-red spectroscopy (GA-FTIR) and their microbial performance and physical properties such as visual observation of fungi growth, moisture content, texture and color change of the sliced bread during storage time were elucidated and discussed. The result revealed that bread packed with SA grafted film showed higher moisture content by 2% and lower hardness by 47% with less significant color changes as compared to bread packed with control LDPE film. Delay in appearance of yeast and mold for up to 5 days was also observed in bread packed with SA grafted film against bread packed with control film. The total coliform of bacteria and yeast and mold on bread packed with SA grafted film showed low level of bacteria spore with the count of 4.36 x 104 cfu/g and 9.66 x 104 cfu/g, respectively, which meet the commission standard limit until the 5th day of storage. This indicates that the developed SA grafted active film successfully protect the food against spoilage micro flora like bacteria and mold.

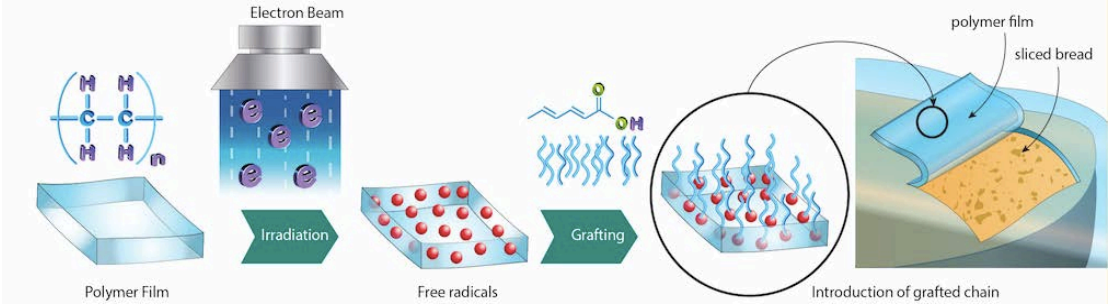


Fig. 1: Schematic diagram of radiation-induced grafting of sorbic acid onto LDPE film.

**Keywords:** Sorbic acid; Active packaging; Antimicrobial packaging; Shelf life; Bread.

## Acknowledgment

The authors are grateful for the International Atomic Energy Atom (IAEA) for granting funding for this project (project number RC17457). The authors also extend their acknowledgement to Malaysian Nuclear Agency and Universiti Teknologi Malaysia for the collaboration and technical supports received in this research.

## References

[1] de Souza, A.C., et al., *Impregnation of cinnamaldehyde into cassava starch biocomposite films using supercritical fluid technology for the development of food active packaging.* Carbohydrate Polymers, 2014. **102**: p. 830-837.
[2] Busolo, M.A. and J.M. Lagaron, *Oxygen scavenging polyolefin nanocomposite films containing an iron modified kaolinite of interest in active food packaging applications.* Innovative Food Science & Emerging Technologies, 2012. **16**: p. 211-217.
[3] Byun, Y., H.J. Bae, and S. Whiteside, *Active warm-water fish gelatin film containing oxygen scavenging system.* Food Hydrocolloids, 2012. **27**(1): p. 250-255.
[4] Foltynowicz, Z., et al., *Nanoscale, zero valent iron particles for application as oxygen scavenger in food packaging*. Food Packaging and Shelf Life, 2017. **11**: p. 74-83.
[5] Gaikwad, K.K., S. Singh, and Y.S. Lee, *A pyrogallol-coated modified LDPE film as an oxygen scavenging film for active packaging materials.* Progress in Organic Coatings, 2017. **111**: p. 186-195.
[6] Chopra, S., et al., *Metal-organic frameworks have utility in adsorption and release of ethylene and 1-methylcyclopropene in fresh produce packaging.* Postharvest Biology and Technology, 2017. **130**: p. 48-55.
[7] López-de-Dicastillo, C., et al., *Active antioxidant packaging films: Development and effect on lipid stability of brined sardines.* Food Chemistry, 2012. **131**(4): p. 1376-1384.

2ND ENERGY SECURITY AND CHEMICAL ENGINEERING CONGRESS 2021
*"Sustainable Technological Solution for a Better World"*
VIRTUAL CONFERENCE | 3-5 NOVEMBER 2021

**FOOD SCIENCE AND TECHNOLOGY**

**Paper ID: ESCE094**

# THIN-LAYER DRYING OF PAPAYA (*CARICA PAPAYA*) SEEDS: DRYING KINETICS, MATHEMATICAL MODELING AND EFFECTIVE MOISTURE DIFFUSIVITY

**Misbahudin Alhanif[1,2], Andri Cahyo Kumoro[1,2]*, Dyah Hesti Wardhani[1,2]**

[1] *Department of Chemical Engineering, Faculty of Engineering,* [2] *Institute of Food and Remedies Biomaterial, Department of Chemical Engineering Faculty of Engineering, Universitas Diponegoro, Semarang, Indonesia 50275.*
*Corresponding author: andrewkomoro@che.undip.ac.id

## Extended Abstract

Recently, papaya seeds are well-recognized for their nutritional and nutraceutical properties. As a by-product, papaya seeds are rich in nutrients (fat, protein, carbohydrates, minerals, fiber), which promising potential in developing new products in the food and pharmaceutical industries [1]. Papaya seed with kernels (±12.77% of seeds) also contains numerous bioactive compounds that are antiviral, antibacterial, cardioprotective, and antioxidants, so it bears enormous potential for future development of functional and nutritional food products [2].

Apart from the various superiorities, papaya seeds also suffer from serious a drawback. Their high moisture content (60-90% wt.) can trigger an inevitable microbial degradation process. Therefore, papaya seeds must be dried to a safe moisture content before storage and further processing [3]. This study aims to assess the drying kinetics of papaya seeds and investigate the effect of drying air temperature on the physicochemical properties of papaya seeds. In this study, mathematical 67odelling was used to predict the moisture removal behavior, predict the thin-layer drying model, and evaluate the use of energy-exergy. The drying experiments were carried out using natural convection oven at various drying air temperatures of 40, 55, 70, and 85$^{o}$C for papaya seeds with and without sarcotesta. The thin-layer drying models used include Weibul, Wang and Singh, Silva, Henderson and Pabis, Two-term, etc. Determination of the best fit model was based on the statistical parameters ($R^2$, RMSE, and $\chi^2$).

The results presented that an increase in drying air temperature led to increasing the drying rate as indicated by a reduction of drying time (22-89%). Another phenomenon that can be observed is that the difference in high moisture concentration between papaya seeds and the surrounding air will also contribute to an increase in the diffusion rate of water to the surface. Due to the high initial moisture content of the papaya seeds, especially the free moisture in the surface, most of the moisture was removed in the initial drying period and subsequently decreases with a decrease in the moisture content of the seeds. It is due to the low moisture content between the pores, which results in high adhesion forces on the seeds, which eventually causes shrinkage [4]. This research also proved that the Wang-Singh model was the most suitable model for the papaya seeds drying. Effective moisture diffusivity and mass transfer coefficient increases for drying with and without sarcotesta. The effective moisture diffusivity and mass transfer coefficient of papaya seeds without sarcotesta higher than papaya seeds with sarcotesta. It indicates that the sarcotesta significantly inhibits the water diffusion to the surface of the seeds. Further observations provide information that there is a free water layer between the sarcotesta and endosperm in fresh papaya seeds, strengthening the notion that the sarcotesta has tighter pores than the endosperm.

A higher drying air temperature leads to more intensive energy utilization, which requires a lower energy supply. The energy supply is also related to energy efficiency, where a high energy supply indicates low efficiency. Thus, drying at high air temperatures is more energy-efficient than low air temperatures. The exergy analysis resulted in significant exergy loss, which offers exergy improvement potential as indicated by the low efficiency and exergy sustainability index. Lower final moisture content has a higher shrinkage percentage and a smaller rehydration ratio on the physical properties. Low water content can cause the barrier between the pores to get closer together (shrinkage). It is difficult for water to enter the material leading to a low value of rehydration ratio. Besides, the external pressure generated by convection heating can cause the papaya seed structure to shrink.

**FOOD SCIENCE AND TECHNOLOGY**

After the drying process, the nutritional contents of papaya seeds showed that the moisture content of papaya seeds without sarcotesta dried at 85oC had already met its standard for agricultural products (<14%). As expected, the carbohydrate, protein, and fat contents also decreased with the increasing drying air temperature (Table 1). Protein experienced the most severe reduction and followed by carbohydrate and fat. Thermal denaturation is probably the dominant phenomenon, inducing a remarkable decrease in protein content in papaya seeds [5]. Besides, the presence of naturally occurring papain enzyme, which is active at pH 4 – 10 and temperatures up to 80ºC, is believed to play a significant role in breaking peptide bonds through autohydrolysis and contributes to the loss of protein content [6]. An alternative way to prevent thermal denaturation of protein during drying agricultural products is by using drying air temperature lower than 63.35ºC [7]. Under this consideration, drying air temperatures at 40 and 55ºC are both recommended for drying papaya seeds.

Table 1: Nutritional compounds of papaya seeds after 100 minutes drying.

| No. | Parameter | Nutritional compounds (% wet basis) | | | | Nutritional compounds (% dry basis) | | | |
|---|---|---|---|---|---|---|---|---|---|
| | | With Sarcotesta | | Without Sarcotesta | | With Sarcotesta | | Without Sarcotesta | |
| | | 40ºC | 85ºC | 40ºC | 85ºC | 40ºC | 85ºC | 40ºC | 85ºC |
| 1 | Carbohydrate | 6.59 | 15.86 | 11.43 | 28.25 | 30.41 | 27.72 | 37.43 | 31.38 |
| 2 | Protein | 10.56 | 25.06 | 8.46 | 17.57 | 48.72 | 43.80 | 27.70 | 19.51 |
| 3 | Fat | 1.14 | 1.51 | 0.88 | 1.62 | 5.25 | 2.64 | 2.88 | 1.80 |
| 4 | Water | 78.33 | 42.79 | 69.47 | 9.98 | - | - | - | - |
| 5 | Ash content | 2.64 | 10.91 | 5.06 | 17.69 | 12.61 | 19.07 | 16.56 | 19.65 |
| 6 | Crude fibre | 0.75 | 3.88 | 4.71 | 24.90 | 3.46 | 6.77 | 15.44 | 27.66 |

Based on the experimental results, it is clear that the drying rate increases at high drying air temperatures as indicated by a more rapid decline in moisture content of the papaya seeds and a shorter drying time. The same trends are also found for the effective moisture diffusivity and mass transfer coefficient. The high temperature gradient promotes accelerated diffusion of water to the surface of the seed. The most representative thin layer model for papaya seeds drying is the Wang and Sing model, which is a second order polynomial equation. Energy analysis showed that higher drying air temperatures lead to more intensive high energy utilization and subsequently require a lower energy supply ratio. In addition, it also results in large exergy loss and exergy improvement potential, indicated by low efficiency and exergy sustainability index. On the physical properties, a lower final moisture content has a higher shrinkage percentage and a smaller rehydration ratio. Nutritional analysis revealed that increasing the drying air temperature causes a significant loss of some essential nutrients, especially the protein due to possible denaturation and autohydrolysis processes. Based on the drying rate, drying, energy utilization and seed's nutritional composition point of views, the drying of papaya seeds at 55ºC can be considered as the most promising drying condition for commercial applications. The steps that can be taken for further research development are to recycle the hot air that comes out with the dry product or an integrated drying process. Thus, energy demand can be minimized, economic efficiency increases, and dry product quality is maintained.

**Keywords:** Drying kinetics; Energy; Exergy; Nutritional; Papaya seeds; Physical properties.

## Acknowledgment

This study is fully funded by the Directorate General of Higher Education, Ministry of Education, Culture, Research and Technology, Republic of Indonesia. Misbahudin Alhanif received scholarship assistance from the Program Magister Menuju Doktor Sarjana Unggul (PMDSU) for M. Eng. And Ph.D. studies.

## References

[1] C. S. Pavithra, S. S. Devi, J. W. Suneetha, and C. V Durga Rani, "Nutritional properties of papaya peel," *Pharma Innov. J. NAAS Rat. TPI*, vol. 6, no. 7, pp. 170–173, 2017.
[2] I. S. Afolabi and K. Ofobrukweta, "Physicochemical and nutritional qualities of Carica papaya seed products," *J. Med. Plants Res.*, vol. 5, no. 14, pp. 3113–3117, 2011.
[3] B. Mocelin *et al.*, "Mathematical modeling of thin layer drying of papaya seeds in a tunnel dryer using particle swarm optimization method," *Part. Sci. Technol. An Int. J.*, vol. 32, no. 2, pp. 123–130, 2014.
[4] B. A. Fu, M. Q. Chen, and Q. H. Li, "Heat transfer characteristics and drying kinetics of hematite thin layer during hot air convection," *Thermochim. Acta*, vol. 682, no. May, pp. 1–7, 2019.
[5] O. D. Ogundele, S. Thompson, K. Lawalsonsimisola, and B. F. Demehin, "Effects of Drying Temperature on Proximate Composition and Effects of Drying Temperature on Proximate Composition and Functional Properties of," *Int. J. Recent*

*Innov. Food Sci. Nutr.*, vol. 2, no. 1, pp. 24–33, 2019.

[6] A. C. Storer and R. Ménard, "Papain," *Handb. Proteolytic Enzym.*, vol. 2, pp. 1858–1861, 2013.

[7] Q. Fang, J. Sun, D. Cao, Y. Tuo, S. Jiang, and G. Mu, "Experimental and modelling study of the denaturation of milk protein by heat treatment," *Korean J. Food Sci. Anim. Resour.*, vol. 37, no. 1, pp. 44–51, 2017.

2ND ENERGY SECURITY AND CHEMICAL ENGINEERING CONGRESS 2021
*"Sustainable Technological Solution for a Better World"*
VIRTUAL CONFERENCE | 3-5 NOVEMBER 2021

**FOOD SCIENCE AND TECHNOLOGY**

**Paper ID: ESCE106**

# EFFECTS OF PRETREATMENT METHOD ON ANTIOXIDANT ACTIVITY OF *FICUS RACEMOSA* (L.) FRUITS

**Thi-Thuy-Dieu Vo[1], Chi-Dung Tran[1], Quoc-Duy Nguyen[1], Thi-Van-Linh Nguyen[1], Thi-Thuy-Dung Nguyen[1]***

[1] *Faculty of Environmental and Food Engineering, Nguyen Tat Thanh University, 700000, Ho Chi Minh City, Vietnam.*
*Corresponding author: dungntt@ntt.edu.vn

## Extended Abstract

*Ficus racemosa* (L.) belongs to the Moraceae family, and this plant has been shown to have an abundant source of phytochemicals and health benefits. It has been widely used in traditional medicine to prevent, treat or cure many diseases such as diseases of the stomach, hyperglycemia, cough, sore throat, kidney, urinary, etc.; and it is also used as food in some countries. The study aimed to evaluate the influence of the pretreatment method on the biological activity of *F. racemosa* (L.) dried fruits to determine the suitable processing parameters to process this material into a high bioactive compound food - medicine products. Specifically, the fruits of *F. racemosa* (L.) were collected from the local area of Ho Chi Minh, Vietnam. These fruits have been sliced, soaked in citric acid 1% (w/v) for 20 minutes, and blanching or blanching and freezing treatment. For blanching method, including steam blanching and hot water blanching, were investigated with time blanching as a factor. For the blanching and freezing method, blanching parameters before freezing at -18 ºC were evaluated with time or temperature blanching as a factor. The one-factor-at-a-time or temperature was used to design the experiment in which four-level. After each pretreatment condition, the sample was dried at 60 °C by hot air drying until the moisture content reached 0.05 g/g of sample on the dry basis (d.b). Then, the dried sample was analyzed to determine the total phenolic content, antioxidant activity by DPPH radical scavenging assay and ferric reducing antioxidant power (FRAP) assay.

The findings indicated that blanching (steam blanching and hot water blanching) is not conducive to maintaining the antioxidant activity of *F. racemosa* fruits. In blanching and freezing before drying, blanching with steam for 2 minutes or blanching with water at 80 ºC for 2 minutes improves the antioxidant activity of the product by about 1.6 to 2 times compared with no blanching. Further studies were required to determine the impact of the drying process on the antioxidant activity of the product to increase the applicability of materials in food - medicine processing.

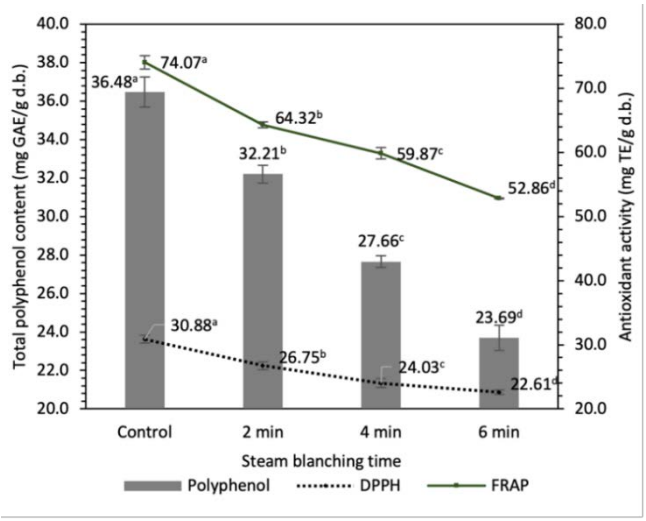


Fig. 1: Effect of steam blanching time on bioactive compounds of *F. racemosa* fruits.

**FOOD SCIENCE AND TECHNOLOGY**

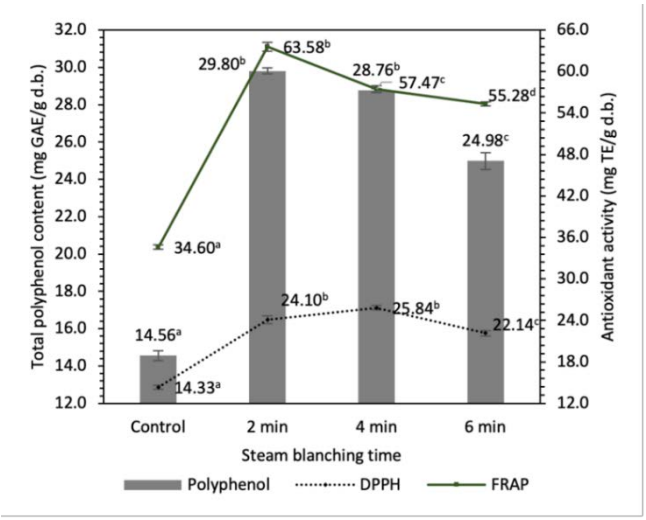


Fig. 2: Effect of steam blanching time on bioactive compounds of frozen *F. racemosa* fruits.

**Keywords:** Antioxidant activity; Blanching; *Ficus racemosa*; Polyphenol.

## Acknowledgment

This research is funded by Nguyen Tat Thanh University (Foundation for Science and Technology Development under the grant 2021.01.22, Ho Chi Minh city, Vietnam.

## References

[1] A. R. Shiksharthi and S. Mittal. (2011) Ficus Racemosa: Phytochemistry, Traditional Uses and Pharmacological Properties: A Review. Int. J. Recent Adv. Pharm. Res., 4:6–15.
[2] A. K. Mohiuddin and S. A. Lia. (2020) Medicinal & Biological Investigations of Ficus Racemosa.1:2:29–81.
[3] A. H. M. Zulfiker, M. R. Saha, S. Sarwar, L. Nahar, K. Hamid, and M. S. Rana. (2011) Hypoglycemic and in vitro antioxidant activity of ethanolic extracts of Ficus racemosa Linn. fruits. Am. J. Sci. Ind. Res., 2:3:391–400.
[4] J. García-Parra, R. Contador, J. Delgado-Adámez, F. González-Cebrino, and R. Ramírez. (2014) The applied pretreatment (blanching, ascorbic acid) at the manufacture process affects the quality of nectarine purée processed by hydrostatic high pressure. Int. J. Food Sci. Technol., 49:4:1203–1214.
[5] X. Sun, X. Jin, N. Fu, and X. Chen. (2020) Effects of different pretreatment methods on the drying characteristics and quality of potatoes. Food Sci. Nutr., 8:11:5767–5775.
[6] R. P. C. Powers, Joseph R, Jose´I.ReyesDeCorcuera. (2004) Blanching of Foods. Encycl. Agric., Food, Biol. Eng., 1–5.
[7] H. Wang, Q. Fu, S. Chen, Z. Hu, and H. Xie. (2011) Effect of hot-water blanching pretreatment on drying characteristics and product qualities for the novel integrated freeze-drying of apple slices. J. Food Qual.
[8] L.-Z. Deng et al. (2019) Chemical and physical pretreatments of fruits and vegetables: Effects on drying characteristics and quality attributes–a comprehensive review. Crit. Rev. Food Sci. Nutr., 59:9:1408–1432.
[9] I. F. F. Benzie and M. Devaki. (2017) The ferric reducing/antioxidant power (FRAP) assay for non-enzymatic antioxidant capacity: Concepts, procedures, limitations and applications. Meas. Antioxid. Act. Capacit. Recent Trends Appl., 77–106.
[10] J. Hou, L. Liang, M. Su, T. Yang, X. Mao, and Y. Wang. (2021) Variations in phenolic acids and antioxidant activity of navel orange at different growth stages. Food Chem., 360:129980.
[11] N. Abu-Ghannam and A. K. Jaiswal. (2015) Blanching as a treatment process: effect on polyphenol and antioxidant capacity of cabbage. Processing and impact on active components in food, Elsevier, 35–4.
[12] R. Moscetti, F. Raponi, D. Monarca, G. Bedini, S. Ferri, and R. Massantini. (2019) Effects of hot-water and steam blanching of sliced potato on polyphenol oxidase activity. Int. J. Food Sci. Technol., 54:2:403–411.
[13] N. Abu-Ghannam and A. K. Jaiswal. (2015) Blanching as a Treatment Process: Effect on Polyphenol and Antioxidant Capacity of Cabbage. Elsevier Inc.
[14] B. Liu, X. Fan, C. Shu, W. Zhang, and W. Jiang. (2019) Comparison of non-contact blanching and traditional blanching pretreatment in improving the product quality, bioactive compounds, and antioxidant capacity of vacuum-dehydrated apricot. J. Food Process. Preserv., 43:3:e13890.

**FOOD SCIENCE AND TECHNOLOGY**

**Paper ID: ESCE119**

# ASSESSMENT OF TOTAL FLAVONOID CONTENTS AND FERRIC REDUCING ANTIOXIDANT POWER IN SEVERAL GREEN AND OOLONG TEA PRODUCTS IN VIETNAM

**Le-Thi Anh-Dao[1], Nguyen Thanh-Nho[1]*, Dang Minh-Phuc[1], Do Minh-Huy[1] and Nguyen Cong-Hau[1]***

[1] *Faculty of Environmental and Food Engineering, Nguyen Tat Thanh University.*
*Corresponding author: nchau@ntt.edu.vn and ntnho@ntt.edu.vn

## Extended Abstract

Tea trees have a long history of cultivation and utilization worldwide, and tea is considered among the most popular beverages, besides water, coffee, and cocoa. According to Chinese mythology, the tea plants were discovered thousands of years ago in South-East Asia, and mankind has been drinking tea for thousands of years due to its medical benefits to prevent and treat a lot of diseases, typically cancers (respiratory, digestive, and urinary) and cardiovascular disorder [1]. The tea polyphenols also help to prevent mutations in genetic materials, regulate detoxification enzyme activities, and inhibit tumorigenesis. *In vivo* tests proved that the tea polyphenols had the ability to increase rat serum catalase, glutathione peroxidase, and superoxide dismutase levels, also reduce the production of malondialdehyde [1, 2]. The habit of drinking tea is considered an art of life and health benefits. Tea leaves have been used to produce tea infusions, and there are many types of tea products depending on the degree of oxidation processes such as white, green, oolong, black or red teas. Thanks to the development of analytical chemistry and biological tests, we are able to better known the various metabolites, particularly the catechins, contributing to the antioxidant capacities. Flavonoid is the most abundant type of phenolic compound present in tea and considered the most important constituent of tea because it is the largest component and behaves as bioactive ingredient to enhance the therapeutic action of tea. In this study, green and oolong tea products were collected in two specific tea-tree plantation regions in the mountainous area (Yen Bai Province-YB, the North) and Central Highland (Da Lat-DL and Lam Ha-LH, Lam Dong Province, the South) of Vietnam for the assessment of the total flavonoid contents (TFCs) and ferric reducing antioxidant power (FRAP). Prior to the coloring procedures for TFCs and FRAP for the measurement by molecular absorption spectrophotometry, the tea products were extracted according to ISO 14502-1:2005 with some modification [3]. Briefly, $0.1(\pm 0.001)$ g of ground tea sample was endure the ultrasound-assisted liquid extraction by 10.00 mL of methanol:deionized water (7:3) within 20 minutes (two extraction times and 10 minutes per each). The TFCs of the extracts were determined by the assay of Kim et al. (2003) [4]. A volume of 1.00 mL of the extract was added to a 300 µ*L* 5 % sodium nitrite solution, followed by 300 µ*L* 5% aluminium chloride. The mixture was incubated at the ambient temperature for five minutes. After that, 2.00 mL of 1 mol $L^{-1}$ sodium hydroxide was added. Then, the reaction mixture was diluted to 10.00 mL by deionized water and shaken thoroughly. The absorbance was measured at 510 nm and quercetin (QE) was used to build up the calibration curve. The TFCs were reported as milligrams quercetin equivalents per gram dried weight (mg QE $g^{-1}$ DW). For FRAP, the assay was followed the published procedure of Benzie et al. (1996) [5]. Shortly, the extract of 100 µL was mixed with 3.00 mL of FRAP reagent (a mixture of 300 mmol $L^{-1}$ sodium acetate-acetic acid buffer, 10 mmol $L^{-1}$ TPTZ solution, and 20 mmol $L^{-1}$ ferric chloride solution at a volume ratio of 10:1:1). The reaction was carried out at room temperature within 4 minutes, and the absorbance was recorded at 593 nm. Trolox was used as a standard, and the results were expressed as micromole Trolox per gram dried weight (µmol $g^{-1}$ DW). The variations of TFCs among several tea products were performed in Figure 1.

**FOOD SCIENCE AND TECHNOLOGY**

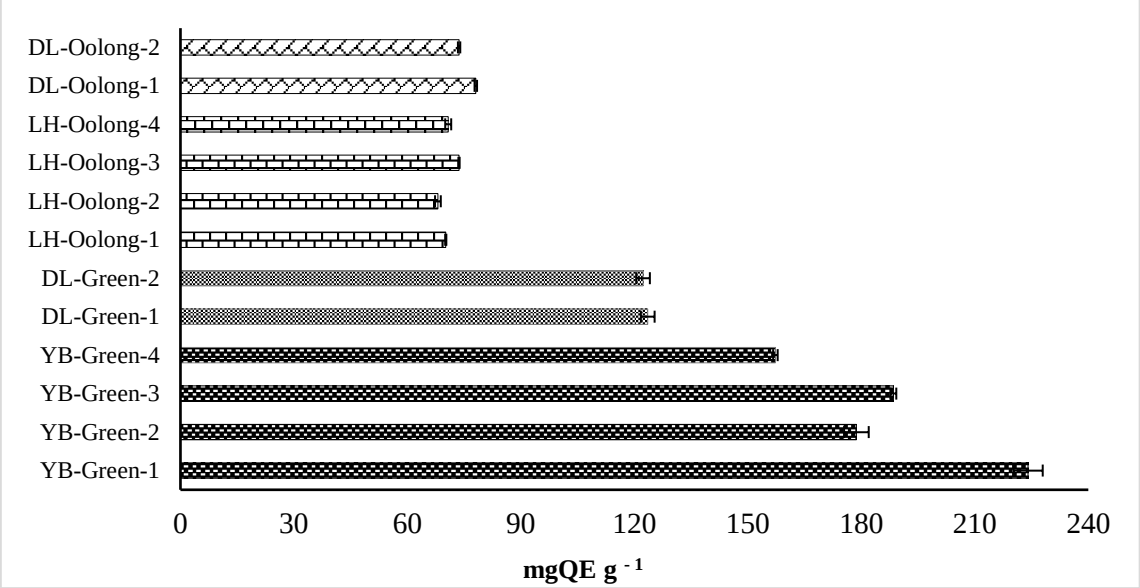


Fig 1: Variations in total flavonoid contents in several green and oolong tea products.

As present in Figure 1, the TFCs of various tea products were varied from 68.06 to 224.06 mg QE $g^{-1}$ with the highest and lowest values recorded in YB-Green-1 and LH-Oolong-2, respectively. The variations in TFCs could be explained due to the different tea species and degrees of oxidation during the fermentation process between green (non-fermented) and oolong (partly fermented) tea products. The processing period, typically the fermentation had certain effects on the antioxidant behavior of tea products due to the oxidation.

**Keywords:** Tea-tree plantation; Total flavonoid; Ferric reducing; Tea products.

## Acknowledgment

This research is funded by Nguyen Tat Thanh University, Ho Chi Minh City, Vietnam under grant number 2021.01.21/ HĐ-KHCN.

## References

[1] Yan Z., Zhong Y., Duan Y., Chen Q. and Li F. (2020) Antioxidant mechanism of tea polyphenols and its impact on health benefits. Anim. Nutr. 6:115–123.
[2] Gramza A., Korczak J. and Amarowicz R. (2005) Tea polyphenols-Their antioxidant properties and biological activity-A review. Polish J. Food Nutr. Sci. 14:219.
[3] ISO-14502-1 (2005) Determination of substances characteristic of green and black tea.
[4] Kim D., Jeong S. and Lee C. (2003) Antioxidant capacity of phenolic phytochemicals from various cultivars of plums. Food Chem. 81:321–326.
[5] Benzie I. and Strain J. (1996) The Ferric Reducing Ability of Plasma (FRAP) as a Measure of "Antioxidant Power": The FRAP Assay. Anal. Biochem. 239:70–76.

**FOOD SCIENCE AND TECHNOLOGY**

**Paper ID: ESCE170**

# PHYSICOCHEMICAL AND MICROBIAL ANALYSIS OF PLANT-BASED FOODWASTE AND POTENTIAL USED AS AN ANIMAL FEED

**W. Nordalilah[1], M. H. Husna Hawa[1], W. Y. Wan Nur Suzilla[1]*, J. Rabiatul Alawiyah[1], M. K. Mohd Mukriz[2], A. R. Mohd Ridzuan[2]**

[1] *Department of Food Technology, Politeknik Sultan Haji Ahmad Shah, Semambu, 25350 Kuantan, Pahang.*
[2] *Department of Agrotechnology and Bio-Industry, Politeknik Jeli Kelantan, Jalan Timur-Barat, 17600 Jeli, Kelantan.*
*Corresponding author: wnsuzilla@polisas.edu.my

## Extended Abstract

One-third of all food produced is lost or wasted globally, amounting to 1.3 billion tonnes (Amaha, Sasaki, and Segawa 1992). Food losses that occur at the end phases of the food supply chain, namely retail and ultimate consumption, are referred to as "food waste". Food waste refers to wasted food nutrients of high quality intended for human consumption and as a result, it usually has a high nutritional value (Afreen and Ucak 2020). By 2025, rising demand for animal products is expected to drive up demand for feed, particularly coarse grains like maize and protein meals (Ominski et al. 2021). Food waste might be utilised to replace a portion of cereal grains and plant protein sources used in animal feeding, reducing food rivalry between people and animals. Furthermore, feed expenses are a key component of meat production and have an influence on financial profits (Truong et al. 2019). As a result of the lower cost of food waste compared to conventional feeds, manufacturing expenses might be reduced (Rahman et al. 2014). Hence, this present study is aimed to evaluate the potential of the plant based food waste such as soybean meal or dreg, pineapple waste and coconut waste to be developed as an animal feed.

In this study, there were two main analyses conducted which are physicochemical analysis of the plant-based food waste involved the physical analysis such as particle size determination and moisture content analysis followed by proximate quantification of fat, protein, crude fiber and ash. From the results, it was showed that coconut waste gave the highest reading of the total yield recovery which is 43.60%, followed by soybean waste 27.58% and pineapple waste 22.91%. For the particle size determination, it was revealed that, all the samples size ranges from 600µm - 850µm. This particle size results were in the optimum range of particle size for animal feed which is between 600-900µm. For the moisture content analysis, it was found that all samples have moisture content below 10% which is suitable to be produced as an animal feed. Determination of moisture content is very crucial as this parameter can influence the shelf life of the product. For the fat content determination, it was found that coconut waste gave the highest content which was 39.17±0.58 %, followed by soybean waste 33.03±0.59 % and the lowest is in the pineapple waste which was 13.67±0.50 %. For the protein content analysis, the highest protein content (7.27±0.67) was found in soybean waste, followed by pineapple waste 1.81±0.03% and coconut waste 0.18±0.0=59%. For the ash content analysis, the highest ash content (10.33±0.12%) was found in pineapple waste followed by soybean waste (7.60±0.20%) and coconut waste 2.8±0.03%. Finally, the crude fiber analysis revealed that, soybean waste gave the highest amount of fibre content which was 101.17±0.10% followed by pineapple waste 88.1±0.10% and lowest in coconut waste 48.67±0.12%. From the results, it was observed that, all this wastes still have a good nutritional content which can benefit the animals by reused it as an animal feed.

**FOOD SCIENCE AND TECHNOLOGY**

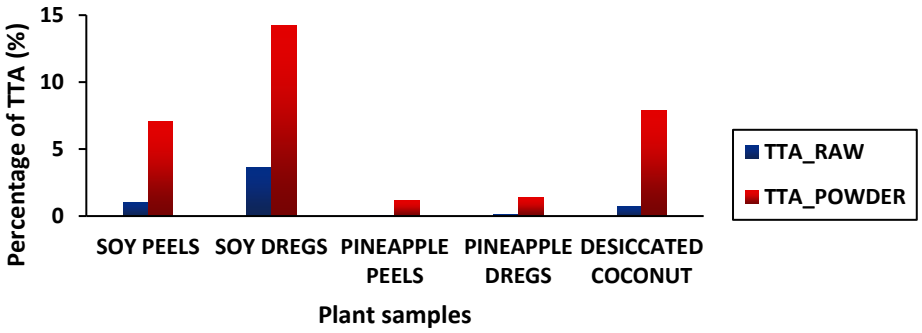


Fig. 1: Percentage of Total Titratable Acidity (TTA) on various of plant waste.

Besides that, for the microbial analysis, it was involved the pH value and total titratable acidity (TTA) analysis followed by Total Plate Count (TPC) to determine the presence of selected bacteria strain such as *E. coli, Lactobacillus* and *Salmonella sp.* For the pH determination, it was found that soybean waste has the lowest pH value which was 4.4±0.01, followed by pineapple waste 5.3±0.5 and coconut waste 6.37± 0.15. From these results, it was observed that soybean waste might have longer shelf life if it was recycled as animal feed as the pH value is most acidic. In general, food with a pH below 4.5 bacterial pathogens will not survive and lower pH value can serve a better environment for the growth of lactic acid bacteria that important in animal feed. For the TTA analysis, soybean waste was found to have highest total acid value which was 4.65±0.19 followed by the pineapple waste 0.69±0.29and coconut waste 0.188±0.02 (Fig 1). These findings correlated with the pH value where the more acidic pH will give higher total acid content. The higher the percentages of total acid are positive correlation with the lactic acid of samples. The highest lactic acid in samples will give the lower pH value of sample. For the TPC analysis, it was observed that for the quantification of the random colonies, soybean waste gave the lowest colony growth which was $6.1x10^2$ cfu/g followed by the pineapple waste $1.4x10^4$ cfu/g and coconut waste $9.5x10^4$ cfu/g. These results can be correlated with the previous data where it was revealed that soybean waste which have the most acidic pH and highest total acid content, have the least growth of the bacterial colony. For the coconut waste which have the almost neutral pH showed the highest colony growth. TPC analysis also conducted to monitor the growth of the selected common food related bacteria species such as *E.Coli, Lactobacillus sp and Salmonella sp.* For the *E.Coli*, it was found that the most growth colony was in pineapple waste ($1.1x10^4$ cfu/g). This result may due to the nature of the pineapple which plant in the soil. For the TPC analysis of *Lactobacillus sp*, it was observed that soybean waste gave the highest colony growth due to the acidic nature of the waste. Acidic condition will promote the growth of the acid tolerate *Lactobacillus sp* bacteria. Finally, for the TPC of the Salmonella sp, all three samples gave negative results where no growth of the colony were observed. From the study, it was showed that soybean waste gave good nutritional content and as for the microbial aspect the findings in compliance with the Microbiology Quality Standard with acceptable range for pH (5.5-7.0), *E.coli* ($10^3$-$10^5$), *Lactobacillus* (< $1.0x10^9$ cfu/g), TPC ($3.0x10^5$ cfu/g for older animals) and ($5.0x10^5$ cfu/g for younger animals) and *Salmonella* (Not Detected). Hence, the soybean waste has the potential to be developed as an animal or fish feed for the future used as one of the more prominent and nature-friendly food waste handling methods which support the sustainable food waste management system and suitable for future implementation in Malaysia.

**Keywords:** Foodwaste; Physicochemical; Antimicrobial; Animal Feed; Plant.

## Acknowledgment

This study was supported by TVET Applied Research Grant Scheme (TARGS) (1001/21). We also would like to thank Department of Food Technology, Politeknik Sultan Haji Ahmad Shah (POLISAS) and Department of Agrotechnology and Bio-Industry, Politeknik Jeli Kelantan for providing the equipments and facilities used in this project.

## References

[1] Afreen, M., and I. Ucak. (2020) Fish Processing Wastes Used as Feed Ingredient for Animal Feed and Aquaculture Feed. Journal of Survey in Fisheries Sciences 6(2): 55–64.
[2] Amaha, K, Y Sasaki, and T Segawa. (1992) Utilization of Tofu (Soybean Curd) by-product as feed for cattle. Characteristics of Fermentation 1–8.

## FOOD SCIENCE AND TECHNOLOGY

[3] Ominski, Kim et al. (2021) Utilization of By-Products and Food Waste in Livestock Production Systems: A Canadian Perspective. Animal Frontiers 11(2): 55–63.
[4] Rahman, Mohammad Mijanur et al. (2014) Feed Intake and Growth Performance of Goats Supplemented with Soy Waste. Pesquisa Agropecuaria Brasileira 49(7): 554–58.
[5] Truong, Linda, Dan Morash, Yanhong Liu, and Annie King. (2019) Food Waste in Animal Feed with a Focus on Use for Broilers. International Journal of Recycling of Organic Waste in Agriculture 8(4): 41729. https://doi.org/10.1007/s40093-019-0276-4.

2ND ENERGY SECURITY AND CHEMICAL ENGINEERING CONGRESS 2021
*"Sustainable Technological Solution for a Better World"*
VIRTUAL CONFERENCE | 3-5 NOVEMBER 2021

**FOOD SCIENCE AND TECHNOLOGY**

**Paper ID: ESCE201**

# A SHORT REVIEW ON PRODUCTION OF ENZYME TREATED SPRAY DRIED TOMATO POWDER

**S M Anisuzzaman[1,2], Collin G. Joseph[3]*, Cleanelley Cosmas[2], Janice L. H. Nga[4]**

[1] *Energy Research Unit (ERU),* [2] *Chemical engineering Programme, Faculty of Engineering,*
[3] *Industrial Chemistry Programme, Faculty of Science and Natural Resources,*
[4] *Planning and Development Economics Programme, Faculty of Business, Economics and Accountancy,*
*Universiti Malaysia Sabah, 88400 Kota Kinabalu, Sabah, Malaysia.*
*Corresponding author: collin@ums.edu.my

## Extended Abstract

This study aims to review papers from different researchers in order to investigate and observe the effect of enzyme and carrier agent into the physicochemical properties of the spray dried tomato powder. In this recent year, consumer demand for high quality and minimally processed goods has skyrocketed despite all the increase in fresh tomato production. Tomatoes which are usually in red colour due to the high lycopene content in it have contributed to the acceptance of the product [1]. Therefore, apart from processing the tomato for a longer lifespan, it is important to maintain its colour at the end of the product produced. Spray drying in the drying process of fruit or vegetable into powder is more effective as it is found that compared to freeze drying method, the spray drying method is much more cost effective due to lower power usage and a faster drying rate [2,3]. Furthermore, spray drying provided several advantages, including a short drying contact time that resulted in the preservation of critical quality features such as nutrition, colour, and so on. Apart from that, the spray drying technology also has benefits on producing a product with a high stability because of its low moisture content as well as low water activity. However, it still does have its own limitations. Spray drying technology has a low thermal efficiency because of the hot air circulation inside the spray drying chamber that has no interaction between the spray droplets. According to Dalmoro et al. [4], spray drying has little control over droplet size, resulting in particles with a wide size distribution and occasionally uneven microstructure. Other than that, the material that is rich in sugar also will be difficult to dry using the spray drying without the addition of carrier agents into the feedstock. This is because sugar-rich materials are sticky and have a low glass transition temperature ($T_g$).

The main purpose of the carrier agent in the powder production using spray drying are actually to increase the yield production and decrease powdered product stickiness and hygroscopicity. Gum Arabic, maltodextrins, gelatine, starches, pectin, methyl cellulose, alginates, and tricalcium phosphate are the most often utilised carrier agents [5,6]. Therefore, the addition of carrier agent into the material used especially with a high sugar content material is necessary in order to mitigate the stickiness problem as well as the low $T_g$ which is actually the main reason for the drying difficulties and wall deposition problem [7]. The application of enzyme treatment into the material before the spray drying process gives a significant effect into the powder product derived from fruit and vegetables. According to Chang et al. [8], the removal of water throughout the drying process has significantly consumed energy which has led to a higher production cost. The enzymatic treatment is proposed by several researchers in order to mitigate this problem which is mainly caused by the higher consumption of energy in the production process [9-14]. Wong and Tan, [10] have found that the application of enzyme in spray drying was the best parameter as it helps the samples to produce a lower viscosity. The usage of enzymes, particularly in the juice and beverage sector, is primarily to boost yield extraction, improve the effectiveness of spray drying operations, liquefy the fruit before processing, improve colour and fragrance, clarify the juice, and hydrolyse insoluble components. However, it is still important to find the best or the optimum conditions of the spray drying as well as the enzyme conditions such as temperature, concentration and time.

The application of enzyme activation with the carrier agents in the spray dried tomato powder have brought significant results as it was found to increase the quality of the tomato powder. The enzyme increases and enhances the total solid content as well as reducing the stickiness of the tomato slurry before going into the drying process in spray drying. The high total solid content in the liquid feed has resulted in an increase of powder yield when the inlet drying temperature is constant. Hence, the powder yield will be found to decrease when the carrier agent's

concentration is increased. Meanwhile, the moisture content tends to decrease when there is an increase in the maltodextrin concentration and the inlet drying temperature. A higher water activity and a higher inlet drying temperature in the tomato powder have significantly reduced the antioxidant activity of the powder product. This can be explained by the damage of the sensitive compound inside the tomato powder as it is highly affected by the changes in temperature. Apart from that, the hygroscopicity is also reduced when the carrier agent's concentration and the moisture content is high. The increase and decrease of all the parameters have pros and cons to the spray-dried tomato powder. Therefore, all it needs is to find the optimum conditions for the spray drying to produce a high quality with maximum benefits to the consumers. It can be concluded that even though all the enzymes that have been certified as safe for food application does not really bring harm to humans, a safety measure must be done.

**Keywords:** Antioxidant; Lycopene; Maltodextrin; Pectinase; Spray Drying.

## Acknowledgement

The authors would like to acknowledge the financial support given by the Universiti Malaysia Sabah, under the SDN Grant Scheme, with code DN21100-Phase 1/2021 to undertake this project.

## References

[1] M. Nguyen, S. Schwartz, *Food Technol.* **1999**, *53*, 38-45.
[2] C. Hammami, F. Rene, *J. Food Eng.* **1997**, *32(2)*, 133-154. DOI: https://doi.org/10.1016/S0260-8774(97)00023-X.
[3] C. Santivarangkna, U. Kulozik, P. Foerst, *Biotechnol. Prog.* **2007**, *23(2)*, 302-315. DOI: 10.1021/bp060268f.
[4] A. Dalmoro, A. Barba, G. Lamberti, M. d'amore, *Eur. J. Pharm. Biopharm.* **2012**, *80(3)*, 471-477. DOI: https://doi.org/10.1016/j.ejpb.2012.01.006.
[5] M. Igual, S. Ramires, L. Mosquera, N. Martinez-Navarrete, *Powder Technol.* **2014**, *256*, 233-238. DOI: https://doi.org/10.1016/j.powtec.2014.02.003.
[6] V. Truong, B. R. Bhandari, T. Howes, *J. Food Eng.* **2005**, 71(1), 66-72. DOI: 10.1016/j.jfoodeng.2004.10.018.
[7] B. R. Bhandari, N. Datta, T. Howes, *Drying Technol.* **1997**, *15(2)*, 671-684. DOI: https://doi.org/10.1080/07373939708917253.
[8] L. S. Chang, S. M. Yau Yong, L. P. Pui, *Walailak J. Sci. & Tech.* **2021,** *18(1)*, 1-15, DOI:10.48048/WJST.2021.6922.
[9] L. S. Chang, Y. Tan, L. P. Pui, L. *Brazilian J. Food Technol.*, **2020**, *23*, 1-16.DOI: https://doi.org/10.1590/1981-6723.18119.
[10] C. W. Wong, H. Tan, *J. Food Eng. Teachnol.* **2017,** 54, 564-571, DOI:10.1007/s13197017-2501-3.
[11] L. Chang, R. Karim, S. Abdulkarim, H. Mohd Ghazali, *J. Food Process Eng.* **2018,** *41*, 1-12. DOI: https://doi.org/10.1111/jfpe.12688.
[12] J. A. Grabowski, V. D. Truong, C. R. Daubert, *Food Eng. Phys. Prop.* **2006**. 71(5), 209-217. DOI: https://doi.org/10.1111/j.1750-3841.2006.00036.x.
[13] M. Kyereme, S. Hale, B. E. Farkas, *J. Food Process Eng.* **1999**. *22*, 235-247 DOI: https://doi.org/10.1111/j.1745-4530.1999.tb00483.x.
[14] C. Wong, L. Pui, J. Ng, *Int. Food Res. J*,. **2015** , *22(4)*, 1631-1636.

**FOOD SCIENCE AND TECHNOLOGY**

**Paper ID: ESCE202**

# REFRACTANCE WINDOW DRYING OF MANGO PULP (*MANGIFERA INDICA*): IMPACT OF HYDROCOLLOIDS ON DRYING CHARACTERISTICS AND COLOR PARAMETERS

**Thi-Van-Linh Nguyen[1]*, Phuoc-Tai Ngo[1], Thi-To-Na Huynh[1], Pham-Quynh-Tram Vo[1], Thi-Ngoc-Anh Hoang[1], Phuoc-Bao-Duy Nguyen[2]**

[1] *Faculty of Environmental and Food Engineering, Nguyen Tat Thanh University, 700000, Ho Chi Minh city, Vietnam.*
[2] *Faculty of Electrical and Electronics Engineering, Vietnam National University Ho Chi Minh city (VNU-HCM), 700000, Ho Chi Minh city, Vietnam.*
*Corresponding author: ntvlinh@ntt.edu.vn

## Extended Abstract

Mango (*Mangifera indica*) is a tropical fruit popularly distributed in India, China, Thailand, Indonesia, Vietnam, etc. Mango possesses high nutritional value containing proteins, carbohydrates, fibers, lipids, amino acids, vitamins, minerals, and phytochemicals (phenolic acids, flavonoids, carotenoids) [1–3]. Mango was considered to belong to the group of tropical fruits with the top increased consumption with high economic value [4, 5] . However, because of the high respiratory activity of mango, leading to the perishability quickly after harvest, it could cause higher losses during postharvest and then limit the distribution and trade [6].

To overcome these drawbacks, food processing would significantly extend shelf-life and develop a new product from mango, bringing added value to mango. Among processed products from mango, mango powder was drawn a lot of interest because fruit powders are considered convenient ingredients in developing other industrial food products (e.g., beverages, baby foods, sauces, confectioneries, yogurts, nutrition bars, etc.) [7]. Besides, moisture removal in fruit powder production reduced volume and weight, so the cost in distribution, storage, packaging was lower [8]. Powder production from mango pulp is an innovative technique but has not been applied efficiently yet. Recently, Refractance window (R.W.) drying is an innovative technology designed to remove moisture from fruit purees to produce powder, leather, or concentrated product [9]. R.W. method was proved to retain the sufficiently high quality of fruits and vegetables such as carrots, strawberries [10], green asparagus purees [11]. Mango powder using R.W. drying had a better physical quality than drum-, spray-drying [6, 8]. However, mango puree was just carried out without/with a fixed concentration of maltodextrin [6, 8].

In this study, the concentration of maltodextrin (6, 7.5, 9, and 10.5 %) and carrageenan (0.3, 0.6, 0.9, and 1.2 %) added mango pulp was investigated to determine the drying behavior and color change in the refractance window drying.

The results showed that the higher maltodextrin or carrageenan concentration was, the higher the drying rate and drying constants were. In a comparison of the control sample, the addition of maltodextrin showed adverse effects on the drying kinetic, but carrageenan with low concentrations (0.3 and 0.6 %) could increase the effectiveness in removing moisture.

**FOOD SCIENCE AND TECHNOLOGY**

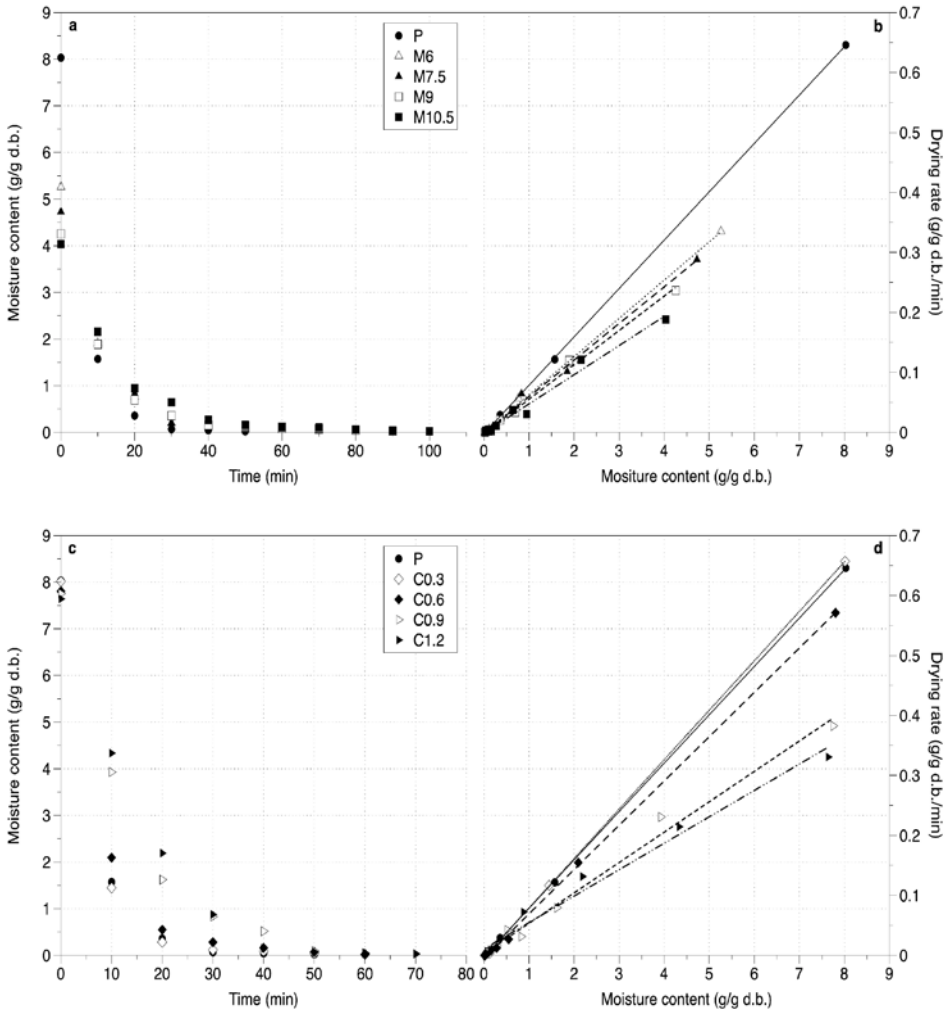


Fig. 1: The changes of moisture content during R.W. drying of different formulations (a, c); and the change drying rate versus moisture content in R.W. drying of different formulations (b, d). Note: P, M and C denoted Puree without hydrocolloids, Maltodextrin and Carrageenan, respectively.

Mathematical models of predicting moisture ratio for each hydrocolloid-supplemented mango pulp were found. The Weibull model was the best fit model for determining the behavior of R.W. drying of mango pulp. The values of Deff were estimated to range from $1.001\times10^{-10}$ to $2.420\times10^{-10}$ $m^2/s$ that is within the standard value range of $D_{eff}$ in typical food drying processes. The addition of hydrocolloid was found to improve the brightness of the dried product than the control sample. When hydrocolloid was used at a high amount (i.e. 9 % maltodextrin), that could obtain the lowest browning pigment in the product. So, hydrocolloids (such as maltodextrin and carrageenan) had significant impacts on drying kinetics and color of R.W. dried mango pulp, led to contribute to changes in the quality of dried products. Therefore, further study has to focus on evaluating the effects of hydrocolloids on the physicochemical properties of the dried product to determine the suitable drying condition obtained the best quality of the product.

**FOOD SCIENCE AND TECHNOLOGY**

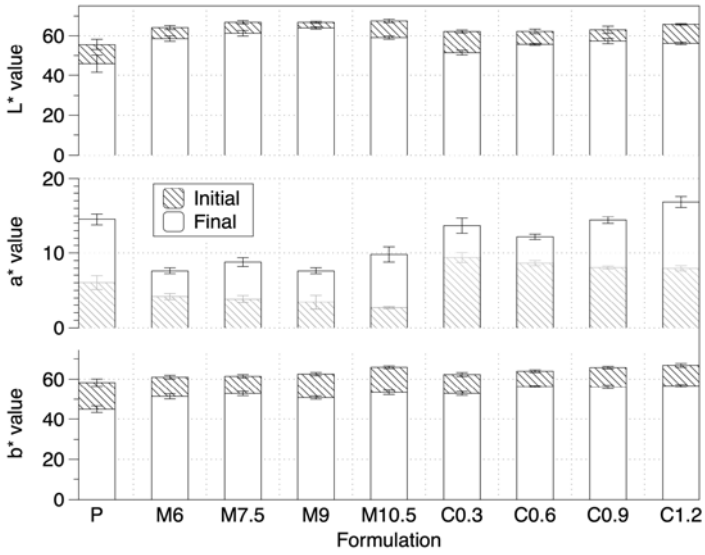


Fig. 2: Change of color parameters in the R.W. drying of mango pulp with different formulations. Note: P, M and C denoted Puree without hydrocolloids, Maltodextrin and Carrageenan, respectively.

**Keywords:** Color parameters; Drying characteristic; Hydrocolloids; Mango pulp; Refractance window drying.

## Acknowledgment

This study was funded by NTTU (Nguyen Tat Thanh University) Foundation for Science and Technology Development under the grant 2021.01.23.

## References

[1] Abbasi AM, Guo X, Fu X, Zhou L, Chen Y, Zhu Y, Yan H, Liu RH (2015) Comparative assessment of phenolic content and in vitro antioxidant capacity in the pulp and peel of mango cultivars. Int J Mol Sci 16:13507–13527.
[2] Haytowitz DB, Wu X, Bhagwat S (2018) USDA Database for the Flavonoid Content of Selected Foods, Release 3.3. US Dep Agric 173:
[3] Shariful H, Parveen B, Maksuda K, Islam SN (2015) Total carotenoid content in some mango (Mangifera indica) varieties of Bangladesh. Int J Pharm Sci Res IJPSR 6:4875–4878.
[4] Fitzpatrick JJ, Ahrné L (2005) Food powder handling and processing: Industry problems, knowledge barriers and research opportunities. Chem Eng Process Process Intensif 44:209–214.
[5] Occena-Po LG (2006) Banana, mango, and passion fruit. Handb Fruits Fruit Process 635.
[6] Caparino O, Tang J, Nindo C, Sablani S, Powers J, Fellman J (2012) Effect of drying methods on the physical properties and microstructures of mango (Philippine 'Carabao'var.) powder. J Food Eng 111:135–148.
[7] Ramaswamy HS, Marcotte M (2005) Food processing: principles and applications. CRC Press.
[8] Zotarelli MF, da Silva VM, Durigon A, Hubinger MD, Laurindo JB (2017) Production of mango powder by spray drying and cast-tape drying. Powder Technol 305:447–454.
[9] Vega-Mercado H, Góngora-Nieto MM, Barbosa-Cánovas GV (2001) Advances in dehydration of foods. J Food Eng 49:271–289.
[10] Nindo C, Tang J (2007) Refractance window dehydration technology: a novel contact drying method. Dry Technol 25:37–48.
[11] Abonyi B, Feng H, Tang J, Edwards C, Chew B, Mattinson D, Fellman J (2002) Quality retention in strawberry and carrot purees dried with Refractance WindowTM system. J Food Sci 67:1051–1056.

**HEAT AND MASS TRANSFER**

**Paper ID: ESCE049**

# ANALYSIS OF DE LAVAL ROCKET ENGINE NOZZLE USING COMPUTATIONAL FLUID DYNAMICS

**M. T. Ahmad[1]*, A. Jagannathan[1], A. Zhahir[2]*, M. H. Azami[3], R. Abidin[1], M. N. H. Noordin[1], N. Nordin[1]**

[1] *Faculty of Engineering, National Defence University of Malaysia, Kem Sungai Besi, 57000 Kuala Lumpur, Malaysia.*
[2] *Department of Aerospace Engineering, Faculty of Engineering, Universiti Putra Malaysia, 43400 UPM Serdang, Selangor, Malaysia.*
[3] *Kulliyyah of Engineering, International Islamic University Malaysia, Jalan Gombak, 53100 Kuala Lumpur, Malaysia.*
*Corresponding author: m.tarmizi@upnm.edu.my and amzari@upm.edu.my

## Extended Abstract

### 1. INTRODUCTION

Rocket engines generate thrust by ejecting high velocity and high pressures gases from the opening of a nozzle. The products of combustion is passed through a supersonic propelling nozzle which converts high combustion pressure energy into useful kinetic energy, hence provides maximum outlet velocity.

Nozzle design is a major step of the rocket development. The performance of a rocket depends to a great degree on its nozzle's performance in thermal energy conversion to kinetic energy.

### 2. LITERATURE REVIEW

The function of the nozzle is to efficiently transform the products of combustions into kinetic energy. De Laval found that when the nozzle first narrowed, the most effective transition occurred, raising the velocity of the gases to Mach one follow by further expansion of the gases. [1.2.3]. The nozzle inlet velocity is less than Mach one and it accelerates to the speed of sound in the throat for choked flow and then accelerates along the divergent portion to supersonic velocities.

CD nozzles design using CFD software were used by many researchers [4, 5, 6, and 7]. Recently there were more studies using CFD [8, 9, 10 and 11] on nozzle flow due to its accuracies as compared to theory. Rocket engines generate thrust by ejecting high velocity and high pressures gases from the opening of a nozzle. Rocket engines have the lightest, the fastest jet speeds and the lowest thermal efficiency of all jet propulsion system.

### 3. OBJECTIVES OF CFD ANALYSIS ON NOZZLE:

This study is done to support the UPNM Faculty of Engineering's research in developing green sustainable hybrid rocket fuel based on stearic acids which is a product of palm oil [15]. The main objective of the study is design and analyze the geometry of the CD nozzles using SOLIDWORK and Compare theoretical results with CFD results.

### 4. METHODOLOGY

In this project, we design and analyze the geometry of the CD nozzles using the CFD (Computational Fluid Dynamics) SOLID WORKS 2010 software. To model both low-speed and supersonic flows, one can use this CFD solution.

The formulated equations, the velocity, temperature and pressure were determined theoretically for different nozzle sections. The theoretical results were used to validate the computer simulation technique.

**HEAT AND MASS TRANSFER**

## 5. RESULTS

The Temperature, Velocity and Pressure contours along the nozzle axis were computed and analyzed. The CFD results show a rapid reduction in the pressure just after the section of the throat due to the shock wave. The velocity value is Mach 1 in the nozzle's throat. This condition is referred to as a condition of choked flow The CFD results show close resemblance with theoretical results.

Figure 1 shows that the CFD Pressures profile versus Area ration graph and comparison with theoretical results.

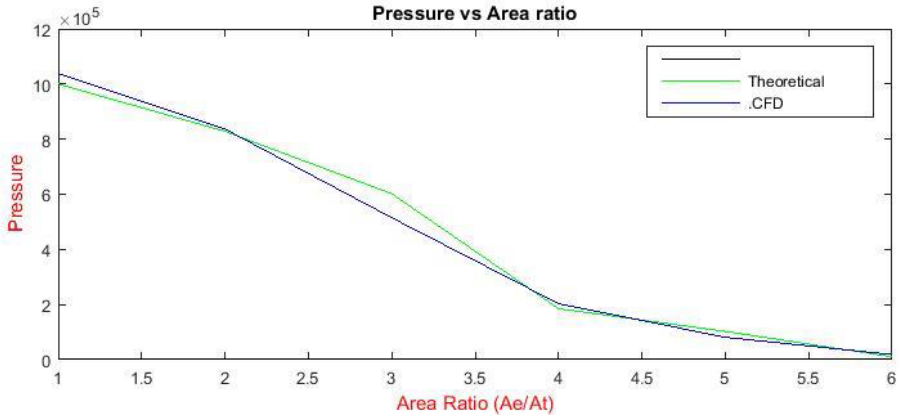


Fig. 1: Pressure plot of CFD results against theoretical Results.

## 6. CONCLUSION

Using CFD, computer-aided solutions are developed. It defines mass flow rates, maximum velocity and maximum pressure. With Mach number, variation in static pressure rises. The variations in velocities at certain given pressures of convergent and divergent nozzle are analyzed in this project. The results obtained with computational modelling (CFD) are almost identical to the results obtained theoretically

**Keywords:** SolidWork; Propellant; Nozzle; Propulsion; C-D nozzle.

### Acknowledgment

The authors would like to thank Brig Gen Prof. Ir. Dr. Norazman Bin Mohamad Nor (Retired) of the National Defence University of Malaysia and his working group; Universiti Putra Malaysia and Tan Sri Syed Azman Syed Ibrahim Endowment Fund (Geran Penyelidikan Industri (Endowmen Tan Sri Syed Azman) No. 2/2020 [Aerodynamic Performance of Two Seater DragonFly Hoverwing]) for funding and support of our research.

### References

[1] P. Parthiban, M. Robert Sagayadoss, T. Ambikapathi, Design And Analysis Of Rocket Engine Nozzle by using CFD and Optimization of Nozzle parameters, International Journal of Engineering Research, Vol.3., Issue.5., 2015 (Sept.-Oct.).
[2] Bogdan-Alexandru Belega, Trung Duc Nguyen, Analysis of Flow in Convergent-divergent rocket engine nozzle using Computational Fluid Dynamics, International Conference Of Scientific Paper Afases 2015 Brasov, 28-30 May 2015.
[3] Hagemann, G., Immich, H. and Preuss, A, (3-6 December 2002) "Advanced Nozzle Concepts for Future Rocket EngineApplications'', 4th International Conference on Launcher Technology, Liege, Belgium.
[4] K.M.Pandey and S.K.Yadav, ,CFD Analysis of a Rocket Nozzle with Two Inlets at Mach .1,vJournal of Environmental Research and Development, Vol 5, No 2,2010, (pp 308-321).
[5] P. Padmanathan, Dr. S. Vaidyanathan, Computational Analysis of Shockwave in Convergent Divergent Nozzle, International Journal of Engineering Research and Applications (IJERA), ISSN: 2248-9622, Vol. 2, Issue 2 Mar-Apr 2012, pp.1597-1605.
[6] Natta, Pardhasaradhi.; Kumar, V.Ranjith.; Rao, Dr. Y.V. Hanumantha; Flow Analysis of Rocket Nozzle Using Computational Fluid Dynamics (Cfd), International Journal of Engineering Research and Applications (IJERA), ISSN: 2248-9622,Vol. 2, Issue 5, September- October 2012, pp.1226-1235.
[7] Pandey,K.M.; Singh, A.P.; CFD Analysis of Conical Nozzle for Mach 3 at V arious Angles of Divergence with Fluent Software, International Journal of Chemical Engineering and Applications, Vol. 1, No. 2, August 2010, ISSN: 2010-0221.

## HEAT AND MASS TRANSFER

[8] Madhu B P, Syed Sameer, Kalyana Kumar M, Mahendra Mani G; "CFD Analysis Of Convergent divergent And Contour Nozzle" International Journal of Mechanical Engineering and Technology (IJMET) Volume 8, Issue 8, August 2017, pp. 670–677, Article ID: IJMET_08_08_073.

[9] S. Srikrishnan and Dr. P. K. Dash. 2D CFD Analysis of Deflagration to Detonation Transition in Closed Pip e Using Different Blockage. International Journal of Mechanical Engineering and Technology, 8(6), 2017, pp. 447–454.

[10] K. Manikandan, Jishu Chandran, A. Devaraj and R. Ganesh. A CFD Analysis for Optimization of Total Disolved Solids in Impeller Mixing Solid Waste Anaerobic Digester. International Journal of Mechanical Engineering and Technology, 8(7), 2017, pp. 283–289.

[11] P.Vinod Kumar, B.Kishore Kumar, Design And CFD Analysis Of Convergent And Divergent Nozzle, International Journal Of Professional Engineering Studies volume 9 /Issue 2 / Sep 2017.

2ND ENERGY SECURITY AND CHEMICAL ENGINEERING CONGRESS 2021
*"Sustainable Technological Solution for a Better World"*
VIRTUAL CONFERENCE | 3-5 NOVEMBER 2021

**HEAT AND MASS TRANSFER**

**Paper ID: ESCE140**

# A NUMERICAL SIMULATION OF THE TWISTED DELTA WINGLET SWIRLER IN A CIRCULAR TUBE WITH A FULLY DEVELOPED W:EG FLOW

**M. A. At-Tasneem[1,2]*, W. H. Azmi[3], M. A. Ismail[4]**

[1] *Faculty of Mechanical and Automotive Engineering Technology, Universiti Malaysia Pahang, 26600 Pekan, Pahang, Malaysia.*
[2] *Centre of Excellence for Advanced Research in Fluid Flow (CARIFF),* [3] *Department of Mechanical Engineering, College of Engineering, Universiti Malaysia Pahang, 26300 Gambang, Pahang, Malaysia.*
[4] *School of Mechanical Engineering, Universiti Sains Malaysia Eng. Campus, 14300 Nibong Tebal, P. Pinang, Malaysia.*
*Corresponding author: tasneem@ump.edu.my

## Extended Abstract

Among the various methods for improving heat transfer, a passive method of inserting a continuous swirler inside a heat exchanger provides a secondary flow along the fluid that reduces the thickness of the thermal boundary layer, thus increasing the efficiency of convection heat transfer performance. The research's primary goal is to conserve energy, materials, and money by operating efficient heat exchanger equipment. However, the presence of the continuous swirler along the fluid flow creates a persistent obstruction, which amplifies the friction factor and increases the working fluid's energy loss. As a result, this research presented the twisted delta winglet swirler (TDWS), a new design of decaying swirler that uses delta winglets twisted to 180° to produce a swirling flow along the tube. The swirler comprises four twisted delta winglets arranged in a circle with a diameter 6% smaller than the tube and a length of L/D=2.2. It was placed at the entrance to a heated tube test section with a diameter of 0.016 m and a length of L/D=93.75. The Reynolds Stress Model was used to simulate the flow of a water-ethylene glycol mixture as the working fluid. TDWS transformed the uniform inlet flow from potential energy to high kinetic energy, resulting in a high intensity of swirling flow downstream of the circular tube up to L/D=46.88 before decaying and reaching a steady state. In comparison to other decaying swirlers, TDWS obtained one of the lowest global relative friction factors, 1.36 with this flow. Despite reaching a maximum relative local relative Nusselt number of 2.0, the maximum global relative Nusselt number increased by only 11% because this value considered the area where the flow reached a steady state. Since the TDWS is a decaying swirler, the local thermal-hydraulic performance was plotted to demonstrate the survivability of the swirling flow down the tube. The results indicate that using a heat exchanger with a length of L/D=20 can improve the maximum average local thermal-hydraulic performance by up to 60% while using the same pumping power. However, to attain the optimal performance of TDWS in the plain tube with a length of L/D=93.75, the dimension or geometric configuration of the TDWS must be modified, or two or more TDWS may be placed in an array orientation.

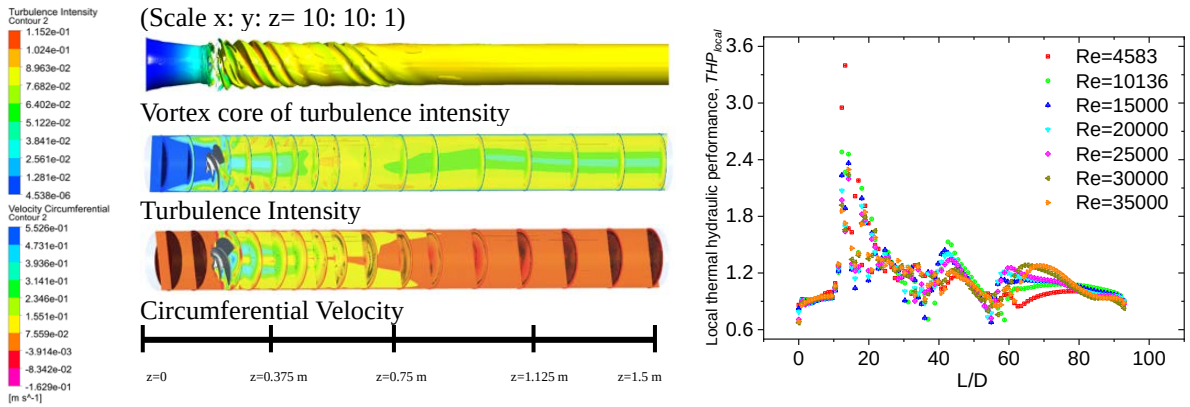


Fig. 1: Flow visualization (left) and local thermal hydraulic performance (right).

**Keywords:** Heat transfer enhancement; Passive method; Swirl flow; Decaying swirler; Delta winglet.

## Acknowledgment

The authors would like to thank the Center of Excellence for Advanced Research in Fluid Flow (CARIFF) for funding assistance under RDU190385 for inventory and the Advance Automotive Liquids Laboratory (A2LL) for providing full access to a high-performance computer. The authors are also grateful to UMP Research and Innovation and Universiti Malaysia Pahang for their financial support through UMP Tabung Persidangan Dalam Negara (TPDN).

## References

[1] M. H. Mousa, N. Miljkovic, and K. Nawaz. (2021) Renew. Sustain. Energy Rev. 137:1277–1287.
[2] P. Promvonge and S. Skullong. (2021) Appl. Therm. Eng. 185.
[3] A. Boonloi and W. Jedsadaratanachai. (2021) Case Stud. Therm. Eng. 27:101242.

2ND ENERGY SECURITY AND CHEMICAL ENGINEERING CONGRESS 2021
*"Sustainable Technological Solution for a Better World"*
VIRTUAL CONFERENCE | 3-5 NOVEMBER 2021

**MODELLING AND SIMULATION**

**Paper ID: ESCE008**

# A MULTI-OBJECTIVE OPTIMIZATION OF HYDROGEN SULFIDE CONVERSION INTO SULFUR BY CLAUS PROCESS USING iCON SIMULATION

**Ramsha Jahan[1], Zulfan Adi Putra[3], Muhammad Ayoub[1,2], Bawadi Abdullah[1,2]***

[1] *Department of Chemical Engineering,* [2] *Centre of Contaminant Control and Utilisation (CenCoU), Universiti Teknologi PETRONAS, 32610, Bandar Seri Iskandar, Perak Darul Ridzuan, Malaysia.*
[3] *PETRONAS Group Technical Solutions, Process Simulation and Optimization, Level 16, Tower 3, Kuala Lumpur Convention Center, Kuala Lumpur 50088, Malaysia.*
*Corresponding author: bawadi_abdullah@utp.edu.my

## Extended Abstract

Hydrogen sulfide (H2S) is an extremely toxic acid gas and is regarded as one of the primary sources of corrosion and odor problems. The work proposed the Claus process, considering the economic, environmental, and safety requirements are the three pillars of sustainability [1-3]. The proposed Claus process's annual benefit, global warming potential (GWP), fire explosion damage index (FEDI), and toxicity damage index (TDI) were estimated utilizing techno-economic analysis, life-cycle assessment, and hazard identification rating techniques. Then, in order to maximize benefit while minimizing GWP, FEDI, and TDI, a multi-objective optimization problem was devised and solved [4]. The process is simulated using Symmetry simulation software for the variation of acid feed gas ability and hydrogen sulfide concentration. The simulation results were used to assess the operating conditions of the sustainability pillars in a comparative manner [5-6].

According to the findings of this study, the Claus process performed better in terms of profitability, the fire and explosion damage index (FEDI), the toxicity damage index (TDI), and the probability of global warming are all factors to consider (GWP). Based on variable feed capacities and hydrogen sulfide concentrations, the regression models created demonstrated the capacity to predict the sustainable approach for hydrogen sulfide conversion that will be employed in industry. The Claus process is projected to be the best sustainable approach for hydrogen sulfide conversion throughout the great majority of the conversion spectrum, based on the data.

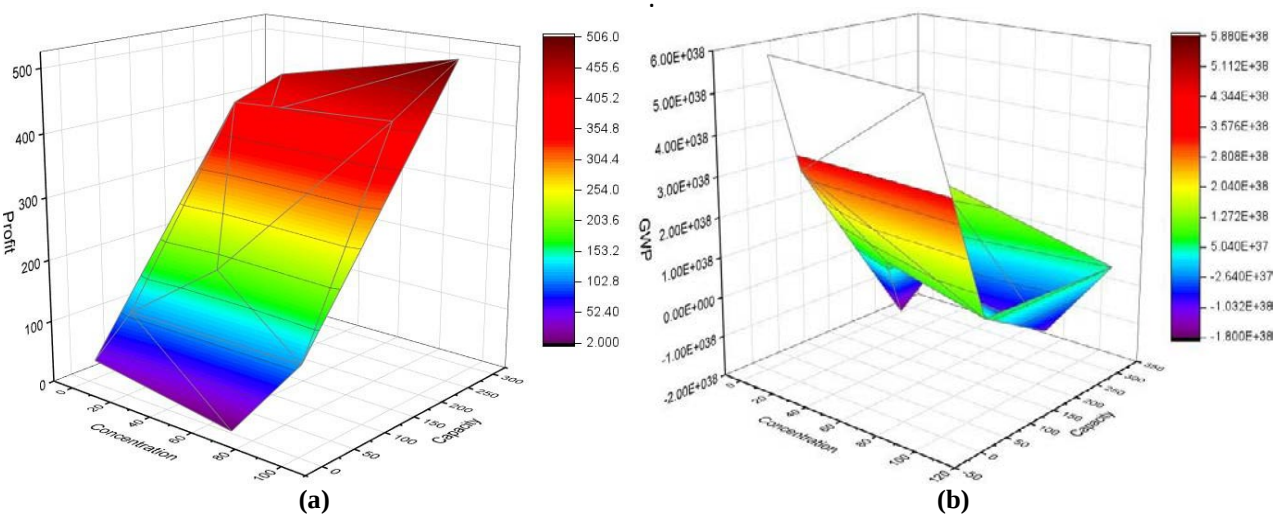


**(a)** **(b)**

Fig. 1: (a) Profit analysis (b) GWP analysis

**Keywords:** Claus Process; Techno-economic analysis; Multi-objective optimization; Sustainability pillars; Symmetry simulation software.

## MODELLING AND SIMULATION

### Acknowledgment

The authors would like to express their gratitude to the Universiti Teknologi PETRONAS (UTP), Chemical Engineering Department for the technical and administrative support and the financial support from the Yayasan UTP grant (Cost centre: 015LC0-268).

### References

[1] Elmawgoud, H. A., Elshiekh, T. M., Khalil, S. A., Alsabagh, A. M., & Tawfik, M. (2015). Modeling of hydrogen sulfide removal from Petroleum production facilities using H2S scavenger. Egyptian Journal of Petroleum, 24(2), 131– 137.
[2] Elshiekh, T. M., Elmawgoud, H. A., Khalil, S. A., & Alsabagh, A. M. (2015). Simulation for estimation of hydrogen sulfide scavenger injection dose rate for treatment of crude oil. Egyptian Journal of Petroleum, 24(4), 469–474.
[3] Selim, H., Gupta, A. K., & Sassi, M. (2012). Novel error propagation approach for reducing H2S/O2 reaction mechanism. Applied Energy, 93, 116–124.
[4] Chiodo, K. (2003, December 2). NIST/SEMATECH e-Handbook of Statistical Methods. Retrieved December **3**, 2019.
[5] Khan, F. I., & Abbasi, S. A. (1997). Accident Hazard Index. Process Safety and Environmental Protection, **75(4)**, 217–224. https://doi.org/10.1205/095758297529093.
[6] Sassi, M., & Gupta, A. K. (2008a). Sulfur Recovery from Acid Gas Using the Claus Process and High Temperature Air Combustion (HiTAC) Technology. American Journal of Environmental Sciences, **4(5)**, 502– 511. https://doi.org/10.3844/ajessp.2008.502.511.

**MODELLING AND SIMULATION**

**Paper ID: ESCE032**

# MATHEMATICAL MODELLING AND ANALYSIS OF DYNAMIC BEHAVIOUR FOR SEEDED BATCH POTASH ALUM CRYSTALLIZATION PROCESS

**S. Z. Adnan[1], N. A. F. A. Samad[1]***

[1] *Chemical Engineering Department, College of Engineering, Universiti Malaysia Pahang, 26300 Gambang, Pahang, Malaysia.*
*Corresponding author: asmafazli@ump.edu.my

## Extended Abstract

Crystallization process is widely used in many industries especially pharmaceuticals and specialty chemicals because of its capability to produce high quality of crystals which makes it beneficial and reliable to be used which is agreed by few researchers [1-2]. Common control factor that has been used to quantify the quality of the crystals is crystal size distribution (CSD). CSD is the main contributor that affects the bioavailability of the crystals and its packing properties [3], and the efficiency of the downstream operations [1-3].

Temperature is the main key factor to be controlled and manipulated in the crystallization process to achieve desired CSD, as the solubility of the solution is the function of temperature. The crystallization operation usually starts in the metastable zone which enables the seed crystals to grow until the end of the operation. However, along with grown seed crystals, fine crystals which is induced by secondary nucleation are also produced significantly which causes low purity and smaller final crystals [4], and inefficiency issues on the latter downstream system such as long filtration and drying time [1-3]. This undesired generation of fine crystals is caused by the high supersaturation level at the beginning of the crystallization process due to the high difference of solute concentration against saturation concentration. Proper temperature trajectory that operates within metastable region is needed to be determined to avoid this problem. Several trajectories such as natural, linear and cubic are adapted from literature to obtain an insight for development of crystallization process [5]. Therefore, the purpose of this study is to simulate and develop the mathematical model of seeded batch crystallization process and evaluate the dynamic response of such process under open-loop operation.

In this study, the mathematical model and simulations of seeded batch crystallization process are developed and implemented in Matlab 2016b software. Potash alum case study is used to illustrate the dynamic response of the crystallization process which is adapted from [6]. The mathematical model for potash alum crystallization is based on the size dependent growth of one-dimensional population balance equation (PBE) as shown in equation (1).

$$\frac{\partial n(L,t)}{\partial t} + \frac{\partial n(L,t)G(L,C,T)}{\partial L} = B_{nuc} \quad (1)$$

where $n$ is the population density function (which is a function of particle size, $L$ and crystallization time, $t$), $G$ is the linear growth rate (which is a function of particle size, $L$, solute concentration, $C$ and solution crystallizer temperature, $T$), and $B_{nuc}$ is the nucleation rate.

From the simulations of potash alum crystallization process, Figure 1 (a) showed the temperature profile of potash alum that is needed to be maintained until the end of the process for natural cooling policy. The solution is cooled steeply from 40 °C to 17 °C. Next, Figure 1 (b) which correspond to the concentration profiles of the process, showed that saturation concentration profile (dashed line) is following the descending trend of temperature profile in which proved the relationship of saturation concentration that depends on temperature. The potash alum concentration profile (solid line) dropped accordingly from 0.104 to 0.049 g/g water to achieved desired supersaturation for the growth of seed crystals. The gap between these two lines clearly demonstrated high supersaturation level throughout the whole process which proved that the crystallization process started in the beginning until the end of the operation. Therefore, overall results showed a good agreement with the literature.

**MODELLING AND SIMULATION**

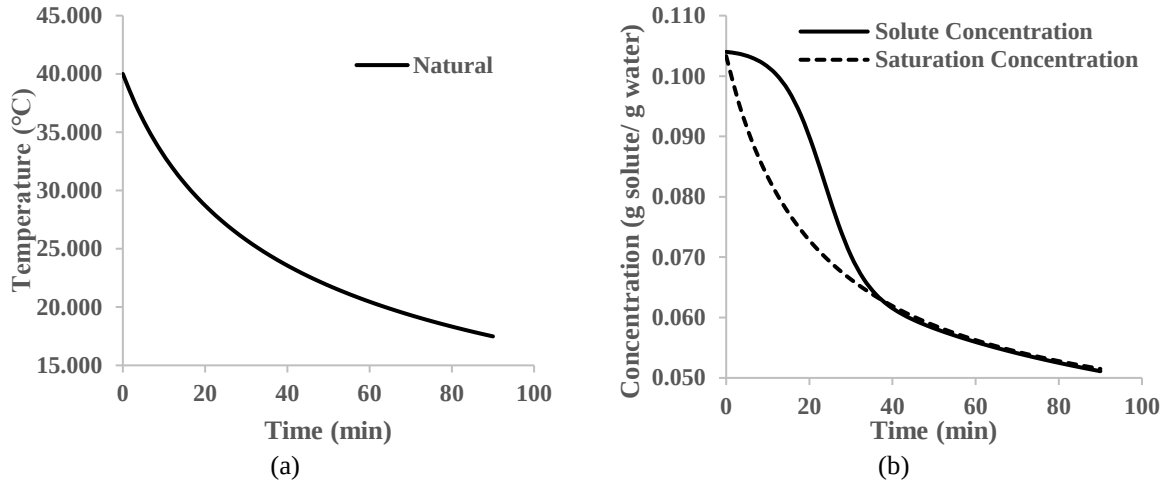


Fig. 1: Temperature (a) and concentration (b) profiles for natural cooling policy

**Keywords:** Dynamic Behaviour; Crystal Size Distribution; Potash Alum Crystallization.

**Acknowledgment**

This study was supported by Universiti Malaysia Pahang (UMP) under Doctorate Research Scheme (DRS).

**References**

[1] Adnan S. Z., Samad N. A. F. A. (2019) Application of Extended Method of Classes for Solving Population Balance Equations and Optimization Study for Crystallization Process Involving Dissolution Phenomena. {IOP} Conf. Ser.:Mater. Sci. Eng. 702:012021.
[2] Unno J.,Hirasawa I. (2020) Partial Seeding Policy for Controlling the Crystal Quality in Batch Cooling Crystallization. Chem. Eng. Technol. 43:1065-1071.
[3] Trampuž M., Teslić D., Likozar B. (2020) Process Analytical Technology-Based (PAT) Model Simulations of Combined Cooling, Seeded and Antisolvent Crystallization of an Active Pharmaceutical Ingredient (API). Powder Technol. 366:873-890.
[4] Nagy Z. K., Aamir E. (2012) Systematic Design of Supersaturation Controlled Crystallization Processes for Shaping the Crystal Size Distribution using an Analytical Estimator. Chem. Eng. Sci. 84:656-670.
[5] Jones A. (1974) Optimal Operation of a Batch Cooling Crystallizer. Chem. Eng. Sci. 29:1075-87.
[6] Aamir E. (2010) Population Balance Model-Based Optimal Control of Batch Crystallisation Processes for Systematic Crystal Size Distribution Design. PhD Thesis, LU Chem. Eng. Dept., Loughborough.

2ND ENERGY SECURITY AND CHEMICAL ENGINEERING CONGRESS 2021
*"Sustainable Technological Solution for a Better World"*
VIRTUAL CONFERENCE | 3-5 NOVEMBER 2021

**MODELLING AND SIMULATION**

**Paper ID: ESCE095**

# ASSESSMENT OF THERMAL CONDUCTIVITY AND VISCOSITY OF ALUMINA-BASED ENGINE COOLANT NANOFLUIDS USING RANDOM FOREST APPROACH

**K. X. Tan[1], S. U. Ilyas[2], R. Pendyala[1]***

[1] *Chemical Engineering Department,* [2] *Institute of Hydrocarbon Recovery, Universiti Teknologi PETRONAS, 32610 Seri Iskandar, Perak Darul Ridzuan, Malaysia.*
*Corresponding author: rajahshekhar_p@utp.edu.my

## Extended Abstract

Thermal conductivity and viscosity are crucial thermophysical properties of nanofluids. They play a pivotal role in industries involved with heat transfer applications. Alumina ($Al_2O_3$) nanoparticles are known to be a good additive for thermophysical properties enhancement with favorable results in countless researches. However, the measurement of thermophysical properties of nanofluids through experimental is expensive. Therefore, the random forest (RF), an advanced computational intelligence approach, is proposed to correctly predict the thermal conductivity and viscosity of alumina-based engine coolant nanofluids in this research. Experimental data from past literature are utilized as input parameters for the development of the RF models. The input parameters for the prediction of thermal conductivity are temperature and concentration, whereas the input parameters for the prediction of viscosity are temperature, concentration, and shear rate. Error metrics consisting of R2, A-R2, MSE, RMSE, and MAE are used to analyze and determine the performance of each RF model. Based on the results, it is observed that all RF models exhibit significantly high and consistent predictive accuracy with R2 of 0.9877 for thermal conductivity prediction and R2 of 0.9974 for viscosity prediction.

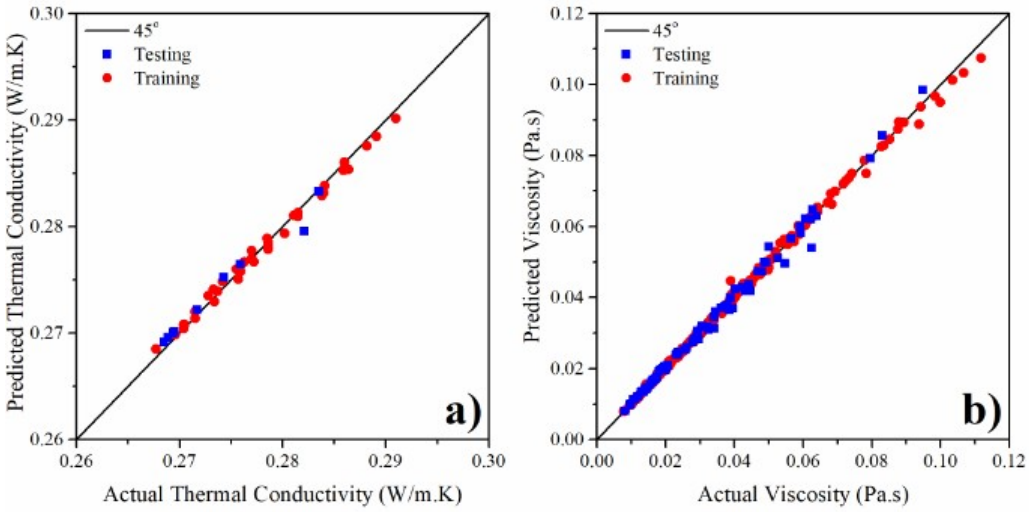


Fig. 1: Testing and training scattered parity plots for
(a) thermal conductivity and (b) viscosity of alumina nanofluids

**Keywords:** Random Forest (RF); Prediction; Alumina Nanofluids; Thermal Conductivity; Viscosity.

**Acknowledgment**

This research was fully supported by the Chemical Engineering Department of Universiti Teknologi PETRONAS (UTP).

## MODELLING AND SIMULATION

### References

[1] Y. Zhang and X. Xu, "Predicting the thermal conductivity enhancement of nanofluids using computational intelligence," Phys. Lett. Sect. A Gen. At. Solid State Phys., vol. 384, no. 20, p. 126500, 2020, doi: 10.1016/j.physleta.2020.126500.
[2] S. U. Ilyas, R. Pendyala, and M. Narahari, "Experimental investigation of natural convection heat transfer characteristics in MWCNT-thermal oil nanofluid," J. Therm. Anal. Calorim., vol. 135, no. 2, pp. 1197–1209, 2019, doi: 10.1007/s10973-018-7546-7.
[3] W. Yu and H. Xie, "A review on nanofluids: Preparation, stability mechanisms, and applications," J. Nanomater., vol. 2012, 2012, doi: 10.1155/2012/435873.
[4] R. Saidur, K. Y. Leong, and H. A. Mohammed, "A review on applications and challenges of nanofluids," Renew. Sustain. Energy Rev., vol. 15, no. 3, pp. 1646–1668, 2011, doi:10.1016/j.rser.2010.11.035.
[5] S. U. S. Choi, "Nanofluids: From vision to reality through research," J. Heat Transfer, vol. 131, no. 3, pp. 1–9, 2009, doi: 10.1115/1.3056479.
[6] J. Buongiorno, "Convective transport in nanofluids," J. Heat Transfer, vol. 128, no. 3, pp. 240–250, 2006, doi: 10.1115/1.2150834.
[7] Y. Xuan and Q. Li, "Heat transfer enhancement of nanofluids," Int. J. Heat Fluid Flow, vol. 21, no. 1, pp. 58–64, 2000, doi: 10.1016/S0142-727X(99)00067-3.
[8] J. Sarkar, P. Ghosh, and A. Adil, "A review on hybrid nanofluids: Recent research, development and applications," Renew. Sustain. Energy Rev., vol. 43, pp. 164–177, 2015, doi:10.1016/j.rser.2014.11.023.
[9] S. U. Ilyas, R. Pendyala, and N. Marneni, Stability of Nanofluid. 2017.
[10] G. Huminic and A. Huminic, "Application of nanofluids in heat exchangers: A review," Renew. Sustain. Energy Rev., vol. 16, no. 8, pp. 5625–5638, 2012, doi:10.1016/j.rser.2012.05.023.
[11] M. Gupta, V. Singh, R. Kumar, and Z. Said, "A review on thermophysical properties of nanofluids and heat transfer applications," Renew. Sustain. Energy Rev., vol. 74, no. March, pp. 638–670, 2017, doi:10.1016/j.rser.2017.02.073.
[12] M. Kole and T. K. Dey, "Experimental investigation on the thermal conductivity and viscosity of engine coolant based alumina nanofluids," AIP Conf. Proc., vol. 1249, no. May 2013, pp. 120–124, 2010, doi:10.1063/1.3466537.
[13] S. U. Ilyas, R. Pendyala, M. Narahari, and L. Susin, "Stability, rheology and thermal analysis of functionalized alumina-thermal oil-based nanofluids for advanced cooling systems," Energy Convers. Manag., vol. 142, pp. 215–229, 2017, doi: 10.1016/j.enconman.2017.01.079.
[14] G. D. Xia, R. Liu, J. Wang, and M. Du, "The characteristics of convective heat transfer in microchannel heat sinks using Al2O3 and TiO2 nanofluids," Int. Commun. Heat Mass Transf., vol. 76, pp. 256–264, 2016, doi: 10.1016/j.icheatmasstransfer.2016.05.034.
[15] J. Xu, K. Bandyopadhyay, and D. Jung, "Experimental investigation on the correlation between nano-fluid characteristics and thermal properties of Al2O3 nano-particles dispersed in ethylene glycol-water mixture," Int. J. Heat Mass Transf., vol. 94, pp. 262–268, 2016, doi: 10.1016/j.ijheatmasstransfer.2015.11.056.
[16] M. Kole and T. K. Dey, "Viscosity of alumina nanoparticles dispersed in car engine coolant," Exp. Therm. Fluid Sci., vol. 34, no. 6, pp. 677–683, 2010, doi: 10.1016/j.expthermflusci.2009.12.009.
[17] Y. R. Sekhar and K. V. Sharma, "Study of viscosity and specific heat capacity characteristics of water-based Al2O3 nanofluids at low particle concentrations," J. Exp. Nanosci., vol. 10, no. 2, pp. 86–102, 2015, doi: 10.1080/17458080.2013.796595.
[18] M. Gholizadeh, M. Jamei, I. Ahmadianfar, and R. Pourrajab, "Prediction of nanofluids viscosity using random forest (RF) approach," Chemom. Intell. Lab. Syst., vol. 201, no. January, p. 104010, 2020, doi: 10.1016/j.chemolab.2020.104010.
[19] F. Livingston, "Implementation of Breiman's Random Forest Machine Learning Algorithm," Mach. Learn. J. Pap., pp. 1–13, 2005.

2ND ENERGY SECURITY AND CHEMICAL ENGINEERING CONGRESS 2021
*"Sustainable Technological Solution for a Better World"*
VIRTUAL CONFERENCE | 3-5 NOVEMBER 2021

**MODELLING AND SIMULATION**

**Paper ID: ESCE097**

# CFD MODELLING OF CHLORINE LEAK DISPERSION AND RISK ZONE FORECAST IN TELOK KALONG INDUSTRIAL AREA

**Jolius Gimbun[1,2]*, Woon Phui Law[2]**

[1] *Department of Chemical Engineering,* [2] *Centre for Research in Advanced Fluid and Processes (Fluid Centre), College of Engineering, Universiti Malaysia Pahang, 26300 Gambang, Pahang, Malaysia.*
*Corresponding author: jolius@ump.edu.my

## Extended Abstract

Chlorine is commonly produced as chlor-alkali product for application in the polymer manufacturing and water treatment plant. The incident involving chlorine gas leaks from chlor-alkali plant occurred occasionally causing emergency evacuation to the nearby residential area (Yeap, 2016). Malay-Sino Chemical Industries Sdn. Bhd. at Teluk Kalong is the largest manufacturer of chlor-alkali product in Malaysia. Teluk Kalong industrial area is surrounded by a number of residential areas, which may be affected by the accidental chlorine release. No previous study on the chlorine dispersion at Teluk Kalong. Therefore, it is vital to evaluate the potential risk of chlorine leakage from chlor-alkali plant in Teluk Kalong industrial area to the nearby residential areas.

The effect of different wind direction, wind speed and time in the meteorological mesoscale area to the gas chlorine dispersion was evaluated. A hypothetical chlorine leakage from the chlor-alkali plant was modelled using a computational fluid dynamics (CFD). The wind speed ranging from 1.55 to 11.1 m/s obtained from a local weather station was considered. All the major incident probability was studied by considering all the major wind speed and direction at night and daytime. The turbulent flow was resolved using a scale-adaptive simulation (SAS) model, whereas the chlorine dispersion was modelled using the species transport equation and compared with the area location of hazardous atmosphere (ALOHA) model (Law et al., 2019). The simulation was compared with the particle image velocimetry (PIV) measurement on a scaled-down terrain model. A good agreement between the CFD prediction and PIV measurement was obtained (Fig. 1). The finding showed that the terrain surface, wind direction and wind speed have a combined effect on the dispersion of chlorine (Fig. 2). A suitable safety evacuation routes were proposed to reduce the risk of exposure to hazardous gas in the event of accidental chlorine leakage incident. Finding from this work is useful to understand the risk of hazardous gas dispersion around Teluk Kalong industrial area.

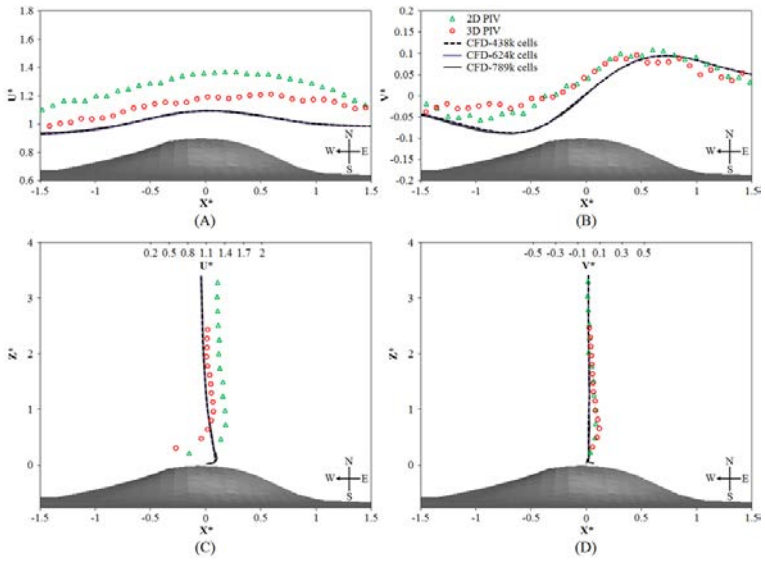


Fig. 1: Comparison of CFD and PIV data for (A) *U** along *X**, (B) *V** along *X**, (C) *U** along *Z**, (D) *V** along *Z**

**MODELLING AND SIMULATION**

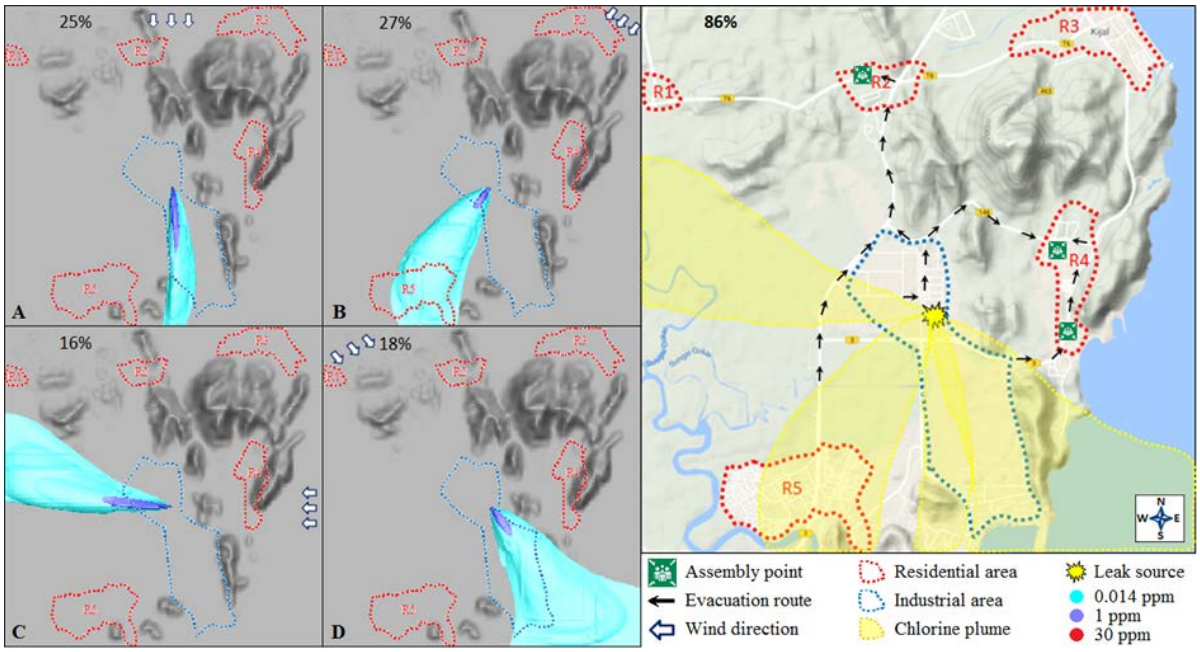


Fig. 2: Chlorine plume dispersion at day time with wind direction (A) 0º, (B) 45º, (C) 90º, (D) 315º and the proposed evacuation route for the case of chlorine leakage during Northeast monsoon 1.

**Keywords:** Monsoon; Chlorine dispersion; CFD; Scale adaptive simulation; Evacuation route.

**Acknowledgement**

This project is funded by FRGS/1/2018/TK02/UMP/02/17 (UMP Ref: RDU190145).

**References**

[1] Law W. P., Erain N., Ramli N. I. & Gimbun J. (2019). Assessment of chlorine leak dispersion around Gebeng industrial area and potential evacuation route. *Atmospheric Research*, 216, 117-129.
[2] Yeap A. (2016). Chlorine gas causes scare around plant. Retrieved from https://www.thestar.com.my/ (accessed on 4 October 2017).

**MODELLING AND SIMULATION**

**Paper ID: ESCE116**

# NUMERICAL SIMULATION AND PARAMETRIC STUDY OF PULVERIZED COAL COMBUSTION BY USING CFD

**P. Sakolaree[1], K. Rattanaphaibun[1], W. Sukhanonsawas[1], Y. Sukjai[1]***

[1] *Department of Mechanical Engineering, Faculty of Engineering, King Mongkut's University of Technology Thonburi, 126 Pracha Uthit Road, Bang Mod, Thung Khru, Bangkok, 10140, Thailand.*
*Corresponding author: yanin.suk@kmutt.ac.th

## Extended Abstract

Nowadays, pulverized coal has become one of the most preferable forms of burning coal as it offers a more complete combustion, and a cleaner and more efficient way of handling coal dust because the entire system from coal silo to coal burner is contained a closed system [1]. Pulverized coal combustion cannot be easily observed and characterized without sophisticated instruments, thus, developing and improving the performance of pulverized coal burners experimentally requires a lot of efforts and resources. Therefore, using numerical simulation to study the combustion of pulverized coal is one of the most efficient methods for developing and improving the performance of pulverized coal burners as it can analyze for the temperature distribution and combustion reaction of coal particles [2]. However, the study with 3D models needs extensive computer resources. Studying with a symmetrical 2-D model is therefore an alternative way of studying pulverized coal combustion that can reduce the computational resources and the computation time [3].

The objective of this research is to numerically model and analyze the combustion characteristics of pulverized coal in an axisymmetric 2-D combustion chamber model by using CFD. For experimental validation, this work focuses on the following simulation conditions: coal particle diameter smaller than 74 µm, primary air mass fraction of 25%, secondary air mass fraction of 65%, and tertiary air mass fraction of 10%. The pulverized coal is sprayed into the burner along with the primary air and mixed with the secondary and the tertiary air in the burner due to the effect of the secondary air vortex flow. The governing equations for the turbulent flow analysis in the combustion chamber is the Turbulence Model Standard K-ε. For particle motion analysis, including devolatilization and heterogeneous combustion is analyzed by Discrete Particle Model (DPM). Homogeneous combustion is analyzed by using Eddy-Dissipation model. It is assumed that the concentration of the chemical reaction is fast kinetics, thus, the reaction rate is therefore dominated by the turbulent flow concentration. In addition, the Discrete Ordinates method is used to model thermal radiation phenomena. The flow behavior of fuel, air, and the combustion gases as well as the combustion reaction are modeled and analyzed the ANSYS FLUENT program. In this study, the experimental results of internal burner temperature at 300 kW were used to validate the simulation results from CFD. The installed site of the burner analyzed in this work is located at a coal storage and handling facility in Phra Nakhon Si Ayutthaya Province, Thailand. The burner is used to produce a stream of hot air for controlling moisture content in the pulverized coal. The simulation results showed that the flame in the burner will be a spiral before converging into the flame line in the main combustion chamber as shown in Figure 1. The maximum temperature inside the combustion chamber was 1637 °C and the maximum temperature inside the burner 1370 °C, which was slightly higher than the results from experiment at the burner temperature of 1325 °C. The first-law combustion efficiency of this burner was found to be 80% primarily due to incomplete combustion, energy loss from excess air, and unburned coal particles leaving the combustion chamber. The results of this study will be used as a body of knowledge for further analysis of combustion characteristics of pulverized coal and for the improvement of pulverized coal burners in the future.

**MODELLING AND SIMULATION**

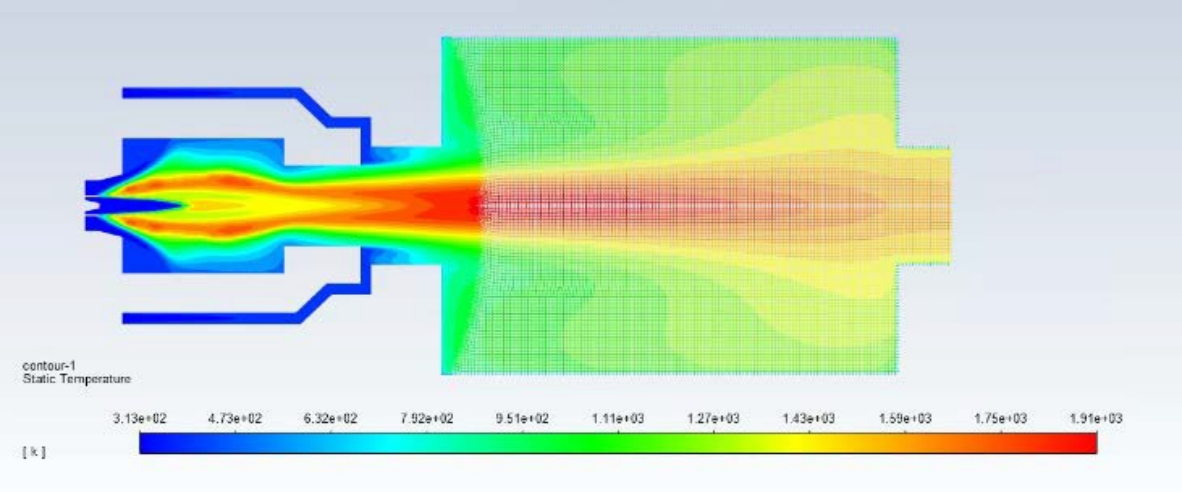


Fig. 1: Flame characteristics of pulverized coal combustion inside the combustion chamber.

**Keywords:** Numerical Simulation; CFD; Pulverized Coal Combustion; Pulverized Coal Burner.

## Acknowledgment

The authors would like to thank Assoc. Prof. Dr. Jaruwat Charoensuk of King Mongkut's Institute of Technology Ladkrabang (KMITL) for assistance and advice during model development and computer simulation. The financial resources and supporting information from Premium Energy Corporation Co., Ltd. are greatly appreciated.

## References

[1] Jiade Han, Lingbo Zhu, Yiping Lu, Yu Mu, Azeem Mustafa, Yajun Ge, "Numerical Simulation of Combustion in 35 t/h Industrial Pulverized Coal Furnace with Burners Arranged on Front Wall," Processes, 2020.
[2] V. Sahajwall, A. Eghlimi, K.Farrell, "Numerical Simulation of Pulverised Coal Combution," in Inter Conf on CFD in Mineral & Metal Processing and Power Generation , 1997.
[3] J. Macphee, "CFD Modelling of a Rotary Lime Kiln," Department of Mechanical Engineering, University of Canterbury Christchurch, New Zealand, 2010.

**MODELLING AND SIMULATION**

**Paper ID: ESCE138**

# EFFECT OF DRYING TECHNIQUE ON *Hermetia illucens* PREPUPAE FATTY ACID

**S. Y. Leong[1]*, V. H. Yap[1], S. R. M. Kutty[2]**

[1] *Department of Petrochemical Engineering, Faculty of Engineering and Green Technology, Universiti Tunku Abdul Rahman, Jalan Universiti, Bandar Barat, 31900 Kampar, Perak Darul Ridzuan, Malaysia.*
[2] *Department of Civil and Environmental Engineering, Universiti Teknologi PETRONAS, 32610 Seri Iskandar, Perak Darul Ridzuan, Malaysia.*
*Corresponding author: leongsy@utar.edu.my

## Extended Abstract

Insect meal has given priority towards achieving sustainable development goals such as novel food and feed protection, economic stimulus, job creation, the promotion of new scientific development and the mitigation of greenhouse gases by waste recycling. Insect-derived protein sources have become a new, sustainable and novel food for human and animal consumption [1]. The processing and transformation of the original form of the insect and/or insect larvae is therefore required [3-4]. Drying is the most basic drying method used to preserve food and to extend the lifetime of food storage. During drying, water from the food material may be dehydrated by different techniques [5]. Today, a large number of food products with very different physical and chemical properties are dehydrated in a variety of dryer designs with a variety of processing conditions [6-7]. The selection of the drying method for a specific food product is an essential step, as the drying technique and operating conditions have an effect on the quality and cost of the dried product.

Hence, the purpose of this study is to investigate the effects of oven and microwave drying on the fatty acid characteristics of *Hermetia illucens* prepupae. Prior to drying, larvae of *Hermetia illucens* were grown to the prepupae stage and harvested for further studies. A palm decanter was used as the larvae's substrate. The influence of oven drying time (24 - 72 hours) and temperature (40 - 80ºC) upon fatty acid was investigated, while that of microwave drying power (200 - 250 W) and time (10 - 15 mins) was investigated. An evaluation of the effects of different drying methods on fatty acid chemical properties was conducted, measuring free fatty acids (FFA), acid value (AV) and iodine value (IV). In addition to the biochemical properties of *Hermetia illucens* prepupae, the compositional fatty acid methyl ester yield (FAME) of *Hermetia illucens* prepupae was examined for both drying techniques.

Microwave-dried materials showed higher values for free fatty acids, acid values, and iodine values than oven-dried products. Following microwave drying, the values obtained for free fatty acids, acid values, and iodine values were respectively 132.44% oleic acid, 263.30 mg KOH/g oil and 46.67 gI/100g. In terms of oven drying, the value attained were 118.34% oleic acid, 232.27 mg KOH/g oil, and 42.54 gI/100g, respectively. Microwave drying of *Hermetia illucens* prepupae shows higher iodine value due to its higher unsaturated fatty acid content at 37.16% as compared with its oven-dried *Hermetia illucens* prepupae's which attained at 34.78% of unsaturated fatty acid. For both oven and microwave drying, FAME yields were 90.41 and 94.05%, respectively. Lauric acid (C12:00) was the highest compositional FAME at 32.44 and 28.53% for both oven and microwave drying, respectively. An increased level of saturation in FAME is observed in oven drying, which achieved 65.18% compared to microwave drying (62.84%).

Based on the findings, the choice of various drying technique can significantly influence the fatty acid characteristics [6]. For instance, higher C12:0 were obtained from oven drying as compared to microwave drying. The study provides an insight on the suitability of the drying process by taking into consideration the compounds of interest and therefore the potential end-use such as biodiesel production.

**Keywords:** *Hermetia illucens* pre-pupae; Oven drying; Microwave drying; Fatty acid methyl ester; Organic waste.

**MODELLING AND SIMULATION**

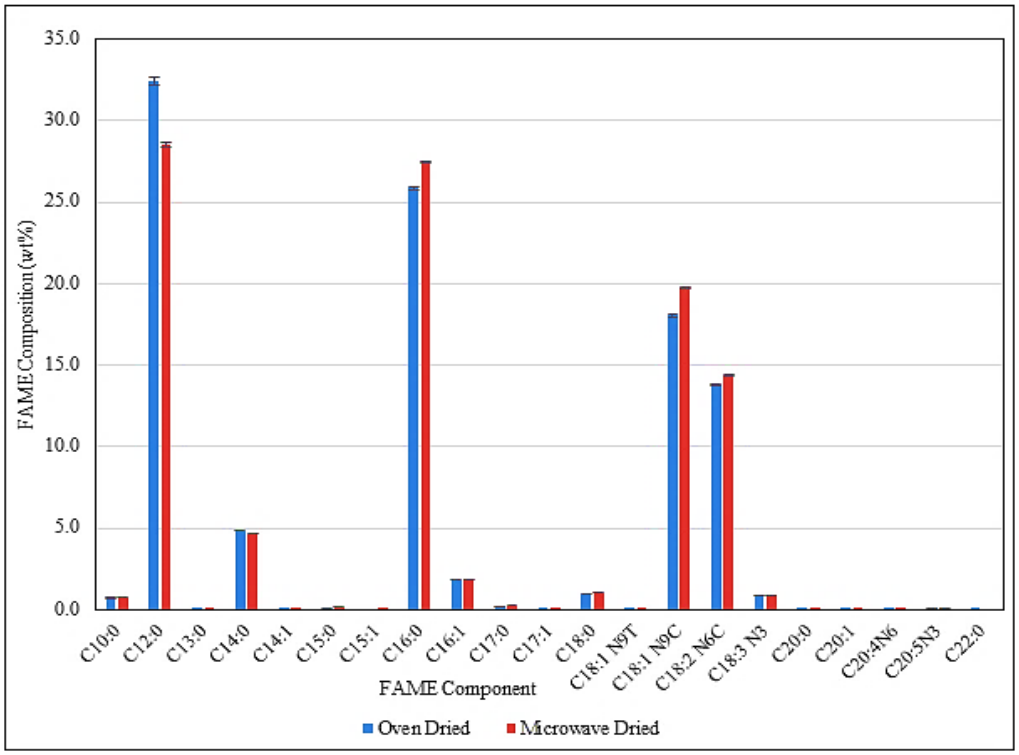


Fig. 1: FAME compositional yield of oven dried vs. microwave dried *Hermetia illucens* prepupae.

**Acknowledgment**

The authors would like to thank the Universiti of Tunku Abdul Rahman, Kampar, Perak for their research facilities and financial support from Universiti Tunku Abdul Rahman Research Funding (IPSR/RMC/UTARRF/2018-C01/L07).

**References**

[1] Huang, C., Feng, W., Xiong, J., Wang, T., Wang, W., Wang, C. and Yang, F. (2018) Impact of drying method on the nutritional value of the edible insect protein from black soldier fly (*Hermetia illucens* L.) larvae: amino acid composition, nutritional value evaluation, in vitro digestibility, and thermal properties. European Food Research and Technology, 245(1): 11-21.

[2] Larouche, J., Deschamps, M., Saucier, L., Lebeuf, Y., Doyen, A. and Vandenberg, G. (2019) Effects of Killing Methods on Lipid Oxidation, Colour and Microbial Load of Black Soldier Fly (*Hermetia illucens*) Larvae. Animals, 9(4):1-19.

[3] Mai, H., Dao, N., Lam, T., Nguyen, B., Nguyen, D. and Bach, L. (2019) Purification Process, Physicochemical Properties, and Fatty Acid Composition of Black Soldier Fly (*Hermetia illucens* Linnaeus) Larvae Oil. Journal of the American Oil Chemists' Society, 96(11):1303-1311.

[4] Vandeweyer, D., Lenaerts, S., Callens, A. and Van Campenhout, L. (2017) Effect of blanching followed by refrigerated storage or industrial microwave drying on the microbial load of yellow mealworm larvae (*Tenebrio molitor*). Food Control, 71: 311-314.

[5] Kröncke, N., Grebenteuch, S., Keil, C., Demtröder, S., Kroh, L., Thünemann, A., Benning, R. and Haase, H. (2019) Effect of Different Drying Methods on Nutrient Quality of the Yellow Mealworm (*Tenebrio molitor* L.). Insects, 10(4): 1-13.

[6] Lenaerts, S., Van Der Borght, M., Callens, A. and Van Campenhout, L. (2018) Suitability of microwave drying for mealworms (*Tenebrio molitor*) as alternative to freeze drying: Impact on nutritional quality and colour. Food Chemistry, 254: 129-136.

[7] Dong W., Hafiz U. J., Ying S., Safina N., Sajid A. and Chang-Qing D. (2020) Impact of Drying Method on the Evaluation of Fatty Acids and Their Derived Volatile Compounds in 'Thompson Seedless' Raisins. Molecules. 2020 Feb; 25(3): 1-13.

**MODELLING AND SIMULATION**

**Paper ID: ESCE187**

# 2D AND 3D PARTICLE IMAGE VELOCIMETRY MEASUREMENT OF AIR FLOW OVER A SCALED-DOWN MODEL OF BUKIT GEMOK IN TELOK KALONG INDUSTRIAL AREA

**Jolius Gimbun[1,2]*, Woon Phui Law[1], Siti Ilyani Rani[3]**

[1] *Department of Chemical Engineering,* [2] *Centre for Research in Advanced Fluid and Processes (Fluid Centre), College of Engineering, Universiti Malaysia Pahang, 26300 Gambang, Pahang, Malaysia.*
[3] *Faculty of Chemical Engineering Technology, TATI University College, 24000, Malaysia.*
*Corresponding author: jolius@ump.edu.my

## Extended Abstract

Malay-Sino Chemical Industries Sdn. Bhd. at Teluk Kalong is the largest manufacturer of chlor-alkali product in Malaysia. Teluk Kalong industrial area (TKIA) is surrounded by a number of residential areas, which may be affected by the accidental chlorine release. The incident involving chlorine gas leaks from chlor-alkali plant occurred occasionally causing emergency evacuation to the nearby residential area (Yeap, 2016). The chlorine gas dispersion is affected by the meteorological mesoscale condition such as surface terrain, wind speed and direction. Presence of obstacle such as hill may generate turbulent vortices which may affect the chlorine dispersion.

Telok Kalong area experience the wind gusts ranging from 8.7 to 12.3 m/s and average wind speed from 2.1 to 3.1 m/s. Majority of wind direction are from north east and east from October to April, meanwhile from south eastern in May to September, annually. The wind direction, wind speed and surface terrain in the meteorological mesoscale area affect the gas chlorine dispersion (Law et al., 2019). Therefore, it is vital to study the effect of fluid flow over the surface terrain in Telok Kalong. The surface terrain feature of Telok Kalong is almost flat except the hill (Bukit Gemok) closed to coastal area that may interfere the wind coming from eastern direction (Fig. 1A). Thus, this work focuses on evaluation of fluid flow over scaled down model of TKIA terrain. The surface terrain map was obtained from google earth which was then converted to a CAD format and the scaled down model was made using a 3D printer.

The flow was seeded with Safex fog into the lab–scale wind tunnel driven by an axial fan with air velocity of 1.78 m/s. The double pulsed Nd:Yag laser (MicroVec, Singapore) was triggered to deliver a thin laser sheer to define the measurement plane indicated by red line in Fig. 1A. The laser model used in this PIV system is Vlite-200 with a wavelength 532 nm. The particles movements in a specific measurement plane were captured by the CCD camera (Dantec Dynamics, Denmark). Only one CCD camera was used for 2D PIV, whereas 2 CCD cameras was used for 3D PIV. Calibration was performed in the measurement plane using the calibration target. A time interval of 400 µs was set for the measurement. The camera and laser system was synchronized by a MicroPulse725 processor. The velocity data was then processing using MicroVec software. The experimental setup is shown in Fig. 2. Fig. 1B shows the 2D view of the hill (Bukit Gemok) and Fig. 1C shows the velocity vector obtained from PIV.

## MODELLING AND SIMULATION

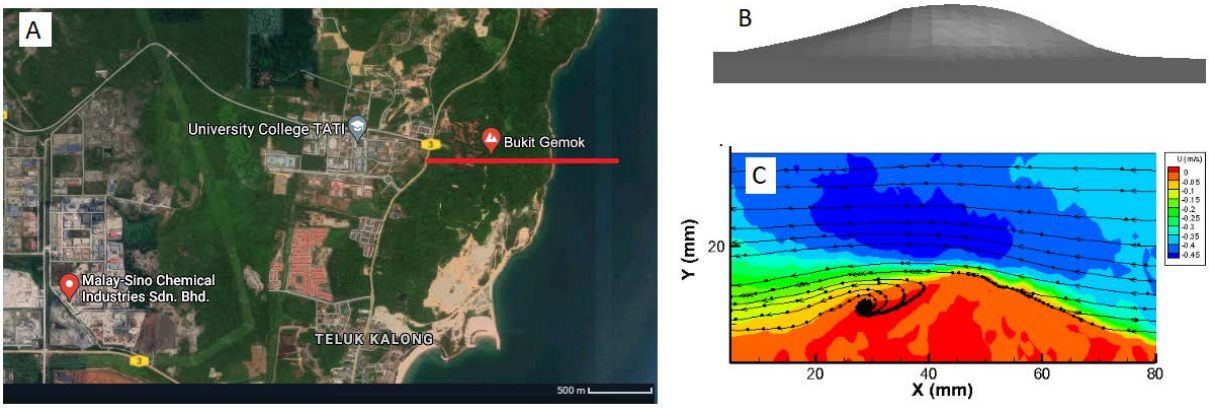


Fig. 1: A) Satellite image of the study area, B) 2D view of the hill Bukit Gemok, C) Velocity vector and contour

Figure 3 shows the comparison between the 2D and 3D PIV measurement of axial ($u$) and horizontal ($v$) over Bukit Gemok. The $u^*$ and $v^*$ is a normalized velocity with respect to the inlet velocity. The $v^*$ of both 2D and 3D PIV measurement is in good agreement because the CCD camera is set perpendicular to the interrogation window illuminated by the laser sheet. However, there is a difference in $u^*$ because the axial velocity component is affected by the three-dimensional velocity components. In fact, the real flow is highly three-dimensional with presence of a tangential velocity ($w$) component, therefore the 2D PIV cannot measure all the 3D velocity component as good as that of a 3D PIV. As it can be seen, the wake flow behind the hill is better captured by the 3D PIV, whereby a bigger vortex was measured compared to the 2D PIV. Finding from this work is useful to understand the air flow pattern around Teluk Kalong industrial area.

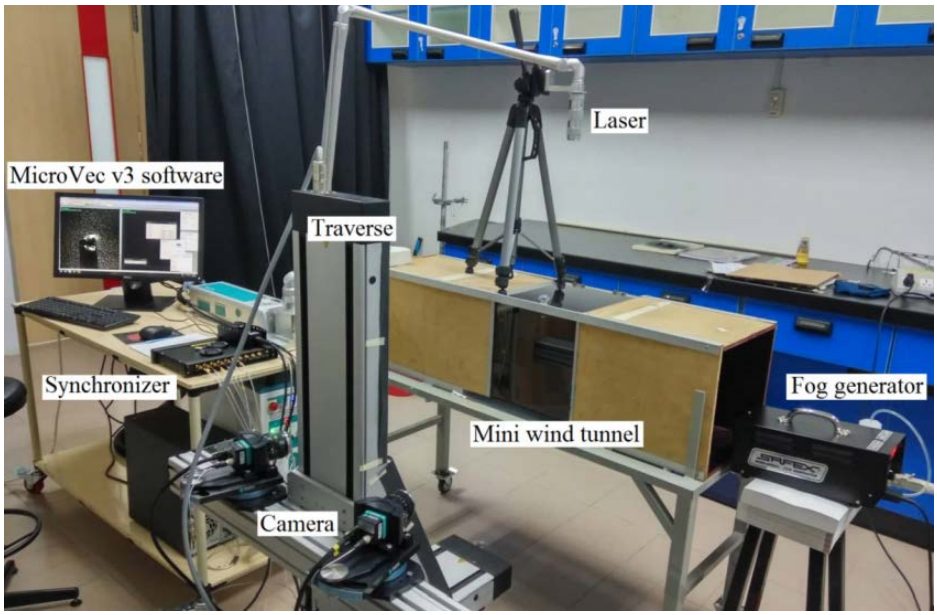


Fig. 2: Experimental setup.

**MODELLING AND SIMULATION**

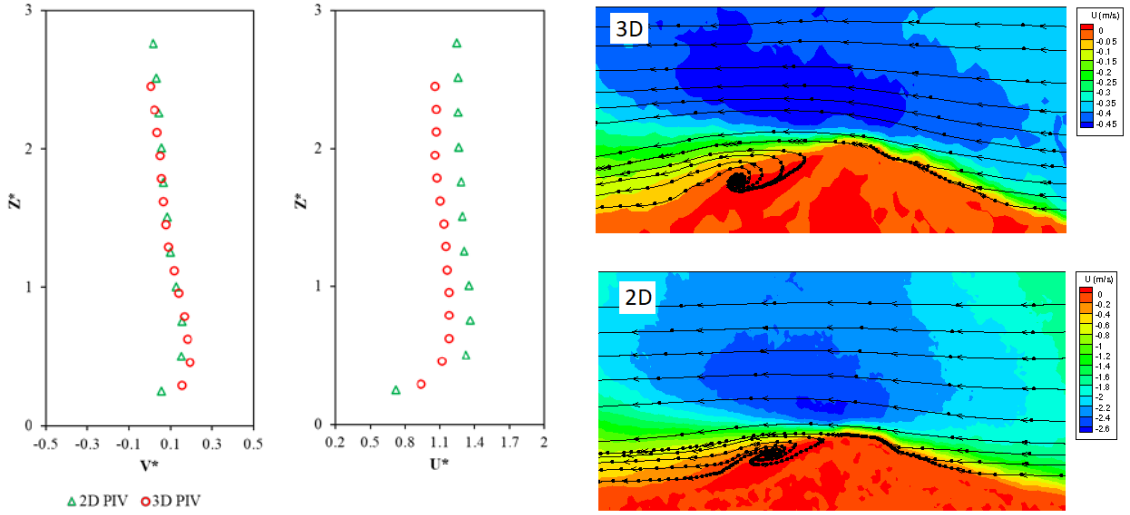


Fig. 3: Comparison of 2D and 3D PIV measurement.

**Keywords:** Particle image velocimetry; 2D PIV; 3D PIV; Flow over terrain.

## Acknowledgement

This work is funded by Ministry of Education Malaysia (FRGS/1/2018/TK02/UMP/02/17) managed by Department of Research and Innovation, Universiti Malaysia Pahang (RDU190145).

## References

[1] Law W. P., Erain N., Ramli N. I. & Gimbun J. (2019). Assessment of chlorine leak dispersion around Gebeng industrial area and potential evacuation route. *Atmospheric Research*, 216, 117-129.
[2] Yeap A. (2016). Chlorine gas causes scare around plant. Retrieved from https://www.thestar.com.my/ (accessed on 4 October 2017).

**NATURAL PRODUCTS AND INDUSTRIAL CROPS**

**Paper ID: ESCE036**

# HYDRODISTILLATION OF ESSENTIAL OIL FROM THE WHOLE BLACK PEPPER AND LIGHT BERRIES BLACK PEPPER (*PIPER NIGRUM* L.) HARVESTING IN DAK NONG, VIETNAM ON PILOT SCALE: THE STUDY ON EXTRACTION PROCESS AND ANALYSIS OF COMPONENTS IN ESSENTIAL OILS

**D. N. Do[1]***

[1] *Faculty of Environmental and Food Engineering, Nguyen Tat Thanh University, Ho Chi Minh City 700000, Vietnam.*
*Corresponding author: ddnhat@ntt.edu.vn

## Extended Abstract

Black pepper (*Piper nigrum* L.) is a tropic plant with large applications due to its commercial, economic, nutritional, and medicinal value. Besides good quality whole black pepper, which meets export demand, lower quality pepper is commonly known as light berries black pepper, and the market price is much lower than that of good quality pepper. However, pepper oil is concentrated mainly in the shell, so extracting pepper essential oil from this raw material is an option to improve its economic value [1]. For this study, the pilot-scale hydrodistillation process was employed to extract essential oil from two types of pepper from Vietnam, including whole black pepper (570 g/l) and light berries black pepper (300 g/l). Extraction parameters such as time, temperature, rate, and the material to water ratio were optimized. The quantitative analyses of the essential oils were performed by Gas Chromatography-Mass Spectrometry. The optimum yield was achieved up to 2.38% for light berries black pepper when the extract conditions were set up at a material-water ratio of 1:12.5 (kg/l) for 180 minutes under the extraction temperature of 130 $^{o}$C. For whole black pepper (570 g/l), the maximum yield was 1.65% at distillation conditions: material-water ratio of 1:15 (kg/l), distillation time of 210 minutes, and temperature of 140 $^{o}$C.

In comparison with previous studies, some main points concerning the conditions of extraction by hydro-distillation method are summarized as follows (Table 1).

Table 1: Comparison of black pepper oil yields from different studies.

| | Study 1 [2] | Study 2 [3] | This study | This study |
|---|---|---|---|---|
| Material | Vietnamese black pepper | Vietnamese black pepper | Vietnamese whole black pepper | Vietnamese light berries black pepper |
| Experimental scale | Lab scale (20g) | Lab scale (40g) | Pilot scale ( 5kg) | Pilot scale ( 5kg) |
| Yield (%) | 2.4 | 2.19 | 1.65 | 2.38 |
| Time (h) | 5.2 | 1 | 3.5 | 3 |
| The material to water ratio (kg/l) | 1:21 | 1:15 | 1:15 | 1:12.5 |

The results in Table 1 show that the yield of light berries black pepper oil was higher than that of whole black pepper. This can be explained by the fact that pepper oil was concentrated mainly in the outer part of the pepper fruit [4], so with the same amount of raw material, the amount of essential oil in light berries black pepper will be higher than that of whole black pepper. In addition, we saw the difference between the pepper oil extraction yield at laboratory scale and pilot scale. In fact, when increasing from laboratory scale to pilot scale, oil recovery efficiency tended to decrease. Therefore, pilot-scale studies are needed to have expansion at larger scales.

The result of GC-MS showed that 3-Carene, D-limonene, and β-caryophyllene were presented as major components of both types of pepper. In addition, the content of β-caryophyllene compound in light berries black pepper (28.28%) is higher than that in whole black pepper (21.94%). Research results showed the potential of extracting essential oil from light berries black pepper (a product with a much lower value than whole black pepper) to enhance its economic value. Besides, the results of this study on the pilot scale could be useful for technology transfer, which might become the solution to shorten the gap between research and production.

**Keywords:** Hydrodistillation; Light berries black pepper; Essential oil; Pilot scale.

## Acknowledgment

We would like to thank Nguyen Tat Thanh University, Ho Chi Minh City, Vietnam for the support of time and facilities for this study.

## References

[1] Srinivasan, K. (2007) Black Pepper and its Pungent Principle-Piperine: A Review of Diverse Physiological Effects. Crit Rev Food Sci Nutr 47(8):735-748.
[2] Tran, T. H., Le Ha, K., Nguyen, D. C., Dao, T. P., Le Nhan, T. H., Nguyen, D. H., ... & Bach, L. G. (2019) The study on extraction process and analysis of components in essential oils of black pepper (Piper nigrum L.) seeds harvested in Gia Lai Province, Vietnam. Processes 7(2): 56.
[3] Dinh, P. N., Cam, H. D. T., & Quoc, T. P. (2020) Comparison of essential oil extracted from black pepper by using various distillation methods in laboratory scale. IOP Conf. Ser.: Mater. Sci. Eng 991(1):012050.
[4] Myszka, K., Leja, K., & Majcher, M. (2019) A current opinion on the antimicrobial importance of popular pepper essential oil and its application in food industry. J. Essent. Oil Res 31(1):1-18.

**NATURAL PRODUCTS AND INDUSTRIAL CROPS**

**Paper ID: ESCE037**

# PILOT SCALE PRODUCTION OF TAMANU (*CALOPHYLLUM INOPHYLLUM*) OIL BY USING HYDRAULIC PRESSING: EFFECT OF PROCESSING PARAMETERS

**D. N. Do[1]***

[1] *Faculty of Environmental and Food Engineering, Nguyen Tat Thanh University, Ho Chi Minh City 700000, Vietnam.*
*Corresponding author: ddnhat@ntt.edu.vn

## Extended Abstract

Tamanu oil (Calophyllum inophyllum L.) was traditionally used for wound healing and to cure various skin problems and cosmetic purposes. Tamanu oil obtained from fruit was one of the most valuable products of the Tamanu tree. In solid-liquid extracts, some common methods include solvent extraction, microwave extraction, mechanical pressing, enzymatic extraction, ultrasonic-assisted extraction, and supercritical fluid extraction. Of these methods, hydraulic pressing is the most common method to recover oil from seeds. In the hydraulic press technique, operating conditions such as pressing pressure, pressing time, moisture content, size, and the mass of material significantly affect the yield and the quality of the oil obtained [1, 2]. In this research, crude Tamanu oil was extracted from Tamanu fruit by hydraulic press method at pilot scale. The effect of various critical factors on the oil yield was considered. One of the most important factors affecting the extraction process of Tamanu oil is pressing pressure [1]. The effect of the pressing pressure was determined with different levels of 150 to 200 kg/cm$^2$. After this experiment, we selected optimal pressure to consider the effect of pressing time on the oil yield. The pressing time range of 5, 10, 15, 20, 25, and 30 minutes was considered. Some researchers suggested that a reduction in particle size slightly increases the oil yield [3]. In contrast, some studies suggested that the oil yield can decrease with decreasing particle size [4]. Therefore, we investigated the effect of the size of material on the oil yield. The moisture content of the material may affect the oil extraction process performance [5]. Various heat treatment conditions corresponding to different material moisture were considered. The volume of pressing materials is an important factor in expanding industrial-scale applications. The input volume of material effect on the oil yield was done by varying the seed material from 1 to 4 kg/time. Tamanu oil was stored at room temperature in a dark bottle. The physical and chemical properties of Tamanu oil, such as density, viscosity, saponification, acid, peroxide, and iodine value, were determined according to ISO standards.

It was found that the oil yield increased with increasing applied pressure and pressing time. Material moisture content and size had a significant effect on oil extraction process efficiency. Figure 1 reveals the impact of material moisture on the oil yield.

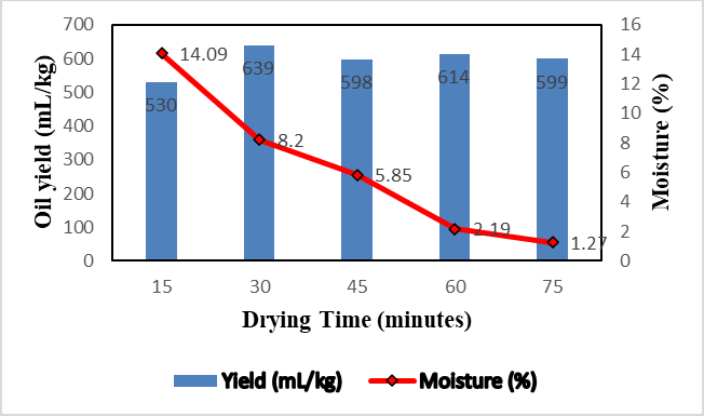


Fig. 1: The yield of Tamanu oil at various material moisture, the pressure of 180 (kg/cm$^2$), pressing time of 15 min.

In general, material moisture had a strong influence on oil collection efficiency. At moisture of 14.09%, the obtained oil yield was the lowest. High material moisture, the structure of Tamanu seeds was not hard enough, easy to slide into each other, leading to reduced oil yield. When the material moisture was decreased, oil yield was increased. The oil yield increased from 530 mL/kg (at the moisture of 14.09%) to 639 mL/kg (moisture of 8.2%). When the moisture was reduced from 8.2% to 1.27%, the yield decreased but not significantly. In summary, the material moisture of 8.2% was suitable for pressing Tamanu oil in this study. Our results differ from some previous studies that the oil yield decreases with decreasing the material moisture content [5]. This could be due to material structure differences.

The highest Tamanu oil extraction yield was 639 mL/kg at conditions: material moisture of 8.2%, extruded kernels, pressing pressure of 180 kg/cm$^2$, and pressing time of 15 minutes. Chromatography and mass spectrometry analysis indicated that prime fatty acids identified in Tamanu oil were palmitic acid (12.69%), stearic acid (13.52%), oleic acid (41.88%), and linoleic acid (29.94%). The research that the hydraulic press method was suitable to separate the Tamanu oil, and it could be used to manufacture Tamanu oil at an industrial scale.

**Keywords:** Tamanu oil; Calophyllum inophyllum; Hydraulic press; Omega 3; Pilot scale.

## Acknowledgment

We would like to thank Nguyen Tat Thanh University, Ho Chi Minh City, Vietnam for the support of time and facilities for this study.

## References

[1] Jahirul, M. I., Brown, J. R., Senadeera, W., Ashwath, N., Laing, C., Leski-Taylor, J., & Rasul, M. G. (2013) Optimisation of bio-oil extraction process from beauty leaf (Calophyllum inophyllum) oil seed as a second generation biodiesel source. Procedia Eng. 56:619-624.
[2] Sundur, S., Shrivastava, B., Sharma, P., Raj, S. S., & Jayasekhar, V. L. (2014) A review article of pharmacological activities and biological importance of Calophyllum inophyllum. Int J Adv Res 2(12):599-603.
[3] Follegatti-Romero, L. A., Piantino, C. R., Grimaldi, R., & Cabral, F. A. (2009) Supercritical CO2 extraction of omega-3 rich oil from Sacha inchi (Plukenetia volubilis L.) seeds. J. Supercrit. Fluids 49(3):323-329.
[4] Adeeko, K. A., & Ajibola, O. O. (1990) Processing factors affecting yield and quality of mechanically expressed groundnut oil. J. Agric. Eng. Res. 45:31-43.
[5] Subroto, E., Manurung, R., Heeres, H. J., & Broekhuis, A. A. (2015) Mechanical extraction of oil from Jatropha curcas L. kernel: Effect of processing parameters. Ind Crops Prod 63:303-310.

**NATURAL PRODUCTS AND INDUSTRIAL CROPS**

**Paper ID: ESCE044**

# THE EFFECT OF AQUEOUS EXTRACT PARAMETERS ON TOTAL PHENOLIC CONTENT AND ANTIOXIDANT ACTIVITY OF MORINGA OLEIFERA LEAVES

**Tran Bui-Phuc[1], T.K.N. Nguyen[1], N. X. Ngo[1], Q. A. Trieu[1]***

[1] *Faculty of Environmental and Food Engineering, Nguyen Tat Thanh University, Ho Chi Minh, Vietnam.*
*Corresponding author: tqan@ntt.edu.vn

## Extended Abstract

Currently, thanks to the diversity of beneficial bioactive substances in the composition of Moringa oleifera leaves, much attention has been focused on Moringa oleifera (*Moringa oleifera Lam*). In this report, the effects of Moringa oleifera extraction conditions with thermal bath support for total polyphenol content and antioxidant resistance of the leaf extract were investigated. The best suitable conditions for aqueous extraction were as follows: material/water ratio of 1/30 g/mL, the extraction temperature of 80°C, the extraction time of 30 mins. The total phenolic content reached the highest value of 23.9 mg Gallic acid equivalent/g dry leaf. The antioxidant capacities of aqueous leaf extracts ranged from 16 to 30 mg Trolox equivalent/g dry leaf. Overall, with its high antioxidant capacity, Moringa oleifera shows not only potential value in medicine but also has high economic value.

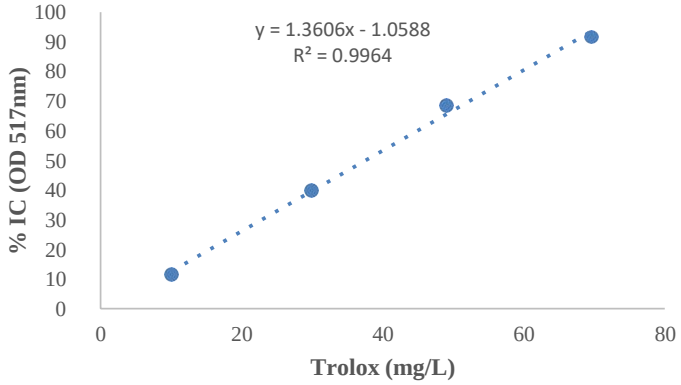


Fig. 1: The calibration curve antioxidant activity DPPH against Trolox concentration.

**Keywords:** *Moringa oleifera Lam*; Total phenolic; Antioxidant activity; Extraction; Thermal bath.

### Acknowledgment

This study was supported by Nguyen Tat Thanh University, Ho Chi Minh City, Vietnam.

### References

[1] Olufunsho Awodele, Ibrahim Adekunle Oreagba, Saidi Odoma, Jaime A. Teixeira da Silva, Vincent Oluseye Osunkalu, Toxicological evaluation of the aqueous leaf extract of Moringa oleifera Lam. (Moringaceae), *Journal of Ethnopharmacology* 139, 330– 336, 2012.

[2] C. Rodríguez-Pérez, R. Quirantes-Piné, A. Fernández-Gutiérrez, A. Segura-Carretero Optimization of extraction method to obtain a phenolic compounds-rich extract from Moringa oleifera Lam leaves, *Industrial Crops and Products*, Volume 66, 246-254, 2015.

[3] Mohammad Afzal Hossain, Nadia Khan Disha, Jahid Hasan Shourove, Pappu Dey, Determination of Antioxidant Activity and Total Tannin from Drumstick (Moringa oleifera Lam.) Leaves Using Different Solvent Extraction Methods, *Turkish Journal of Agriculture - Food Science and Technology*, 8(12): 2749-2755, 2020.

**NATURAL PRODUCTS AND INDUSTRIAL CROPS**

**Paper ID: ESCE050**

# CHEMICAL COMPOSITION AND ANTIOXIDANT ACTIVITY OF CORNMINT GROWN IN VIETNAM

**Tran Bui-Phuc[1], Nguyen Dinh-Phong[1], Ngo Hoang-Duy[1], Le-Thi Anh-Dao[1], and Nguyen Cong-Hau[1]***

[1] *Faculty of Environmental and Food Engineering, Nguyen Tat Thanh University.*
*Corresponding author: tbphuc@ntt.edu.vn

## Extended Abstract

Cornmint (*Mentha arvensis* L.) belongs to the family Lamiaceae, about 10-150 cm tall. Cornmint is an herb that has been grown for a long time in many countries in Europe and Asia. Mint flowers are pale purple, while the leaves are the organ that contains the highest content of essential oils [1]. The main ingredient of cornmint is menthol ($C_{10}H_{20}O$), which accounts for approximately 60-90%, and various other minor components, including camphene, limonene, and 1, 8-cineole, etc. [2]. Menthol is an anesthetic and analgesic and is widely used to treat respiratory diseases [3]. In addition to being beneficial for the digestive system and cold treatment [4], the cornmint oil helps to reduce insomnia, reduce stress, support blood circulation to make the mind feel comfortable [5]. Besides, the cornmint assists to boost the immune system, relieve pain, beautify the skin, and fade bruises. Also, mint is widely used in the food fields as detox, spices, confectionery, and flavoring [6]. Thanks to its high economic value, mint is produced in many countries such as India, China, Vietnam, Japan, and Brazil, etc.

With a tropical climate, high humidity, and a lot of rain, Vietnam is quite suitable for growing mint due to its extreme weather-resistant properties. The goal of the study was to investigate conditions for the extraction of cornmint essential oil by using the pilot-scale, using the four-month cornmint plants were collected in Binh Thuan Province (Vietnam). Then, the obtained essential oil was determined the total polyphenol contents [7], DPPH and ABTS radical scavenging activity [8, 9] to evaluate the antioxidant capacities.

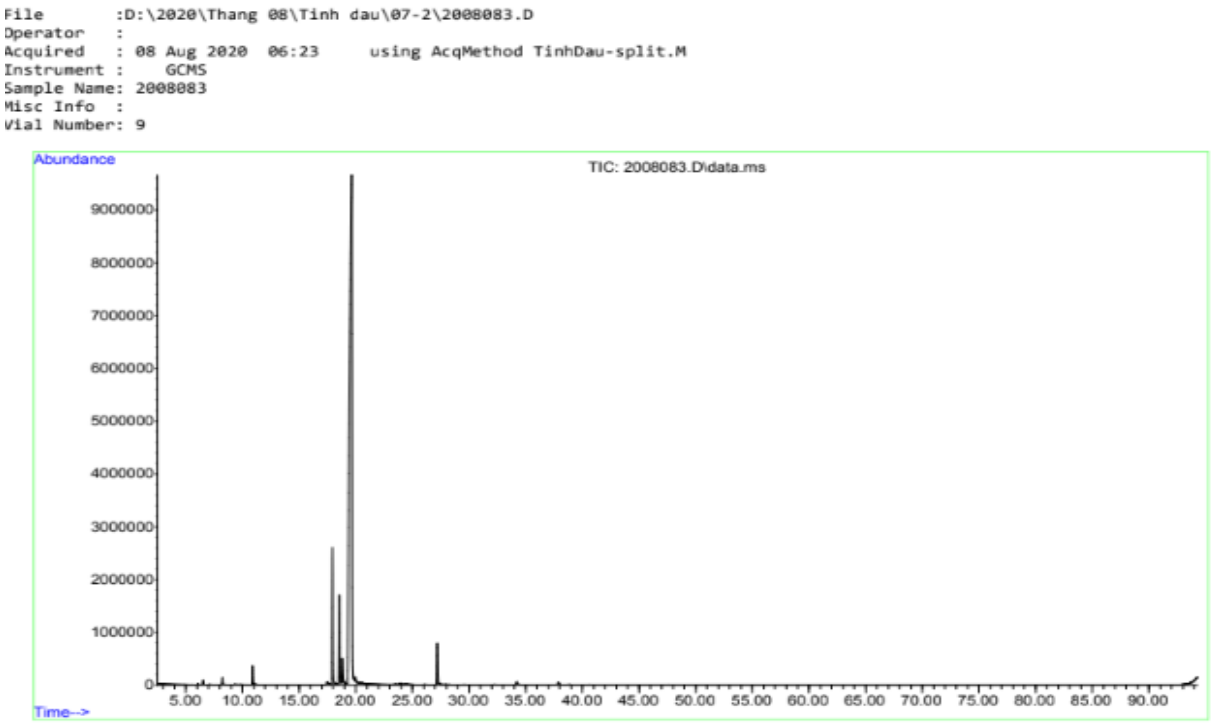


Fig. 1: Chromatogram of Cornmint essential oilreached by the pilot-scale with some main compositions listed as trans-menthone 7.5%, menthol 80.07 %.

The essential oil content reached the highest value of 0.051 (g/mL) when using cut material size of 5-10 cm (moisture about 80%), material/solvent ratio 1:7 (g/mL), extraction temperature 130ºC, extraction time 150 minutes. GC-MC analysis (Figure 1) showed that essential oil has two main compounds: Menthol (80,075%) and L-Menthone (7,519%). The total polyphenol content of Cornmint essential oil was 0.7 mg/mL. Furthermore, DPPH and ABTS radical scavenging activity of essential oil were measured 53.1% and 68.2% respectively. Experimental results could be applied for large-scale industrial production.

**Keywords:** Cornmint; *Mentha arvensis*; Pilot scale; Extraction; Menthol.

**Acknowledgment**

This study was supported by Nguyen Tat Thanh University, Ho Chi Minh City, Vietnam.

**References**

[1] Lawrence B. M. (2006) Mint: The Genus Mentha. CRC Press, Florida.
[2] Bakkali F., Averbeck S., Averbeck D., and Idaomar M. J. F. (2008) Biological effects of essential oils-A review. Food Chem. Toxicol. 46:446.
[3] Patel T., Ishiuji Y., and Yosipovitch G. (2007) Menthol: A refreshing look at this ancient compound. J. Am. Acad. Dermatol. 57.
[4] Birring, S. S., Brew, J., Kilbourn, A., Edwards, V., Wilson, R., and Morice, A. H. (2017) Rococo study: a real-world evaluation of an over-the-counter medicine in acute cough (a multicentre, randomised, controlled study). BMJ open, 7(1), e014112.
[5] Blackburn L., Achor S., Allen B., Bauchmire N., Dunnington D., and Klisovic R. B. (2017) The effect of aromatherapy on insomnia and other common symptoms among patients with acute leukemia. Oncol. Nurs. Forum, 44:185.
[6] Sachan, A. K., Kumar, S., Kumari, K., and Singh, D. (2018). Medicinal uses of spices used in our traditional culture: Worldwide. Journal of Medicinal Plants Studies, 6(3):116–122.
[7] Sánchez-Rangel, J. C., Benavides, J., Heredia, J. B., Cisneros-Zevallos, L., & Jacobo-Velázquez, D. A. (2013). The Folin–Ciocalteu assay revisited: improvement of its specificity for total phenolic content determination. Analytical Methods, 5(21):5990–5999.
[8] Xiao, F., Xu, T., Lu, B., and Liu, R. (2020). Guidelines for antioxidant assays for food components. Food Frontiers, 1(1):60-69.
[9] Cleverdon, R., Elhalaby, Y., McAlpine, M. D., Gittings, W., and Ward, W. E. (2018). Total polyphenol content and antioxidant capacity of tea bags: comparison of black, green, red rooibos, chamomile and peppermint over different steep times. Beverages, 4(1):15.

**NATURAL PRODUCTS AND INDUSTRIAL CROPS**

**Paper ID: ESCE058**

# BLACK PEPPER ESSENTIAL OIL BASED MOSQUITO REPELLENT LOTION

**D. P. Nguyen[1]*, Q. H. Tran[1], T. Q. Phan[1]**

[1] *Faculty of Environmental and Food Engineering, Nguyen Tat Thanh University, Ho Chi Minh, Vietnam.*
*Corresponding author: ndphuc@ntt.edu.vn

## Extended Abstract

For thousands of years, black pepper has been a functional plant with nutritional and medicinal benefits. Besides, D-Limonene, Terpinolene, 1R-□-Pinene are the major bioactive compounds in black pepper applied for repelling mosquitoes. This study determined a combination of operating parameters that optimize the hydrodistillation of essential oil, including distillation time, distillation temperature, feed particle size, time to soak NaCl solution, and NaCl concentration solution, and feed-solvent ratio on yield of essential oil extraction. The results obtained placed the optimum extraction condition at 5 hours of distillation time, at 180□C of distillation temperature, 0.25 mm of particle size, and 1:20 of feed-solvent ratio. With these parameters, the highest yield of distillate essential oil process is 2.3%. The lotion product with 2% of black pepper essential oil was reported that was the ability to repel mosquitoes effectively in 186 minutes. The development and use of black pepper essential oil effectively applied in repellent products provide an enormous potential for cosmeceutical.

The purpose of this study is to provide optimum conditions for the distillation process of black pepper essential oils from Daklak (Viet Nam), such as NaCl soaking time, the concentration of NaCl solution, distillation time, particle size, feed-solvent ratio, distillation temperature, as well as provide a product was applied from black pepper essential oil. The results of this study will be very potential for the cosmetic and pharmaceutical. The product was from familiar and cheap materials, no affect the environment, and friendly with human health.

Distillation process: The essential oils were obtained by hydrodistillation with a Clevenger-type apparatus (Appendix 1). The yield of the essential oil depends on factors such as temperature, distillation time, NaCl soaking time, the concentration of NaCl, etc. The material was treated, ground, and sieved to 20-60 mesh size. After that, it would be preserve before the distillation process to ensure the oil content. Black pepper is weighed with determined mass into the flask. Add NaCl solution with concentration from 0%-4% to the flask contains black pepper, lightly shake. Then, they were soaked in the required time to survey. The solution will be distilled at a temperature from 140 to 220□C; the time is from 3h to 7h. After the distillation is completed, the oil is recovered, anhydrous with Na2SO4, and stored in a container. Distilled samples with optimum conditions were stored, physicochemical determination, and GC-MS analysis.

Lotion process: Weigh tween 80, launryl in the same cup; coconut oil, almond oil in the same becher with a determined ratio. Then, pour a cup of tween 80 + launryl into coconut + almond oil. Start heating and stirring at a temperature of 60-70 degrees Celsius. Start adding the water slowly into that mixture until the stirring is completed for 40 minutes. Keep stirring with the cetyl alcohol and the emulsifier, lower the temperature to about 45 degrees Celsius. Continue stirring for 10 minutes and then turn off the heat exchanger but still stirring. Start slowly stirring to gradually reduce the temperature, and then add all components such as vitamin E, vitamin B3, glyceryl, and black pepper or citronella essential oil.

Conclusion: Black pepper in Daklak (VietNam) has a high yield of essential oil and repellent compounds. The lotion shows that resonance scent has potential ineffective mosquito repellent. The aim of this work was to study the extraction efficiency of the black pepper EO distillation process. The extractions were carried out by a hydrodistillation method. Optimized extraction yields of essential oil were achieved by decreasing the particle diameter as far as practical, operating of extraction temperature at which all actives are stable, an extraction time sufficient to overcome diffusion limitations, the solvent-to-material ratio, which is efficient and feasible, and a solvent composition capable of extracting the lipophilic and hydrophilic bioactive components. The optimal extraction conditions that satisfied the above constraints were found to be a particle diameter of 0.25 mm, at an

extraction temperature of 180 °C, an extraction time of 5 hours, the solvent-to- material ratio of 20:1, 2% NaCl solution soaking time of 2h. Extraction yield results were found to be in good agreement with those at a laboratory scale, which gives confidence that the optimized process can be carried out without loss of efficiency at an industrial scale. However, the flavor of the product has some limitations, not really impressive. Other next studies need to improve that problem to have a better product.

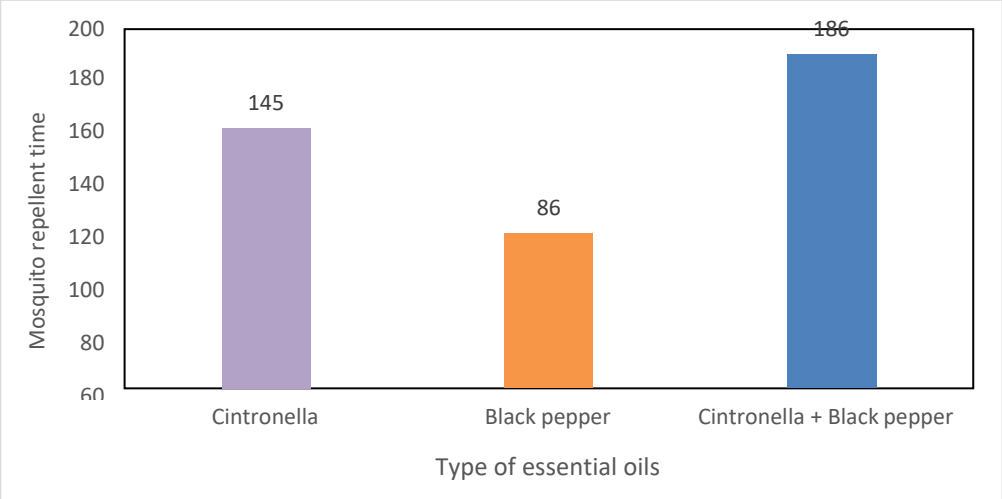


Fig. 1: Mosquito repellent time of 3 lotion samples.

**Keywords:** Black pepper; Mosquitoes; Repellent, Hydrodistillation.

**Acknowledgment**

This study was supported by the Faculty of environmental and food engineering, Nguyen Tat Thanh University, Ho Chi Minh, Vietnam.

**References**

[1] R. Pavela, "Essential oils for the development of eco-friendly mosquito larvicides: A review," *Industrial Crops and Products*, vol. 76, pp. 174-187, 2015.
[2] E. A. Gould and T. Solomon, "Pathogenic flaviviruses," *The Lancet*, vol. 371, pp. 500-509, 2008/02/09/ 2008.
[3] A. M. A. Elourfi, "Evaluation of various essential oils as repellents and insecticides against mosquitoes," 2005.
[4] Y. Trongtokit, Y. Rongsriyam, N. Komalamisra, and C. Apiwathnasorn, "Comparative repellency of 38 essential oils against mosquito bites," *Phytother Res*, vol. 19, pp. 303-9, Apr 2005.
[5] A. M. Pohlit, N. P. Lopes, R. A. Gama, W. P. Tadei, and V. F. Neto, "Patent literature on mosquito repellent inventions which contain plant essential oils--a review," *Planta Med*, vol. 77, pp. 598-617, Apr 2011.
[6] M. Chellappandian, P. Vasantha-Srinivasan, S. Senthil-Nathan, S. Karthi, A. Thanigaivel, A. Ponsankar, *et al.*, "Botanical essential oils and uses as mosquitocides and repellents against dengue," *Environ Int*, vol. 113, pp. 214-230, Apr 2018.
[7] M. C. Ou, Y. F. Lee, C. C. Li, and S. K. Wu, "The effectiveness of essential oils for patients with neck pain: a randomized controlled study," *J Altern Complement Med*, vol. 20, pp. 771-9, Oct 2014.
[8] S. R. S. Ferreira, "Supercritical fluid extraction of black pepper (Piper Sigrun L.) essential oil," *Journal of Supercritical Fluids 14*, pp. 235–245, 1999.
[9] H. H. Jelen and A. Gracka, "Analysis of black pepper volatiles by solid-phase microextraction-gas chromatography: A comparison of terpenes profiles with hydrodistillation," *J Chromatogr A*, vol. 1418, pp. 200-209, Oct 30 2015.
[10] H. Bagheri, M. Y. Abdul Manap, and Z. Solati, "Antioxidant activity of Piper nigrum L. essential oil extracted by supercritical CO(2) extraction and hydrodistillation," *Talanta*, vol. 121, pp. 220-8, Apr 2014.
[11] Y. Wang, R. Li, Z.-T. Jiang, J. Tan, S.-H. Tang, T.-T. Li, *et al.*, "Green and solvent-free simultaneous ultrasonic-microwave assisted extraction of essential oil from white and black peppers," *Industrial Crops and Products*, vol. 114, pp. 164-172, 2018.

**NATURAL PRODUCTS AND INDUSTRIAL CROPS**

**Paper ID: ESCE075**

# ONE-POT LEVULINIC ACID PRODUCTION FROM RICE STRAW IN DEEP EUTECTIC SOLVENT

**Chenda Hak[1], Panadda Panchai[3], Tanawut Nutongkaew[1,2], Nurak Grisdanurak[3], Sarttrawut Tulaphol[1,2]***

[1] *Department of Chemistry,* [2] *Sustainable Polymer & Innovative Composite Materials Research Group, Faculty of Science, King Mongkut's University of Technology Thonburi 10140, Bangkok,Thailand.*
[3] *Center of Excellence in Environmental Catalysis and Adsorption, Department of Chemical Engineering, Faculty of Engineering, Thammasat University 12121, Pathum Thani, Thailand.*
*Corresponding author: Sarttrawut.tul@kmutt.ac.th

## Extended Abstract

### Introduction

Current productions of fuels, chemicals and plastic precursors use petroleum as a feedstock. With the increasing demand for these petroleum-derived products and their limited supply, alternative renewable feedstocksare sought-after. Lignocellulosic biomass has been shown as a potential alternative feedstock. Its cost- effectiveness, renewability, and abundance make it an ideal alternative feedstock of petroleum [1]. Rice straw isclassified as an abundant lignocellulose feedstock consisting of cellulose between 32 to 47%, hemicellulose between 19 to 20%, and lignin between 5 to 24% [2]. High cellulose content makes it a promising lignocellulose feedstock.

Levulinic acid (LA), a biomass-derived product, is a high-valued chemical for pharmaceuticals, plasticizers, solvents, flavoring agents, other additives and even cosmetics. Production of levulinic acid from cellulose undergoes three sequential steps: (1) cellulose hydrolysis to glucose; (2) glucose dehydration to 5- hydroxymethyl furfural (HMF); and (3) HMF hydrolysis to LA with formic acid as a by-product (see fig. 1).

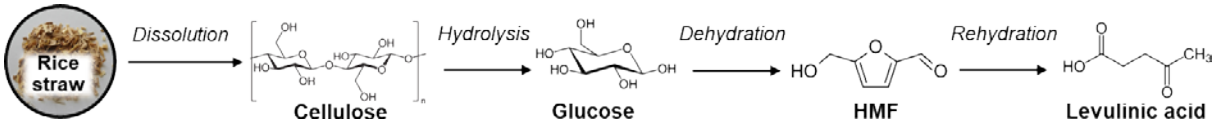


Fig. 1: Reaction pathway of levulinic acid production from lignocellulose.

Lignocellulosic biomass consists of three major components, (1) cellulose, (2) hemicellulose, and (3) lignin, glued together via strong hydrogen bonding, forming a robust matrix. This robust structure, in turn, makesit very difficult for us to process lignocellulosic biomass conversion. Hence, lignocellulosic biomass must be processed fractionations/pretreatments to improve cellulose accessibility and unlock carbohydrates in biomass. Cellulose solvent pretreatment (e.g., ionic liquids) has shown to be effective because it can partially disrupt hydrogen bonding among crystalline cellulose chains, resulting in enhanced cellulose accessibility to catalysts/enzymes [3]. A previous study investigated levulinic acid production from hemp hurd in one pot by ionic liquid in acid. Dissolution hemp hurd in ionic liquid enabled acid to catalyze dissolved hemp hurd to levulinic acid (47 % yield) in mild conditions [4]. Although ionic liquids show high efficiency in cellulose dissolution, it is hard to process in large-scale applications because of its cost.

Recently, Deep eutectic solvent (DES), a new green, renewable, biodegradable and inexpensive ionic solvent, has become an outstanding solvent that shares similar physical and chemical properties to ionic liquid. DES is a mixture of a hydrogen-bond acceptor (HBA) and a hydrogen-bond donor (HBD) with a specific molar ratio to form a eutectic mixture. Choline chloride (ChCl)-based DESs have exhibited their capability to biomass fractionation which enhances cellulose accessibility to catalyst.

This study aims to produce levulinic acid in choline chloride-based deep eutectic solvent in one pot. Wescreened carboxylic acid-based deep eutectic solvents for rice straw dissolution. The suitable DES, which had thehighest rice straw dissolution, was selected to study levulinic acid production further.

## NATURAL PRODUCTS AND INDUSTRIAL CROPS

### Methodology

Deep eutectic solvents were synthesized by mixing ChCl (HBA) and hydrogen bond donor (acetic acid (Ace), oxalic acid (Oxa), malonic acid (Mal) and succinic acid (Suc)) with 1:1 molar ratio. The mixture was heated at 80°C until clear liquid formed. Levulinic acid production was conducted into a one-pot two- step process, (1) rice straw dissolution in DES at 5% solid loading, (70-150°C) for (1-6 h). and (2) acid hydrolysis by 1.5 wt.% HCl, 120°C for 1-6 h. HCl was selected as a catalyst to avoid anions exchange in ChCl:Oxa. The resulting hydrolysate has analyzed the products using HPLC.

### Results and discussion

To obtain the suitable DES for levulinic acid production, we screen various carboxylic acid-based DESs by the dissolution of rice straw (120°C for 2h) and acid hydrolysis (120°C for 2 h). Choline chloride- oxalic acid (ChCl-Oxa) gave the highest dissolved biomass with the highest levulinic acid yield (10 %). Thus, ChCl-Oxa was selected to study further. To understand the effect of dissolution time to levulinic acid yield, we varied the dissolution temperature of rice straw in ChCl-Oxa from 100 – 150°C for 2 h, while maintainingacid hydrolysis condition at 120°C, 1.5 wt.% HCl and 2 h. We found the maximum levulinic acid yield (13%) at 100°C and 2 h. A further increase in dissolution temperature from 100°C to 150°C caused levulinic acid yield to drop. We selected dissolution temperature at 100°C to study the effect of dissolution time. We varied the dissolution time of rice straw in ChCl-Oxa from 1 – 4 h. An increase in dissolution time from 1 to 4 h promotedglucan conversion from 21% to 56%. Longer dissolution time improved hydrolysis of cellulose, resulting in highglucan conversion. These results suggested that an increase in dissolution temperature or time promoted the interaction between DES with rice straw by cleavage of LCC in rice straw by protons in DES and disrupting or swelling inter-and intra-molecular hydrogen bonds in cellulose chains in rice straw.

To examine hydrolysis profile of dissolved rice straw in DES with HCl, the dissolved rice straw in ChCl-Oxa at 100°c for 2 h was hydrolyzed by 1.5 wt.% HCl at 120°C. We observed the maximum levulinic acid yield (52%) at 10 h and longer hydrolysis time (10 to 12 h) slightly lowered levulinic acid yield from 52% to 47%, suggesting the degradation of levulinic acid to undesired humin. We obtained a high levulinic acid yield of 52% with a dissolution condition of 5% solid loading, 100°C for 2 h and acid hydrolysis condition of 1.5 wt.% HCl, 120°C and 10 h. Under 100 kg rice straw as an assumption, we obtained 12.5 kg levulinic acid. To elucidate the change in the chemical structure of rice straw after dissolution and acid hydrolysis, we characterized regeneratedsolid after dissolution and residual solid after acid hydrolysis by XRD and FTIR against raw straw as a control. An increase in the lateral order index (LOI), total crystallinity index (TCI) and crystallinity index (CrI) of regenerated solid after ChCl-Oxa dissolution indicated that amorphous cellulose was solubilized into the soup. After acid hydrolysis, we observed an increase in LOI, TCI and CrI of residual solid suggested that amorphous cellulose was easily hydrolyzed, leaving crystalline cellulose in the residual solid.

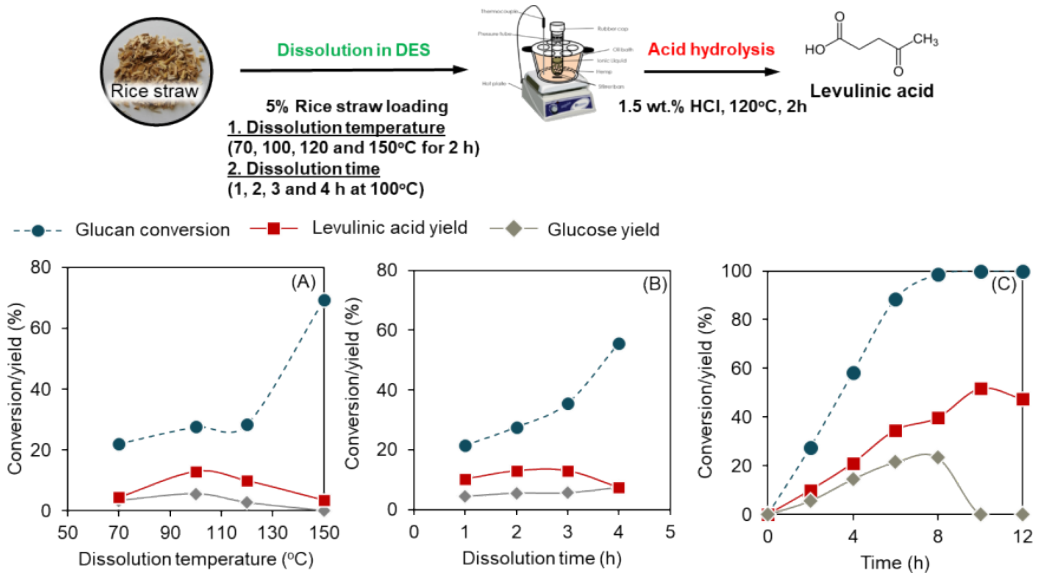


Fig. 2: Effect of dissolution temperature (A), effect of dissolution time (B), Acid hydrolysis profile of rice straw dissolution at 100°C for 2 and acid hydrolysis at 120°C for 10 h (C).

## Conclusion

We presented a one-pot two-step process for levulinic acid from rice straw. This study can reduce production costs from ionic liquid and eliminate the separation cost of glucose and HMF in levulinic acid production. However, life cycle assessment (LCA) and techno-economic assessment (TEA) studies will make thisprocess economical.

**Keywords:** Deep eutectic solvent; Rice straw; Levulinic acid; Acid hydrolysis; One-pot process.

## Acknowledgment

The authors would like to thank the Petchra Pra Jom Klao scholarship, the Pra Jom Klao research funding, the Post-doctoral Fellowship and Department of Chemistry, Faculty of Science, King Mongkut's University of Technology Thonburi (KMUTT), Thailand, for the financial support.

## References

[1] Morgan, H.M., et al. (2017) Bioresour. Technol. 230:112-121.
[2] Imman, S., et al. (2015) Chem. Eng. J. 278:85-91.
[3] Karimi, K. and M.J. Taherzadeh. (2016) Bioresour. Technol.203:348-356.
[4] Tulaphol, S., et al. (2020) Energy Fuels 34(2):1764-1772.

**NATURAL PRODUCTS AND INDUSTRIAL CROPS**

**Paper ID: ESCE117**

# ANTIAGING AND ANTIBACTERIAL EFFICIENCY OF COPPER ION ON CUT ROSE VASE LIFE (*ROSA L. HYBRID)*

**Le Nguyen[1], Nguyen Thanh-Nho[1]*, Le Trung-Hieu[2], Nguyen Viet-Cuong[1]**

[1] *Faculty of Environmental and Food Engineering, Nguyen Tat Thanh University, Ho Chi Minh City, Vietnam.*
[2] *Ewater Engineering Co.Ltd, Vietnam.*
*Corresponding author: ntnho@ntt.edu.vn

## Extended Abstract

The plantation area and output of cut flowers are increasing worldwide. Post-harvest preservation is an important step of production to reduce losses and improve product quality, values, and competitiveness. Many preservation methods are applied to reduce the impact of adverse factors on the quality and shelf life of cut flowers after harvest. The main techniques include refrigeration, atmospheric, low pressure, and chemical conditions. Vietnam has three primary cut flower growing regions: the Red River Delta, Da Lat city (Lam Dong province, central highland), and the Mekong Delta. The flower is mainly cultivated in conditions without coverage. Only a tiny area of the experimental garden is covered using nylon, net, cork, bamboo, etc., to preserve flowers. The post-harvest preservation is almost based on spontaneous experiences, leading to a quantity loss that causes the increased cost of cut flowers in markets far from flower farms. The proliferation of bacteria in vase water in and on cut flowers is the main cause of the shortened lifespan of some cut flowers and foliage. Consequently, the vase life of cut flowers is decreased. Therefore, it is necessary to have suitable preservation for extending the freshness of cut flowers after harvesting and vases life to increase their values. In the present study, we used copper solutions to the cut rose vase to study its antiaging and antibacterial efficiency. Our hypothesis, metal ions dissolved in water at low concentrations can play as bactericides, fungicides, and wood preservatives [1-3]. Copper ions can create the necessary energy source for the operation of cells, from which the metabolism takes place quickly, helping to eliminate toxins and replace the new layer of healthier and more quality cells.

The morphological changes of flowers over the four stages (Table 1): (a) flowering stage, (b) full bloom stage, (c) flowering stage begins to wilt, (d) full wilted flower stage. The significance of evaluation is to find out which treatments can extend stages (a), (b), and slow down stages (c), (d). The results showed that stage (a) only occurred in the first two days, and stage (d) appeared in the last two days in the control solution. Meanwhile, stage (d) did not present in vases containing copper ions at concentrations of 1 mg $L^{-1}$ and 3 mg $L^{-1}$ at the end of the experimental time. Besides, stage (c) appeared on the $8^{th}$ day of the experiment in vases with 1 mg $L^{-1}$ of copper ion. Stage (a) lasted for the first three days, and stage (b) was maintained until the $8^{th}$ day with 3 mg $L^{-1}$ of copper ion in vases. At the end of the experiment ($9^{th}$ day), there were signs of stage (c). Similar observations were reported for cut Acacia holosericea by Kamani Ratnayake [4]. The lifespan of A. holosericea was improved with copper ion treatment. The petal shape and color assessment aimed to determine flower distinctness, uniformity, and stability during growth. The observed abnormalities explain the vulnerability as well as the ability to maintain growth in the tested subjects. The primary color on the inner petal side was still *pink* (P) to the end of the experiment using 1 mg $L^{-1}$ and 3 mg $L^{-1}$ of copper ion. Meanwhile, *light yellow* (P-Y), the color of the inner side of the petals, was recorded in the control vases. At the same time, the freshness was entirely lost at the end of the experiment with wilted *yellow* (Y) (Table 1). These phenomena may be related to water stress [5] or low carbohydrate concentrations [6]. In another observation for reflexing of petals one by one described as two signals as Absent (Ab.) and Present (Pr.), the "present" signal appeared from the $2^{nd}$ day for control vases during the testing process. For vases, copper concentrations using 1 mg $L^{-1}$ and 3 mg $L^{-1}$ appeared on the $6^{th}$ and $7^{th}$ day, respectively. Another important feature when observing growth in flower diameter was observed. In the present study, it was observed that the flower diameters on the last day of the experiment were in descending of using 3 mg $L^{-1}$ of copper ion > 1 mg $L^{-1}$ of copper ion > control vases without copper ion (i.e., ranging from 6.0 cm to 7.2 cm > from 6.2cm to 6.8cm > 5.2 cm - 5.5 cm).

## NATURAL PRODUCTS AND INDUSTRIAL CROPS

Table 1: Morphological change and color state, petal shape in 9 days of testing.

| Experiment | Day | 1 | 2 | 3 | 4 | 5 | 6 | 7 | 8 | 9 |
|---|---|---|---|---|---|---|---|---|---|---|
| ***Control vases*** | *Morphological Changes* | a | a | b | b | c | c | c | d | d |
| | *Petal: primary color on the inner side* | P | | P-Y | | | | | Y | |
| | *Reflexing of petals one by one* | Ab. | | Pr. | | | | | | |
| | *Flower: diameter (cm)* | 2.5 – 3.0 | | 4.0 – 5.0 | | | | | 5.2 - 5.5 | |
| **1 mg $L^{-1}$ of copper ion** | *Morphological Changes* | a | a | b | b | b | b | b | c | c |
| | *Petal: primary color on the inner side* | P | | | | | | | | |
| | *Reflexing of petals one by one* | Ab. | | | | Pr. | | | | |
| | *Flower: diameter (cm)* | 3.0 - 4.0 | | 4.5 – 5.0 | | 5.5 - 6.0 | | 6.2 – 6.8 | | |
| **3 mg $L^{-1}$ of copper ion** | *Morphological Changes* | a | a | a | b | b | b | b | b | c |
| | *Petal: primary color on the inner side* | P | | | | | | | | |
| | *Reflexing of petals one by one* | Ab. | | | | | | Pr. | | |
| | *Flower: diameter (cm)* | 2.5 – 3.0 | | | 3.5 - 5 | | | 6.0 – 7.2 | | |

This study showed that copper ions have great promise as an antimicrobial agent, i.e., restricting the proliferatio n of coliforms. The rose vases containing copper ions at 1 mg $L^{-1}$ and 3 mg $L^{-1}$ exhibited superior anti-coliform a ctivity, and better efficiency at copper ion level increased. We suggest that the copper ion were absorbed into the rose, increasing its antiaging and antibacterial ability. As a result, it was no significant difference in the residual copper ion concentration in the rose vases after 9 days of the investigation. The results were consistent with the recorded sensory states. The morphological change, color state, petal shape occurred slower on rose in vases usi ng 3 mg $L^{-1}$ $Cu^{2+}$ than others. Because of its color-changing from green to blue at a higher concentration of 3 mg $L^{-1}$, we need to carefully evaluate the effects of $Cu^{2+}$ on the flower appearance before use. To extend the applica tion of metal ions for post-harvest preservation on the cut flower life, such as rose, a combination of different ion s can provide a complete bactericidal effect preventing mixed bacterial populations.

**Keywords:** Antibacterial; Antiaging; Cut flower; Rose; Copper ion.

### Acknowledegment

This study was supported by Nguyen Tat Thanh University, *Ewater Engineering Co.Ltd.*

### References

[1] S. Mittapally, R. Taranum, and S. Parveen, "Metal ions as antibacterial agents," *Journal of Drug Delivery and Therapeutics* **8**, 411-419 (2018).
[2] A. J. Macnish, R. T. Leonard, and T. A. Nell, "Treatment with chlorine dioxide extends the vase life of selected cut flowers," *Postharvest Biology and Technology* **50**, 197-207 (2008).
[3] W. G. Van Doorn, D. Zagory, and M. S. Reid, "Role of ethylene and bacteria in vascular blockage of cut fronds from the fern Adiantum raddianum," *Scientia horticulturae* **46**, 161-169 (1991).
[4] K. Ratnayake, D. C. Joyce, and R. I. Webb, "Investigation of potential antibacterial action for postharvest copper treatments of cut Acacia holosericea," *Postharvest Biology and Technology* **70**, 59-69 (2012).
[5] R. E. Paull, "Temperature-induced leakage from chilling-sensitive and chilling-resistant plants," *Plant Physiology* **68**, 149-153 (1981).
[6] M. Reid, "Rose, spray rose, sweetheart rose–recommendations for maintaining postharvest quality," *Produce Facts Article. Postharvest Technology research and Information Center, University of California, Davis* **1**, (2004).

**NATURAL PRODUCTS AND INDUSTRIAL CROPS**

**Paper ID: ESCE131**

# RECOVERY OF OMEGA-3 FISH OIL FROM *MONOPTERUS ALBUS* EEL FISH USING MICROWAVE ASSISTED EXTRACTION PROCESS

**N. A. Hashim[1], M. S. R. Mazilan[1], S. K. Abdul Mudalip[1,2]***

[1] *Department of Chemical Engineering, College of Engineering,* [2] *Centre for Research in Advanced Fluid and Processes, Universiti Malaysia Pahang, 26300 Gambang, Pahang, Malaysia.*
*Corresponding author: kholijah@ump.edu.my

## Extended Abstract

Fish oil is currently high in demand due to its wide range of therapeutic benefits. High contents of eicosapentaenoic acid (EPA) and docosahexaenoic acid (DHA) derived from various sources of marine life are essential in human metabolism and mental developments [1,2]. Swamp Eel Fish, scientifically known as *Monopterus Albus* (Figure 1) is a freshwater fish that highly in demands across South-East Asia and can easily be found in Malaysia. There was a growing interest in extracting fish oil from *Monopterus Albus* since it constitutes significant amount of DHA and EPA [3]. Microwave assisted extraction (MAE) offer advantages in time-saving, low consumption of solvent, and less heat lost into environment [4]. Fish oil from local *Monopterus Albus* extracted using MAE techniques with different range of ethanol concentration and solid-to-solvent ratio, 0 % v/v to 100 % v/v and 0.04 g/ml to 0.13 g/ml, respectively. Concentrated extract was analysed for its free fatty acid content, acid value and chemical composition using 785 DMP Titrino Metrom. Increase of ethanol concentration and solid-to-solvent ratios had increased the extracted fish oil, with the highest yield of 14.60 % at 100 % v/v and 0.13 g/ml, respectively. Acid values and free fatty acid recorded was 2.19 mg KOH/g and 1.14 %. Morphology of the before and after extraction process displayed significant structural changes on the surfaces of the sample. The use microwave-assisted extraction technique had successfully extract fish oil from *Monopterus Albus.*

Fig. 1: Swamp Eel Fish or scientifically known as *Monopterus Albus.*

**Keywords:** *Monopterus Albus*; Omega-3; Microwave Assisted Extraction (MAE).

### Acknowledgment

This work was funded by Universiti Malaysia Pahang via Postgraduate Research Grants Scheme (PGRS), PGRS2003180 and Fundamental Research Grant Scheme (FRGS) FRGS/1/2019/K02/UMP/02/9 Grant No. RDU1901134 by Ministry of Education, Malaysia.

### References

[1] S. Das, B. Paul, J. Sengupta, and A. Datta, "Beneficial effects of fish oil to human health: A review," *Agric. Rev.*, vol. 30, no. 3, pp. 199–205, 2009.
[2] D. S. Siscovick *et al.*, "Omega-3 Polyunsaturated Fatty Acid (Fish Oil) Supplementation and the Prevention of Clinical Cardiovascular Disease: A Science Advisory from the American Heart Association," *Circulation*, vol. 135, no. 15, pp. e867–e884, 2017, doi: 10.1161/CIR.0000000000000482.

## NATURAL PRODUCTS AND INDUSTRIAL CROPS

[3] Z. K. A. Razak, M. Basri, K. Dzulkefly, C. N. A. Razak, and A. B. Salleh, "Extraction and Characterization of Fish Oil from Monopterus Albus," *Malaysian J. Anal. Sci.*, vol. 7, no. 1, pp. 217–220, 2001 [4] Cancer Research UK (2003). Cancer statistics reports for the UK.

[4] H. K. Afolabi, S. K. A. Mudalip, and O. R. Alara, "Microwave-assisted extraction and characterization of fatty acid from eel fish (Monopterus albus)," *Beni-Suef Univ. J. Basic Appl. Sci.*, vol. 7, no. 4, pp. 465–470, 2018, doi: 10.1016/j.bjbas.2018.04.003.

**NATURAL PRODUCTS AND INDUSTRIAL CROPS**

**Paper ID: ESCE155**

# THERMAL-INDUCED ANDROGRAPHOLIDE, 14-DEOXY-11, 12-DIDEHYDROANDROGRAPHOLIDE AND NEOANDROGRAPHOLIDE SYNTHESIS FROM *ANDROGRAPHIS PANICULATA* EXTRACTS

**Vi Vien Chia[1,2,3], Sook Fun Pang[2], Jolius Gimbun[1,2]***

[1] *Department of Chemical Engineering, College of Engineering,* [2] *Centre of Excellence for Advanced Research in Fluid Flow (CARIFF), Universiti Malaysia Pahang, 26300 Gambang, Pahang, Malaysia.*
[3] *School of Bioscience, Faculty of Medicine, Bioscience and Nursing, MAHSA University, Selangor 42610, Malaysia.*
*Corresponding author: jolius@ump.edu.my

## Extended Abstract

*Andrographis paniculata* (King of bitter) is categorised under family name of Acanthaceae. Generally, it is widely utilised in prevention and treatment of common cold in Asia and Scandinavia [1]. Besides that, *A. paniculata* (AP) is known to have the medicinal effects such as anti-inflammatory, hypoglycemic, antibacterial, anti-cancer, anti-platelet aggregator, poses a vasorelaxing effects and useful for the treatment of endocrine disorders [1-3]. In Malaysia, this plant is used in folk medicine to treat diabetes and hypertension. The aforementioned pharmaceutical properties are attributed to the presence of major bioactive compounds in AP such as, andrographolide (AND), 14-deoxy-11,12-didehydroandrographolide (DDA) and neoandrographolide (NEA), which must be extracted before it can be routinely used.

As a result, various extraction methods were studied in past 20 years to maximize the yield of terpene extraction. The AP extract is subjected to spray drying to form a powder in order to prolong the shelf-life as well as to ease for handling and transportation. Both the extraction and spray drying process involves exposure of heat which may cause the terpene degradation. For instance, Thisoda et al. reported a reduction in AND content after several month in storage [1]. The degradation of the original terpene may produce new byproduct which may have an adverse effect to human health when consumed, besides the drop of terpene content reduced the efficacy of AP extracts as functional food. There is a limited study on terpene degradation of AP extracts in the literature. Therefore, the aims of this work is to evaluate the thermal degradation kinetics of the main terpenes from AP, i.e., AND, DDA and NEA because its efficacy for medicinal application is a dose-dependent [4]. The thermal degradation kinetics and mechanism of AND, DDA and NEA are elucidated in this work by performing an ultra-performance liquid chromatography coupled with quadrupole time-of-flight mass spectrometry (UPLC-QTOF-MS) of the heated and unheated extracts as well as the pure AND, DDA and NEA standards [5].

Figure 1 shows the degradation induced synthesis pathway of various terpenes from AP. The marker compounds of interest were marked as A1 (AND), B1 (DDA) and C1 (NEA). It was found that AND can degrade to synthesize DDA. Earlier, Chia et al. (2020) proved the existence of terpene E1 and E2 from AP which can undergo degradation-synthesis process to produce DDA [5]. Thermal degradation kinetics of terpenes from AP extract followed zero-order ($R^2$>0.88). The degradation enthalpy (ΔH) of AND, DDA and NEA are 14.6, 1.6 and -66.2 kJ/mol, respectively. The activation energy for AND, DDA and NEA were 18.2, 5.1 and -62.7 kJ/mol.K, respectively. Both standards of andrographolide and neoandrographolide exhibited gradual decrease throughout heat treatment whereas; 14-deoxy-11, 12-didehydroandrographolide showed an increment which implies a synthesis reaction occurred. The degradation kinetics developed in this work may serve as a useful guide to maximize the specific terpene extraction from AP.

## NATURAL PRODUCTS AND INDUSTRIAL CROPS

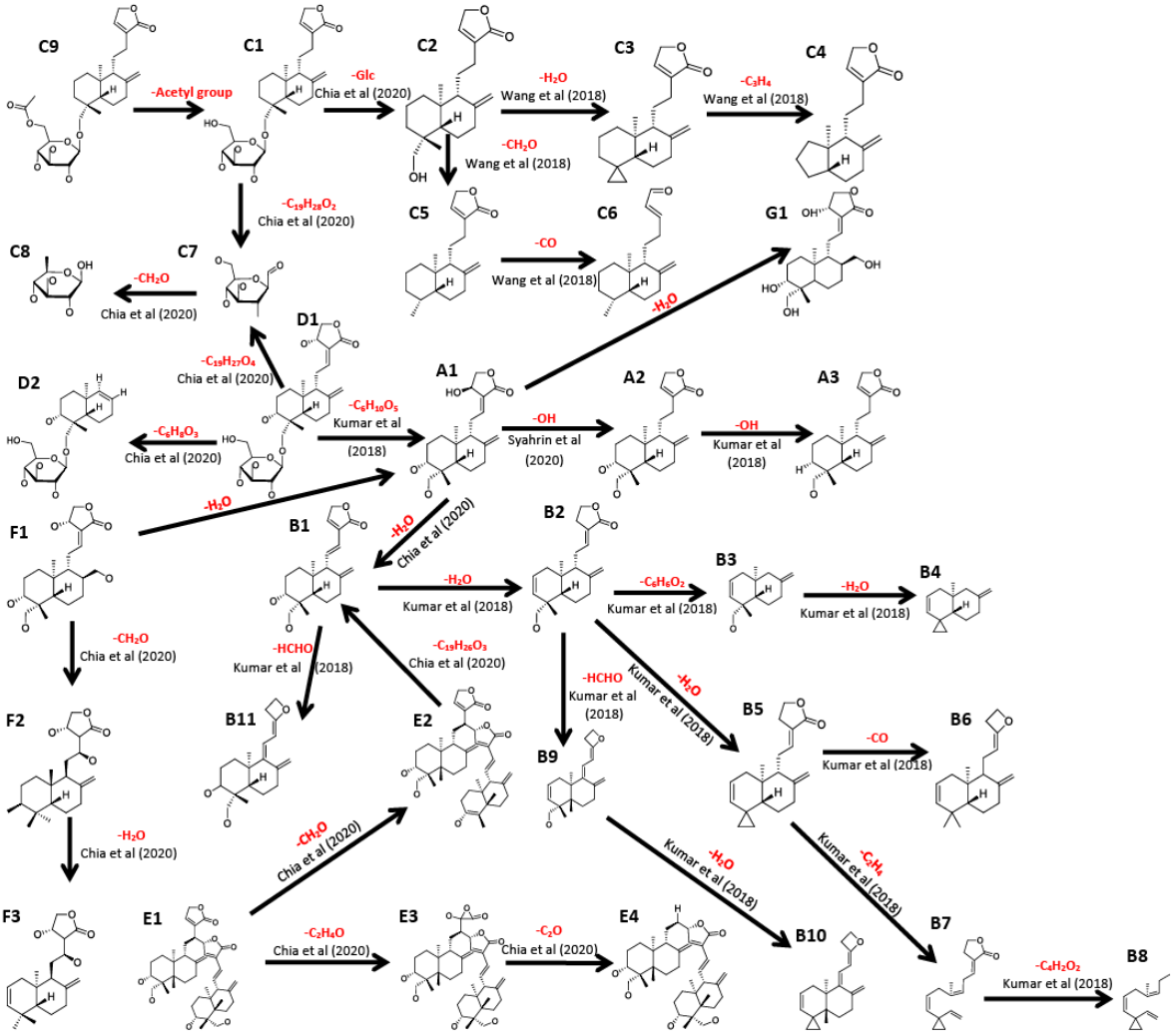


Fig. 1: Thermal degradation and synthesis pathway of terpene *A. paniculata* deduced using QTOF-MS.

Table 1: Kinetic parameters (k, $t_{1/2}$, $E_a$, ΔH, ΔG and ΔS) of terpenes in *A. paniculata* extracts.

| Terpene | Temperature (°C) | k value ($min^{-1}$) | $t_{1/2}$ (min) | $E_a$ (kJ/mol.K) | ΔH (kJ/mol) | ΔG (kJ/mol) | ΔS (J/mol.K) |
|---|---|---|---|---|---|---|---|
| **AND** | 100 | 0.0071 | 70.42 | 18.16 | 15.06 | 107.43 | -0.25 |
| | 120 | 0.0012 | 416.67 | | 14.90 | 119.17 | -0.27 |
| | 150 | 0.0118 | 42.37 | | 14.65 | 120.48 | -0.25 |
| **DDA** | 100 | 0.0080 | 62.50 | 5.11 | 2.01 | 107.06 | -0.28 |
| | 120 | 0.0085 | 58.82 | | 1.84 | 112.77 | -0.28 |
| | 150 | 0.0097 | 51.55 | | 1.60 | 121.17 | -0.28 |
| **NEA** | 100 | 0.0062 | 80.65 | -62.69 | -65.80 | 107.85 | -0.47 |
| | 120 | 0.0040 | 125.00 | | -65.96 | 115.24 | -0.46 |
| | 150 | 0.0006 | 833.33 | | -66.21 | 130.96 | -0.47 |

**Keywords:** *Andrographis paniculate*; Terpene synthesis; Thermal degradation kinetics; QTOF-MS.

**Acknowledgment**

This study was supported by supported by the Research and Innovation Department of Universiti Malaysia Pahang (PGRS 180324 & RDU 1803121). Chia Vi Vien is grateful to the Doctorate Research Scheme scholarship from Universiti Malaysia Pahang.

## NATURAL PRODUCTS AND INDUSTRIAL CROPS

### References

[1] Thisoda, Rangkadilok N, Pholphana N, Worasuttayangkurn L, Ruchirawat S, Satayavivad J. Inhibitory effect of Andrographis paniculata extract and its active diterpenoids on platelet aggregation. *Eur J Pharmacol*. 2006;553(1-3):39-45. doi:10.1016/j.ejphar.2006.09.052.

[2] Chen L, He H, Xia G, Zhou K. A new flavonoid from the aerial parts of Andrographis paniculata. *Nat Prod Res*. 2013;28(3):138-143. doi:10.1080/14786419.2013.856907.

[3] Hsieh YL, Shibu MA, Lii CK, et al. Andrographis paniculata extract attenuates pathological cardiac hypertrophy and apoptosis in high-fat diet fed mice. *J Ethnopharmacol*. 2016;192:170-177. doi:10.1016/j.jep.2016.07.018.

[4] Shen Y, Chen C, Chiou W. Suppression of Rat Neutrophil Reactive Oxygen Species Production and Adhesion by the Diterpenoid Lactone Andrographolide. *Planta Med*. 1999;66(4):314-317.

[5] Chia VV, Pang SF, Gimbun J. Mass spectrometry analysis of auxiliary energy-induced terpenes extraction from Andrographis paniculata. *Ind Crop Prod*. 2020;155:112828-112835. doi:10.1016/j.indcrop.2020.112828.

**NATURAL PRODUCTS AND INDUSTRIAL CROPS**

**Paper ID: ESCE164**

# THERMODYNAMICS AND KINETIC STUDIES FOR THE MICROWAVE-ENHANCED EXTRACTION OF PHENOLICS FROM *PHYLLANTHUS NIRURI* LEAF

**O. R. Alara[1]*, N. H. Abdurahman[1], H. A. Ali[2]**

[1] *Department of Chemical Engineering, College of Engineering, Universiti Malaysia Pahang, 26300 Gambang, Pahang, Malaysia.*
[2] *Eastern Unity Technology, Suite 01, 12th Floor Plaza, 138 Annex Hotel Maya, Jalan Ampang, 50450, Kuala Lumpur, Malaysia.*
*Corresponding author: ruthoalao@gmail.com

## Extended Abstract

*Phyllanthus niruri* is one of the medicinal plants found in Malaysia. It is mostly employed in folk medicine to treat gallbladder and kidney stones, viral infections including tuberculosis and hepatitis, diabetes, malaria, fever, liver cancer, and jaundice [1]. The process of solid-liquid extraction entails solute recovery from solid materials by utilizing a solvent [2]. This solid-liquid extraction is being carried out through different techniques including conventional and unconventional. The microwave-enhanced extraction technique is one of the commonly used methods; it involves using microwave radiation to transfer mass. When using microwave-enhanced extraction, the extraction process is faster because of the changes in the cell wall of the solid materials emanating from the influence of irradiation. This might be due to the synergistic action of concentration and temperature gradients that work in the same direction [3]. Given this, the thermodynamics and kinetic studies of total phenolic (TP) concentration from *P. niruri* leaf through microwave-enhanced extraction were studied. These were done to investigate the effects of microwave power (200-600 W), solid/solvent (1:10-1:16 g/mL) and temperature (40-70 ºC). The TP concentrations against extraction time were evaluated by utilizing a second-order kinetic model to evaluate the extraction constant. The factors showed significant impact on TP yield and the intensification process of microwave-enhanced extraction of TP yielded 135.05 mg GAE/g extract with the following conditions: Extraction time of 2 min; microwave power of 400 W; solid/solvent ratio of 1:12 g/mL; and temperature of 50 ºC. As presented in Fig. 1, the highest yield of TP was achieved at 2 min. Moreover, the effective diffusivity was maximum at these conditions as the second-order rate model was best in describing the process. Thus, the thermodynamics and kinetic studies presented valuable information on the microwave-enhanced extraction of TP from *P. niruri* leaf.

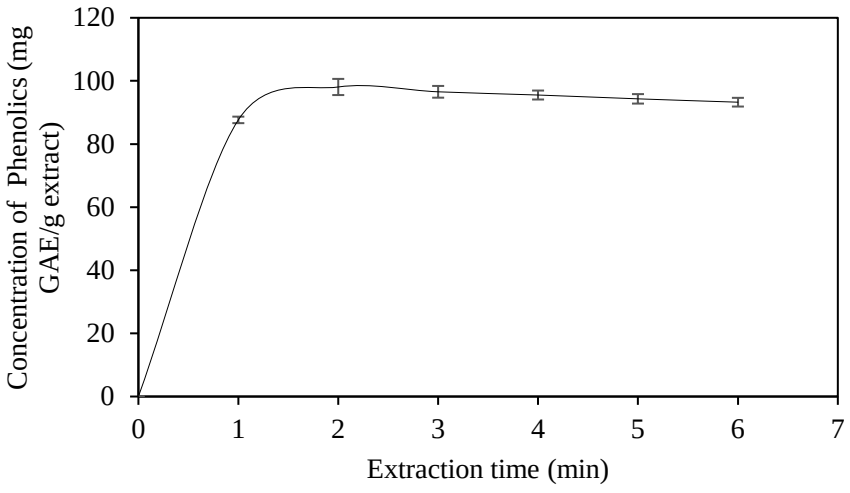


Fig. 1: Effect of extraction time on TP concentration from *P. niruri* leaf.

**Keywords:** Microwave-enhanced extraction; Kinetics; Thermodynamics; *Phyllanthus niruri.*

**Acknowledgement**

This study was supported by an industrial grant (UIC190806) from Eastern Unity Technology, Malaysia.

**References**

[1] Markom M., Hasan M., Daud W.R.W., Singh H., Jahim, J.M. (2007) Extraction of Hydrolysable tannins from *Phyllanthus niruri* Linn.: Effects of Solvents and Extraction Methods. Sep. Purif. Tech. 52: 487–496.
[2] Krishnan R.Y., Rajan K.S. (2016) Microwave Assisted Extraction of Flavonoids from *Terminalia bellerica*: Study of Kinetics and Thermodynamics. Sep. Purif. Tech. 157: 169–178.
[3] Alara O.R., Abdurahman N.H. (2019) Microwave-assisted Extraction of Phenolics from *Hibiscus sabdariffa* Calyces: Kinetic Modelling and Process Intensification. Ind. Crop Prod. 528–535.

2ND ENERGY SECURITY AND CHEMICAL ENGINEERING CONGRESS 2021
*"Sustainable Technological Solution for a Better World"*
VIRTUAL CONFERENCE | 3-5 NOVEMBER 2021

**NATURAL PRODUCTS AND INDUSTRIAL CROPS**

**Paper ID: ESCE167**

# EXTRACTION OF CAROTENOIDS FROM CRUDE PALM OIL BY SOLVOLYTIC MICELLIZATION: ECONOMIC EVALUATION AND LIFE CYCLE ASSESSMENT

**B. C. Hoe[1], A. Priyangaa[1], I.M.L. Chew[1,2], J. Tan[1], C.W. Ooi[1,2]***

[1] *Chemical Engineering Discipline, School of Engineering,* [2] *Monash-Industry Palm Oil Education and Research Platform (MIPO), Monash University Malaysia, 47500, Bandar Sunway, Selangor, Malaysia.*
*Corresponding author: ooi.chien.wei@monash.edu

## Extended Abstract

Carotenoids are a class of commercially important phytonutrient and they are widely used as natural colourant and antioxidant in food formulation. Palm oil contains the highest concentration of plant-derived carotenoids but most of them are destroyed during palm oil processing. Among the extraction methods used in the recovery of carotenoids from palm oil, solvolytic micellization is attractive in terms of extraction performance and scalability. However, the environmental and economic performances of solvolytic micellization for industrial- scale extraction of palm-based carotenoids have not been reported. In this study, economic evaluation and life- cycle assessment (LCA) were performed on the extraction of palm carotenes from crude palm oil (CPO). A good profitability of this extraction scheme was demonstrated using a base-case scenario targeting 50000 kg CPO feedstock/day. The main expense was the cost of CPO, which was the highest among all raw materials. The working capital was significantly lower than operating and capital costs because the extraction process did not involve solid particulate processing. A gate-to-gate LCA based on ISO 14040 was performed to evaluate ten midpoint impact categories, namely global warming potential, photochemical ozone formation potential, acidification potential related to terrestrial acidification, water consumption potential, fossil fuel scarcity, eutrophication potential, human toxicity, and particulate matter formation potentials. Figure 1 shows the system boundary of LCA. From LCA, global warming potential and fossil fuel scarcity are the main contributors of the environmental impact mainly because of the methanol recovery process. Overall, solvolytic micellization shows good commercialization potential because of its energy efficiency and the high output processing of carotenoids from CPO.

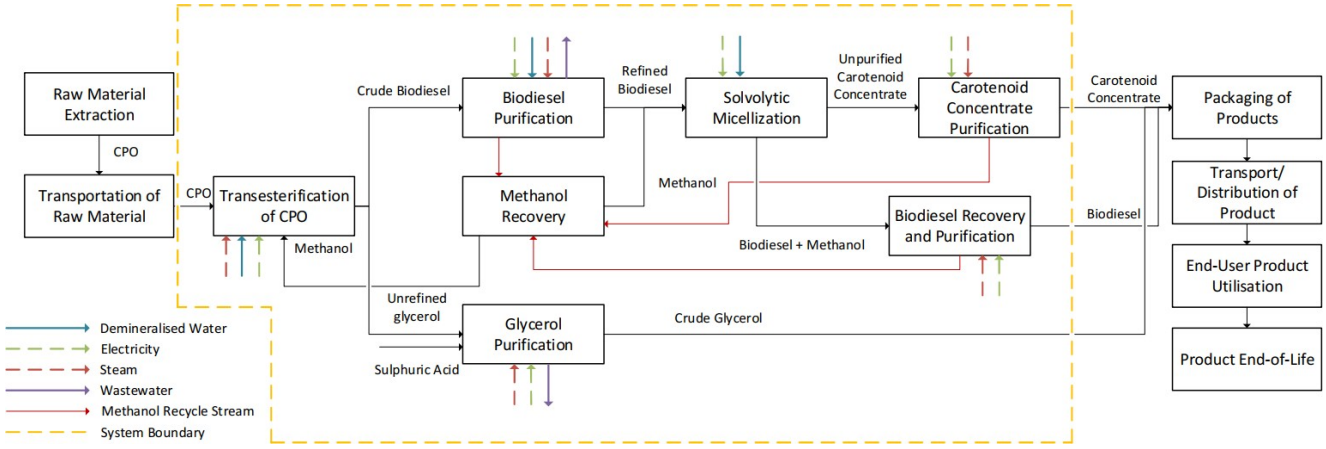


Fig. 1: Block flow diagram of carotenoid extraction by solvolytic micellization and system boundary of LCA study.

**Keywords:** Carotenoids; Solvolytic micellization; Life-cycle assessment; Environmental impact.

**NATURAL PRODUCTS AND INDUSTRIAL CROPS**

**Acknowledgment**

This study was supported by Monash-Industry Palm Oil Education and Research Platform (MIPO) and Industry Feasibility Grant (SIEC_FG0022021) by School of Engineering, Monash University Malaysia.

2ND ENERGY SECURITY AND CHEMICAL ENGINEERING CONGRESS 2021
*"Sustainable Technological Solution for a Better World"*
VIRTUAL CONFERENCE | 3-5 NOVEMBER 2021

**NATURAL PRODUCTS AND INDUSTRIAL CROPS**

**Paper ID: ESCE178**

# SYNERGISTIC EFFECTS OF PALM BUNCH ASH AND GLUTATHIONE ON PLANT GROWTH AND DEVELOPMENT

**Yi Sze Koh[1], See Kiat Wong[1], Acharaporn Duangjai[3], Surasak Saokaew[3,4,5,6,7], Pochamana Phisalprapa[8]*, Bey Hing Goh[9,10], Siah Ying Tang[1,2]***

[1] *Chemical Engineering Discipline, School of Engineering,* [2] *Tropical Medicine and Biology Platform, School of Science, Monash University Malaysia.*
[3] *Unit of Excellence in Research and Product Development of Coffee, Division of Physiology, School of Medical Sciences,* [4] *School of Pharmaceutical Sciences, Center of Health Outcomes Research and Therapeutic Safety (Cohorts),* [5] *Unit of Excellence on Clinical Outcomes Research and IntegratioN (UNICORN), School of Pharmaceutical Sciences,* [6] *Unit of Excellence on Herbal Medicine, School of Pharmaceutical Sciences,*
[7] *Division of Pharmacy Practice, Department of Pharmaceutical Care, School of Pharmaceutical Sciences, University of Phayao, Phayao, Thailand.*
[8] *Division of Ambulatory Medicine, Department of Medicine, Faculty of Medicine Siriraj Hospital, Mahidol University, Bangkok, Thailand.*
[9] *Biofunctional Molecule Exploratory Research Group, School of Pharmacy, Monash University Malaysia.*
[10] *College of Pharmaceutical Sciences, Zhejiang University, China.*
*Corresponding author(s): a.pochamana@gmail.om and patrick.tang@monash.edu

## Extended Abstract

Palm bunch ash (PBA), a waste biomass from the palm oil industry has been widely used as alternative source of fertilizer to improve soil health and reduce waste disposal problems. However, the use of PBA in combination with plant growth regulator has not yet been explored and remains as new gap in the literature. Herein, we aimed to investigate the individual and the combinatory effects of PBA and glutathione (GSH) on vegetative plant growth performance. Using okra as the model plant, the cultivation of okra was performed in outdoor pots under well-watered conditions. The experimental design included a control and 3 treatment groups with 4 replicates per test group. For each treatment and control group, 6 okra seeds were sown in each replicate pot. In this experiment, GSH was introduced through seed soaking method while PBA was added to soil by physical mixing. Plant growth parameters such as seedling emergence, plant height, stem girth, number of leaves, and leaf surface area were carefully examined over a period of 8 weeks. It was found that the GSH-treated group recorded the highest seedling emergence (83%) and tallest mean plant height (47.19 cm). Whereas the combinatory application of PBA and GSH presented the thickest mean stem girth (4.45 mm), highest mean number of leaves per plant (6.35), biggest mean leaf surface area (118.38 $cm^2$). The results implied that the combinatory application of PBA and GSH led to a synergistic effect on okra plant growth. Hence, our studies suggest the combination of PBA and GSH application is recommended to improve okra plant growth and development.

**NATURAL PRODUCTS AND INDUSTRIAL CROPS**

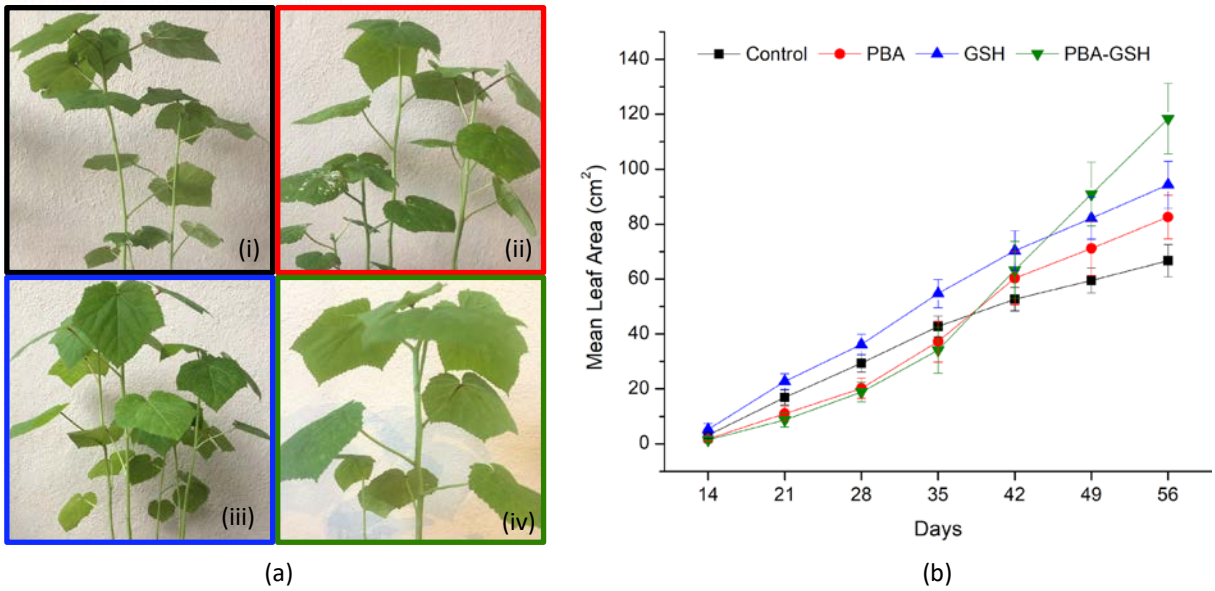


(a) (b)

Fig. 1: (a) Picture of okra plant leaves from (i) control group, (ii) PBA group, (iii) GSH group, and (iv) PBA-GSH group at day 56 (b) Graph of the mean leaf area of okra plants from different treatment groups from day 14 till day 56 after planting. Colours and symbols represent: (Black ■) control, (Red ●) PBA, (Blue ▲) GSH and (Green ▼) PBA-GSH

**Keywords:** Palm bunch ash; Glutathione; Fertilizer; Plant growth regulator.

**Acknowledgment**

This work was supported by School of Engineering and Tropical Medicine and Biology Platform, School of Science, Monash University Malaysia.

**References**

[1] Ojeniyi, S., Ezekiel, P. O., Asawalam, D. O., Awo, A. O., Odedina, S. A., & Odedina, J. (2009) Root Growth and NPK Status of Cassava as Influenced by Oil Palm Bunch Ash. Afr. J. Biotechnol 8(18):4407-4412.
[2] Hasanuzzaman, M., Nahar, K., Anee, T. I., & Fujita, M. (2017) Glutathione in Plants: Biosynthesis and Physiological Role in Environmental Stress Tolerance. Physiol. Mol. Biol. Plants, 23(2):249-268.
[3] Vittoria Locato, Sara Cimini, & Gara, L. D. (2017) Glutathione as a Key Player in Plant Abiotic Stress Responses and Tolerance. In Glutathione in Plant Growth, Development, and Stress Tolerance. Springer Nature, Switzeland.
[4] Khattab, H. (2007). Role of Glutathione and Polyadenylic Acid on the Oxidative Defense Systems of Two Different Cultivars of Canola Seedlings Grown under Saline Condition. Aust. J. Basic & Appl. Sci, 1(3):323-334.

**OIL AND GAS**

**Paper ID: ESCE163**

# DEMULSIFIER: AN IMPORTANT AGENT IN BREAKING CRUDE OIL EMULSION

**O. R. Alara[1]*, N. H. Abdurahman[1], H. A. Ali[2]**

[1] *Department of Chemical Engineering, College of Engineering, Universiti Malaysia Pahang, 26300 Gambang, Pahang, Malaysia.*
[2] *Eastern Unity Technology, Suite 01, 12th Floor Plaza, 138 Annex Hotel Maya, Jalan Ampang, 50450, Kuala Lumpur, Malaysia.*
*Corresponding author: ruthoalao@gmail.com

## Extended Abstract

Crude oil is an unrefined natural oil found underneath the surface of the earth. The production of crude oil is associated with the presence of water; crude oil often contains about 1-60% volume of water [1]. The water content emulsified through the naturally occurred surface-active substances in the crude. Hence, different operational problems such as corrosions in pipelines and equipment occur because of the presence of water; this can generally increase the production cost of oil. The produced water in crude oil happens in two categories including emulsion or free water. It is therefore important to separate crude oil from the water before refining processes. In addition, several challenges are faced during the production of oil due to the emergence of emulsion. The water-in-oil emulsion is one of the challenges facing the petroleum industry. Asphaltenes and resins are the main interfacial active components of oil; they are absorbed into the water-oil interface and generate interfacial films. The presence of asphaltenes and polar naphthenic acids in crude oil secure the distributed water droplets. Moreover, the occurrence of sub-micron size solids such as clay and silica in crude oil can interact with asphaltenes and polar naphthenic acids; thus, initiate the formation of emulsion stability. The formation of stable water-in-crude oil emulsion can generate problems in separating crude oil and water. Controlling and understanding demulsification is highly essential in breaking the emulsion. Although, several review article have been published in relation to the demulsification processes, nonetheless, this review presents the currents start-of-art demulsifiers used in combating the challenges facing the breaking of emulsions in crude oil.

Demulsification that refers to the breaking of emulsions into water and oil phases (Fig. 1), is needed in several applications, including waste-water treatment, painting, environmental technology, and petroleum industry [2]. Because of this, different chemical (addition of demulsifier) and physical techniques (mechanical, thermal, and electrical) have been developed over the past years to break up this emulsion as the crude oil reaches the surface. These techniques or their combinations are used for treating water-in-oil emulsions [3].

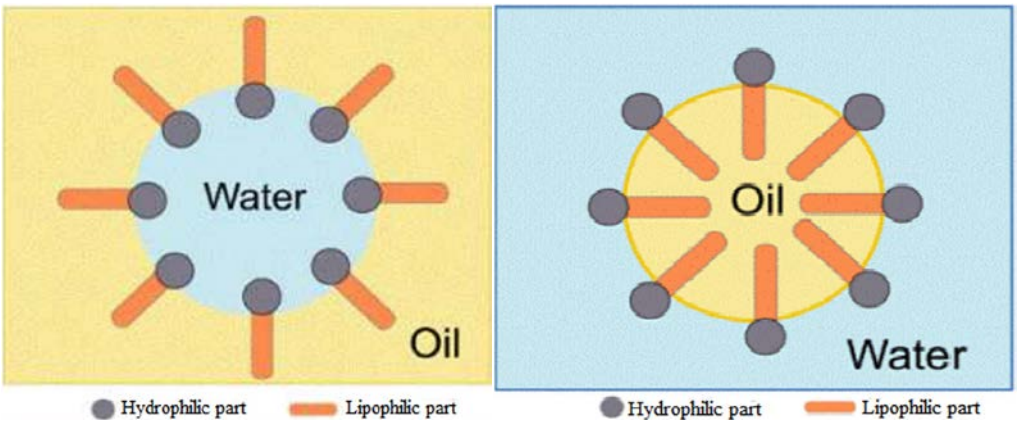


Fig. 1: Water-in-oil (a) and oil-in-water emulsions [4].

**Keywords:** Demulsification; Emulsions; Resins; Asphaltenes.

**OIL AND GAS**

## Acknowledgement

This study was supported by an industrial grant (UIC190806) from Eastern Unity Technology, Malaysia.

## References

[1] Ramesh V. (2002) Demulsification of Water-in-oil Emulsion. 1:1–7.
[2] Abdurahman H.N., Yunus R.M., Jemaat Z. (2007) Chemical Demulsification of Water-in-crude Oil Emulsions. J. Appl. Sci. 7(2):196–201.
[3] Zolfaghari R., Fakhru-Razi A., Abdullah L.C., Elnashaie S.S.E.H. (2016) Demulsification Techniques of Water-In-Oil and Oil-Water Emulsions in Petroleum Industry. Sep. Purif. Tech. 170:377–407.
[4] Khan B.A., Akhtar N., Khan H.M.S., Waseem K., Mahmood T., Rasul A., Iqbal M., Khan H. (2011) Basics of Pharmaceutical Emulsions: A Review. African J. Pharm. Pharmacol. 5(25):2715–2725.

2ND ENERGY SECURITY AND CHEMICAL ENGINEERING CONGRESS 2021
*"Sustainable Technological Solution for a Better World"*
VIRTUAL CONFERENCE | 3-5 NOVEMBER 2021

**OIL AND GAS**

**Paper ID: ESCE193**

# COLOR MONITORING IN PETROLEUM INDUSTRY: METHODS AND DEVELOPMENTS

**Nurliana Farhana Salehuddin[1]*, Madiah Omar[1,3], Rosdiazli Ibrahim[2]**

[1] *Department of Chemical Engineering,* [2] *Department of Electrical and Electronic Engineering,* [3] *Institute of Autonomous System, Universiti Teknologi PETRONAS (UTP), Bandar Seri Iskandar, Perak, Malaysia.*
*Corresponding author: lianafarhana@gmail.com

## Extended Abstract

Color is a quantifiable property that conveys information on the type and quality of a sample. In the petroleum industry, color serves as an important indicator to determine a suitable refinement process and monitor the level of contamination in petroleum products. Since the acceptability of a product relies on color, it is crucial for it to meet the standard of visual perception. Colors can be quantified in various ways, the best of which is with the human eye. However, this method is found to be inaccurate and inconsistent, as every human being has a slightly different perception of color expression. Thus, numerous strategies have been developed to overcome the reliance on the human eye, primarily by using instruments such as colorimeters or spectrophotometers. The color measurement advancements have mostly concentrated on modifying existing instruments rather than on the method itself. However, as the world is currently moving towards digital transformation through the Industry 4.0 drive, there is great effort to replace the available methods with using automated color determination through a correlation model. It is expected that this new method can be an alternative to conventional laboratory analysis. Hence, this review has focused on the methods and global standards used to measure the color of petroleum products from the early twentieth century to date. Besides that, an overview of the factors that can influence color measurement and correlation model development between petroleum colors and their properties have been discussed. It is predicted that this study will lead to further exploration and advancement in color measurement technology, especially in the petroleum industry.

**Keywords:** Color Measurement; Saybolt; Regression Analysis; Colorimeter; Spectrophotometers.

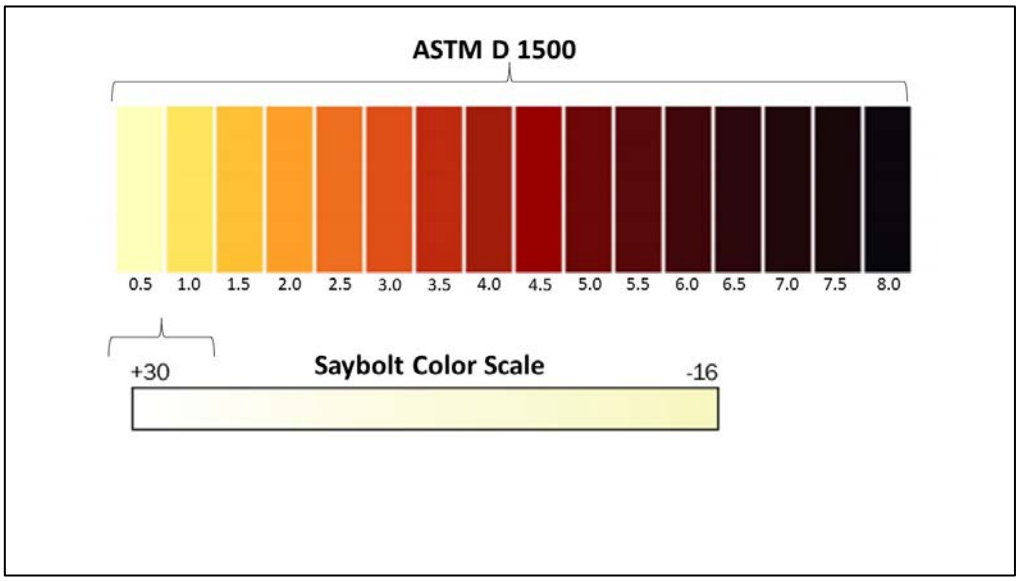


Fig. 1: Comparison between the ASTM and Saybolt color scales [1, 2].

**OIL AND GAS**

Table 1: Modification of method or instrument for color measurement in the petroleum industry.

| Method/Instrument | Modification | References |
|---|---|---|
| Photoelectric colorimeter | - | [3] |
| Photoelectric colorimeter | The instrument was designed to minimize the effects of variations in the refractive index and fluorescence of the sample. | [4] |
| Spectrophotometer | - | [5] |
| Spectrophotometer | Optimization of measurement. | [6] |
| Mobile micro-colorimeter and micro-spectrometer | Multispectral micro-sensors with different calibration methods are applied with smart pads for the calculation of measurement. | [7] |
| Microcomputer | Detection system with the aid of RGB (red, green, blue) sensor | [8] |
| Spectrometer | White LED is incorporated into the spectroscopic method and processed using CIE 1931 color space. | [9] |
| Correlation model | Prediction of Saybolt color using single and multiple regression models | [10] |
| Correlation model | Correlation-based on forward, backward and bidirectional elimination methods. | [11] |

**Acknowledgment**

The authors would like to offer their utmost appreciation to Yayasan Universiti Teknologi PETRONAS (YUTP) for funding (015-LCO166) and supporting the project.

**References**

[1] Kytola (2021). Application Note-Oil Color. https://insatech.com/downloads/Oilcolor_app15.pdf (accessed August 2021).
[2] Optek (2021). Saybolt Color Analyzer. https://www.optek.com/en/saybolt-color-analyzer.asp (accessed August 2021).
[3] Story B.W. and Kalichevsky V.A. (1933) Photoelectric Colorimeter for Measuring Color Intensities of Liquid Petroleum Products. Industrial and Engineering Chemistry Research. 5:214-217.
[4] Diller I., DeGray R., and Wilson J., J. (1942) Photoelectric Color. Description and Mensuration of the Color of Petroleum Products. Industrial and Engineering Chemistry Research. 14:607-614.
[5] Santana D.W.E.A., Sepulveda M.P., and Barbeira P.J.S. (2007) Spectrophotometric Determination of the ASTM Color of Diesel Oil. Fuel 86:911-914.
[6] Yang J., Xiong D., Wang G., Zhang T., Xu G., Chen C., Zheng S., and Chen J (2014) The Optimization Research of Petroleum Products Chroma by Spectrophotometry. Journal of University of Science and Technology of China.
[7] Dittrich M.E.P.-G. and Hofmann D. (2015) Photonic Micro Sensors for Mobile Color and Spectral Characterization of Colored Liquids in Laboratories and in Field. XXI IMEKO World Congress. Prague, Czech Republic.
[8] Jinbo S. and Zhiwei D. (2015) Petroleum Products Color Detecting System Using RGB Color Sensor. IOSR Journal of Computer Engineering. 5:6-11.
[9] Rodriguez J., Comstock M., Auz B., Olmstead T (2017) A Spectroscopic Method of Determining Color of petroleum Products Using CIELab Color Space with LED Illumination. Proceedings of SPIE 10110.
[10] Khor C.S., Nurazrin N.N.S., Hanafi F.M., Asallehan F.N., Rosman N.Z, Leam J.J., Dass S.C., Abidin S.A.Z., Anuar F.S (2020) Correlation Model Development for saybolt Colour of Condensates and Light Crude Oils. ASM Science Journal 13:434.
[11] Leam J.J., Khor C.S., and Dass S.C. (2021) Saybolt Color Prediction for Condensates and Light Crude Oils. Journal of Petroleum Exploration and Production 11:253-268.
[12] Men'kov P., Isvanov V., and Loginov V. (1981) Determination of Color of Petroleum Products. Chemistry and Technology Fuels Oils.
[13] Montemayor R. (2010) Petroleum Solvents. ASTM International.
[14] Lipták B.G. (1994) Analytical instrumentation. CRC Press.
[15] HACH (2016). Objective Color Assessment and Quality Control in the Chemical, Pharmaceutical and Cosmetic Industries. https://uk.hach.com (accessed August 2021).
[16] Yajima Y. and Funayama M. (2006) Spectrophotometric and Tristimulus Analysis of The Colors of Subcutaneous Bleeding in Living Persons. Forensic Science International 156:131-137.
[17] Pathare P., Opara U., and Al-Said F. (2013) Colour Measurement and Analysis in Fresh and Processed Foods: A review. Food Bioprocess Technology.
[18] Jose G., Thomas V., Joseph C., Ittyachen M.A., Unnikrishnan N (2004) Optical Characterization of Eu 3+ ions in CdSe

## OIL AND GAS

Nanocrystal Containing Silica Glass. Journal of Fluorescence 14:733-738.
[19] Setchell Jr J. (2012) Colour Description and Communication, Colour Design. Elsevier. 219-253.
[20] Hunt R.W.G. and Pointer M.R. (2011) Measuring Colour. John Wiley & Sons.
[21] Douglas R.K., Nawar S., Alamar M.C., Mouazen A., Coulon F (2018) Rapid Prediction of Total Petroleum Hydrocarbons Concentration in Contaminated Soil using Vis-NIR Spectroscopy and Regression Techniques. Science of the Total Environment 616:147-155.
[22] Nadkarni R. (2007) Guide to ASTM Test Methods for The Analysis of Petroleum Products and Lubricants. ASTM International West Conshohocken.
[23] ASTM (2012) Standard Test Method for ASTM Color of Petroleum Products (ASTM color scale). In Annual Book of Standards. West Conshohocken, PA, USA.
[24] Leong Y.S., Ker P.J., Jamaludin M.Z., Nomanbhay S., Ismail A., Abdullah F., Looe H.M., Lo C.K (2018) UV-Vis spectroscopy: A New Approach for Assessing The Color Index of Transformer Insulating Oil. Sensors 18:2175.
[25] ASTM (2015) Standard test method for saybolt color of petroleum products (Saybolt chromometer method), ASTM International. West Conshohocken, PA.
[26] Diller I., Dean J., DeGray R., Wilson Jr J. (1943) Color index. Light-colored petroleum products. Industrial of Engineering Chemistry Research 15:365-373.
[27] Choudhury A.K.R. (2014) Principles of Colour and Appearance Measurement: Object Appearance. In Colour Perception and Instrumental Measurement. Elsevier.
[28] Becker D. (2016) Color Trends and Selection for Product Design: Every Color Sells a Story. William Andrew.
[29] Dittrich P.-G., Grunert F., Ehehalt J., Hofmann D. (2015) Mobile Micro-Colorimeter and Micro-Spectrometer Sensor Modules as Enablers for The Replacement of Subjective Inspections by Objective Measurements for optically Clear Colored Liquids In-Field. Proceedings SPIE.
[30] Chandrasekhar V., Reddy L.P., Prakash T.J., Rao G.A., Pradeep M. (2011) Spectrophotometric and Colorimetric Evaluation of Staining of The Light Cured Composite After Exposure With Different Intensities of Light Curing Units. Journal of Conservative Dentistry 14:391-394.
[31] Rodriguez J., Comstock M., Bingemann D., Olmstead T. (2018) A Spectroscopic Method to Determine Color of Petroleum Products. In Applied Industrial Optics: Spectroscopy, Imaging and Metrology. Optical Society of America.

**OIL AND GAS**

**Paper ID: ESCE200**

# INVESTIGATION OF RHEOLOGICAL AND FILTRATION BEHAVIOR OF POLYANIONIC CELLULOSE AND TAPIOCA STARCH IN NONDAMAGING WATER BASED MUDS

**I. Ali[1]*, M. Ahmad[1]*, T. Ganat[1]**

[1] *Department of Petroleum Engineering, Universiti Teknologi PETRONAS, 32610, Seri Iskandar, Perak, Malaysia.*
*Corresponding authors: imtiaz_17003333@utp.edu.my and maqsood.ahmad@utp.edu.my

## Extended Abstract

Drilling fluid is a combination of continuous phase with other additives, that is used as circulation medium in oil and gas drilling. Numerous additives either in liquid or in solid form are added for several functions. A properly designed and maintained drilling fluid system performs various functions. All the mud functions are strongly dependent on rheological and filtration properties of mud. These properties can be maintained using different additives. Typically, drilling fluids are considered as thixotropic having shear-thinning behavior, which shows an inverse relationship between viscosity and shear rate. Drilling induced problems in the near-wellbore region are directly associated with drilling fluids rheological and filtration characteristics. These properties are dependent on the appropriate selection of additives utilized in the mud.

Water based mud (WBM) is the most commonly used mud system and about 80% of the oil wells are drilled using water-based muds. For specialized functions, various mud additives are added including clays, polymer, pH control, lubricating agents and bridging control. For rheological properties enhancement, different polymers have been used to minimize the fluid loss into the formation. For example, polyanionic cellulose (PAC) is considered a suitable filtrate loss control agent in water-based drilling mud systems. It is a water-soluble anionic cellulose ether that could also be synthesized employing alkali-catalyzed method. Compared with carboxymethyl cellulose (CMC), it has a better purity as well as degree of substitution. Owing to its better performance, it acts as an efficient fluid loss reducer and viscosity enhancer in WBMs. Due to the cost and environmental concerns, the oil industry is looking for green alternatives which could have no serious impact on the environment. Hence, this study is focusing on the utilization of a locally available starch which have almost no negative impact on the ecosystem. It forms a gelled fluid when the amylose polymers present in the starch granules are dissolved in water. Thus, improving the viscosity of the entire mud system.

In this paper, the performance of locally available tapioca starch has been assessed for the improvement of rheological and filtration properties of water-based mud. Tapioca starch has been studied because of its easy availability and its better gelling properties at elevated temperatures which further enhances the rheological and filtration characteristics. The objectives of this work are to formulate a non-damaging drilling mud composed of locally available tapioca starch and to investigate its rheology and filtration in the presence of xanthan gum and polyanionic cellulose (PAC) as primary viscosifier and filtrate control agent respectively. Non damaging WBM is consisted of polymers and other solids additives and is used in the drilling of a payzone section. It can reduces the chances of formation damage due to solid invasion into the porous and permeable rocks. In this study, tapioca starch in various concentrations has been examined in combination with calcium carbonate as a weighting agent. The mud rheological and filtration characteristics have been measured according to API specifications. The obtained results were compared with a commercial fluid loss additive. Nine (9) mud formulation have been designed to assess the effect of PAC and tapioca starch on the rheology and filtration characteristics of drilling mud. The laboratory results concluded that tapioca starch can be applied as the rheology modifier and filtrate loss control additive (Fig. 1). The optimum concentration of starch for plastic viscosity and AV was found as 6 ppb while 5 ppb for yield point optimum values. Similarly, the lowest fluid loss volume and cake thickness were found with 5 ppb starch at API filter press, while 6 ppb showed the lowest fluid loss and cake thickness at 280$^{o}$F.

**OIL AND GAS**

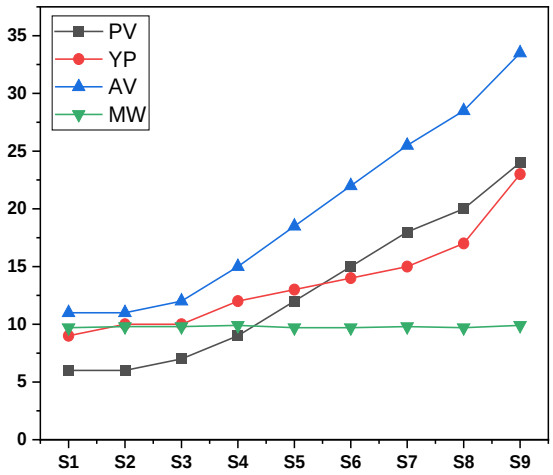


Fig. 1: Effect of starch on the mud properties.

**Keywords:** Water Based Muds; Nondamaging Mud; Solid Free Mud; Rheological Properties; Fluid Loss Control.

## Acknowledgment

This study was supported by Ministry of Education (MOE), Malaysia by providing financial assistance under FRGS/1/2020/TK0/UTP/02/3 and Universiti Teknologi PETRONAS for providing the required facilities to conduct this research work.

## References

[1] W.-J. Sun *et al.*, "Synthesis and characterisation of a multifunctional oil-based drilling fluid additive," *Environmental earth sciences*, vol. 77, no. 24, p. 793, 2018.
[2] R. Caenn and G. V. Chillingar, "Drilling fluids: State of the art," *Journal of Petroleum Science and Engineering*, vol. 14, no. 3-4, pp. 221-230, 1996.
[3] H. Jia *et al.*, "Investigation of inhibition mechanism of three deep eutectic solvents as potential shale inhibitors in water-based drilling fluids," *Fuel*, vol. 244, pp. 403-411, 2019.
[4] M.-C. Li *et al.*, "Cellulose nanocrystals and polyanionic cellulose as additives in bentonite water-based drilling fluids: Rheological modeling and filtration mechanisms," *Industrial & Engineering Chemistry Research*, vol. 55, no. 1, pp. 133-143, 2016.
[5] D. C. Thomas, "Thermal stability of starch-and carboxymethyl cellulose-based polymers used in drilling fluids," *Society of Petroleum Engineers Journal*, vol. 22, no. 02, pp. 171-180, 1982.
[6] P. Talukdar, S. Kalita, A. Pandey, U. Dutta, and R. Singh, "Effectiveness of different Starches as Drilling Fluid Additives in Non Damaging Drilling Fluid," *International Journal of Applied Engineering Research*, vol. 13, no. 16, pp. 12469-12474, 2018.
[7] J. K. Adewole and K. B. Muritala, "Some applications of natural polymeric materials in oilfield operations: a review," *Journal of Petroleum Exploration and Production Technology*, pp. 1-11, 2019.
[8] O. Nwosu and C. Ewulonu, "Rheological behaviour of eco-friendly drilling fluids from biopolymers," *Journal of Polymer and Biopolymer Physics Chemistry*, vol. 2, no. 3, pp. 50-54, 2014.
[9] A. R. Ismail, W. Sulaiman, W. Rosli, M. Z. Jaafar, I. Ismail, and E. Sabu Hera, "Nanoparticles performance as fluid loss additives in water based drilling fluids," in *Materials Science Forum*, 2016, vol. 864: Trans Tech Publ, pp. 189-193.

**OIL AND GAS**

**Paper ID: ESCE209**

# PROSPECTS OF ENERGY RECOVERY IN OFFSHORE OIL AND GAS OPERATIONS

**Q. Y. Koh[1,2]*, S. Rajoo[1,2], K. Y. Wong[1,2]**

[1] *School of Mechanical Engineering,* [2] *Institute for Vehicle Systems and Engineering (IVESE), Universiti Teknologi Malaysia, 81310 Skudai, Malaysia.*
*Corresponding author: qiyunkoh@utm.my

## Extended Abstract

Offshore oil and gas platforms are one of the energy industries that generate huge amount of waste heat and CO2 emission that causes the increase in $CO_2$ concentration level [1] and lead to environmental problems nowadays [2]. According to the Malaysia Energy Statistics Handbook 2018 prepared by the Energy Commission [3], from 2005 to 2016, the natural gas is concluded to be the primary energy supply in Malaysia, followed by crude oil and petroleum as shown in Fig. 1. According to this statistic, the offshore oil and gas platform can be seen to play a vital role in Malaysia to generate and provide energy to different sectors or people. Without new policies to confine the energy consumption, the CO2 emission produced by the energy industries will continue to grow in a rate of 130% by 2050 [4]. However, there are very least review done to find out the potential source of waste heat on offshore oil and gas platform. Therefore, this paper performed an investigation on the potential source of waste heat on the offshore oil and gas operation. Technologies that were utilized by previous researchers were reviewed and the future direction on the waste heat recovery of offshore operation was described.

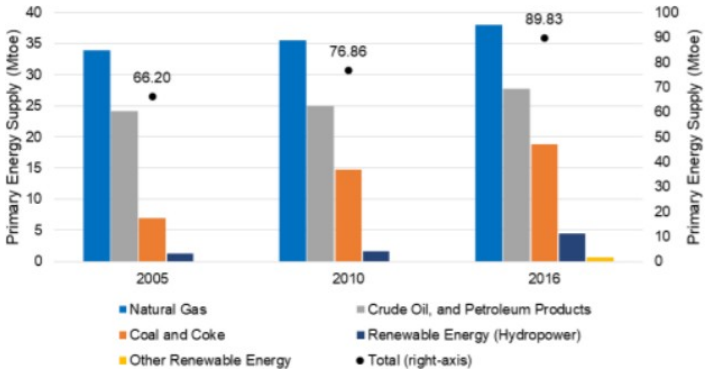


Fig. 1: Primary Energy Supply Breakdown for 2005, 2010 and 2016 in Malaysia [3].

In a standard offshore oil project, it usually comprises four offshore platform. The platforms employed includes the oil extraction and processing platform, the oil storage platform, the support and maintenance platform and the mooring platform. The oil extraction and processing platform or it is also called the central power platform among all of the platforms as it provides power for them through sea cables [5]. According to standard operations, two engines will operate by sharing the loads and the other one will be on stand-by or maintenance mode. The two gas turbines of the machines will be running in low loads to lower the risk of system failure which lead to high economic loss. Nonetheless, with this type of strategy applied, the system performance will reduce seriously and generate even more waste heat to the environment [6]. As a result, the potential for energy recovery on the offshore platform will be the power system of it as it is the major contributor of overall emissions and major source of energy wastage. In the oil extraction and processing platform, there are processing plant that purifies and separates raw gases into different chemicals and other processes that support the operation of the platform. The power and heat generation and other utilities systems are named as Auxiliary systems. In the processing plant, there are several stages on oil and gas extraction such as production separation, $CO_2$ removal system, flare system, sales gas compression, condensate separation, etc. By taking the cakerawala offshore platform located approximately 150km northeast of Kota Bahru, Kelantan as an example, the process flow diagram of Carigali Hess Operating Company is presented in Fig. 2.

**OIL AND GAS**

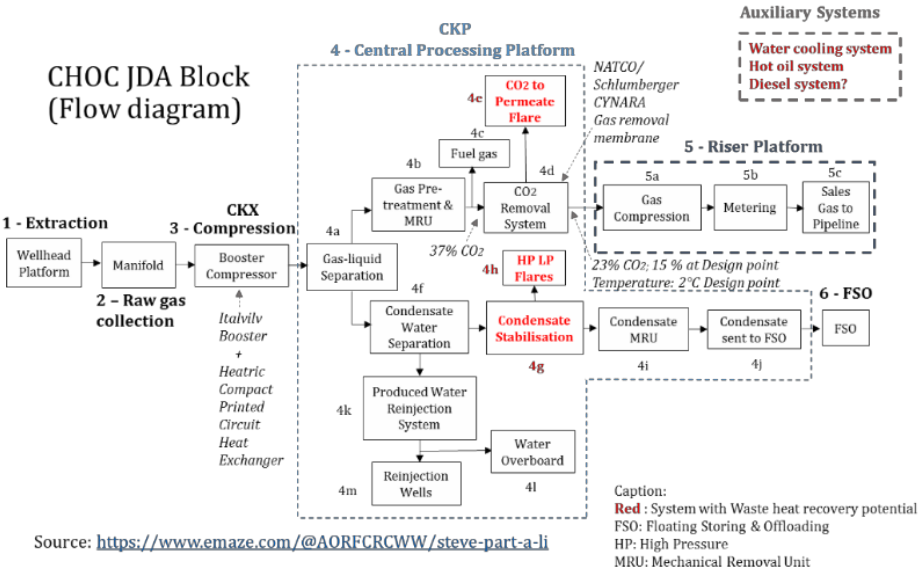


Fig. 2: Flow Diagram of the Malaysia-Thailand Joint Authority Carigali Hess Operating Company Production Facility.

Technologies that were utilized by previous researchers were reviewed and the future direction on the waste heat recovery of offshore operation was analyzed too. Organic Rankine Cycle, Steam Rankine Cycle, Air Bottoming Cycle and transcitical $CO_2$ power cycle had been utilized on the offshore oil and gas operation as waste heat recovery system [7-9]. However, they were just analysis made and were not put into practical use on the offshore oil and gas operation. Although there have been studies conducted utilizing different technologies on the waste heat recovery of offshore oil and gas sector, more improvements could be made in the future to the efficiency of the power system by applying other waste heat recovery technologies such as turbo compound, thermoelectric generator etc. or combination of several technologies to recover more waste heat released by the offshore oil and gas operation and released to the environment.

**Keywords:** Oil and Gas; Waste heat recovery; Offshore platform.

## Acknowledgment

The authors are grateful to Malaysia-Thailand Joint Authority (MTJA), UTM-LoCARtic and IVESE UTM for the support in publishing this work.

## References

[1] Malaysia Biennail Update Report to the UNFCCC 2016. (2016) Ministry of Environment and Water Malaysia, Putrajaya.
[2] Omara, A., Saghafifar, M., Mohammadi, K., Alashkar, A., and Gadalla, M. (2018) A Review of Unconventional Bottoming Cycles for Waste Heat Recovery: Part II - Applications. Energy Conversion and Management 180(1):559-583.
[3] Malaysia Energy Statistics Handbook 2018. (2019) Energy Commission, Putrajaya.
[4] Oh, T.H. (2010) Carbon Capture and Storage Potential in Coal-fired Plant in Malaysia—A Review. Renewable and Sustainable Energy Reviews 14(9):2697-2709.
[5] Zhang, A., Zhang, H., Qadrdan, M., Yang, W., and Jin, X. (2019) Optimal Planning of Integrated Energy Systems for Offshore Oil Extraction and Processing Platforms. Energies 12(4):756.
[6] Pierobon, L., Benato, A., Scolari, E., Haglind, F., and Stoppato, A. (2014) Waste Heat Recovery Technologies for Offshore Platforms. Applied Energy 136(1):228-241.
[7] Kolahi, M., Yari, M., Mahmoudi, S.M.S., and Mohammadkhani, F. (2016) Thermodynamic and Economic Performance Improvement of ORCs Through Using Zeotropic Mixtures: Case of Waste Heat Recovery in an Offshore Platform. Case Studies in Thermal Engineering 8:51-70.
[8] Pierobon, L., Nguyen, T.-V., Larsen, U., Haglind, F., and Elmegaard, B. (2013) Multi-objective Optimization of Organic Rankine Cycles for Waste Heat Recovery: Application in an Offshore Platform. Energy 58(1):538-549.
[9] Walnum, H.T., Nekså, P., Nord, L.O., and Andresen, T. (2013) Modelling and Simulation of Carbon Dioxide Bottoming Cycles for Offshore Oil and Gas Installations at Design and Off-design Conditions. Energy 59:513-520.

**OIL AND GAS**

**Paper ID: ESCE210**

# ORGANIC RANKINE CYCLE FOR WASTE HEAT RECOVERY ON OFFSHORE OIL AND GAS PLATFORM

**Q. Y. Koh[1,2]*, S. Rajoo[1,2], K. Y. Wong[1,2]**

[1] *School of Mechanical Engineering,* [2] *Institute for Vehicle Systems and Engineering (IVESE), Universiti Teknologi Malaysia, 81310 Skudai, Malaysia.*
*Corresponding author: qiyunkoh@utm.my

## Extended Abstract

Recently, the environmental awareness of people has increase, making them willing to pay more attention to the serious environmental issues and depletion of fossil fuels. Both stated phenomena happened due to the rapid industrialization nowadays that lead to growing of global energy consumption and $CO_2$ concentration level [1]. In Malaysia, 55% from the overall $CO_2$ emission came from the energy industries in 2015 [2]. Although the CO2 emission had reduced to a percentage of 39% in 2020 [3], energy industries are still its biggest contributor and oil and gas exploitation sector is one of the energy industries which release vast amount of waste heat and carbon dioxide to the atmosphere. Several numbers of studies have been carried out by researchers to find out methods to enhance the performance of power generation by making use of the potential source of wasted energy. Waste Heat Recovery (WHR) system is one of the methods used and Organic Rankine Cycle (ORC) had been widely studied recently in application of many sectors, but there is no practical case on offshore oil and gas operation. An extensive overview of the ORC for the WHR of offshore oil and gas platform has been performed in this paper to investigate the capability of this technology in this application.

As presented in Fig. 1, a typical Rankine cycle is made up of a condenser, a turbine, a pump and an evaporator. The working principle of a Rankine cycle is first having fuel to burn in the evaporator which makes the working fluid performing phase changes from liquid phase into superheated vapor phase. The power is produced with the turbine by directing the working fluid in superheated vapor state into it. Then, at the turbine outlet, the fluid will flow to the condenser, and it will undergo the process of losing heat and change back into liquid form. Lastly, the fluid is pumped into the evaporator again and the cycle repeats. To generate electrical power instead of mechanical power, a generator is connected to the turbine's shaft [4].

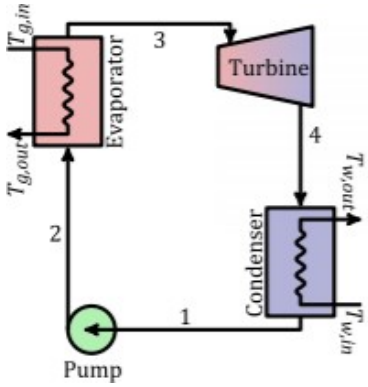


Fig. 1: Simple Organic Rankine Cycle [4].

Kolahi and Yari [5] has conducted a comparative analysis on ORC with Internal Heat Exchanger (IHE) and simple ORC as the WHR system for the 425°C high grade heat of large diesel engines using pure and zeotropic mixtures in phase 12 of South Pars Gas on Persian Gulf offshore platform. Results showed that from the economic and thermodynamic aspects, ORC with IHE had better results than simple ORC. Moreover, on power system of the Draugen offshore oil and gas platform, comparison of ORC, single pressure Steam Rankine Cycle (SRC) and air bottoming cycle (ABC) to recover the medium temperature waste heat produced at 379°C by the Siemens SGT500 twin-spool gas turbine was done by Pierobon and Nguyen [6]. Optimization using the multi-objective genetic

algorithm (MOGA) was applied on each of them to discover the optimal system designs. ORC and SRC are appropriate to be used when a highly efficient offshore platform was desired, but its cost needed to be reduced for better economic revenue. From the aspect of applicability range and system performance, the combination of ORC with turbo generators stands out but with poor economic revenue too. Besides the Draugen offshore oil and gas platform, ORC had been utilized on a Brazilian floating oil platform by Barrera and Bazzo [7] to conduct an exergetic analysis related to 2$^{nd}$ law of thermodynamic. The working fluid selected was Cyclopentane and ORC with optimal configuration was discovered according to the vapor saturation curve. The results showed that the exhaust gas exergy could be considered to improve the output power and ORC could save the fuel consumption up to 15-20%. Apart from that, the basic and recuperated ORCs were analyzed by Khatita and Ahmed [8] which aimed to apply a WHR system on an existing oil and gas facilities in Egypt. The reaction of decision parameters to the systems efficiency and net output power were investigated by conducting simulation with several working fluids. The results have shown that an ORC with recuperator with either cyclohexane or benzene as working fluids is the best choice for the current case. Furthermore, Bhargava and Bianchi [9] also conducted an overall investigation of ORC with different types of gas turbines that are normally used by offshore platform with different power ratings as the bottoming cycle for WHR. Thermal connections with the presence or absence of secondary heat transfer fluid between the ORC and gas turbine exhaust gas are both considered in this analysis. Dowtherm A was used as the thermal fluid while cyclopentane was the ORC working fluid. The results have shown that although having secondary thermal fluid had several feasible advantages than the direct evaporation, it led to poor thermodynamic performance. Eveloy and Rodgers [10] had proposed and analyzed a cogeneration system which targeted to produce heat, power and clean water from the waste heat released from a Persian Gulf offshore sector. A reverse osmosis desalination system applied in the ORC was used in this research to recover the heat content of the exhaust gas. Additionally, heat dissipated from the process of condensation in ORC was utilized in the process of heating. The results showed that with working fluid octamethyltrisiloxane utilized on the ORC, the cogeneration system boosted the exergetic efficiency of gas turbine by 6%.

ORC was found out to be able to adapt to low or medium grade heat source with different type of configurations. The platform size and the available heat source are the main factors when choosing the working fluid for the ORC. ORC also has low operating pressure and low maintenance cost which is suitable for the WHR of offshore oil and gas platform. The flexibility of ORC on the selection of working fluids makes it easier to be used on offshore oil and gas platform with different configuration. Dry and isentropic fluids with good thermal stability are more suitable to be the working fluid of ORC system on offshore application which could lead to better system performance and efficiency [7, 8]. Besides, the turbine inlet temperature and pressure were stated to be the most effective parameters on the performance of ORC system [6, 11]. Moreover, the simple ORC is suggested to be in a configuration where the temperature of exhaust gases is consistently higher than the dew point temperature of the water contained in the exhaust gases to avoid damage to the equipment caused by the condensation of acid components.

**Keywords:** Oil and Gas; Waste heat recovery; Offshore platform; Organic Rankine cycle.

## Acknowledgment

The authors are grateful to Malaysia-Thailand Joint Authority (MTJA), UTM-LoCARtic and IVESE UTM for the support in publishing this work.

## References

[1] Omara, A., Saghafifar, M., Mohammadi, K., Alashkar, A., and Gadalla, M. (2018) A Review of Unconventional Bottoming Cycles for Waste Heat Recovery: Part II - Applications. Energy Conversion and Management 180(1):559-583.
[2] Malaysia Biennail Update Report to the UNFCCC 2016. (2016) Ministry of Environment and Water Malaysia, Putrajaya.
[3] Malaysia Biennail Update Report to the UNFCCC 2020. (2020) Ministry of Environment and Water Malaysia, Putrajaya.
[4] Jouhara, H., Khordehgah, N., Almahmoud, S., Delpech, B., Chauhan, A., and Tassou, S.A. (2018) Waste Heat Recovery Technologies and Applications. Thermal Science and Engineering Progress 6(1):268-289.
[5] Kolahi, M., Yari, M., Mahmoudi, S.M.S., and Mohammadkhani, F. (2016) Thermodynamic and Economic Performance Improvement of ORCs Through Using Zeotropic Mixtures: Case of Waste Heat Recovery in an Offshore Platform. Case Studies in Thermal Engineering 8:51-70.
[6] Pierobon, L., Nguyen, T.-V., Larsen, U., Haglind, F., and Elmegaard, B. (2013) Multi-objective Optimization of Organic Rankine Cycles for Waste Heat Recovery: Application in an Offshore Platform. Energy 58(1):538-549.
[7] Barrera, J.E., Bazzo, E., and Kami, E. (2015) Exergy Analysis and Energy Improvement of a Brazilian Floating Oil Platform Using Organic Rankine Cycles. Energy 88:67-79.

## OIL AND GAS

[8] Khatita, M.A., Ahmed, T.S., Ashour, F.H., and Ismail, I.M. (2014) Power Generation Using Waste Heat Recovery by Organic Rankine Cycle in Oil and Gas Sector in Egypt: A Case Study. Energy 64:462-472.
[9] Bhargava, R.K., Bianchi, M., Branchini, L., De Pascale, A., and Orlandini, V. (2015) Organic Rankine Cycle System for Effective Energy Recovery in Offshore Applications: A Parametric Investigation with Different Power Rating Gas Turbines. Turbo Expo: Power for Land, Sea, and Air. American Society of Mechanical Engineers, Montreal, Canada.
[10] Eveloy, V., Rodgers, P., and Qiu, L. (2016) Performance Investigation of a Power, Heating and Seawater Desalination Poly-generation Scheme in an Off-shore Oil Field. Energy 98:26-39.
[11] Roy, J., Mishra, M., and Misra, A. (2010) Parametric Optimization and Performance Analysis of a Waste Heat Recovery System using Organic Rankine Cycle. Energy 35(12):5049-5062.

**PHARMACEUTICAL AND DRUG DELIVERY**

**Paper ID: ESCE004**

# CONTROL ANALYSIS OF BIOMASS GASIFICATION WITH COMBINED HEAT AND POWER SYSTEM

**Y.H. Kok[1], N. Kamarulzaman[1], Z. F. Mohd Shadzalli[1], N. Abdul Manaf[1]***

[1] *Department of Chemical and Environmental Engineering, Malaysia-Japan International Institute of Technology (MJIIT).*
*Corresponding author: norhuda.kl@utm.my

## Extended Abstract

The development of science and technology has a strong correlation with the energy demand. Rapid growth of technological development and population contributes to the enhanced electricity production which then lead to extreme environmental problems such as global warming and climate change. Innovation in biomass gasification with combined heat and power (BG-CHP) system emerges as a potential technology to overcome those environmental challenges. The major problem of BG-CHP is its bulkiness and inconvenient form of biomass along with the multifaceted process behavior. All these feature non-linearities as well as high process interactions, and therefore require understanding of the dynamics if responsive and flexible operation of the plant is to occur. Therefore, it is of significant importance to ensure the operational stability and feasibility of BG-CHP subjected to the optimal operation at maximum power output.

Daniel and Gandhi (2017) studied a design of mathematical modelling and control of downdraft biomass gasifier. A Proportional, Integral, Derivative (PID) controller was used to control the temperature to achieve an optimal result by manipulating the airflow. Their analysis showed that PID controller is able to improve the performance of the process in terms of time-domain specifications, setpoint tracking, and regulatory changes. Huang and Shen (2019) carried out a study by adjusting the amount of water to improve the output of synthetic gas and reduce the slag in an updraft gasifier base on the adaptive control design, PID. From the study, combination control of MANFIS and PSO is useful to improve the hydrogen production efficiency by 25.43% and slag formation of the gasifier by 36.8%. Based on the existing studies, there is scarce work has been done on the performance of BG-CHP system using MPC controller and targeted to power output.

In this work, Aspen Plus (Aspen Technology, Inc.) and Matlab (Mathworks, Inc.) software are used to demonstrate a control analysis of BG-CHP system as illustrated in Figure 1. A steady state BG-CHP system is initially developed using Aspen Plus software based on the actual unit operation of 25kW pilot scale manufactured by APL Power Pallet. The Aspen Plus model of the steady state BG-CHP system is consequently converted to a dynamic model by Aspen Plus Dynamics. A dynamic dataset of BG-CHP model is generated which consist of 3 inputs and 1 output. The inputs are syngas flowrate, air flowrate and temperature while the output is power output. From the dataset, an empirical model describes the BG-CHP process is developed in Simulink/Matlab environment via System Identification toolbox. In this research, we are using Simulink environment as the control analysis platform due to its computational efficiency in evaluating and simulating the controller performance with more realistic plant dynamics (Chinprasit and Panjapornpon 2020). Two different types of controllers (*viz;* PID and Model Predictive Controller (MPC)) are designed and compared to meet the plant objective (power output) by manipulating the syngas flow rate and/or air flowrate.

Control analysis is conducted based on the set point trajectories at 15-20-10 kW for 24-hour operation via two control configurations. A control pairing for PID controller is syngas flowrate and power output, while for MPC controller, the control pairing involves syngas and air flow rates with power output. It is expected that MPC is outperformed the PID controller performance in meeting the set points of power output in BG-CHP system. This is because MPC is able to explicitly predict the future behavior of the plant as well as capable to optimally reduced the process variance. This preliminary control study of BG-CHP system is able to provide insight for the feasible and optimal operation of large scale BG-CHP plant subsequently contribute to reduction in costs of the plant.

**PHARMACEUTICAL AND DRUG DELIVERY**

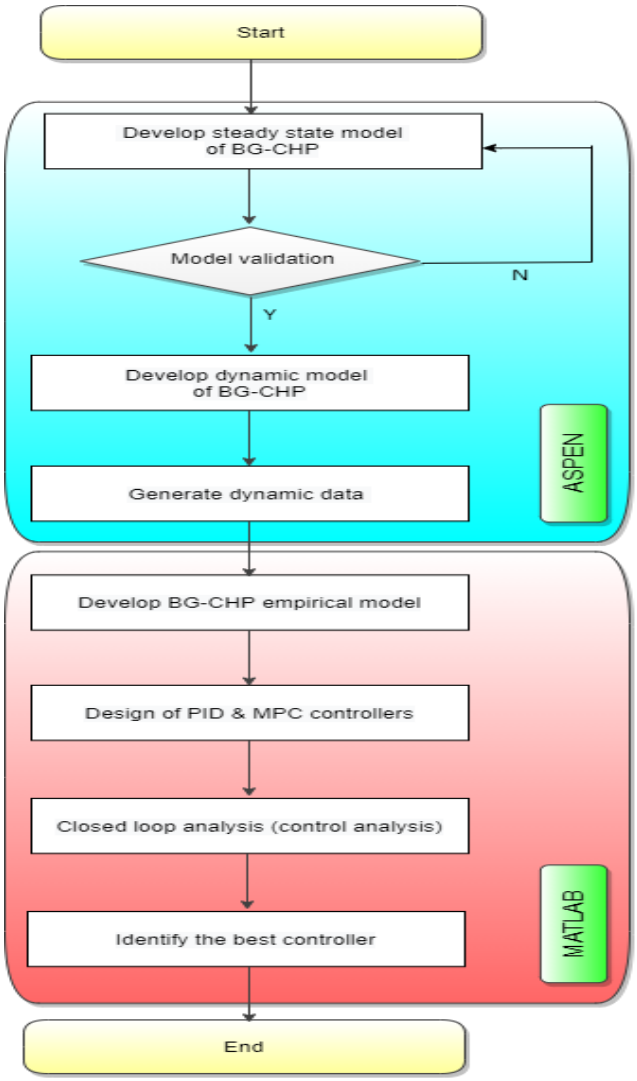


Fig. 1: Modelling and control analysis procedure for BG-CHP system.

**Keywords:** Palm Kernel Shell; Gasification; MPC; Control; Energy.

## Acknowledgment

This study was supported by Ministry of Education (MOE) through Fundamental Research Grant Scheme (FRGS), project no. FRGS/1/2018/TK02/UTM/02/27, vot no. 4F996 and Tier 2, Universiti Teknologi Malaysia, project no. Q.K130000.2643.15J77.

## References

[1] Chinprasit, J. and C. Panjapornpon (2020). "Model predictive control of vinyl chloride monomer process by Aspen Plus Dynamics and MATLAB/Simulink co-simulation approach." IOP Conference Series: Materials Science and Engineering 778: 012080.
[2] Daniel, V. and S. Gandhi (2017). "Design of Mathematical Modelling and Control of Downdraft Biomass Gasifier." International Journal of Control and Automation 10: 175-184.
[3] APL Power Labs (2021), http://www.allpowerlabs.com/ [access on 28.2.2021]."
[4] Huang, C.-N. and H.-T. Shen (2019). "Maximum hydrogen production by using a gasifier based on the adaptive control design." International Journal of Hydrogen Energy 44(48): 26248-26260.

**PROCESS CONTROL AND OPTIMISATION**

**Paper ID: ESCE014**

# MODELLING OF ETHYLENE GLYCOL PRODUCTION IN PLUG FLOW REACTOR USING BLOCK-ORIENTED MODEL

**F. S. Rohman[1], D. Muhammad and N. Aziz[1]***

[1] *School of Chemical Engineering, Engineering Campus, Universiti Sains Malaysia, Seri Ampangan,14300 Nibong Tebal, Seberang Perai Selatan, Penang, Malaysia.*
*Corresponding author: chnaziz@usm.my

## Extended Abstract

To control the process at its optimum conditions is the effective ways to improve the productivity of ethylene glycol (EG). The dilemma of any model based control is the development and accuracy process model. Model needs to be simple but still accurate. An appropriate model which is required to develop, is noteworthy to establish the best control performance for model based controller. One of the well-known model identification technique is block-oriented models [1]. Unlike black-box modeling, the block-oriented modeling approach is more transparent due to its straightforward physical interpretation based on its combined block gains [2,3] It can be applied as an estimator to predict the process system [4,5]. The block-oriented model class comprises a wide range of model configurations, which involved a linear dynamic and nonlinear static element. The most widely implement block-oriented model is the Wiener model, which has been applied in many modeling case studies and displayed the capability of describing a broad class of nonlinear systems.

In this works, a block-oriented model consists of linear block, state space (SS), and nonlinear elements, neural wiener (NW) models, were developed for EG production in plug flow reactor. There is no other prior research that has been carried out in the same field of EG production. From theoretical perspective, nonlinear system characteristics can only be fully captured by nonlinear model. However, in a model based control application, a linear model will be the first choice for nonlinear process if the model can satisfactorily fulfil its purpose to representing the process under consideration [6]. This can be decided by comparing the capability of the linear and nonlinear model representing the process. Therefore, the main objective of this work is to compare and analysed the state space (SS) model and the neural wiener (NW) models. The identification and validation data SS and NW models were generated from the ASPEN model within Matlab 2017b environment.

In order to generate data for the empirical model identification, a steady state and dynamic model of the EG production is developed using Aspen Plus and Aspen Dynamic software, respectively. The multi-inputs data included were jacket flowrate and hydrogen flowrate. Meanwhile, the multi-outputs data were temperature in reactor and EG flowrate. Figures 1 and 2 show the regression plots for SS and NW models validation results The distribution of data points, which scatter almost evenly along the fit line, suggests that the model is excited with sufficient inputs perturbation. The values of $R^2$ for the SS and the NW models for the reactor temperature were 68.86.80% and 93.63%, respectively, while for the EG flowrate the values of $R^2$ for the best SS and NW models were 77.61% and 96.48%, respectively. The results showed that the accuracy of NW models for predicting the real data is better than the SS models. Thus, the application of nonlinear block-oriented models in simulating the EG production is well justified in capturing nonlinear effect of the MIMO system.

## PROCESS CONTROL AND OPTIMISATION

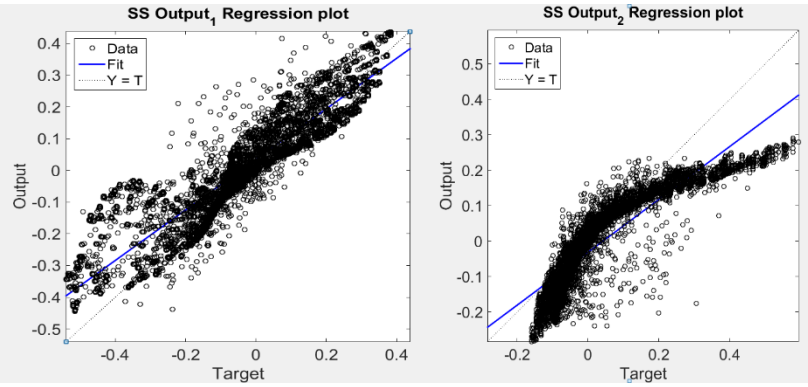


Fig. 1: Regression plot for SS model.

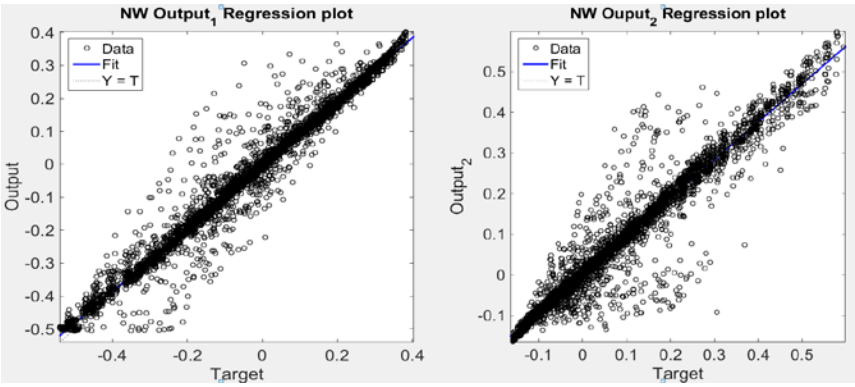


Fig. 2: Regression plot for NW model.

**Keywords:** State space; Neural wiener; Ethylene glycol; Plug flow reactor.

**Acknowledgment**

The financial support from Universiti Sains Malaysia through Research University Grant (RUI) 203.PJKIMIA.8014146 is greatly acknowledged.

**References**

[1] Schoukens, M., and Tiels, K., (2017). Identification of block-oriented nonlinear systems starting from linear approximations: A survey. Automatica 85: 272-292.
[2] Lawryńczuk, M., (2019) Identification of Wiener models for dynamic and steady-state performance with application to solid oxide fuel cell. Asian J Control 21: 1836-1846.
[3] Lawryńczuk, M., and Tatjewski, P. (2020) Offset-free state-space nonlinear predictive control for Wiener systems. Inf. Sci. 511: 127-151.
[4] Rohman, F.S., Sata, S.A., Othman, M.R., Aziz,N. (2020) Optimizing autocatalysis with uncertainty by derivative-free estimators, Optim Control Appl Methods, 1–15.
[5] Rohman, F.S., Sata, S.A., Othman, M.R., Aziz,N (2015) Application of Derivative-Free Estimator for Semi Batch Autocatalytic Esterification Reactor: Comparison Study of Unscented Kalman Filter, Divided Difference Kalman Filter and Cubature Kalman Filter, Comput. Aided Chem. Eng. 37, 329-334.
[6] Rohman, F.S, Muhammad, D., Aziz,N. (2020) Implementation of model predictive control in tracking dynamic optimal profiles of semi batch autocatalytic esterification reactor, Asia-Pac. J. Chem. Eng. , 1-9.

**PROCESS CONTROL AND OPTIMISATION**

**Paper ID: ESCE067**

# PARETO SOLUTION OF AUTOCATALYTIC ESTERIFICATION IN SEMI BATCH BY USING CONTROL VECTOR PARAMETERIZATION (CVP) AND ε-CONSTRAINT

**F. S. Rohman[1] and N. Aziz[1]***

[1] *School of Chemical Engineering, Engineering Campus, Universiti Sains Malaysia, Seri Ampangan, 14300 Nibong Tebal, Seberang Perai Selatan, Penang, Malaysia.*
*Corresponding author: chnaziz@usm.my

## Extended Abstract

The esterification process is an important process in the food, cosmetic and pharmaceutical which is mainly used for flavors and fragrance components in products. Moreover, ester products also have wide applications in areas such as pesticides and herbicides, metal extraction agents, synthetic lubricants, polymerization aids for acrylic acid esters, insect attractants, repellants and photographic applications [1]. In industry, the ester is a specialty chemical product and commonly produced in batch processes which are typically applied to yield high productivity and selectivity [2]. The ester (sec-butyl propionate) can be produced by catalyzed reaction between propionic anhydride and 2-butanol [3]. Mathematical modeling of esterification in semi batch process operating under dynamic conditions composes of ordinary differential equations (ODE) and differential algebraic equations (DAE). Dynamic optimization generates optimal trajectories of feed flow rate and temperature which leads to the maximum productivity and efficiency [4].

The available literature on the dynamic optimization of the esterification reaction between propionic anhydride and 2-butanol for sec-butyl propionate production was carried out by solving single objective optimization problems [5]. Actually, contradictory objective functions have been found in this esterification process, i.e. maximum conversion and minimum process time which generates various combinations of optimal controls trajectories. The optimum results from the single-objective optimization problem cannot interpret the correlation between conflicting objective functions, and unable to provide a combination set of optimal trajectories. Thus, it is suggested that application of a multi-objective optimization MOO approach for the improving optimal policy can offer a better way for predicting performance trade-offs obtained due to opposite actions of operating objectives for the esterification process. Notwithstanding this, the application of multi-objective optimization to the esterification for sec-butyl propionate production using ε-constraint approach has been unexplored. The investigation of dynamic MOO in autocatalytic esterification can fill the gap of optimization study for semi batch esterification process.

The objective of this paper is to solve the multi-objective optimization problem using ε-constraint approach in autocatalytic esterification process the esterification reaction between propionic anhydride and 2-butanol. The aim of this optimization problem is to determine the optimal feed flowrate and temperature profiles to optimize the opposite objective functions which are minimization process time and maximization conversion.

This resulted in a set of several pareto optimal solutions with the two objectives: maximum conversion ranging from 0.90 to 0.99 is accompanied by minimum final time ranging from 45 to 70 min. Thus, the two objectives are contradictory leading to the optimal pareto front in the Fig. 1 Each point of Pareto solutions consists of different optimal temperature reactor and feed rate profiles, which lead to a variation conversion and process time. These solutions give multiple alternatives in evaluating the trade-offs and selecting the most suitable operating policy.

**PROCESS CONTROL AND OPTIMISATION**

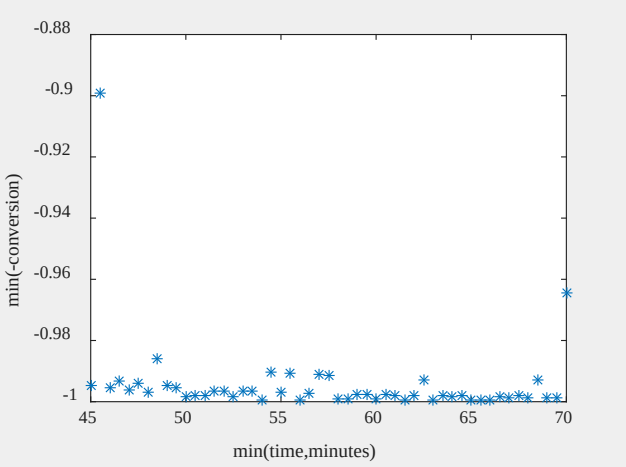


Fig. 1: Pareto front.

**Keywords:** Dynamic optimization; Multi-objective optimization; ε-constraint; Autocatalytic esterification.

**Acknowledgment**

The financial support from Universiti Sains Malaysia through Research University Grant (RUI) 203.PJKIMIA.8014146 is greatly acknowledged.

**References**

[1] Zulkeflee, S.A. Sata, S.A., Rohman, F.S., Aziz, N. (2020) Modelling of immobilized Candida Rugosa lipase catalysed esterification process in batch reactor equipped with temperature and water activity control system. Biochem Eng J 107669.
[2] Chang J, and Chen K. (2004) An integrated strategy for early detection of hazardous states in chemical reactors. Chem Eng J 98199:211.
[3] Zaldivar J M, Hernandez H, Molga E, Galvan I M. & Panetsos F. (1993) The use of neural networks for the identification of kinetic functions of complex reactions. In Proceedings of the third European symposium on computer aided process engineering, ESCAPE 3.
[4] Faust, J M M, Hamzehlou S, Leiza J R, Asua J M, Mitsos A, (2019) Dynamic optimization of a two-stage emulsion polymerization to obtain desired particle morphologies Chem Eng J 359:1035-1045.
[5] Rohman, F.S., Sata, S.A., Othman, M.R., Aziz, N. (2021) Dynamic optimization of autocatalytic esterification in semi-batch reactor. Chem Eng Technol,early view.

**PROCESS CONTROL AND OPTIMISATION**

**Paper ID: ESCE069**

# OPTIMIZATION OF FUZZY LOGIC IN THE INTEGRATION OF SURFACE WATER TREATMENT BASED ON WATER QUALITY INDEX (WQI)

**N. F. Rahim[1,2], N. Kasmuri[1]*, A. Z. Amir[2], J. Jani[1], A. R. Abbas[2], M. Alias[2], A. H. Amer[2], N. I. Ruslan[2], M. Stapah[2]**

[1] *School of Civil Engineering, College of Engineering, Universiti Teknologi MARA, 40450 Shah Alam, Selangor, Malaysia.*
[2] *Built Environment and Climate Change, TNB Research, Malaysia.*
*Corresponding author: norhafezahkasmuri@uitm.edu.my

## Extended Abstract

River water pollution has been critically reported in recent years. This environmental issue needs to be urgently overcome to prevent a severe impact on the surrounding ecosystem. Thus, an artificial intelligence (AI) system of mobile automated water treatment has been developed to enhance surface water quality. This method used the fuzzy logic technique for decision-maker instead of a human. This research focused on implementing the fuzzy logic technique to analyze the water quality index results and determine the appropriate treatment for the surface water based on AI. Implementing fuzzy logic by determining the dose of treatment based on the sensor results will also integrate the mobile water treatment as it will be automated instead of manually analyzing and deciding on the dosing requirement. The fuzzy logic techniques have been built by using MATLAB software where the membership functions for the input are six (6) parameters according to the Water Quality Index (WQI) based on Department of Environment (DOE), Malaysia. Here, the fuzzy logic was created and analyzed based on the 181 rules set and the membership functions for output, WQI values, and the classes based on WQI. The classes of WQI will be determined from Class I to II of water quality, a non-chemical treatment, whereas Class III to IV will be chemical treatment required. The fuzzy logic techniques will be implemented in the fuzzy logic block diagram in SIMULINK, and the simulation will show the results of WQI and the class of treatment. For future development of mobile water treatment plant, the overall fuzzy logic block diagram will then be built, including the dosing required for coagulation and the demineralization water process.

### INTRODUCTION

Fuzzy Logic controllers do not need an accurate mathematical model and can work with imprecise inputs. They also can handle nonlinear systems and control unstable systems [1]. The basic structure of any fuzzy logic controller is shown in Figure 1 and consists of the following stages: fuzzification, rule base and inference engine, and defuzzification. In the fuzzification stage, numerical input variables are converted into linguistic variables, such as CI (Class I), CII (Class II), CIII (Class III), CIV (Class IV) and CV (Class V) using a basic fuzzy subset. The fuzzy inference engine processes the inputs according to the rules base table and produces the linguistic output. The defuzzification stage is used to convert the output linguistic variable back to a numerical variable [2].

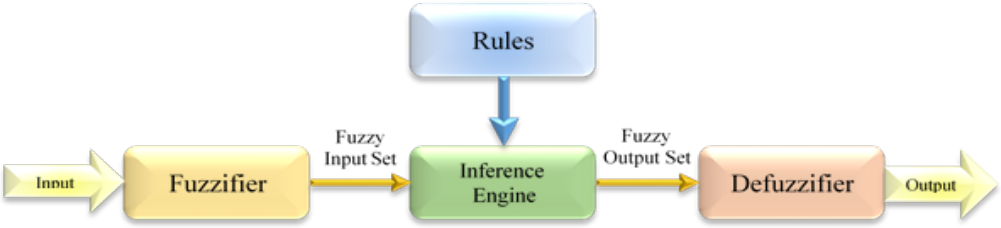


Fig. 1: Fuzzy Logic Fundamentals [2].

## PROCESS CONTROL AND OPTIMISATION

### METHODS

Here in the study, the inputs for fuzzy logic techniques for determining surface water treatment is the water quality index (WQI). It can be denoted, that the water quality index can be obtained by calculating six water quality parameters set up by the Department of Environment (DOE). Fuzzy logic results in not inherently true or false outputs but can be anywhere in the middle, apart from regular Boolean Logic, where it generates only true and false values. In this case, the method distributes the quality of water into five classes based on the logical performance of the parameters.

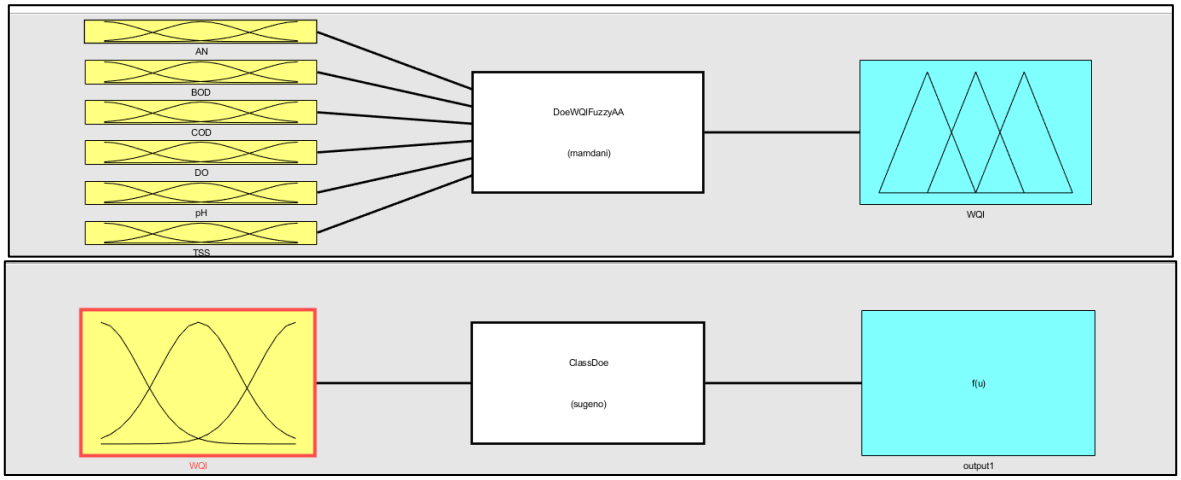


Fig. 2: Fuzzy Logic Input, Rules and Output Set-up.

The establishment of water quality indexes (WQI) from various water sources based on multiple identified key parameters and finally optimize the fuzzy logic control in determining the type of water treatment system to develop smart green technology incorporating control system employing the fuzzy logic technique for the future development of mobile water treatment plant [3]. Based on the results, all value in the fuzzy logic simulation had been verified by the other application and turned out the same value.

It can be concluded that fuzzy logic techniques for decision support system had been successfully established, and the overall block diagram can be implemented in the future mobile water treatment plant.

**Keywords:** Artificial intelligence; Fuzzy logic; Optimization; Water quality index.

### Acknowledgment

This study was supported by the Ministry of Higher Education (MOHE) and Universiti Teknologi MARA, Shah Alam, in providing FRGS-RACER Grant (600-IRMI/FRGS-RACER 5/3 (065/2019) for financially supported this research study.

### References

[1] Afroz, R., & Rahman, A. (2017). Health impact of river water pollution in Malaysia. International Journal of Advanced and Applied Sciences, 4(5), 78-85.
[2] Argyrou, M. C., Christodoulides, P., & Kalogirou, S. A. (2018, June). Modeling of a photovoltaic system with different MPPT techniques using MATLAB/Simulink. In 2018 IEEE International Energy Conference (ENERGYCON) (pp. 1-6). IEEE.
[3] Alias, M., Amer, A. H., & Abbas, A. R. (2019). Pilot Automated Mobile Water Treatment. Kajang: TNB Research.

**PROCESS CONTROL AND OPTIMISATION**

**Paper ID: ESCE107**

# MODEL PREDICTIVE CONTROL IN FERMENTATION PROCESS – A REVIEW

**W. Y. Chai[1], K. T. K. Teo[2], M. K. Tan[2], H. J. Tham[1]***

[1] *Chemical Engineering Programme,* [2] *Electrical & Electronics Engineering Programme, Faculty of Engineering, Universiti Malaysia Sabah, Jalan UMS, 88400 Kota Kinabalu, Sabah, Malaysia.*
*Corresponding author: hjtham@ums.edu.my

## Extended Abstract

Fermentation process, in the aspect of industrial field, is defined as the involvement of microbes in mass production of valuable products. It shows tremendous application in food processing, renewable energy, bulk chemical production, and pharmaceutical [1]. Microorganisms can produce complex compound which is difficult and costly to obtain through chemical synthesis. Also, bioprocess consumes less energy and is more environmental friendly [2]. However, microorganisms are very sensitive to their surroundings, particularly pH, temperature, presence of oxygen amount and type of nutrients. Therefore, optimal operational control becomes the concern of biomanufacturing industries to promote the microbial growth and metabolic activity for maximum desired product formation while prohibiting any possible by-product yield. The nonlinear and complex process behaviour, incomplete process modelto describe the actual process mechanism and deficient of dependable and cost-effective direct measuring devices [3-5] make fermentation process more challenging to be controlled and optimised. Model predictive control (MPC) is an advanced control approach which performs prediction on a sequence of future output response and take optimal control action according to objective function. Earlier remedy can be performed as problem is detected earlier through the future prediction. It has been studied extensively in fermentation process regulation. This paper reviews the application of MPC in different fermentation process with different selection of the manipulated and controlled variables. Basic concept of MPC strategy is also presented, together with the development of MPC application in fermentation over the years. Although MPC can deal with great variety of control and optimisation problem, there are still some challenges that need to be overcome include the accuracy of prediction model, computational load and cost-effective of online measurement. Mathematical modelling of fermentation process has been studied since a few decades ago, like simple unstructured model, structured segregated model, dynamic balance flux model and neural network model. The more complicated model, the more accurate description on process, however, at the same time, the more computational burden for MPC. Recent development in technology and more powerful CPU has increased the computational efficiency of MPC, therefore the use of complicated but detailed model has become feasible. On the other hand, the selection for manipulated and controlled variables are also considered as a vital task depend on the availability of cost-effective online measurement. The variables that most costly and complicated to measure directly are the component concentrations inside the bioreactor. The development of advanced process analytical equipment such as Raman spectroscopy [3] and soft sensor [6] have become the alternative way, replacing the indirect measurement [7], for the state measurement or estimation.

**Keywords:** Fermentation; Model Predictive Control; Non-linear model; Optimisation.

### Acknowledgment

The authors gratefully acknowledge the financial support from Ministry of Higher Education under Fundamental Research Grant Scheme number FRG0548-2020.

### References

[1] Pohorecki, R., Bridgwater, J., Molzahn, M., Gani, R., Gallegos, C. (2010) Chemical Engineering and Chemical Process Technology: Chemical Engineering Education and Main Products, Volume V. United Kingdom: EOLSS.
[2] Rocha, M., Mendes, R., Rocha, O., Rocha, I., Ferreira, E. C. (2014) Optimization of fed-batch fermentation processes with bio-inspired algorithms. Expert Systems with Applications, 41:2186-2195.
[3] Craven, S., Whelan, J., Glennon, B. (2014) Glucose concentration control of a fed-batch mammalian cell bioprocess using

## PROCESS CONTROL AND OPTIMISATION

a non-linear model predictive controller. J. Process Control 24: 344–357.
[4] Shimizu H, Miura K, Shioya S, Suga K. (1993) An overview on the control system design of bioreactors. Advanced Biochemical Engineering Biotechnology, 50: 65–84.
[5] Alford, J. S. (2006) Bioprocess control: advances and challenges. Computer & Chemical Engineering, 30: 1464-1475.
[6] Karakuzu, C., Turker, M., Ozturk, S. (2006) Modelling, on-line state estimation and fuzzy control of production scale fed batch baker's yeast fermentation. Control Engineering Practice, 14: 959-974.
[7] Dewasme, L.,Fernandes S., Amribt, Z., Santos, L. O., Bogaerts, Ph., Vande Wouwer, A. (2015) State estimation and predictive control of fed-batch cultures of hybridoma cells. Journal of Process Control, 30: 50-57.

**PROCESS CONTROL AND OPTIMISATION**

**Paper ID: ESCE123**

# PERFORMANCE EVALUATION FOR LINEAR BASED MODEL PREDICTIVE CONTROL IN CONTROLLING PRODUCTION RATE AND REACTOR TEMPERATURE OF ETHYLENE GLYCOL REACTOR

**M. S. Sulaiman[1], F. S. Rohman[1], N. Aziz[1]***

[1] *School of Chemical Engineering, Engineering Campus, Universiti Sains Malaysia, Seri Ampangan, 14300 Nibong Tebal, Seberang Perai Selatan, Penang, Malaysia.*
*Corresponding author: chnaziz@usm.my

## Extended Abstract

Process Automation Systems are widely known to be a crucial element in processing plants worldwide. In an environment that is ever-changing, process automation is applied in industries when possible to mitigate complexities with advance process control (APC) systems specifically leading to higher efficiency, less operator interaction and increased profits. APC is a proven control and optimization technology delivering measurable and sustainable improvements in production yield, coupled with the added value of energy savings [1]. Many researches focused on modeling the Ethylene glycol (EG) production process each with distinct reactors and reactions. On the other hand, the advances on its control system were poor. Thus, this research fills the gap on the implementation of APC for the EG reactor. In this work, a linear based model predictive control (LMPC) is developed and implemented in EG reactor [2]. The aim of LMPC is to control the production rate and reactor temperature for an optimized hydrogenation reactor. The optimal set point used is based on multi-objective optimization approach as provided by Sulaiman et al. [3]. A state-space model is used in the prediction control is constructed with the best fit of 91.51% and 83.34% for EG production rate and reactor temperature, respectively. Based on Figure 1, the LMPC is developed in Simulink and tuned via the MPC design toolbox in Matlab. The LMPC performance was evaluated based on the graphical and error analyses results obtained from set point tracking (shown in Figure 2) and disturbance rejection. The results showed that the LMPC can operate efficiently under tight boundary constraint. The offset as error increases once the limit is exceeded. This sums up that the LMPC can control both control variables with an acceptable degree of error under strict boundary conditions.

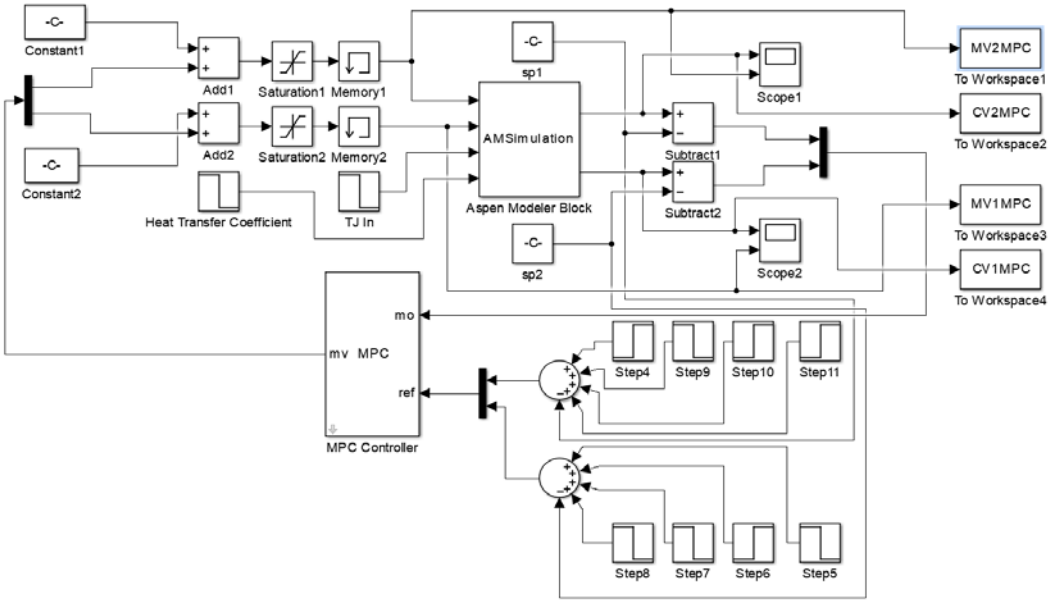


Fig. 1: Simulink model of LMPC controller for EG reactor.

**PROCESS CONTROL AND OPTIMISATION**

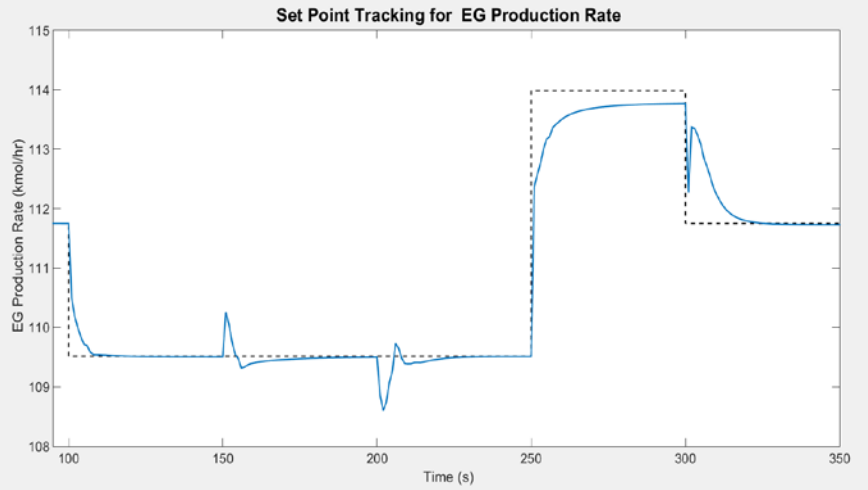


Fig. 2: Result of set point tracking for EG production rate.

**Keywords:** Model Predictive Control; Advance Process Control; Ethylene Glycol; Model Based Control; Multi-Input-Multi-Output System.

**Acknowledgment**

This study was supported by Universiti Sains Malaysia through Research University Grant (RUI) 203.PJKIMIA.8014146.

**References**

[1] Nordh, P. (2016) Understand advance process control, American Institute of Chemical Engineering (AIChE), 69-72.
[2] Yu, B.Y. and Chien, I.L. (2017) Design and optimization of dimethyl oxalate (DMO) hydrogenation process to produce ethylene glycol (EG). Chemical Engineering Research and Design, 121, 173-190.
[3] Sulaiman, M.S., Rohman, F.S. & Aziz, N. (2021) Optimization process for ethylene glycol production using the Pareto solution, IOP Conference Series: Materials Science and Engineering, 1011.

2ND ENERGY SECURITY AND CHEMICAL ENGINEERING CONGRESS 2021
*"Sustainable Technological Solution for a Better World"*
VIRTUAL CONFERENCE | 3-5 NOVEMBER 2021

**REACTION ENGINEERING AND CATALYSIS**

**Paper ID: ESCE079**

# SYNTHESIS AND CHARACTERIZATION OF SODIUM TUNGSTATE: INVESTIGATION OF SURFACTANT EFFECT AND ITS PHOTOCATALYTIC APPLICATION

**N. A. M. Razali[1,2], W. N. W. Salleh[1,2] *, F. Aziz[1,2], W. J. Lau[1,2], N. Yusof[1,2], A. F. Ismail[1,2]**

[1] *Advanced Membrane Technology Research Centre (AMTEC),* [2] *School of Chemical and Energy Engineering, Universiti Teknologi Malaysia, 81310 Skudai, Johor, Malaysia.*
*Corresponding author: hayati@petroleum.utm.my

## Extended Abstract

The palm oil mill effluent (POME) discharges a vast amount of wastewater from palm oil industry that contain high organic and inorganic voluminous colloidal particles in suspension that subsequently results in high biochemical oxygen demand (BOD), chemical oxygen demand (COD), and total suspended solid (TSS) coupled with a high acidity [1]. Among conventional method, biological treatments, such as a ponding system, are widely used for treating POME, as it is still influenced by the discharge limit specified by Malaysia Sewage and Industrial Effluent Discharge Standard from the Department of Environment (DOE) [2]. Therefore, the photocatalytic technology that is categorized in advanced oxidation processes (AOPs) can be applied to treat POME [3]. Sodium tungstate ($Na_2WO_4$) are isostructural, exhibiting rich polymorphism and is considered a good catalyst in photocatalytic technology that is classified into spinel typed crystal structure, with Fd-3m symmetry and a general formula of $Na_2X_nO_{3n+1}$ (X = W) [4-5]. Besides, the synthesis of $Na_2WO_4$ influenced with addition of surfactant and different calcination temperature that had shown significant effects on their characterization, which might influence its photocatalytic performance of POME.

In the present work, $Na_2WO_4$ was synthesized for photocatalytic degradation towards POME. The synthesized $Na_2WO_4$ was characterized of their thermal and optical properties via thermogravimetric analysis (TGA) and diffuse reflectance spectroscopy (DRS), respectively. The energy storage potential as the newest scheme in photocatalytic performance was assessed by their color and COD removal. Result revealed that $Na_2WO_4$ photocatalyst is inconsistent for photocatalysis of the aforementioned decolorization and degradation towards POME. In addition, result showed an optimal calcination temperature for maximal degradation of POME at 400°C. The highest efficiency of decolorization and degradation of POME were found to be W4 (25%) under visible-light-driven (VLD) scheme, and W6 (53%) for energy storage material (ESM) scheme under visible-light irradiation. The results indicated that the influence of calcination temperature of $Na_2WO_4$ with addition of citric acid used in the synthesis procedure did not have a strong influence on the thermal and optical properties. Meanwhile, the decolorization and degradation of POME have been observed during temperature increment. It was found that increased calcination temperature led to smaller bandgaps, which emerged at the optical absorption edges. This shows synthesized $Na_2WO_4$ demonstrated suitable bandgap of photocatalyst and can, therefore, have promising photocatalytic applications.

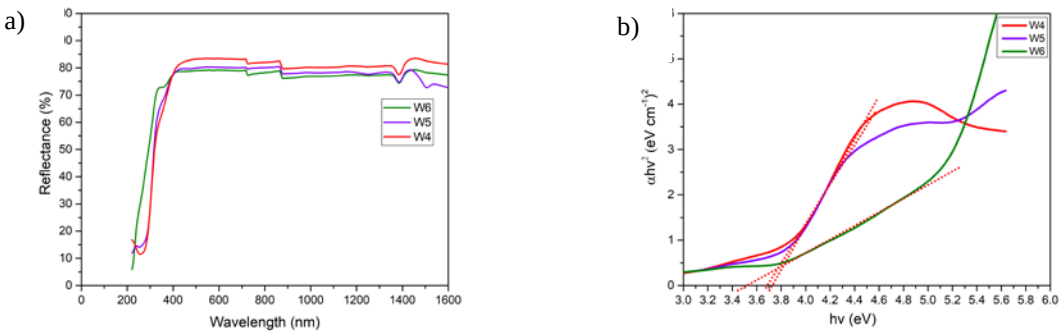


Fig. 1: Evaluation of a) reflectance and b) band gap for W4, W5 and W6 photocatalysts

Fig. 1 illustrates that the $Na_2WO_4$ was able to absorb light in the visible range of 200-700 nm, whereby absorption from photons with appropriate energy had led to the initiation of photocatalytic reaction. Results showed that bandgap energy of $Na_2WO_4$ decreased from 3.74 eV to 3.7 eV and 3.6 eV subsequently at annealing temperature of 400°C, 500°C, and 600ºC, respectively, which is in well agreement with a good photocatalyst bandgap. By increasing the calcination temperature, the thermal energy of electrons was also increased, causing the abrupt movement of electrons from valence band to conduction band and thereby, reduction in bandgap [6].

**Keywords:** Photocatalytic degradation; Sodium tungstate; Palm oil mill effluent; Co-precipitation.

## Acknowledgment

This study was supported by the Ministry of Education and Universiti Teknologi Malaysia for the financial support provided under Higher Institution Centres of Excellence Grant Scheme (Project Number: R.J090301.7851.4J423) and UTM High Impact Research Grant (Project Number: Q.J130000.2451.08G36). N.A.M. Razali would like to acknowledge the support from Universiti Teknologi Malaysia for ZAMALAH scholarship.

## References

[1] García-pérez U M., Cruz A M., Peral J. (2012) Electrochim. Acta. 81:227–32.
[2] Environment D of 1974 Environmental Quality Sewage Regulations. (2009).
[3] Charles A., Kui C. (2019) J. Environ. Manage. 234:404–11.
[4] Lima C L., Saraiva G D., Freire P T C., Maczka M., Paraguassu W., Sousa F F De., Filho J M. (2011) J. Raman Spectrosc. 799–802.
[5] Yang D., Hernandez J A., Katiyar RS., Fonseca L F. (2016) Chem. Phys. Lett. 653:73–7.
[6] Tauc J, Grigorovici R., Vancu A. (1966) Phys. status solidi. 15:627–37.

**REACTION ENGINEERING AND CATALYSIS**

**Paper ID: ESCE126**

# A BIMETALLIC-CATALYZED OXIDATIVE ESTERIFICATION REACTION FORMING α-ACYLOXY ETHER

**O.K.T. Nguyen[1], T.D. Nguyen[1]***

[1] *Advanced Catalysis and Reaction Engineering Lab, Institute of Environmental Sciences, Nguyen Tat Thanh University, Add: 298A-300A Nguyen Tat Thanh, Ward 13, District 4, Ho Chi Minh City, Vietnam.*
*Corresponding author: ndtrinh@ntt.edu.vn

## Extended Abstract

A basic ethers are one of the most common and crucial themes in various natural products, bioactive molecules and organic synthons [1]. Hence, the fact that finding an efficient method for the synthesis of structurally numerous ethers is of necessary issues [2]. A bimetallic-catalyzed oxidative esterification reaction has been created between non-activated C($sp^3$)−H bonds of symmetric ethers and carboxylic acids with the presence of di-tert-butyl peroxide (DTBP) as the oxidant through a cross-dehydrogenative coupling (CDC) reaction. This approach allows the derivatives of cyclic ether substrates to interact with aromatic acids, giving excellent yields when formed the α-acyloxy ethers. The bimetallic organic frameworks catalyst ($Fe_2$Ni-BDC) was synthesized by solve thermal method. The typical structures of material were verified by a several modern analytic methods such as X-ray Diffraction (XRD), Fourier Transform Infrared spectroscopy (FT-IR) and Scanning Electron Microscope (SEM), Raman Spectroscopy, Brunauer-Emmett-Teller (BET) and X-ray Photoelectron Spectroscopy (XPS). The $Fe_2$Ni-BDC catalyst was successfully utilized for the formation α-Acyloxy ethers based on the CDC reaction of carboxylic acid with diethylene oxide (approx. 84% product yield). Besides, this material was also used as catalyst for research scope of benzoic acid containing various substituents. The bimetallic catalyst was reused many times without a significant reducing in catalytic activity. Moreover, α-Acyloxy ethers were not created through the donation of leaching catalytic species. It was verified that this is first study which uses the bimetallic catalyst for reaction to form the α-acyloxy ethers via direct esterification of aromatic acids.

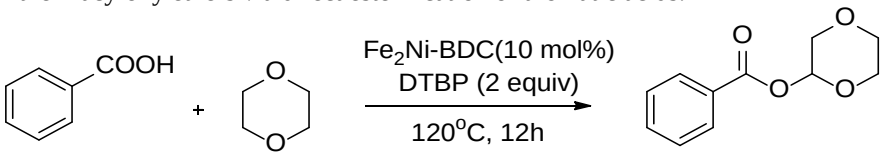


Scheme 1: The synthetic reaction of α-acyloxy ether compound.

**Keywords:** α-Acyloxy ethers; Metal-organic framework; Bimetallic metal-organic frameworks; Esterification reaction.

### Acknowledgment

This study was supported by NTTU Foundation for Science and Technology Development under grant number 2019.01.24/HĐ-KHCN.

### References

[1] M. A. A. Orabi, S. Taniguchi, M. Yoshimura, T. Yoshida, K. Kishino, and H. Sakagami, "Hydrolyzable Tannins of Tamaricaceous Plants. III.1 Hellinoyl- and Macrocyclic-Type Ellagitannins from Tamarix nilotica," *J. Nat. Prod*, vol. 78, pp. 870–879, 2010.
[2] G. Majji, S. Guin, S. K. Rout, A. Behera, and B. K. Patel, "Cyclic ethers to esters and monoesters to bis-esters with unconventional coupling partners under metal free conditions via sp3C-H functionalisation," *Chem. Commun.*, vol. 50, no. 81, pp. 12193–12196, 2014.

**REACTION ENGINEERING AND CATALYSIS**

**Paper ID: ESCE137**

# MO-PROMOTED Ni/$CeO_2$ SYNTHESIZED VIA SONOCHEMICAL METHOD AS POTENTIAL CATALYST IN AQUEOUS PHASE REFORMING OF GLYCEROL FOR PRODUCTION OF 1,3-PROPANEDIOL

**Mohamad Razlan bin Md Radzi[1,2], Mohd Hizami Mohd Yusoff[1,2]*, Suzana Yusup[1,2], Mohammad Tazli bin Azizan[3]**

[1] *HICoE–Center for Biofuel and Biochemical Research, Institute of Self-Sustainable Building,* [2] *Department of Chemical Engineering, Universiti Teknologi PETRONAS, Seri Iskandar, 32610, Perak, Malaysia.*
[3] *Faculty of Chemical Engineering Technology, Universiti Malaysia Perlis, Kompleks Pusat Pengajian Jejawi 3, 02600 Arau, Perlis, Malaysia.*
*Corresponding author: hizami.yusoff@utp.edu.my

## Extended Abstract

Selection of catalyst preparation method is vital in determining the performance of the catalyst in aqueous phase reforming of glycerol. Production of glycerol to 1,3-propanediol via aqueous phase reforming specifically, requires catalysts with good physicochemical properties to ensure high yield of the targeted product. It was then discovered that sonochemical method, which utilizes ultrasonic propagation to assist in catalyst synthesis, yield catalysts with excellent physicochemical properties [1]. Further studies on sonochemical synthesis on bimetallic Ni-based catalysts has revealed that the catalyst synthesized via sonochemical method has better surface morphology, smaller particle sizes and less particle agglomeration compared to other technologies such as wet impregnation. Studies have also shown that sonochemically-synthesized catalyst are more active in aqueous phase reforming and has better yields of product compared to other synthesis [2, 3]. Inspired by the previous studies, in this research, physicochemical properties of bimetallic Mo-promoted Ni/$CeO_2$ were studied, where five catalysts were synthesized via sonochemical method with fixed 10% Ni loading and varying percentage of Mo promoter (0-7%) doped on support $CeO_2$, propagated using sonicator probe for 45 minutes via pulse method of 10s on and 10s off at 80% amplitude. Ni/$CeO_2$ catalyst combination was a staple metal-support combination in reforming technology such as steam reforming and hydrothermal processes. Mo promoter were selected due to its high Brønsted acid sites which is crucial in ensuring high selectivity of 1,3-propanediol, good product selectivity in reforming technologies, and its benefits in enhancing physicochemical properties. The resulted catalysts were then subjected to two characterization techniques, Field-Emission Scanning Electron Microscope (FESEM) and Hydrogen-Temperature Programmable Reduction ($H_2$-TPR). From the characterization, FESEM micrographs obtained revealed that catalyst prepared has good surface morphology, with all the proposed elements Ni, Ce and Mo present, with good elemental distribution and minimal particle agglomeration, benefited from the effect of ultrasonic cavitation. However, addition of Mo has also significantly increased catalyst reduction temperature from 350°C up to 700°C as observed from $H_2$-TPR reductograms, where the increase in reduction temperature leads to difficulty in catalytic reduction. This increase in reduction temperature indirectly affects its catalytic activity. Future work is suggested to further examine the physicochemical properties of the catalyst and study the performance of the catalyst in aqueous phase reforming

**Keywords:** Sonochemical synthesis; Bimetallic catalysts.

**Acknowledgment**

The authors would like to greatly acknowledge Malaysian Ministry of Higher Education (MoHE) for the conferment of HICoE award (015MA0-052) to Centre for Biofuel and Biochemical Research (HICoE-CBBR), and Centralized Analytical Lab (CAL), Universiti Teknologi PETRONAS, for the excellent catalyst characterization techniques.

## REACTION ENGINEERING AND CATALYSIS

### References

[1] M. Abdollahifar, M. Haghighi, A. A. Babaluo, and S. K. Talkhoncheh, "Sono-synthesis and characterization of bimetallic Ni–Co/Al2O3–MgO nanocatalyst: Effects of metal content on catalytic properties and activity for hydrogen production via CO2 reforming of CH4," *Ultrasonics Sonochemistry,* vol. 31, pp. 173-183, 7// 2016, doi: http://dx.doi.org/10.1016/j.ultsonch.2015.12.010.

[2] M. Ameen, M. T. Azizan, A. Ramli, S. Yusup, and M. S. Alnarabiji, "Catalytic hydrodeoxygenation of rubber seed oil over sonochemically synthesized Ni-Mo/γ-Al2O3 catalyst for green diesel production," *Ultrasonics Sonochemistry,* vol. 51, pp. 90-102, 2019/03/01/ 2019, doi: https://doi.org/10.1016/j.ultsonch.2018.10.011.

[3] M. I. Shahbudin *et al*., "Liquid value-added chemicals production from aqueous phase reforming of sorbitol and glycerol over sonosynthesized Ni-based catalyst," *Journal of Environmental Chemical Engineering*, vol. 9, no. 4, p. 105766, 2021/08/01/ 2021, doi: https://doi.org/10.1016/j.jece.2021.105766.

**REACTION ENGINEERING AND CATALYSIS**

**Paper ID: ESCE142**

# INTEGRATING PHOTOCATALYSIS AND MICROFILTRATION FOR METHYLENE BLUE DEGRADATION: KINETIC AND COST ESTIMATION

**Duc Chinh Pham[1], Thi Mai Duyen Cao[1], Manh Cuong Nguyen[1], Thanh Dong Nguyen[2], Thi Thu Trang Nguyen[2]***

[1] *Institute for R&D of Natural Products, Hanoi University of Science and Technology – 1, Dai Co Viet, Hanoi, 10999, Vietnam.*
[2] *Institute of Environmental Technology, Vietnam Academy of Science and Technology - 18 Hoang Quoc Viet, Hanoi, 10000, Vietnam.*
*Corresponding author: thutrangnguyen1210@gmail.com

## Extended Abstract

### Introduction

Advanced oxidation process using $TiO_2$ photocatalysts has emerged as a potential technique for the treatment of polluted organic compounds [1-3]. The enhance of the reaction rate of decomposition of toxic organic compounds has attracted many researchers. Recently, combined processes such as $UV/TiO_2/H_2O_2$ and $UV/O_3/H_2O_2$ have shown potential for enhancing the treatment efficiency of toxic organic compounds compared with single $UV/TiO_2$ processes [4-5]. However, in these studies, the efficiency of the $UV/TiO_2/H_2O_2$ process has not been considered in-sync with the activity of the microfiltration membrane process for catalytic separation. Therefore, the integrated study of $UV/TiO_2/H_2O_2$ process and microfiltration (MF) is essential for practical applications. Besides operation parameters, economics is a crucial factor that needs attention in exploring and developing the wastewater treatment system to an industrial scale.

The objective of this study was to evaluate the efficiency of methylene blue (MB) degradation by an integrated system of $UV/TiO_2/H_2O_2$ and a cross-flow microfiltration membrane in the lab scale. Methylene blue degradation kinetics, cake layer formation on the membrane surface, and the energy consumption of system were discussed. Finally, the capital cost and operating costs of the photocatalytic membrane reactor for MB degradation were evaluated and were compared with the UV only, $UV/H_2O_2$, and $UV/TiO_2$- MF.

### Material and methods

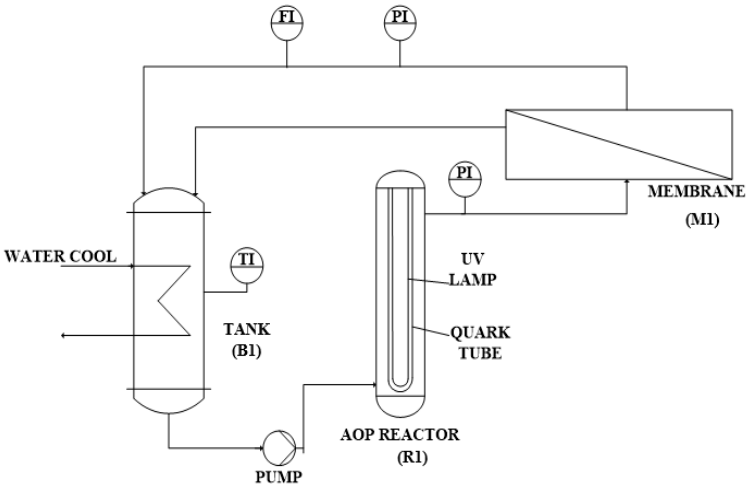


Fig. 1: Schematic of experiment.

**REACTION ENGINEERING AND CATALYSIS**

The experimental scheme was shown in Figure 1. The reaction mixture (methylene blue, $TiO_2$, and $H_2O_2$) was pumpedpassed from the container (B1) through the reaction vessel (R1) and into the microfiltration membrane module (M1). The retentate flow and permeate flow of membrane module are were recirculated back to the feed tank (B1). Degradation of methylene blue solution was checked by UV-VIS measurements (AL-800, Germany) at a wavelength of 664 nm. The degradation kinetics of methylene blue can be described by the pseudo-first-order model.

The capital cost, operating costs and specific wastewater treament of the photocatalytic membrane reactor for methylene blue degradation were calculated according Mahamuni et al. and Samhaber et al. [6-8].

**Results and discussion**

Operational parameters and MB degradation test results by advanced oxidation processes based on UV/$TiO_2$/$H_2O_2$ and MF were presented in Table 1.

Table 1: Operation conditions and the results of MB degradation test.

| Process | AOPs conditions | MF | Results |
|---|---|---|---|
| UV only (Exp. 1) | - | - | kapp= 0.0008 $min^{-1}$; $R^2$= 0.997<br>EE/O = 559.64 kWh/$m^3$.oder |
| UV/$H_2O_2$ (Exp. 2) | $H_2O_2$ conc.: 0.025 mol/l | - | kapp=0.0087 $min^{-1}$; $R^2$= 0.996<br>EE/O = 55.15 kWh/$m^3$.oder |
| UV/ $TiO_2$ (Exp. 3) | $TiO_2$ conc.: 0.5 g/l | ΔP = 2.5 atm,<br>Pore-size: 0.2 µm<br>Membrane area: 0.0048$m^2$ | kapp= 0.0052 $min^{-1}$; $R^2$=0.999<br>J= 48.1 l/$m^2$.h<br>EE/O = 92.25 kWh/$m^3$.oder |
| UV/ $TiO_2$ (Exp. 4) | $TiO_2$ conc.: 0.3 g/l<br>$H_2O_2$ conc.: 0.005 mol/l | | kapp =0.0105 $min^{-1}$; $R^2$= 0.998<br>J= 66.3 l/$m^2$.h<br>EE/O = 45.69 kWh/$m^3$.oder |

(PUV= 25 W, V= 2l, flow rate= 1.5 l/min membrane at adjust pH)

In addition, cost estimation of the treatment of MB by different AOP processes was carried out. As a result, specific MB treatment costs by UV, UV/$H_2O_2$ and UV/$TiO_2$-MF, and UV/$TiO_2$/$H_2O_2$-MF processes were \$91.19, \$9.77, \$12.86, and \$8.21 for 1 $m^3$, respectively. Although the treatment costs were relatively high, the UV/$TiO_2$/$H_2O_2$-MF process was at the experimental stage in the laboratory scale; thus, the operation parameters can be improved and optimized to compete with commercially available processes on an industrial scale.

**Conclusion**

UV/$TiO_2$/$H_2O_2$- microfiltration process allows for the treatment of methylene blue solution. The specific cost to treat 1$m^3$ of methylene blue solution ($C_0$= 20 mg/l) is \$8.51, 36.16%, and 15.97% lower compared to UV/$TiO_2$-MF and UV/$H_2O_2$ processes. These results are the basis for the experimental design of wastewater treatment systems at the pilot scale.

**Keywords:** Photocatalytic membrane reactor; Cost estimation; Wasterwater, methylene blue; Degradation.

**Acknowledgment**

This study was supported by the Ministry of Science and Technology (MOST) of Vietnam through Vietnam - Germany Cooperation Research Project coded NĐT.59.GER/19.

**References**

[1] Rochetto U.L., Tomaz E. (2015) Degradation of volatile organic compounds in the gas phase by heterogeneous photocatalysis with titanium dioxide/ultraviolet light, Journal of the Air & Waste Management Association vol 65 (7).
[2] Chiou C.H, Wu C.Y., Juang R.S. (2018) Influence of operating parameters on photocatalytic degradation of phenol in UV/$TiO_2$ process, *Chemical Engineering Journ*al vol 139, pp 322–329.

## REACTION ENGINEERING AND CATALYSIS

[3] Al- Mamun M.R., Kader S., Islam M.S., Khan M.Z.H. (2019) Photocatalytic activity improvement and application of UV-TiO2 photocatalysis in textile wastewater treatment: A review, *Journal of Environmental Chemical Engineering*, vol 7 (5).
[4] Li X., Chen C., Zhao J. (2001) Mechanism of photodecomposition of H2O2 on TiO2 surfaces under visible light irradiation, Langmuir", vol 17, pp 4118-4122.
[5] Saquib M., Tariq M.A., Haque M.M. (2008) Muneer M., Photocatalytic degradation of disperse blue 1 using UV/TiO2/H2O2 process, Journal of Environmental Management, vol 88, pp 300–306.
[6] Mahamuni N.N, Adewuyi Y.G. (2010) Advanced oxidation processes (AOPs) involving ultrasound for waste water treatment: A review with emphasis on cost estimation, Ultrasonics Sonochemistry vol 17, pp 990–1003.
[7] Samhaber W.M, Tan N.M. (2019), Chapter 11: Economical Aspects in Photocatalytic Membrane Reactors, Elselvier.
[8] Rani C.N, Karthikeyan S. (2021), Synergic effects on degradation of a mixture of polycyclic aromatic hydrocarbons in a UV slurry photocatalytic membrane reactor and its cost estimation, Chemical Engineering and Processing - Process Intensification, vol 159, 2021.

**REACTION ENGINEERING AND CATALYSIS**

**Paper ID: ESCE146**

# PERFORMANCE OF Ni-Sr/MgO-$ZrO_2$ BIMETALLIC CATALYST FOR $CO_2$ REFORMING OF METHANE: EFFECT OF Sr ADDITION

**A. S. Farooqi[1], M. Yusuf[1], NA.M. Zabidi[2], M.U. Mushtaq[4], B. Abdullah[1,3]***

[1] *Chemical Engineering Department,* [2] *Fundamental and Applied Sciences Department,*
[3] *Centre of Contaminant Control and Utilization (CenCoU), Institute of Contaminant Management for Oil and Gas, Universiti Teknologi PETRONAS, Bandar Seri Iskandar, 32610 Perak, Malaysia.*
[4] *Department of Chemical Engineering, Wah Engineering College, University of Wah, Quaid Avenue, 47040, Wah Cantt, Pakistan.*
*Corresponding author: bawadi_abdullah@utp.edu.my

## Extended Abstract

$CO_2$ (CRM) is emerging as an enticing research area due to the crucial need to mitigate global warming and offers as an alternative energy resource. However, there has been a serious challenge to the scale-up of the process to commercial production due to the catalyst deactivation. In the present study, the effect of strontium on activity and stability of mixed oxide MgO-$ZrO_2$ supported Ni-based catalysts has been investigated. The $ZrO_2$- MgO mixed oxide support was prepared by coprecipitation method and subsequently impregnated with Ni and Strontium metal. The Ni-Sr/MgO-$ZrO_2$ catalysts showed an improved performance in the CRM reaction in terms of activity and stability compared to the Ni/$ZrO_2$-MgO. The findings indicated a high level of catalytic activity and stability of synthesized catalysts for CRM. Combining $ZrO_2$-MgO binary oxide would combine many peculiar properties that are crucial for a robust catalyst formulation. MgO has high thermal stability and pronounced surface basicity, and $ZrO_2$ is characterized by substantial oxygen mobility which plays an essential role in the oxidation type of reactions [1]. The prepared catalysts were characterized by X-ray diffraction (XRD), Brunauer-Emmett-Teller (BET) analysis, temperature programmed reduction (TPR), temperature programmed desorption ($CO_2$-TPD) and field emission scanning microscopy (FESEM) techniques. BET results revealed that the addition of $La_2O_3$ increases the surface area of the synthesized catalyst due to the high surface area of the support. TPR analysis showed reduction in chemical interaction between nickel and support resulting in an increase in reducibility and higher dispersion of nickel [2]. The characterization of the spent Ni/MgO-$ZrO_2$ catalyst using Raman spectroscopy, Transmission Electron Microscopy (TEM) and FESEM and analysis revealed the formation of amorphous carbon that could be responsible for its fast deactivation.

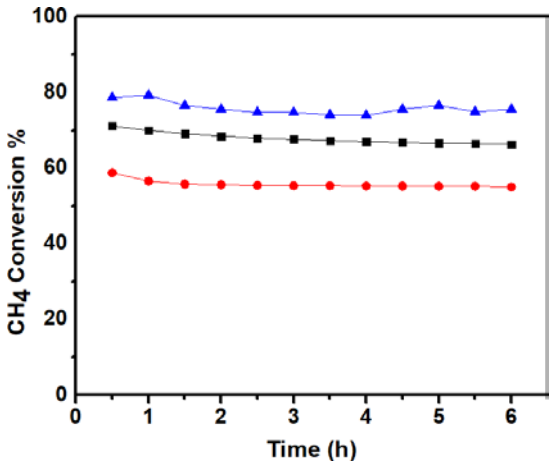


Fig. 1: $CH_4$ conversion in CRM. Symbols represent: (▲) Ni-3%Sr/$ZrO_2$-MgO, Ni-1%Sr/$ZrO_2$-MgO (■) and Ni/$ZrO_2$-MgO (●).

**REACTION ENGINEERING AND CATALYSIS**

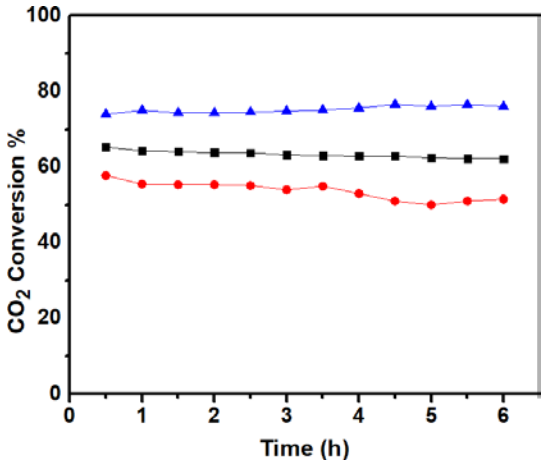


Fig. 2: $CO_2$ conversion in CRM Symbols represent: (▲) Ni-3%Sr/$ZrO_2$-MgO, Ni-1%Sr/$ZrO_2$-MgO (■) and Ni/$ZrO_2$-MgO (●).

The CRM reaction was performed in a tubular furnace reactor at 1073.15 K, 1 atm and a $CH_4/CO_2/N_2$ ratio of 1:1:1. The Ni-3%Sr/$ZrO_2$-MgO was found to be the most appropriate choice for CRM which depicts higher conversion (80.5% for $CH_4$ conversion and 81.0% for $CO_2$ conversion) as shown in Figure 1 and Figure 2. using an equimolar feed ratio by means of strong metal-support interaction and high resistance to coke formation. According to [3], higher stability of MgO supported Ni catalysts is due to suppressing coke formation by enhancing $CO_2$ concentration at the basic La sites and thus accelerating the Boudouard reaction towards CO.

**Keywords:** Catalyst; Sol-gel; Reforming; Dispersion; Carbon resistance.

**Acknowledgment**

The authors would like to thank Yayasan Universiti Teknologi PETRONAS (YUTP), Malaysia for providing financial assistance under grant no: 015LC0-343 and Universiti Teknologi PETRONAS for providing the required facilities to conduct this research work.

**References**

[1] Park J. E., Koo K. Y., Yoon W. L. (2015) Syngas Production by Combined Steam and $CO_2$ Reforming of Coke Oven Gas over Highly Sinter-Stable La-Promoted Ni/$MgAl_2O_4$ Catalyst. Int. J. Hydrogen Energy 40:909-917.
[2] Tao W. (2014). Syngas Production by $CO_2$ Reforming of Coke Oven Gas over Ni/$La_2O_3$-$ZrO_2$ Catalysts. Int. J. Hydrogen Energy 39:650–658.
[3] Rezaei. M., Bai. P., Liu. X., and Yan Z. F. (2008) $CO_2$ Reforming of $CH_4$ over Nanocrystalline Zirconia-Supported Nickel Catalysts. Appl. Catal. B Environ 77:346-354.

**REACTION ENGINEERING AND CATALYSIS**

**Paper ID: ESCE159**

# RECENT CATALYTIC SYNTHESIS OF 5-HYDROXYMETHYLFURFURAL (HMF) FROM CARBOHYDRATES WITH PROCESS DEVELOPMENT ANALYSIS – A REVIEW

**M.A.A. Abdul Rani[1], N.A. Karim[1] *, S.K. Kamarudin[1,2]**

[1] *Fuel Cell Institute*, [2] *Department of Chemical Engineering, Universiti Kebangsaan Malaysia, 43600 Bangi, Selangor, Malaysia.*
*Corresponding author: nabila.akarim@ukm.edu.my

## Extended Abstract

5-hydroxymethylfurfural (HMF), is one of the leading versatile biomass-derived chemicals as it is a multi-functional compound, and it is also a promising intermediate compound that is beneficial in numerous chemical and fuel applications, including pharmaceuticals, solvents, thermo-resistant polymers, surfactants, biofuel precursor, fuel additives, and other organic intermediates. The need for finding new strategies for alternative renewable energy resources has increased due to reduce the dependency on fossil fuel and to seek economic and environmental-friendly strategies in providing energy to the world. HMF can be synthesized from the carbohydrates, such as fructose, glucose, cellulose, and lignocellulosic material. High substrate costs, the use of costly solvents, and low reaction yields have prevented HMF synthesis from being commercially viable. This review provides the previous studies on the development of high yield and selectivity of HMF from technical and economic perspectives. The paper highlighted a few significant parameters for the synthesis of HMF in lab-scale and through the development of process modeling using simulation software such as ASPEN Plus to perform the techno-economic analysis (TEA) which analyzed the economic feasibility of the developed production process. The techno-economic analysis can estimate the capital cost investment needed, including the cost of feedstock, catalyst, and equipment, and the minimum selling price (MSP) of the final products. HMF is less economically feasible due to higher operational cost from higher cost of fructose feedstock. By studying this analysis, the overall cost for HMF production can be minimized and make it more economically competitive with current commercial production. Besides, to make production of HMF more cost-effective, more research into alternative lignocellulosic feedstocks, and the development of novel catalytic systems may be needed.

**Keywords:** 5-Hydroxymethylfurfural (HMF); Catalyst; Carbohydrates; Process modeling; Technoeconomic analysis (TEA).

### Acknowledgment

The authors gratefully acknowledge the financial support for this work by the Ministry of Higher Education under FRGS/1/2019/TK02/UKM/02/4.

### References

[1] Kazi F. K. et al. (2011) Techno-Economic Analysis of Dimethylfuran (DMF) and Hydroxymethylfurfural (HMF) Production from Pure Fructose in Catalytic Processes. Chemical Engineering Journal. 169:329-338.
[2] Motagamwala A. H. et al. (2019) Solvent System for Effective Near-Term Production of Hydroxymethylfurfural (HMF) with Potential for Long-Term Process Improvement. J. Energy and Environmental. 12:2212-2222.
[3] Overton J. C. et al. (2020) Single-Vessel Synthesis of 5-Hydroxymethylfurfural (HMF) from Milled Corn. J. ACS Sustainable Chemistry and Engineering. 8:18-21.
[4] Yan P. et al. (2020) Unlocking Biomass Energy: Continuous High-Yield Production of 5-Hydroxymethylfurfural in Water. J. Green Chemistry. 22:5274-5284.

**REACTION ENGINEERING AND CATALYSIS**

**Paper ID: ESCE168**

# LOW THERMAL OXIDATION OF GASEOUS TOLUENE OVER Cu/Ce SINGLE-DOPED AND CO-DOPED OMS-2 ON DIFFERENT SYNTHETIC ROUTES

**K. Wantala[1]*, F.C.L. See Go[2], V. C.C. Garcia[2], R.R.M. Abarca[2], M. D.G. de Luna[3], P. Chirawatkul[4], N. Chanlek[4], P. Kidkhunthod[4]**

[1] *Department of Chemical Engineering, Faculty of Engineering, Khon Kaen University, Khon Kaen 40002, Thailand.*
[2] *Environmental Engineering Program, National Graduate School of Engineering,* [3] *Department of Chemical Engineering, University of the Philippines Diliman, Quezon City 1101, Philippines.*
[4] *Synchrotron Light Research Institute (Public Organization), Nakhon Ratchasima 30000, Thailand.*
*Corresponding author: kitirote@kku.ac.th

## Extended Abstract

Volatile organic compounds (VOC) are insidious gaseous pollutants that emanate from solid/liquid fossil fuels and various household products such as paints, adhesives, coatings, fragrances, inks, and cigarette smoke. VOC concentrations ranging from 2 – 164 µg $m^{-3}$ have been measured from indoor areas such as houses, classrooms, shopping complexes, and offices [1]. Chronic exposure to VOCs even at low concentrations has been linked to liver, kidney, and lung damage [2]. Recently, doping metal ions to the K-OMS-2 framework have resulted in enhanced cryptomelane's thermal stability and catalytic activity towards certain VOCs. Cations such as $Cu^{2+}$, $Zn^{2+}$, $Ni^{2+}$, $Co^{2+}$, $Al^{3+}$, $Mg^{2+}$, $Fe^{3+}$, $Ti^{4+}$, $Ce^{4+}$, $Zr^{4+}$, and $V^{5+}$ may attach to the K-OMS-2 surface, incorporate into its framework, or enter its tunnel network. [3]. One study incorporated $Cu^{2+}$ into the K-OMS-2 framework resulting in high toluene removal efficiencies at low oxidation temperatures [4]. Another study found that active sites on the Cu-doped K-OMS-2 were more rapidly regenerated than undoped K-OMS-2 resulting in consistently high VOC removal efficiencies over a 10.5 h period [5]. Meanwhile, Ce incorporated into the K-OMS-2 tunnel structure improved benzene oxidation due to enhanced lattice oxygen mobility [6]. Unfortunately, Ce replacement of Mn in K-OMS-2 reduced the overall catalytic activity of cryptomelane signifying the importance of the doping procedure. Doping is implemented either via ex-situ and in-situ routes where dopants are added after and during cryptomelane formation, respectively. Ex-situ methods such as the wet impregnation route incorporate dopants by replacing Mn in the K-OMS-2 framework, while in-situ methods incorporate the metal dopant along with $K^+$ within the tunnel structure [6].

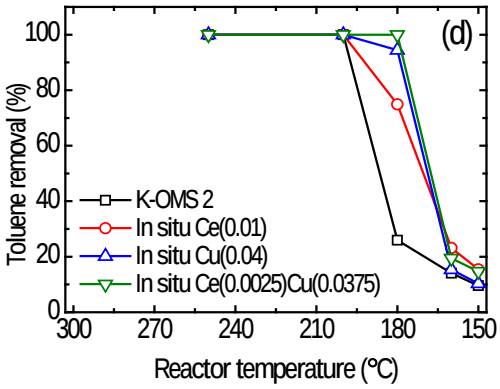


Fig. 1: Thermal catalytic oxidation profile of toluene by single doping and co-doping of Ce and Cu.

## REACTION ENGINEERING AND CATALYSIS

In this study, cryptomelane-type manganese oxide (K-OMS-2) was used as a catalyst for the thermal oxidation of toluene, a toxic volatile organic compound emitted from solid/liquid hydrocarbons. The catalyst was synthesized via the hydrothermal route and doped with Cu, Ce, and co-doped with the same metals by ex-situ and in-situ methods. The effects of dopant type, dopant concentration, and dopant impregnation method on the thermal catalytic activity of K-OMS-2 were examined. Initially, 1%, 2%, and 4% by mole Cu or Ce were incorporated by wet impregnation to the hydrothermally synthesized K-OMS-2. Gaseous toluene was made to react with the doped catalysts in a packed bed reactor attached to gas chromatography equipment with a thermal conductivity detector to measure the amount of unreacted toluene.

Results showed K-OMS-2 doped with 4% by mole Cu and 1% by mole Ce gave excellent thermal catalytic efficiency results. Meanwhile, K-OMS-2 co-doped with Ce and Cu with a mole ratio of 0.25:3.75 per 100 moles of K-OMS-2 gave the best catalytic activity. Comparing K-OMS-2 doped with the same metal ratios, in situ doped catalysts led to higher toluene removal percentages. Fig. 1 shows that co-doping of Ce and Cu in K-OMS-2 by in situ technique gives the highest toluene decomposition at the lowest reaction temperature. Meanwhile, the 72-h stability test showed that the optimum co-doped catalysts are capable of entirely oxidizing toluene even after prolonged and continuous use. Catalyst performance on toluene degradation were validated by X-ray diffraction, X-ray photoelectron spectroscopy, X-ray absorption spectroscopy, Brunauer-Emmett-Teller surface area analysis, and thermal gravimetric analysis. In conclusion, the co-doped catalysts between Ce and Cu give the higher activity than single doped catalysts in both of ex situ and in situ catalyst preparations.

**Keywords:** Advanced oxidation process; Cryptomelane; Heterogeneous catalysis; Indoor air purification; KOMS-2; Volatile organic compounds.

### Acknowledgment

The authors are grateful to the financial support from the Research Center for Environmental and Hazardous Substance Management (EHSM), and the Research and Graduate Studies, Khon Kaen University, Thailand and the Department of Science and Technology, Philippines. In addition, the authors would like to express their appreciation to the Synchrotron Light Research Institute (Public Organization), Thailand for XANES and XPS beamtimes for their helpful support in terms of scientific facilities.

### References

[1] González-Martín J., Kraakman N.J.R., Pérez C., Lebrero R., Muñoz R. (2021) A state–of–the-art review on indoor air pollution and strategies for indoor air pollution control, Chemosphere. 262.
[2] Soltanpour Z., Mohammadian Y., Fakhri Y. (2021) The concentration of benzene, toluene, ethylbenzene, and xylene in ambient air of the gas stations in Iran: A systematic review and probabilistic health risk assessment, Toxicol. Ind. Health. 37, 134–141.
[3] Zhang J., Tse K., Wong M., Zhang Y., Zhu J. (2016) A brief review of co-doping, Front. Phys. 11.
[4] Kaewbuddee C., Chirawatkul P., Kamonsuangkasem K., Chanlek N., Wantala K. (2021) Structural characterizations of copper incorporated manganese oxide OMS-2 material and its efficiencies on toluene oxidation, Chem. Eng. Commun. 1–17.
[5] Yang Y., Huang J., Zhang S., Wang S., Deng S., Wang B., Yu G. (2014) Catalytic removal of gaseous HCBz on Cu doped OMS: Effect of Cu location on catalytic performance, Appl. Catal. B Environ. 150–151,167–178.
[6] Liu Y., Hou J. (2019) Ce ion substitution position effect on catalytic activity of OMS-2 for benzene oxidation, Mater. Res. Bull. 118, 110497.

**REACTION ENGINEERING AND CATALYSIS**

**Paper ID: ESCE205**

# HYDROGEN PRODUCTION VIA GLYCEROL DRY REFORMING REACTION OVER Ru-Ni-SUPPORTED ON EXTRACTED ALUMINA FROM ALUMINUM DROSS: A KINETIC EVALUATION

**N. A. Roslan[1], S. Z. Abidin[1,2]*, S. Y. Chin[1,2], Y. H. Taufiq-Yap[3,4]**

[1] *Department of Chemical Engineering, College of Engineering,* [2] *Centre of Excellence for Advanced Research in Fluid Flow (CARIFF), Universiti Malaysia Pahang, 26300 Gambang, Pahang, Malaysia.*
[3] *Catalysis Science and Technology Research Centre (PutraCAT), Faculty of Science, Universiti Putra Malaysia, 43400, UPM, Serdang, Selangor, Malaysia.*
[4] *Chancellery Office, Universiti Malaysia Sabah, 88400, Kota Kinabalu, Sabah, Malaysia.*
*Corresponding author: sumaiya@ump.edu.my

## Extended Abstract

More than one million tons of aluminum dross as a hazardous waste are produced by aluminum manufacturers per year throughout the world, which imposes high disposal costs and serious environmental problems. Aluminum dross was categorized into two type which are primary and secondary dross. Primary dross contains approximately >50% of aluminum metal and small amounts of oxidic and salt constituents in the form of clump [1], whereas secondary dross contains about 15-30% of aluminum metal and large amounts of oxidic and salt compounds [2]. Primary dross is generally returned to smelter for the purpose of recycling of remaining aluminum metal. Usually, secondary dross is disposed off in landfill sites which could result in leaching of toxic metal ions into ground water causing serious pollution problems and more importantly loss of valued metal [3]. Thus, by finding an appropriate recycling approaches, the volume of wastes, corresponding disposal cost, and the pollution of environment could be diminished. Also, such promising approaches can result in the conservation of natural sources and economic benefits. Recently, the recovery of high value-added products from aluminum dross such as γ-alumina has been explored by the researchers worldwide. γ-alumina was widely applied in various industry and commonly used as a catalyst support in the reforming process due to its high surface area and good metal-support interaction [4].

In recent times, glycerol has been employed as feedstock for the production of syngas ($H_2$ and CO) with $H_2$ as its main constituent in dry reforming reaction. The utilization of carbon dioxide as a greenhouse gas in this reaction has always recognized as one of the most attractive alternatives to produce syngas [5]. Ni-based catalysts are widely used in reforming reactions due to their low price and comparable activity with the noble metal catalysts [6]. However, the major drawback with Ni-based catalysts is due to its severe carbon deposition leading to deactivation of the catalyst [7]. Commonly, Ni-based catalyst was incorporated with suitable promoters and supports to improve the catalytic activity and suppress the carbon formation. Thus, the selection of catalyst support was very crucial to ensure the catalyst stability during the reaction. Extracted γ-alumina (EGA) from aluminum dross has become one of the potentials supports for Ni-based catalyst to obtain a better catalytic performance in glycerol dry reforming (GDR) reaction.

Considering the above literature, kinetic studies is an indispensable step to fully understand the reaction mechanism and catalyst behavior for heterogeneous catalyst involved during the reforming reaction. In the present study, there are no studies in regard to the kinetics and mechanistic over EA supported Ni catalyst for the GDR reaction. Moreover, it was found that operating parameter such as temperature may manipulate the catalytic performance and reforming mechanism, especially in the rate-determining step (RDS) determination [25]. Therefore, the main idea of our work is to evaluate the relationship between operating parameters, such as reforming temperature (873 - 1173 K) and reactant partial pressure (i.e. stoichiometric feed ratio of 0.5-5) on catalytic performance and coke formation, as well as to study the kinetics and mechanism of 3%Ru-15%Ni/EGA3 catalyst on the GDR reaction.

## REACTION ENGINEERING AND CATALYSIS

The performance of Nickel (Ni) supported on extracted alumina (EA) under the influence of reaction temperature (873 – 1173 K) and reactant partial pressure (i.e. 1-5 ratio) for GDR reaction was executed by using a tubular fixed-bed reactor. 3%Ru-15%Ni/EGA3 exhibited great catalytic performance (i.e. 92% glycerol conversion), credited to the well dispersion of Ni within pore EA, strong metal-support interaction, and EA confinement ability. Based on Langmuir-Hinshelwood kinetic analysis, the dissociative adsorption of both reactants on a single Ni active site was selected for this study. The lower value of activation energy (28.9 kJ $mol^{-1}$) suggested that Ni particles were finely scattered on the EA surface. Regardless of carbon types, the amount of coke accumulated on the spent 3%Ru-15%Ni/EGA3 within 8 h of GDR reaction was inhibited due to fine Ni distribution inside EA structure, as well as lessened with the raise of reforming temperature from 873 to 1173 K due to improvement in reverse Boudouard reaction. Figure 1 and 2 represents the data collected from the current study.

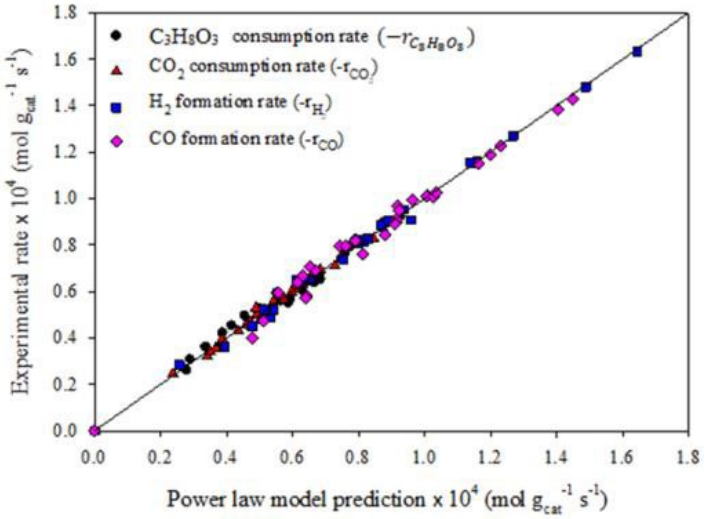


Fig. 1: Parity plot of predicted consumption and formation rates obtained from power law model versus experimental rate.

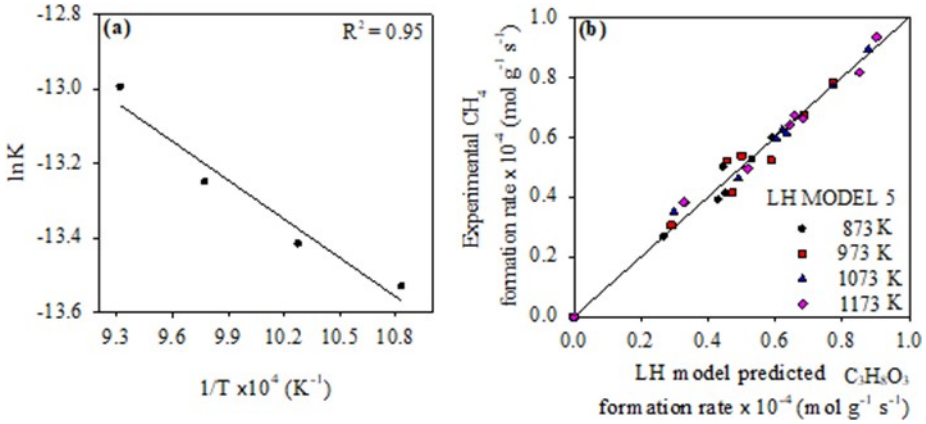


Fig. 2: (a) The estimation of activation energy from LH Model 5 and (b) parity plot for $C_3H_8O_3$ consumption rate by LH model versus experimental rate

**Keywords:** Aluminum dross; Alumina; Glycerol dry reforming; Syngas; Kinetic and Mechanism.

**Acknowledgment**

The authors would like to acknowledge the Ministry of Higher Education, Malaysia for awarding the FRGS research grant vote RDU190197 (FRGS/1/2018/TK02/UMP/02/12) and Universiti Malaysia Pahang (PGRS1903121 and RDU1803118) for financial support.

## REACTION ENGINEERING AND CATALYSIS

### References

[1] Mahinroosta M., ALlahverdi A. (2018). J Environ Manage 223: 452-468.
[2] Saravanakumar R., Ramachandran K., Laly L. G., Ananthapadmanabhan P. V., Yugeswaran S. (2018). Waste Manage 77: 565-575.
[3] Calder G. V., Stark T. D. (2010). J. Hazard. Toxic Radioact. Waste 14: 258-265.
[4] Zhang Z., Wei T., Chen G., Li C., Dong D., Wu W., Liu Q., Hu X. (2019). Fuel 250: 176-193.
[5] Dang C., Wu S., Yang G., Cao Y., Wang H., Peng F., Yu H. (2020). J Energy Chem 43: 90-97.
[6] Wang X., Li M., Wang M., Wang H., Li S., Wang S., Ma X. (2009). Fuel 88: 2148-2153.
[7] Harun N., Abidin S. Z., Osazuwa O U., Taufiq-Yap Y. H., Azizan M T. (2019). Int J of Hydrogen Energy 44: 213-225.

**RENEWABLE ENERGY AND BIOFUELS**

**Paper ID: ESCE043**

# AN OVERVIEW ON THE TREATMENT PROCESSES OF POULTRY MANURE

**M. D. Manogaran[1], M. R. Shamsuddin[1,2], M H Mohd Yusoff[1,2], M S Md Zain[3], M Lay[4]**

[1] *Chemical Engineering Department,* [2] *Centre for Biofuel and Biochemical Research (CBBR), Institute of Sustainable Living, Universiti Teknologi PETRONAS, 32610 Seri Iskandar, Perak, Malaysia.*
[3] *PETRONAS Research Sdn Bhd, Lot 3288 & 3289, Off Jalan Ayer Itam, Kawasan Institusi Bangi, 43000, Kajang, Selangor, Malaysia.*
[4] *School of Engineering, Faculty of Science and Engineering, University of Waikato, Private Bag 3105, Hamilton 3240, New Zealand.*
*Corresponding author: mrashids@utp.edu.my

## Extended Abstract

The poultry industry is a rapidly growing industry driven by consumer demand. Poultry industry generates large quantities of solid waste in the form of manure, feathers, hatchery, bedding materials and abattoir waste [1]. The manure produced is often used raw as fertilizer without any pre-treatment hence, it could become a vector for pathogens and flies as well as contributing to odour problems [2]. Treatment methods using pesticides, microorganisms and daily collection and disposal are normally adopted by the farmers. Other techniques such as composting [3], pyrolysis [4], gasification [5] and anaerobic digestion [6] in particular, are drawing interest due to their ability to convert "waste-to-wealth". In 2012, 38,959 tons of poultry manure was produced on average per day in Malaysia which could have generated 8.95 million $m^3$ biogas on a daily basis through anaerobic digestion [7] which is the equivalent of up to 323.41 TJ of heat and 89.91 GWh of electricity. This fruitful finding depicts the potential of harnessing renewable, clean energy in conjunction of energy security efforts. This paper provides an overview on the technical and practical aspects of the techniques above in terms of ease of operation, performance and limitations as well as the ability of each approach to yield an output while imposing the least burden on the environment.

**Keywords:** Poultry manure; Anaerobic digestion; Composting; Pyrolysis; Gasification.

### Acknowledgement

The authors would like to acknowledge the Ministry of Science, Technology and Innovation Malaysia, for funding the project through grant Fundamental Research Grant Scheme (FRGS) 015MA0-093. The authors also recognize HICoE's support to Centre for Biofuel and Biochemical Research (CBBR) from the Ministry of Higher Education, Malaysia.

### References

[1] P. Singh, T. Mondal, R. Sharma, N. Mahalakshmi, and M. Gupta, "Poultry waste management," *Int J Curr Microbiol App Sci*, vol. 7, no. 8, pp. 694-700, 2018.
[2] A. Bayrakdar, R. Ö. Sürmeli, and B. Çalli, "Dry anaerobic digestion of chicken manure coupled with membrane separation of ammonia," *Bioresource Technology*, vol. 244, pp. 816-823, 2017.
[3] J. Li *et al.*, "Succession of fungal dynamics and their influence on physicochemical parameters during pig manure composting employing with pine leaf biochar," *Bioresource Technology*, vol. 297, p. 122377, 2020/02/01.
[4] X. Hu and M. Gholizadeh, "Biomass pyrolysis: A review of the process development and challenges from initialresearches up to the commercialisation stage," *Journal of Energy Chemistry*, vol. 39, pp. 109-143, 2019/12/01.
[5] I. Janajreh, I. Adeyemi, S. S. Raza, and C. Ghenai, "A review of recent developments and future prospects in gasification systems and their modeling," *Renewable and Sustainable Energy Reviews*, vol. 138, p. 110505, 2021/03/01.
[6] M. Pöschl, S. Ward, and P. Owende, "Evaluation of energy efficiency of various biogas production and utilization pathways," *Applied Energy*, vol. 87, no. 11, pp. 3305-3321, 2010/11/01.
[7] P. Abdeshahian, J. S. Lim, W. S. Ho, H. Hashim, and C. T. Lee, "Potential of biogas production from farm animal waste in Malaysia," *Renewable and Sustainable Energy Reviews*, vol. 60, pp. 714-723, 2016/07/01.

**RENEWABLE ENERGY AND BIOFUELS**

**Paper ID: ESCE074**

# HYDRODEOXYGENATION OF OLEIC ACID FOR EFFECTIVE RENEWABLE DIESEL PRODUCTION USING ZEOLITE-BASED CATALYSTS

**Nur Azreena[1,3,7]*, H. L. N. Lau[2], N. Asikin-Mijan[6], M.A. Hassan[5], Saiman Mohd Izham[3,4], E. Kennedy[7], M. Stokenhuber[7] and Y. H. Taufiq-Yap[3,8]**

[1] *Biomass Technology Unit,* [2] *Energy and environment Unit, Engineering and Processing Division, Malaysian Palm Oil Board, No 6, Persiaran Institusi, 43000 Kajang, Selangor.*
[3] *Catalysis Science and Technology Research Centre, Faculty of Science,* [4] *Department of Chemistry, Faculty of Science,* [5] *Department of Bioprocess Technology, Faculty of Biotechnology and Biomolecular Sciences, Universiti Putra Malaysia, 43400 Serdang, Selangor, Malaysia.*
[6] *Department of Chemical Sciences, Faculty of Science and Technology, Universiti Kebangsaan Malaysia, 43600 UKM Bangi, Selangor Darul Ehsan, Malaysia.*
[7] *Priority Research Centre for Energy, School of Engineering, Faculty of Engineering and Built Environment, The University of Newcastle, Callaghan, NSW 2308, Australia.*
[8] *Faculty of Science and Natural Resources, Universiti Malaysia Sabah, 88400, Kota Kinabalu, Sabah.*
*Corresponding author: azreena@mpob.gov.my

## Extended Abstract

The use of edible oils as an alternative green fuel source for vehicles has sparked debates about the food supply's sustainability, particularly in third-world countries [1]. Green diesel, which is made from vegetable oils or animal fats, is gaining more popularity than other biofuels owing to its higher calorific value, cetane index, and superior storage stability [2]. This study investigates the hydrodeoxygenation (HDO) reaction of oleic acid (OA), which is abundant in palm oil and serves as a model compound for the production of renewable diesel. The HZSM5 and zeolite beta catalysts' efficiency in preferring diesel hydrocarbons was determined. The catalysts were prepared by wet impregnation and their physiochemical properties were determined using X-ray diffraction (XRD), scanning electron microscopy (SEM), temperature-programmed desorption with $NH_3$ probe molecules (TPD-$NH_3$), and Brunauer-Emmet-Teller analysis (BET). HZSM5 and zeolite beta have a high crystalline phase of 24.6 and 84.7 nm, respectively, as determined by XRD. BET analysis revealed that zeolite beta catalysts have a greater surface area (648.0 $m^2/g$) than HZSM5 (464.9 $m^2/g$), but no significant differences in pore size or volume. TPD-$NH_3$ analysis revealed that zeolite beta had excellent strong acid sites for HDO to occur, with a desorption peak of 2883.2 mol/g representing strong acidic sites, whereas HZSM5 had the highest desorption peak of 1377 mol/g. The optimal conditions for both catalysts were 350 °C, 4 MPa hydrogen pressure, and 5wt.% catalyst loading over a 2h reaction time. As a result, the zeolite beta catalysed HDO pathway demonstrated a higher selectivity for diesel (77%) than the HZSM5 catalysed HDO pathway (70%).

**Keywords:** Biofuel; Diesel; Zeolite beta; Hydrocarbon; Hydrodeoxygenation; HZSM5; Oleic acid.

### Acknowledgment

The authors thank the Director-General of MPOB and UPM for permission to publish this work.

### References

[1] H. K. Gurdeep Singh *et al.*, "Production of gasoline range hydrocarbons from catalytic cracking of linoleic acid over various acidic zeolite catalysts," *Environ. Sci. Pollut. Res.*, 2018.
[2] D. Singh, S. S. Sandhu, and A. K. Sarma, "An investigation of green diesel produced through hydroprocessing of waste cooking oil using an admixture of two heterogeneous catalysts," *Energy Sources, Part A Recover. Util. Environ. Eff.*, vol. 40, no. 8, pp. 968–976, 2018.

**RENEWABLE ENERGY AND BIOFUELS**

**Paper ID: ESCE098**

# OPTIMIZATION OF BIOETHANOL PRODUCTION FROM OIL PALM TRUNK SAP

**Mohd Nasir Nor Shahirah[1], Jolius Gimbun[2]*, Chin Kui Cheng[3]**

[1] *Malaysian Institute of Chemical and Bioengineering Technology, Universiti Kuala Lumpur, Lot 1988, Kawasan Perindustrian Bandar Vendor, Taboh Naning, 78000 Alor Gajah, Melaka, Malaysia.*
[2] *Centre for Research in Advanced Fluid and Processes (Fluid Centre), Universiti Malaysia Pahang, 26300 Gambang, Pahang, Malaysia.*
[3] *Department of Chemical Engineering, College of Engineering, Khalifa University, P.O Box 127788, Abu Dhabi, United Arab Emirates.*
*Corresponding author: jolius@ump.edu.my

## Extended Abstract

Malaysia and Indonesia are the two largest producers of palm oil in Asia with its combined output accounts for approximately 88% of global palm oil producer (Kosugi et al., 2010). At an interval of approximately 20-25 years, oil palm trees have to be replanted due to the decrease in oil productivity of old trees besides difficulty in harvesting their fruit (Lim et al., 1997). This means that about 64 to 80 million old palm trees will be felled annually in Malaysia, which can generate 15.2 million tons of oil palm trunks (Lim et al., 1997). These trunks are rich in sugar and may be utilized for production of bioethanol (Shahirah et al., 2014). Therefore, the oil palm trunks must be utilized in the interest of a sustainable palm oil industry (Lim et al., 1997).

This paper presents an optimization study of bioethanol yield from oil palm trunk sap (OPTS) fermentation by *Saccharomyces cerevisiae* with presence of multiple nutrient additions (i.e., $MgSO_4$ and $C_3H_7NO_2$). The sugar content in OPTS from 30-years old oil palm trunk and in fermentation mother liquor was determined using a high-performance liquid chromatography (HPLC). The fermentation parameters such as the initial pH, temperature and agitation rate were optimized by experimental design using response surface methodology (RSM) with applied rotatable central composite design (CCD). Validation of experimental model showed that the optimum bioethanol yield of 75.82% can be achieved at initial pH, temperature, and agitation rate were 5.79, 31.05°C and 164.38 rpm, respectively (Fig. 1). The outcomes were within 2.44% of deviation from the predicted result. Moreover, the supplement employed in this work showed an enhancement of ethanol production from OPTS without complicated pretreatment. Figure 1 showed a successful optimization of parameters for bioethanol production using fermentation process from OPTS by *Saccharomyces cerevisiae*. Findings from this work may provide a guideline to obtain a high yield of ethanol from OPTS fermentation.

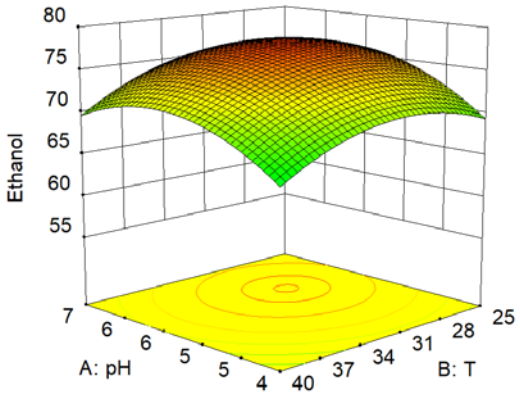


Fig. 1: 3D interaction plot of pH and temperature on bioethanol yield.

**RENEWABLE ENERGY AND BIOFUELS**

**Keywords:** Bioethanol; Oil palm trunk sap; Sugar fermentation; Yeast; Saccharomyces cerevisiae; Nutrient addition; HPLC; Optimization; Parameter; RSM; CCD.

## References

[1] Kosugi A., Tanaka R., Magara K., Murata Y., Arai T., Sulaiman O., Hashim R., Hamid Z.A.A., Yahya M.K.A., Yusof M.N.M., Ibrahim W.A. and Mori, Y. 2010. Ethanol and lactic acid production using sap squeezed from old oil palm trunks felled for replanting. *Journal of Bioscience and Bioengineering*, 110(3), 322–325.

[2] Lim K.O., Ahmaddin F.H. and Vizhi, S.M. 1997. A note on the conversion of oil-palm trunks to glucose via acid hydrolysis. *Bioresource Technology*, 59, 33–35.

[3] Shahirah M.N.N., Gimbun J., Pang S.F., Zakria R.M., Cheng C.K., Chua G.K. and Asras M.F.F. 2014. Influence of nutrient addition on bioethanol yield from oil palm trunk sap fermentation by *Saccharomyces cerevisiae*. *J. Ind. Eng. Chem.* 23, 213-217.

2ND ENERGY SECURITY AND CHEMICAL ENGINEERING CONGRESS 2021
*"Sustainable Technological Solution for a Better World"*
VIRTUAL CONFERENCE | 3-5 NOVEMBER 2021

**RENEWABLE ENERGY AND BIOFUELS**

**Paper ID: ESCE111**

# DENSITY FUNCTIONAL THEORETICAL CALCULATIONS FOR THE ELECTRONIC STRUCTURE OF CARBON AND COPPER CO-DOPED $TiO_2$ RUTILE MODEL

**F. Ullah[1,2,3]*, R. Bashiri[1], N. M. Mohamed[1,2], M. S. M. Saheed[2], F. K. Chong[1,2]**

[1] *Department of Fundamental and Applied Sciences,* [2] *Centre of Innovative Nanostructure and Nanodevices (COINN), Universiti Teknologi PETRONAS, 32610 Bandar Seri Iskandar, Perak, Malaysia.*
[3] *Department of Physics, University of Science and Technology, Bannu 28100, Khyber Pakhtunkhwa, Pakistan.*
*Corresponding author: farman_19001014@utp.edu.my and shuaib.saheed@utp.edu.my

## Extended Abstract

In recent years, a lot of emphasis has been given to the development of an efficient semiconductor photocatalyst for photocatalytic solar hydrogen production. The main problem that restricts the application of the $TiO_2$ is the wide band gap (3 eV for rutile), related to which it absorbs primarily the ultraviolet radiation with wavelength <387 nm in a small portion of only about 3-5% of the total sunlight spectra [1-3]. Recently, co-doping of $TiO_2$ with transition metal and nonmetal ions is reported to be more effective method than mono-doping. Although the performance of the different co-doped modified $TiO_2$ photocatalyst is improved, however, it is still not up to the mark because of the lack of understanding of the complex electronic structure [4, 5]. Understanding of the complex electronic structure and reduction of the band gap to an optimal range is necessary to improve their performance [6, 7]. Therefore, in this work, we theoretically designed an undoped and carbon/copper co-doped $TiO_2$ rutile 2×2×2 supercell models, using first principles density functional theory (DFT) calculations. The electronic structure and optical properties of the rutile $TiO_2$ were investigated. Plane-wave pseudopotential DFT approach with Hubbard's modified Perdew–Burke–Ernzerhof assisted generalized gradient approximation (GGA+PBE+U) exchange correlational functional is employed in order to simulate the characteristics of the designed models. To construct C-Cu co-doped system, a 2×2 ×2 $TiO_2$ rutile supercell model was designed. Computational simulation of the co-doped system with carbon and copper atoms at the substituted position of the titanium atoms was conducted for the said 2×2×2 optimized supercell model. Fig. 1 (a, b) represent a (2×2×2) supercell model for Pure $TiO_2$ rutile and C-Cu co-doped $TiO_2$ models, respectively.

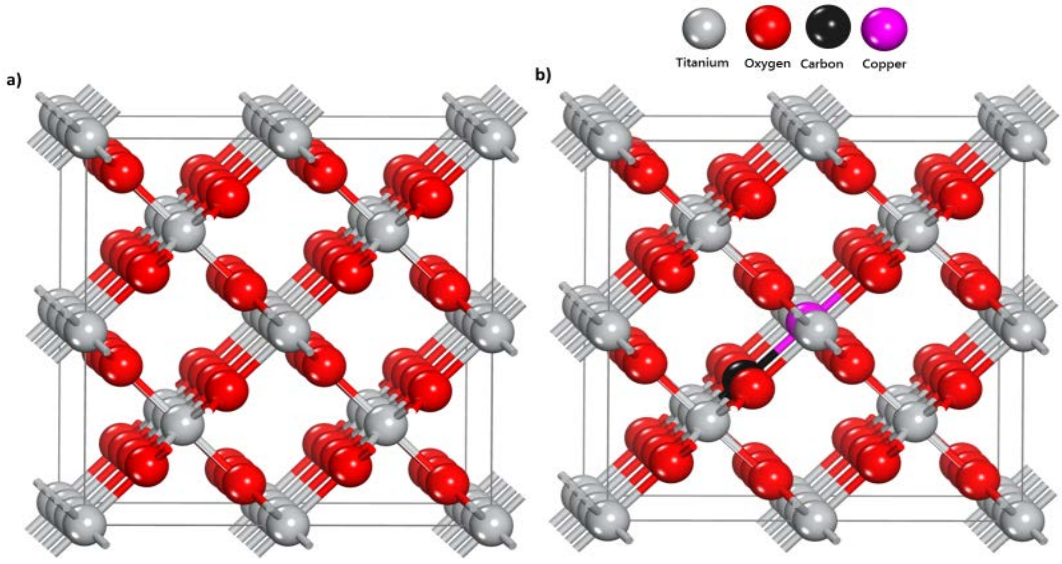


Fig. 1: (2×2×2) supercell model for (a) Pure $TiO_2$ Rutile and (b) C-Cu co-doped $TiO_2$ models.

The photocatalytic performance of the $TiO_2$ photocatalyst is strongly dependent on the electronic structure and their related properties [8-10]. The simulated electronic band structures for the pure and C-Cu co-doped $TiO_2$ models is shown in Fig. 2. The blue dashed line at zero-point energy shows the Fermi energy level. The calculated band gap energy ($E_g$) for pure rutile $TiO_2$ is 2.98 eV with Hubbard U value of 6 eV, as displayed in Fig. 2 (a). and is in close agreement with the experimentally known value of 3 eV for rutile $TiO_2$. A significantly reduced band of 2.21 eV for C-Cu co-doped $TiO_2$ model is shown in Fig. 2(b).

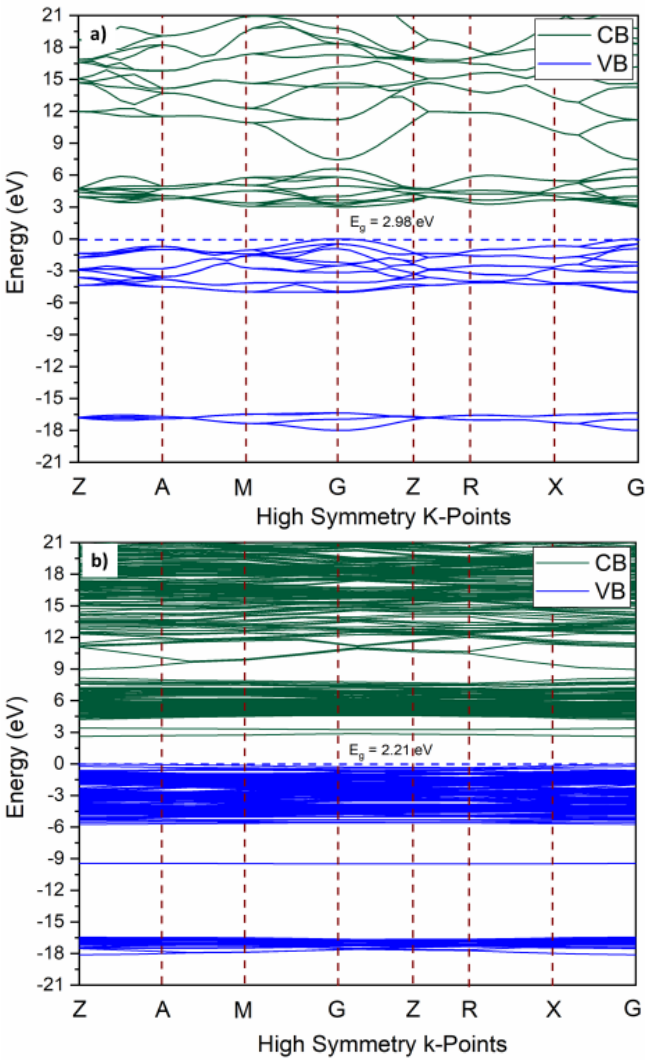


Fig. 2: Simulated electronic band structure of (a) pure $TiO_2$ rutile and (b) C-Cu co-doped $TiO_2$ rutile models

The calculated optimized lattice parameters for bulk $TiO_2$ Ru unit cell are a = b = 4.567 Å, c = 2.934 Å, and are in good agreement with the experimental values of a = b = 4.594 A˚ and c = 2.959 A˚, illustrating also that the adopted calculation method is reliable. To generally summarize this study, it can be concluded that C-Cu co-doping of $TiO_2$ exhibits a significant band gap reduction, as confirmed by the band structure plots and density of states diagrams. Bandgap reduction might shift the optical absorption edge to the visible region which will enhance the photocatalytic performance. Thus overall, it is clear that the C-Cu co-doping could be a feasible doping technique to enhance the photocatalytic performance of $TiO_2$.

**Keywords:** $TiO_2$ rutile; Photocatalyst; Co-doping; Electronic structure; Band gap reduction.

## Acknowledgment

This work is funded by the Universiti Teknologi PETRONAS (UTP) and Ministry of Higher Education (MOHE) Malaysia, Fundamental Research Grant Scheme (FRGS) (Grant no. FRGS/1/2019/STG07/UTP/01/1).

## References

[1] Ren B., Jin Q., Li Y., Li Y., Cui H. Wang C. (2020) Activating Titanium Dioxide as a New Efficient Electrocatalyst: From Theory to Experiment. ACS Appl. Mater. Interfaces. 12(10), 11607-11615.
[2] Zhu J., Deng Z., Chen F., Zhang J., Chen H., Anpo M., Huang J., Zhang L. (2006) Hydrothermal doping method for preparation of $Cr^{3+}$-$TiO_2$ photocatalysts with concentration gradient distribution of $Cr^{3+}$. Appl. Catal. B. 62(3-4), 329-335.
[3] Chen H., Li X., Wan R., Kao-Walter S., Lei Y. Leng C. (2018) A DFT study on modification mechanism of (N, S) interstitial co-doped rutile $TiO_2$. Chem Phys Lett. 695, 8-18.
[4] Li X., Gao H. Liu G. (2013) A LDA+ U study of the hybrid graphene/anatase $TiO_2$ nanocomposites: Interfacial properties and visible light response. Comput. Theor. Chem. 1025, 30-34.
[5] Diebold U., 2003. The surface science of titanium dioxide. Surf Sci Rep. 48(5-8), 53-229.
[6] Bayat A. Saievar-Iranizad E. (2018) Vertically aligned rutile $TiO_2$ nanorods sensitized with sulfur and nitrogen co-doped graphene quantum dots for water splitting: an energy level study. J Alloys Comp. 755, 192-198.
[7] L. Xiao T. Liu M. Zhang Q. Li Yang J. (2018) Interfacial construction of zero-dimensional/one-dimensional g-$C_3N_4$ nanoparticles/$TiO_2$ nanotube arrays with Z-scheme heterostructure for improved photoelectrochemical water splitting," ACS Sustain Chem Eng. 7(2), 2483-2491.
[8] Kudo A. Miseki Y. (2009) Heterogeneous photocatalyst materials for water splitting. Chem Soc Rev. 38(1), 253-278.
[9] Zhou Q., Lin Y., Zhang K., Li M. Tang D. (2018) Reduced graphene oxide/$BiFeO_3$ nanohybrids-based signal-on photoelectrochemical sensing system for prostate-specific antigen detection coupling with magnetic microfluidic device. Biosens Bioelectron, 101, 146-152.
[10] Agegnehu A.K., Pan C.J., Tsai M.C., Rick J., Su W.N., Lee J.F. Hwang B.J. (2016) Visible light responsive noble metal-free nanocomposite of V-doped $TiO_2$ nanorod with highly reduced graphene oxide for enhanced solar $H_2$ production. Int J Hydrog Energy, 41(16), 6752-6762.

**RENEWABLE ENERGY AND BIOFUELS**

**Paper ID: ESCE139**

# MEMBRANELESS ENZYMATIC BIOFUEL CELL POWERED BY STARCHY BIOMASS

**A. Jamaludin[1], C.K.M. Faizal[1]***

[1] *Faculty of Chemical & Process Engineering Technology, Universiti Malaysia Pahang, 26300 Gambang, Pahang, Malaysia.*
*Corresponding author: mfaizal@ump.edu.my

## Extended Abstract

This present work reports an eco-friendly and membraneless enzymatic biofuel cell (EBFC) was developed with direct utilization of starch as the biofuel. Since decades ago, glucose is the most utilized biofuel in EBFC [1]. This study examines the compatibility of Metroxylon Sagu (Sago) starch to be used as a substrate in the production of the biofuel in EBFC via enzymatic hydrolysis using alpha-amylase and glucoamylase enzymes. The hydrolysis is adapted from the idea of simultaneous saccharification and fermentation (SSF) which is widely used in another biofuel production [2], [3]. Glucose oxidase and laccase were immobilized on the bioanode and biocathode, respectively, to catalyze the redox reaction of glucose and oxygen. Membraneless EBFC makes the biofuel cell less bulky and reduces the cost [4]. The presence of glucose after the hydrolysis process was identified using the DNSA method. Meanwhile, the catalytic currents were successfully observed in the cyclic voltammetry analysis to confirm the redox reaction. Further, the electrochemical performances of the membraneless EBFC were evaluated in terms of the open circuit voltage (OCV) and maximum power density. All the measurements were carried out using a potentiostat. The concentrations of Sago substrate and volume of enzymes are varied in the experimental measurements. Fig. 1 (a) shows the best catalytic currents of an EBFC employing 1.5% (w/v) concentration of Sago substrate and 200 µl of enzymes and (b) maximum power density of 37.6 µW $cm^{-2}$. The EBFC can deliver an OCV of 0.32 V. The results proved that the direct use of starchy biomass in EBFC produces biofuel and consequently generate power. Membraneless EBFC is a potential candidate for low-powered implantable and wearable devices.

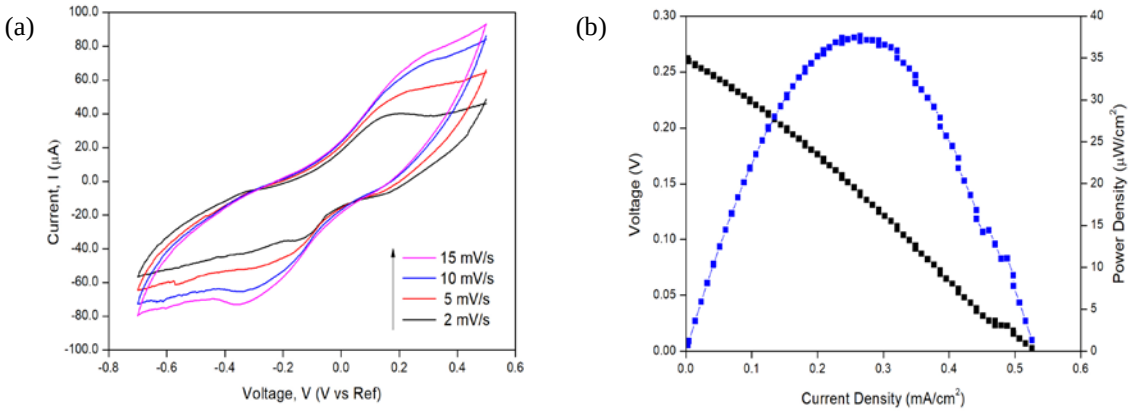


Fig. 1: (a) Cyclic voltammogram and (b) maximum power density of EBFC employing 1.5% (w/v) concentration of Sago substrate and 200µl of enzymes

**Keywords:** Biomass substrate; Metroxylon sagu; Enzymatic biofuel cell; Direct energy conversion.

**Acknowledgment**

This study was supported by the grants RDU140346 and RDU 1901118.

**RENEWABLE ENERGY AND BIOFUELS**

## References

[1] Singh R., Kaur N., Singh M. (2020). Bio-compatible bio-fuel cells for medical devices. Materials Today, 44:241-249.
[2] Srivastava, R., Shetti, N., Reddy, K.R., Kwon, E.E., Nadagouda, M., Aminabhavi, T. (2021). Biomass utilization and production of biofuels from carbon neutral materials. Env. Pollution, 276: 116731.
[3] Valles, A., Alvarez-Hornos, F.J., Martinez-Soria, V., Marzal, P., Gabaldon, C. (2020). Fuel, 282: 118831.
[4] Rewatkar P., Hitaishi V., Lojou E., Goel S. (2019). Enzymatic fuel cells in a microfluidic environment: Status and opportunities. A mini review. Electrochemistry Comm., 107:106533.

**RENEWABLE ENERGY AND BIOFUELS**

**Paper ID: ESCE160**

# THE MECHANISM OF ELECTRO-OXIDATION OF GLYCEROL ON THE Pd-Au CATALYST SURFACES: A DFT STUDIED

**N.A. Karim[1], M.S. Alias[1], N. Yahya[2], S.K. Kamarudin[1] and F. Rusydi[3,4]**

[1] *Fuel Cell Institute, Universiti Kebangsaan Malaysia, Bangi, Selangor, Malaysia.*
[2] *Malaysian Institute of Chemical and Bioengineering Technology, Universiti Kuala Lumpur, Melaka, Malaysia.*
[3] *Department of Physics,* [4] *Research Center for Quantum Engineering Design, Faculty of Science and Technology, Universitas Airlangga, Jl. Mulyorejo, Surabaya, 60115, Indonesia.*
*Corresponding author: nabila.akarim@ukm.edu.my

## Extended Abstract

Clean and efficient energy sources are becoming more important nowadays to reduce environmental pollution and to cater to high energy demand. Therefore, the need to explore various types of clean and efficient energy becomes essential. Biodiesel produced from biomass is one of the sources that lead to the production of excess crude glycerol in the biodiesel industry. Crude glycerol from this biodiesel gives competitive value compared to pure refine glycerol and also gives environmental problems. Therefore, the transformation of glycerol into a valuable chemical for use in other industries or applications such as chemical, biomedical, and pharmaceutical provides an advantage. Direct Glycerol Fuel Cell (DGFC) is one of the alternative energy used to produce electricity without combustion. Therefore, crude glycerol is used as a fuel in DGFC to produce electricity and transform it into value-added chemicals such as glyceraldehyde, dihydroxyacetone, glyceric acid, hydroxypyruvinic acid, glycolaldehyde, glycolic acid, tartronic acid, acetic acid, and formic acid. The conversion of glycerol to various of these value-added chemicals is through the electrochemical oxidation reaction of glycerol (GOR) at the anode of DGFC. The resulting electrons in the GOR are then routed to the cathode side to complete the oxygen reduction reaction in the DGFC and thus generate electricity. Catalysts are used to increase GOR, and the PdAu alloys were seen to have increased reaction activity in DGFC through experimental studies [1-3]. Therefore, this study presents the reaction mechanism of glycerol from a theoretical point of view using the density functional theory method (DFT). The atomic ratios of Pd to Au selected in this study were 3: 1, 1: 3, and 1: 1, leading to the development of catalyst models of Pd3Au1, Pd1Au3, and PdAu, respectively. Au (111) and Pd layer on Au (111) (namely as Pd skin) were also developed as comparisons. Various intermediates are adsorbed on the surface of the catalysts model to find the most stable adsorption energy. Mulliken charge and partial density of state (p-dos) were also performed to observe the change of electrons from catalyst surface to adsorbate and the strength of adsorption, respectively. The reaction mechanism of glycerol is carried out, and $Pd_1Au_3$ attempts to produce oxalic acid as the final product. However, several steps in the pathways require high activation energy that will likely cause other intermediate products to be formed as well.

**RENEWABLE ENERGY AND BIOFUELS**

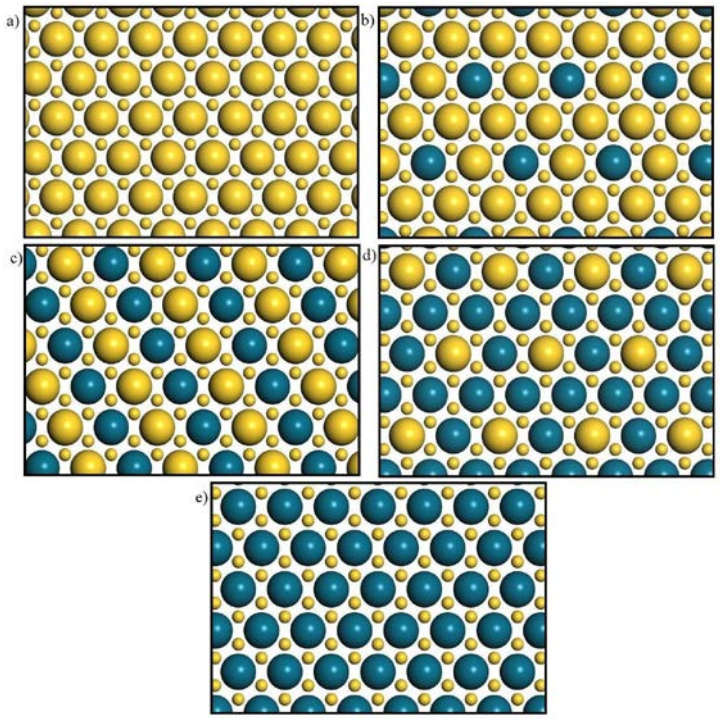


Fig. 1: Model of Au metal and PdAu alloy for the electro-oxidation of glycerol in acidic and alkaline medium: a) Au, b) Pd1Au3, c) PdAu, d) Pd3Au1, and e) Pd skin (gold: Au atom, blue: Pd atom)

**Keywords:** Electro-oxidation; Glycerol; Direct Glycerol Fuel Cell; Alkaline; Acidic.

**Acknowledgment**

The authors gratefully acknowledge the financial support for this work by the Universiti Kebangsaan Malaysia under GUP-2021-075.

**References**

[1] N. Yahya, S. K. Kamarudin, N. A. Karim, M. S. Masdar and K. S. Loh (2017) Nanoscale Research Letters Vol. 12 Issue 1 Pages 605.
[2] N. Yahya, S. K. Kamarudin, N. A. Karim, M. S. Masdar, K. S. Loh and K. L. Lim (2019) Energy Conversion and Management Vol. 188 Pages 120-130.
[3] N. Yahya, S. K. Kamarudin, N. A. Karim, S. Basri and A. M. Zanoodin (2019) Nanoscale Research Letters Vol. 14 Issue 1 Pages 52.

**RENEWABLE ENERGY AND BIOFUELS**

**Paper ID: ESCE171**

# PRODUCTION OF RENEWABLE LIGHT FUEL RANGE OVER HETEROGENOUS CALCIUM OXIDE-BASED CATALYST DERIVED FROM GYPSUM WASTE BY PYROLYTIC CATALYSIS PROCESS: EFFECT OF MAGNESIUM CONTENTS

**W. Chansiriwat[1,2], K. Wantala[1,2,3]*, R. Khunphonoid[4], P. Khemthong[5]**

[1] *Department of Chemical Engineering,*[2] *Chemical Kinetics and Applied Catalysis Laboratory (CKCL),*
[3] Research Center for Environmental and Hazardous Substance Management (EHSM), [4] *Department of Environmental Engineering, Faculty of Engineering, Khon Kaen University, 40002 Khon Kaen, Thailand.*
[5] *National Nanotechnology Center (NANOTEC), 12120 Pathum Thani, Bangkok, Thailand.*
*Corresponding author: kitirote@kku.ac.th

## Extended Abstract

Global warming is a major problem nowadays. This problem must be addressed by every country. The mean temperature of global has risen up from year to year, especially almost 1 degree Celsius from 1850-2012 [1]. One method that can ease this problem is $CO_2$ reduction. Moreover, the popular way for $CO_2$ reduction chosen is green energy use from renewable resource, vegetable oil. Thailand can produce crude palm oil about 3.9% of global production [2]. Using palm oil as a raw material for renewable resources, biofuel, is a proper choice for utilizing domestic source and biofuel production since triglyceride structure resembles hydrocarbon product [3]. Transesterification, hydrotreating process and pyrolytic catalytic cracking, all is able to change palm oil to biofuel. Pyrolytic catalytic cracking is simple and cheap. CaO with MgO as a catalyst could reduce the acidity in biofuel because these two oxides support the reactions, decarboxylation and decarbonylation, that can remove the oxygen in the compound. Also MgO can induce the second cracking to small molecules [4]. Furthermore, no studies have been conducted using gypsum as a raw material for CaO source and mixing it with Mg in pyrolytic catalytic cracking for bio-oil production. Hench, exactly Mg composition was required for producing novel catalysts to produce light biofuel with low acidity via pyrolytic catalytic process. This study of biofuel production by catalytic pyrolysis of palm oil using CaO catalyst derived from synthetic gypsum via a packed bed reactor with different reaction temperatures (500 °C, 525 °C and 550 °C) was investigated. The calcium was prepared from flue-gas-desulfurized gypsum collected from Mae Moh power plant in Thailand following, it was mixed with 2M of NaOH under stirring for 4 hours. Then, it was washed with deionized water until the pH of rinsing water about 12.5. After that it was dried in the oven at 110°C overnight and the white power of $Ca(OH)_2$ was obtained. Next, $Ca(OH)_2$, $MgCO_3$, and 200 g of bentonite were mixed by wet ball mill process with 1000 mL of DI water. The alkaline catalysts were mixed between Ca $(OH)_2$ with different amounts of $MgCO_3$ (0%, 10%, 20%, 30% and 60%) and 40% of binder, bentonite. The total weight of each catalyst was 500 g of $Ca(OH)_2$, $MgCO_3$, and bentonite. The mixers were mixed for 6 h by ball mill process. After that, the mixers were dried at 110°C overnight in the oven, ground by hammer mill, sieved by using a 60-mesh sieve and pelletized by a hydraulic pressing machine at 4000 psi. After pelleting, the pellet was dried at 110°C and calcined at 750 °C for 4 h in a furnace (Electric service device Co., Ltd.). All catalyst was labeled relating with the $MgCO_3$ percentage as $MgCO_3$ 0%, $MgCO_3$ 10%, $MgCO_3$ 20%, $MgCO_3$ 30% and $MgCO_3$ 60%. Only four catalysts, $MgCO_3$ 0%, $MgCO_3$ 10%, $MgCO_3$ 20%, and $MgCO_3$ 30%, were tested in the pyrolytic reactor at different reaction temperatures. The catalyst was characterized by BET method with $N_2$ adsorption-desorption apparatus, XRD, XRF, and TEM techniques. In term of biofuel production, the 180g catalyst was packed in the reactor. Then palm oil was fed in the reactor by peristatic pump. The reaction was taken place at different temperatures. The final products were collected at each temperature and then they were separated by separator funnel to remove water and then was filtrated to remove impurity. After filtration, it was named as pyrolytic oil (PO). The pyrolytic oil was distilled following ASTM D86 and named as distilled oil (DO). PO was characterized by CHNO and GC-MS, while DO was analyzed by many techniques such as heating value, viscosity and acidity. The result confirmed that CaO and MgO were successfully synthesized from synthetic gypsum and $MgCO_3$, respectively, with the low sulfur confirmed by XRD and XRF results. According to XRF result, it showed only 0.8% $SO_3$ in pure CaO and about 0.6-2.4% $SO_3$ in all catalyst while about 50% sulfur existed in raw material, gypsum. Moreover, there are crossed lattice fringes described by

heterojunction between CaO and MgO particle in the catalyst structure as shown in TEM result (Figure 1(a)). In term of BET pore size distribution, it implied that $MgCO_3$ 10-30% showed only micropores while $MgCO_3$ 0% has only mesopores. It might be explained by MgO clogging in CaO pores. The chemical properties of PO were found that CHNO results showed oxygen in the product about 24.6, 18.0, 16.8 and 17.4 for $MgCO_3$ 0%, 10%, 20% and 30%, respectively. Higher MgO tends to lower the oxygen contents comparing with palm oil (29.1%). It can be explained by inducing decarboxylation and decarbonylation by MgO that can remove the oxygen in the compound.

Also basic site, low %Mg displayed a high basic site that could convert carboxylic acid to aldehyde by oxygen removal, confirmed by GC-MS result. The GC-MS results expressed high amount of aldehyde at the product with lower amount of Mg, represented about 1.30%, 0.48%, 0.45% and 0.47% for $MgCO_3$ 0%, 10%, 20% and 30%, respectively.

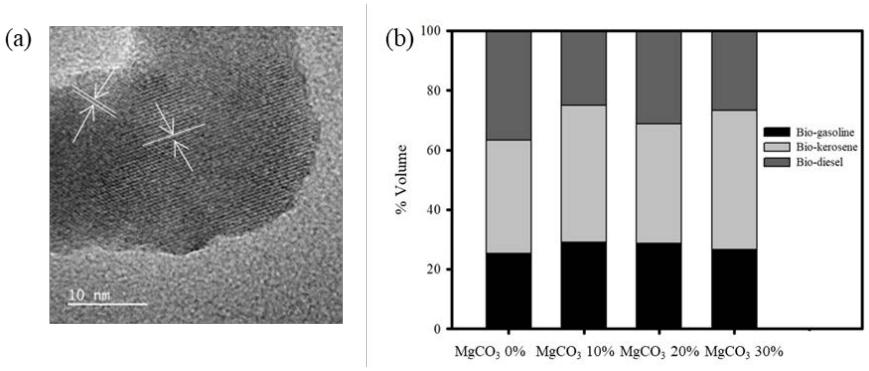


Fig. 1: (a) HR-TEM micrographs of calcined catalysts at 10%$MgCO_3$ percentages, (b) distilled oils at 525°C of reaction temperature

Light renewable biofuel taken place in the packed-bed reactor under atmosphere pressure without external gas feeding over CaO-MgO catalysts was successfully produced. Not only, Mg content was significant on light fuel production, but also the reaction temperature was significant on bio-gasoline and bio-kerosene proportion. The highest volume proportion of light biofuel was found at $MgCO_3$ 10% catalyst and 525°C of reaction temperature at about 75%, as shown in Figure 1(b). The excess of Mg supported second cracking to small molecules and left more bio-diesel or big molecules. The light biofuel increased with increasing reaction temperature. High reaction temperature can induce high fatty acid decomposition and bond cracking of hydrocarbon chains. The properties of biofuel including heating value, viscosity, and density, were under the standard except for their acidity. Especially, heating value was related to oxygen and carbon content in bio-oil.

**Keywords:** Waste gypsum; Renewable fuel; Alkaline catalyst; Pyrolytic catalysis.

## Acknowledgment

This study was supported by a scholarship from the Thailand Research Fund (TRF) through the Royal Golden Jubilee Ph.D. (RGJ) program (Grant No. PHD/0150/2561). Authors would like to thank the Research Center for Environmental and Hazardous Substance Management (EHSM) and Faculty of Engineering, and the Research and Graduate Studies, Khon Kaen University, for a partial scholarship.

## References

[1] Singh S., Singh D. R., Velmurugan A., Jaisankar I., Swarnam T. P. (2008) Chapter 23 - Coping with Climatic Uncertainties Through Improved Production Technologies in Tropical Island Conditions. Eds. Academic Press 623-666.
[2] Sowcharoensuk C., Thani S. (2020) Palm oil industry. no. January 2020:1-11.
[3] Seifi H., Sadrameli S. M. (2016) Improvement of renewable transportation fuel properties by deoxygenation process using thermal and catalytic cracking of triglycerides and their methyl esters. Appl. Thermal Eng 100:1102-1110.
[4] Kalogiannis K. G., Stefanidis S. D., Karakoulia S. A., Triantafyllidis K. S., Yiannoulakis H., Michailof C., Lappas A. A. (2018) First pilot scale study of basic vs acidic catalysts in biomass pyrolysis: Deoxygenation mechanisms and catalyst deactivation. Appl. Catalysis B Environmental 238:346-357.

**RENEWABLE ENERGY AND BIOFUELS**

**Paper ID: ESCE195**

# BIODIESEL PRODUCTION FROM WASTE CATFISH OIL

**N. M. A. A. Amzah[1], A. Ideris[2], A. I. Nafsun[2], R. Abdul Rasid[1]***

[1] *Faculty of Chemical & Process Engineering Technology,* [2] *Department of Chemical Engineering, Universiti Malaysia Pahang, 26300 Gambang, Pahang, Malaysia.*
*Corresponding author: ruwaida@ump.edu.my

## Extended Abstract

Fish oil is a sustainable, abundant, and low-cost raw material, as it is extracted from fish processing waste [1]. Pahang is famous for its catfish, *patin*, or its scientific name *Pangasianodon hypophthalmus*. It can be easily found in local markets and its internals are considered as waste and high in fat content. It would be a good feedstock for biodiesel production due to its low cost, and solving the problem of fish waste disposal [2]. As the oil from the fish waste may have low quality characteristics such as high free fatty acid (FFA) content, it has a potential as a source for biodiesel production. The main objective of this work is to investigate the potential of waste fish oil from the catfish in biodiesel production, specifically the effect of two most important parameters in biodiesel production which are methanol to oil ratio and catalyst loading during the transesterification process with heterogeneous catalyst. It is done via the two-step process; the first step is esterification, followed by the actual transesterification. Esterification reaction using PK resin as catalyst, aims to reduce the high FFA content of waste fish oil while transesterification reaction in which oil reacts with methanol in the presence of an alkaline catalyst, Calcium Oxide (CaO) to form ester and glycerol.

A sample of a significant result from this study is as shown in Figure 1, which is the plot of increasing waste fish oil to methanol ratio to biodiesel yield. It can be observed that the biodiesel produced increased from 58.79 to 87.42% as the molar ratio of oil to methanol was increased from 1:6 to 1:12. Molar ratio is one of the important factors affecting the conversion of oil in the transesterification reaction. Ideally, transesterification reaction requires 3 mol of alcohol to produce 1 mol of biodiesel. However, molar ratio should be higher than the stoichiometric ratio. This is because an excess of alcohol is required for the reaction to move forward and avoid the reversible reaction [3]. An optimum yield of biodiesel was obtained at a molar ratio of 1:12 which was 87.42%. This finding implies that the interaction between oil and methanol molecules was enhanced and the yield of biodiesel increased as the molar ratio of oil to methanol increased up to 1:12, which also indicate the potential of utilizing waste fish oil from catfish as a sustainable resource for biodiesel production.

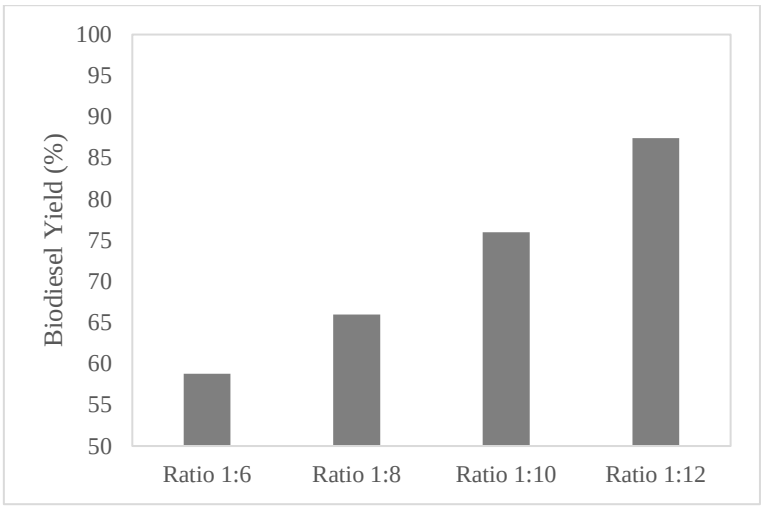


Fig. 1: Effect of oil to methanol ratio on the yield of biodiesel
(reaction temperature of 60ºC, catalyst loading 2wt.% and reaction time of 1 hours).

**Keywords:** Biodiesel; Waste fish oil; *Pangasianodon hypophthalmus*; Esterification; Transesterification.

## Acknowledgment

This study was supported by Universiti Malaysia Pahang Flagship Grant (RDU182204-2).

## References

[1] L. da C. Cardoso, F. N. C. de Almeida, G. K. Souza, I. Y. Asanome, and N. C. Pereira, "Synthesis and optimization of ethyl esters from fish oil waste for biodiesel production," *Renew. Energy*, vol. 133, pp. 743–748, 2019.
[2] Z. Hajamini, M. A. Sobati, S. Shahhosseini, and B. Ghobadian, "Waste fish oil (WFO) esterification catalyzed by sulfonated activated carbon under ultrasound irradiation," *Appl. Therm. Eng.*, vol. 94, pp. 1–10, 2016.
[3] G. K. Ayetor, A. Sunnu, and J. Parbey, "Effect of biodiesel production parameters on viscosity and yield of methyl esters: Jatropha curcas, Elaeis guineensis and Cocos nucifera," *Alexandria Eng. J.*, vol. 54, no. 4, pp. 1285–1290, 2015.

**RENEWABLE ENERGY AND BIOFUELS**

**Paper ID: ESCE211**

# INVESTIGATION OF THE STABILITY OF CERIUM OXIDE IN DIESEL FUEL FOR NANO-ENHANCED FUEL FORMULATION

**Ali Ba Saleem[1]*, R. Mamat[1], Ftwi Y. Hagos[2], A. Abdul Adam[3], Abdulwahid Arman[1]**

[1] *College of Engineering, Department, Universiti Malaysia Pahang, Malaysia, 26300, Gambang, Pahang, Malaysia.*
[2] *Mechanical and Industrial Engineering Department, College of Engineering, Sultan Qaboos University, Al Khoud, 123, Seeb, Muscat, Oman.*
[3] *Automotive Engineering Centre, Universiti Malaysia Pahang, 26600 Pekan, Pahang, Malaysia.*
*Corresponding author: alibasleem1995@gmail.com

## Extended Abstract

Enhancing fuels through nano-addition has become a prospect in keeping both renewable and non-renewable fuels as energy sources for the transportation sector. One of the challenges when using nanofluids in a specific system is the fluid's ability to be stable for a longer period. Undesired settlement of nanoparticles can cause damage to the system operating within its limits due to contamination. Stability study has paramount importance in the nano-enhanced fuel introduction in internal combustion engines. Three-step method using UV-vis spectral absorbency device was selected to enhance the nanofluid and ensure the stability of the solution daily. Cerium oxides consider one of the challenging nano additives to blend with fuel. To measure its stability, it was observed that when the nanofluid fuel was mixed with nanoparticles in quantities estimated at 25, 50, and 75 ppm, the nano fuel solution showed a high stability capacity in the first days, which indicate revealed that blending at high speeds followed by ultrasonication in an ultrasonic homogenizer for 40 minutes increases the stability of the mixes. The nano fluid fuel was gradually decreasing during the next following 8 days, but all of the blended fuel remains stable for percentage above 80 percent.

**Keywords:** Nano-enhanced fuel; Stability; Diesel; Cerium oxide; UV-Vis; Ultrasonic.

### References

[1] Green Technologies Thermal decomposition study of high density polyethylene nano composite National Conference On Recent Trends And Developments In Sustainable Green Technologies," no. 7, pp. 240–244, 2015.
[2] M. Tomar and N. Kumar, "Influence of nanoadditives on the performance and emission characteristics of a CI engine fuelled with diesel, biodiesel, and blends – a review," Energy Sources, Part A Recover. Util. Environ. Eff., vol. 0, no. 0, pp. 1–18, 2019.
[3] M. V. Kumar, A. V. Babu, and P. R. Kumar, "Influence of metal-based cerium oxide nanoparticle additive on performance, combustion, and emissions N. Conference, O. Recent, D. In, and S. Green, "National Conference On Recent Trends And Developments In Sustainable with biodiesel in diesel engine," Environ. Sci. Pollut. Res., vol. 26, no. 8, pp. 7651–7664, 2019.
[4] S. Madiwale, A. Karthikeyan, and V. Bhojwani, "A Comprehensive Review of Effect of Biodiesel Additives on Properties, Performance, and Emission," IOP Conf. Ser. Mater. Sci. Eng., vol. 197, no. 1, 2017.
[5] W. T. Urmi, M. M. Rahman, K. Kadirgama, D. Ramasamy, and M. A. Maleque, "An overview on synthesis, stability, opportunities and challenges of nanofluids," Mater. Today Proc., no. xxxx, 2021.
[6] H. A. Dhahad and M. T. Chaichan, "The impact of adding nano-Al 2 O 3 and nano-ZnO to Iraqi diesel fuel in terms of compression ignition engines ' performance and emitted pollutants," Therm. Sci. Eng. Prog., vol. 18, no. August 2019, p. 100535, 2020.
[7] T. E. Irjmt, "Experimental studies on Diesel Engine using Aluminium Nano Particles as Additives," no. January, 2019.
[8] P. K. Mondal and B. K. Mandal, "A comparative study on the performance and emissions from a CI engine fuelled with water emulsified diesel prepared by mechanical homogenization and ultrasonic dispersion method," Energy Reports, vol. 5, pp. 639–648, 2019.
[9] A. Rameshbabu and G. Senthilkumar, "Emission and performance investigation on the effect of nano-additive on neat biodiesel," Energy Sources, Part A Recover. Util. Environ. Eff., vol. 0, no. 0, pp. 1–14, 2019.
[10] S. Shrestha, B. Wang, and P. Dutta, "Nanoparticle processing: Understanding and controlling aggregation," Adv. Colloid Interface Sci., vol. 279, p. 102162, 2020.

[11] A. Ghadimi, R. Saidur, and H. S. C. Metselaar, "International Journal of Heat and Mass Transfer A review of nanofluid stability properties and characterization in stationary conditions," Int. J. Heat Mass Transf., vol. 54, no. 17–18, pp. 4051–4068, 2011.
[12] S. Chakraborty and P. K. Panigrahi, "Stability of nanofluid: A review," Appl. Therm. Eng., vol. 174, no. December 2019, 2020.
[13] X. Hou, H. Liu, X. Li, H. Jiang, Z. Tian, and M. K. A. Ali, "An experimental study and mechanism analysis on improving dispersion stability performance of Al2O3 nanoparticles in base synthetic oil under various mixing conditions," J. Nanoparticle Res., vol. 23, no. 4, 2020.
[14] A. K. Nassir and H. A. K. Shahad, "Experimental study of effect of nanoparticles addition on combustion phasing in diesel engine," Int. J. Mech. Mechatronics Eng., vol. 18, no. 1, pp. 87–97, 2018.
[15] M. Z. Sharif, W. H. Azmi, A. A. M. Redhwan, and N. M. M. Zawawi, "Preparation and stability of silicone dioxide dispersed in polyalkylene glycol based nanolubricants," vol. 01049, 2017.
[16] A. Zawadzki, D. S. Shrestha, and B. He, "Biodiesel Blend Level Detection Using Ultraviolet Absorption Spectra," Trans. ASABE, vol. 50, no. 4, pp. 1349–1353, 2007.
[17] A. G. N. Sofiah, M. Samykano, S. Shahabuddin, K. Kadirgama, and A. K. Pandey, "An experimental study on characterization and properties of eco-friendly nanolubricant containing polyaniline (PANI) nanotubes blended in RBD palm olein oil," J. Therm. Anal. Calorim., vol. 145, no. 6, pp. 2967–2981, 2021.
[18] R. Sadeghi, S. G. Etemad, E. Keshavarzi, and M. Haghshenasfard, "Investigation of alumina nanofluid stability by UV–vis spectrum," Microfluid. Nanofluidics, vol. 18, no. 5–6, pp. 1023–1030, 2015.
[19] M. Z. Sharif, W. H. Azmi, A. A. M. Redhwan, N. N. M. Zawawi, and R. Mamat, "Improvement of nanofluid stability using 4-step UV-vis spectral absorbency analysis," J. Mech. Eng., vol. SI 4, no. 2, pp. 233–247, 2017.

**SAFETY AND HEALTH MANAGEMENT**

**Paper ID: ESCE002**

# DECISION-MAKING TOOL FOR PROCESS HAZARD EVALUATION AND RISK ASSESSMENT DURING PRELIMINARY DESIGN STAGE

**Muhammad F. Husin[1]*, Hamidah Kamarden[2], Mimi H. Hassim[2], Syaza I. Ahmad[3], Iswaibah Mustafa[1]**

[1] *Faculty of Chemical Engineering, Universiti Teknologi MARA Bukit Besi, 23200 Dungun, Terengganu, Malaysia.*
[2] *School of Chemical and Energy Engineering/Centre of Hydrogen Energy, Universiti Teknologi Malaysia, 81310, UTM Johor Bahru, Malaysia.*
[3] *Centre of Advanced Process Safety (CAPS), Universiti Teknologi PETRONAS, 32610 Bandar Seri Iskandar, Perak Darul Ridzuan, Malaysia.*
*Corresponding author: firdaushusin@uitm.edu.my

## Extended Abstract

A conventional process design lifecycle starts with a screening process of alternative chemical reaction pathways until the detailed design of the entire plant. During the design of the process mainly the flow diagram of the process, errors may arise due to wrong decisions and basis made, which will later cause problems to the following stages of the process lifecycle. Despite the availability of enormous safety assessment methods, a proper detailed framework which guides users in selecting the appropriate method for their assessment is still missing. Therefore, this paper aims to address the above issue by proposing a systematic framework for safety assessment based on process information generated from PFDs during preliminary design stage. The research on R&D and basic engineering design is currently on-going to develop the entire framework and will be presented in other papers. Technically, the framework was developed based on the inherent safety methods screened to be suitable for application within the PFD-based context. The framework also provides recommendations on the strategies for reducing the safety hazard and risk in the process in the respective design stage. A case study on process design of biorefineries is solved to illustrate the functionality and benefit of the proposed framework.
**Keywords:** Safety assessment; Systematic framework; Safety hazard and risk; Process flow diagram (PFD); Safety index.

### Introduction

In chemical engineering, one of the targets of the process design is the creation or modification of flow diagrams capable of manufacturing the desired chemical. It is also essential to consider safety aspects when designing any new process or in the case of retrofitting. As a result, several methods have been introduced for safety assessment during process design phase [2]. Unfortunately, there are lacks of guideline in selecting an appropriate method for him/her based data availability, target of assessment and budget constraints. Therefore, a systematic framework is required for the design of safe chemical processes – this is not only to ensure a safe plant but can also to speed up the process development work. This paper presents a new framework that applies selected index-based methods to evaluate the risk and minimize hazard using inherent safety design (ISD) keywords based on process flow diagram.

### Methodology

In order to achieve the objective of this study, a well-ordered steps are constructed which starts from reviewing and classifying the available process safety assessment methods to the stage of demonstrating the proposed framework on case study as shown in Figure 1.

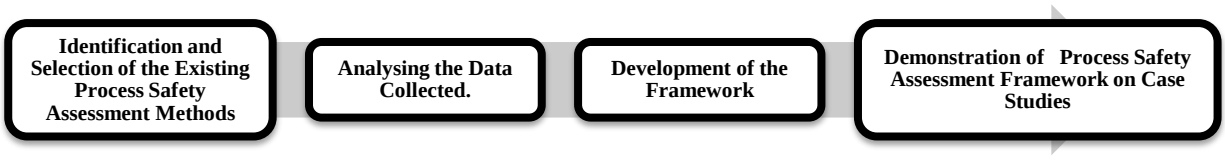


Fig. 1: Overall Research Methodology Steps.

## SAFETY AND HEALTH MANAGEMENT

The first step of this research methodology is to identify existing process safety assessment method to be included in proposed framework. There are 13 methods were selected to be analyzed before develop the framework. Classification of methods and identification safety parameters are steps in analyzing the data collected step. After all data have been collected and analyzed, the next step is to develop a framework to quantify the level of safety based in PFD. The mitigation strategies also included by introducing ISD keywords which is explained in the following section.

**Results and Discussion**

The primary goal of this framework is to guide or assist user in selecting an appropriate method for performing safety assessment based on availability of process information generated from PFD only as shown in Figure 2. Instead of assessing the safety level of process design phase, this framework also can use to analyse the root of the safety problems and recommend the possible solutions through ISD keywords (minimization, substitution, simplification and moderation).

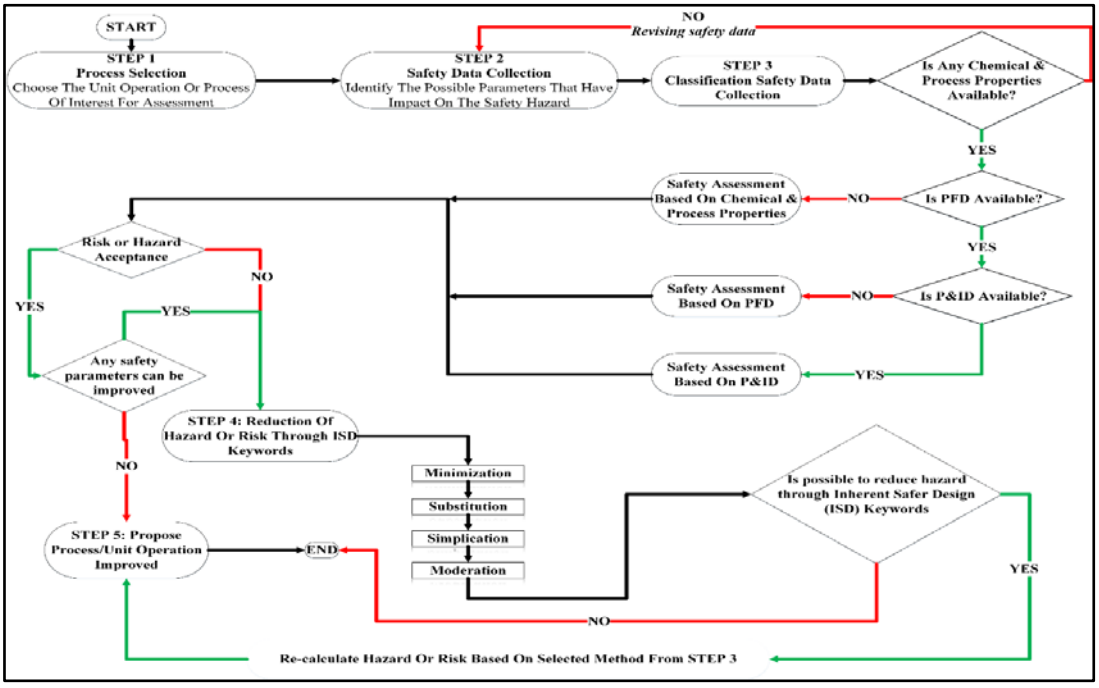


Fig. 2: Heuristic Framework for Process Safety Assessment based on Different Process Infromation.

The selected case study is based on the process development of biorefinery– processing facility that converts biomass into value added products such as bio-hydrogen and succinic acid. This case study is intended to evaluate the safety level of integrated biorefineries consists of two sections in the process - gasification and fermentation. In this assessment, scoring value is assigned to process in situation where hazards are present in order to indicate the level of hazard. A higher value represents the greater hazards. Table 1 shows that, the total inherent safety index for gasification section is higher than for fermentation section, hence indicating that the fermentation section is inherently safer than the gasification section. This could be attributed to:

i. A toxic chemical of carbon monoxide, CO presents in the gasification and not in fermentation section.
ii. The process temperature in gasification is higher than in fermentation section.
iii. There is possibility for gas explosion to occur in biomass gasification facilities when a mixture of combustible gases consisting of CO, hydrogen and oxygen within the flammability limits meets an ignition source [1].

Table 1: Safety Analysis for Integrated Biorefineries.

| Process Section | CISI | PISI | Total (CISI+PISI) |
|---|---|---|---|
| Gasification and Purification Process | 16 | 11 | 27 |
| Succinic Fermentation and Purification Process | 11 | 9 | 20 |

## Conclusion

The proposed frameworks shall serve as a great help for engineers to select appropriate method for safety assessment based on the availability of process information during the chemical process design. In order to extend the functionality of framework, more specific ISD keywords (i.e. error tolerance, limitation of effects) also can be considered for more effective and various options to reduce the hazards.

## Acknowledgment

Special thanks to Universiti Teknologi MARA (UiTM) Cawangan Terengganu for the financial support received to conduct this research under the provided research grant, 600-UiTMCTKD (PJI/RMU 5/2/1) RCF-RACER 2021 (8/2021).

## References

[1] Abidin,N.A., Ariffin, M.A and Rusli, R. (2011). Preliminary risk assessment for the bench-scale of biomass gasification system. Proceedings of the 2011 *National Postgraduate Conference* (NPC), 2011, 1-6.

[2] Khan, F. I. and Abbasi, S. A. (1998c). Techniques and methodologies for risk analysis in chemical process industries. Journal of Loss Prevention in the Process Industries, 11(4), 261-277.

**SAFETY AND HEALTH MANAGEMENT**

**Paper ID: ESCE011**

# CARBON FOOTPRINT CALCULATION AND PROPOSING SOLUTIONS TO REDUCE CARBON FOR GARMENT TECHNOLOGY PROCESSES IN VIETNAM

**N. Le[1], H. A. Le[1*], K. L. P. Nguyen[1], P. H. Le[1]**

[1] *Faculty of Environmental and Food Engineering, Nguyen Tat Thanh University, Ho Chi Minh City, Vietnam.*
[2] *Faculty of Environment, University of Science, Vietnam National University-Ho Chi Minh City, Ho Chi Minh City, Vietnam.*
*Corresponding author: lhanh@hcmus.edu.vn

## Extended Abstract

The textile & garment industry is one of the key industries in Vietnam, contributing great value to Vietnam's exports and GDP as well as solving employment [1]. Vietnam has known as the world's second largest exporter of ready-made garments (RMG), Fashion United, an international B2B fashion platform, quoted the World Trade Statistical Review 2021 released by World Trade Organization (WTO). The way to set a sustainable development pathway for fabric and garment production is to truly embrace principles and best practices on environmental protection, green production [2] and will be assist the transition of Vietnam's textile and apparel sector towards sustainable development and actively support the achievement of national development goals to get green growth model, as a means to achieve a low carbon economy and to enrich natural capital, will become the principal direction in sustainable economic development [3] of Viet Nam in the future. To meet these challenges, Viet Nam needs to continue strengthening its institutional capacity, tackling economic reforms, massively adopting clean technologies and paying attention to the evolving people consumption patterns [4]. It is to be expected that a diversity of carbon footprint standards will persist for years to come [6].

Vietnam needs to have research and publication on carbon footprint to move towards a sustainable development model, especially the garment industry in Vietnam, choosing a very important development model in which green growth is critical approach in line with global trends.

The objective of the thesis is to calculate carbon footprint unit (CFU) for the sewing technology process of some enterprises of Vietnam national textile and garment group (VINATEX), thereby comparing, giving out strengths and weaknesses in the production process. Based on the achieved results, concluded the advantages and disadvantages of each process and the ability to apply technology in Vietnam. Finally, giving recommendations and initially proposing solutions to reduce emissions to move towards a low-carbon economy and green growth under current Vietnam's conditions.

Objectives to be achieved of the study:
- Inventory of the amount of greenhouse gas emitted (kgCO2e) of the garment technology processes of the company under VINATEX.
- Comparing the shortcomings of each CF calculation process to draw experience to initially propose proposals to reduce CF emissions, thereby integrating green growth towards a low-carbon economy under Vietnam's conditions.

Due to the specificity of the textiles and garment industry, it can be easily calculated when we divide the production into 3 sectors and each sector has its own (CFU). Those 3 sectors are: Sector 1 (S1) is the manufacturing process, Sector 2 (S2) is the auxiliary process of production, Sector 3 (S3) is the production operation process. For the plants, monthly or annual data contained used energy and materials consumption data is easy to obtain. Accordingly, a solution combining the highly informative value of CF with a reasonable process-level allocation methodology is thought to be appropriate [5].

**SAFETY AND HEALTH MANAGEMENT**

The case study results are as follows: at Nha Be Garment JSC, the S2 of veston sewing accounts for the most, the highest in the finished product stage S2, up to more than 80% up to 80927,672 $KgCO_2e$, the average of 8 months. Because the space at the high-end veston garment factory has little natural light, production activities depend heavily on bulbs of up to 1100 bulbs that operate continuously for 10 hours/day. Hence the very high-power consumption in S2 leads to the highest GHG emissions in S2. While the highest value of the operating process is the loosing fabric process reaching a peak of 70039.25 kgCO2e. Because in the office block at this garment factory, many high-capacity devices such as computers, air conditioners, printers are installed. So the GHG emissions at this stage are the highest compared to the other 2 stages In particular, we see that S3 accounts for the highest percentage of the total in the stages, in the checking stage, the GHG emissions due to S3 is the highest, followed by S2. Specifically, in the checking stage S2 accounts for more than 60% of the GHG released in this process in Phong Phu JSC.

Enterprises should focus on GHG mitigation and solid waste reduction. Calculate the input materials, waste and associated costs at each stage of the production process. Enterprises need to fully comply with current environmental laws and understand the environmental requirements in the near future. Green production must be central to the management portfolio of the company. Pay real attention to employees and control the business development towards efficient green production. The goals can be to reduce production costs, reduce input costs, lower emissions and work safety.

Choosing the direction to reduce costs and meet environmental requirements. To cut costs and meet environmental requirements, businesses can choose from two directions. The non-tech direction needs to take precedence over because most involving operational improvements, controls, the idea of removing waste or changing materials are ideas that employees or staff members can suggest and execute. The main direction of technology is to improve or change technology, but this direction requires high costs and large changes in operations at the enterprise, so it is less priority and should only be considered.

**Keywords:** Carbon footprint; Greenhouse gas; Green growth; Vinatex.

**Acknowledgment**

This study was supported by Nguyen Tat Thanh University, Nhabe Garment Corporation, Phong Phu Internation al JSC.

**References**

[1] T.T.B.Nhung, T.T.P.Thuy, "Vietnam's Textile and Garment Industry: An Overview, journal Business & IT" **1**, 45-53 (2018).
[2] WWF Viet Nam, "*Guidelines for Greening the Textile Sector in Viet Nam*' **63**, (2019).
[3] N.T.Dung, *"Decision Approval of the National Green Growth Strategy"* **2,** No.1393/QĐ-TTg (2012).
[4] Jerome.M, Claude.C, Paul.V, "*The Viet Nam Green Growth Strategy: A review of specificities, indicators and research perspectives*" **11,** (2015).
[5] X.Li, L.Chen, X.Ding *"Allocation Methodology of Process-Level Carbon Footprint Calculation in Textile and Apparel Products"* **1,** Sustainability, (2019).
[6] Peters, M. Svanstrom, S. Roos, G. Sandin, B. Zaman, "*Handbook of Life Cycle Assessment (LCA) of Textiles and Clothing*" **22**. Elsevier. (2015).
https://en.vietnamplus.vn/vietnam-becomes-second-largest-garment-exporter/205709.vnp / (accessed 21.09.15).

2ND ENERGY SECURITY AND CHEMICAL ENGINEERING CONGRESS 2021
*"Sustainable Technological Solution for a Better World"*
VIRTUAL CONFERENCE | 3-5 NOVEMBER 2021

**SAFETY AND HEALTH MANAGEMENT**

**Paper ID: ESCE046**

# RECOGNIZING DESIGN ISSUES IN CHEMICAL PROCESS INDUSTRIES

**Z. Zakaria[1]*, K. Kidam[1,2]**

[1] *Faculty of Chemical & Natural Energy Engineering,* [2] *Centre of Hydrogen Energy Institute of Future Energy, Universiti Teknologi Malaysia, 81300 Skudai, Johor.*
*Corresponding author: zafirahbintizakaria@gmail.com

## Extended Abstract

Inherent Safety (IS) concept has been introduced for more than 45 years ago yet the application on chemical industries is still low. The accident in chemical industries did not decrease moreover some accident keep occurring. Researchers has found out that accident contributors are mainly related to design error of 45%. Therefore, this research was conducted to point out the design issues which exist in chemical processes. Knowing the design issue right before starting designing a process at early stages can eliminate and reduce most of process hazard which leads to a safer chemical process.

To achieve the objective, this research looked up into the accident cause analysis to listed up numbers of design failure elements (DFE) so that the general classification of design error can be highlighted. Then, a database of cases (that suggested design changes from unsafe to safe design) from journal, accident corrective action, product brochure and patents were assembled out to bring as many design issues (DI) that encountered by chemical process industries. The DI were then specifically classified under DFE.

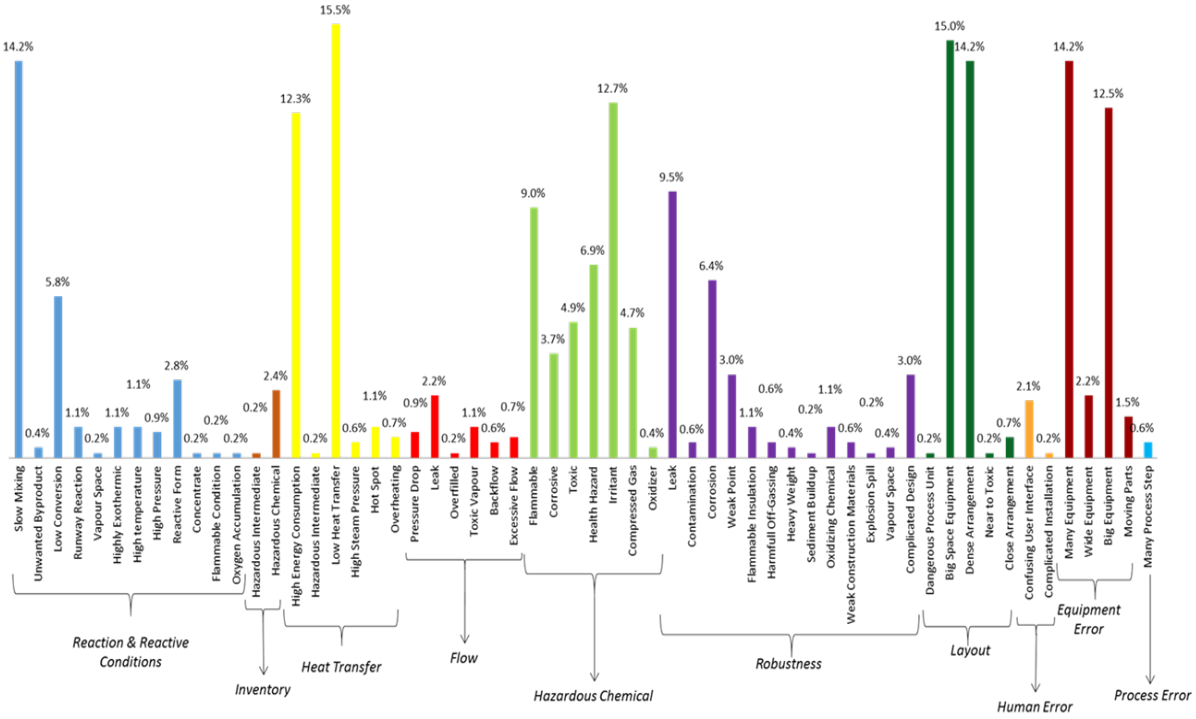


Fig. 1: Design Issues (DI) frequency according to Design Failure Elements (DFE).

The contribution of this paper includes frequency of DFE (equipment error 17.2%, heat transfer 17.2%, layout 17.1%, reaction & reactive condition 16.0%, robustness 15.2%, hazardous chemical 10.8%, flow 3.3%, inventory 1.5%, human error 1.3% and process error 0.3%), critical DI (low heat transfer 15.5%, big space equipment 15.0%, slow mixing 14.2%, dense arrangement 14.2%, many equipment 14.2%, irritant chemical 12.7%, big equipment 12.5%, high energy consumption 12.3%, leak 9.5%, and flammable chemical 9.0%). Moreover, DI were also classified according to 5 type of equipment (reaction equipment, separation equipment, heat transfer equipment, storage equipment and piping & piping system) and at different design stages (research & development, preliminary engineering, basic engineering and detailed engineering).

**Keywords:** Inherently Safer Design (ISD); Accident Contributor; Accident Analysis; Design Issues.

## Acknowledgment

The authors might want to acknowledge Universiti Teknologi Malaysia (UTM) and Ministry of Education Malaysia for the MyBrain15 scholarship.

## References

[1] Don, N. (2014) Human Error? No, Bad Design. Retrieved from https://www.linkedin.com/pulse/20140414212456-12181762-human-error-no-bad-design.
[2] Hussin, N.A.E., Kidam, K., Johari, A., Hashim, H. (2017) Suitability Analysis of Corrective Actions to Prevent Major Chemical Process Accidents. Jurnal Teknologi *3*(79), 97–106.
[3] Jalani, J.A., Kidam, K., Shahlan, S.S., Kamarden, H., Hassan, O., Hashim, H. (2015) An Analysis of Major Accident in the US Chemical Safety Board (CSB) Database. Jurnal Teknologi, 75(6), 53–60. https://doi.org/10.11113/jt.v75.5186.
[4] Jensen, R.C. (2007) Risk Reduction Strategies: Past, Present and Future. Professional Safety, *52*(1), 24–30.
[5] Kang, S. J. (1999) Trends in Major Industrial Accidents in Korea. Journal of Loss Prevention in the Process Industries, 12(1), 75–77. https://doi.org/10.1016/s0950-4230(98)00040-0.
[6] Kidam, K., Hurme, M., Hassim, M.H. (2010) Technical Analysis of Accident in Chemical Process Industry and Lesson Learnt. Chemical Engineering Transaction, 19, 451–456.
[7] Kidam, K., Hurme, M. (2012) Design as a Contributor to Chemical Process Accidents. Journal of Loss Prevention in the Process Industries, 25(4), 655–666. https://doi.org/10.1016/j.jlp.2012.02.002.
[8] Kidam, K., Hurme, M. (2013) Analysis of Equipment Failures as Contributors to Chemical Process Accidents. Process Safety and Environmental Protection, 91(1–2), 61–78. https://doi.org/10.1016/j.psep.2012.02.001.
[9] Koteswara R, G., Yarrakula, K. (2016) Analysis of Accidents in Chemical Process Industries in the Period 1998-2015. International Journal of ChemTech Research, 9(4), 177–191.
[10] Mannan, M.S., Sachdeva, S., Chen, H., Reyes-Valdes, O., Liu, Y., Laboureur, D.M. (2015) Trends and Challenges in Process Safety. AIChe Journal 61:11.
[11] Moura, R., Beer, M., Patelli, E., Lewis, J. (2012) Learning from Major Accidents to Improve System Design. Safety Science, 84, 37–45. https://doi.org/10.1016/j.ssci.2015.11.022.
[12] Nivolianitou, Z., Konstandinidou, M., Michalis, C. (2006) Statistical Analysis of Major Accidents in Petrochemical Industry Notified to the Major Accident Reporting System (MARS). Journal of Hazardous Materials, 137(1), 1–7. https://doi.org/10.1016/j.jhazmat.2004.12.042.
[13] Prem, K.P., Ng, D., Mannan, M.S. (2010) Harnessing Database Resources for Understanding the Profile of Chemical Process Industry Incidents. Journal of Loss Prevention in the Process Industries, 23(4), 549–560. https://doi.org/10.1016/j.jlp.2010.05.003.
[14] Tammineni, Y., Dakuri, T. (2020) Vizag Gas Leak – A Case Study on the Uncontrolled Styrene Vapour Release for the First Time in India. EPRA International Journal of Research & Development (IJRD), pp.13–24.
[15] Taylor, J.R. (2007) Statistics of Design Error in the Process industries. Safety Science, 45(1–2), 61–73. https://doi.org/10.1016/j.ssci.2006.08.013.
[16] Sales, J., Mushtaq, F., Christou, M.D., Nomen, R. (2007) Study of Major Accidents Involving Chemical Reactive Substances Analysis and Lessons Learned. Process Safety and Environmental Protection, 85(2 B), 117–124. https://doi.org/10.1205/psep06012.
[17] Vílchez, J.A., Sevilla, S., Montiel, H., Casal, J. (1995) Historical Analysis of Accidents in Chemical Plants and in the Transportation of Hazardous Materials. Journal of Loss Prevention in the Process Industries, 8(2), 87–96. https://doi.org/10.1016/0950-4230(95)00006-M.
[18] Zhao, L., Qian, Y., Hu, Q. M., Jiang, R., Li, M., Wang, X. (2018) An Analysis of Hazardous Chemical Accidents in China Between 2006 and 2017. Sustainability (Switzerland), 10(8). https://doi.org/10.3390/su10082935.
[19] Zhao, L., Zhu, W., Papadaki, M.I., Mannan, M.S., Akbulut, M. (2019) Probing into Styrene Polymerization Runway Hazard: Effects of the Monomer Mass Fraction. ACS Omega 8136-8145.

2ND ENERGY SECURITY AND CHEMICAL ENGINEERING CONGRESS 2021
*"Sustainable Technological Solution for a Better World"*
VIRTUAL CONFERENCE | 3-5 NOVEMBER 2021

**SAFETY AND HEALTH MANAGEMENT**

**Paper ID: ESCE101**

# INTEGRATED SPATIAL RISK ASSESSMENT OF GAS ACCUMULATION DURING ATMOSPHERIC INVERSION OVER OPERATING AREA IN THE DEEP OPEN PIT COAL MINE

**Somprasong K.[1]*, Hattakosol P.[1], Inta T.[1], Assawadithalerd M.[2]**

[1] *Department of Mining & Petroleum Engineering, Faculty of Engineering, Chiang Mai University, Chiang Mai, Thailand.*
[2] *Center of Excellence on Hazardous Substance Management (HSM), Chulalongkorn University, Pathumwan, Bangkok, 10330, Thailand.*
*Corresponding author: s.komsoon@gmail.com

## Extended Abstract

Opencast coal mining has been considered as one of the core industries, serving the energy sustainability of Thailand. In the increasing demand of electricity, the Mae Moh mine, the largest open pit coal mine in the Southeast Asia will reach approximately 600 m from the surface. The material removal capacity requires over 2,000 machineries during its full load, causing combustion gas emission. The numerous challenges in both monitoring and mitigation for safety, health, and environment's operation (SHE) of ambient air quality. In this study, the spatial multiple criteria decision-making scheme (SMDMC), meteorological simulation results from CALMET software and primary data of significant contaminants including CO, SO2, and NO2 from the monitoring station were integrated in a purpose of defining the possible area of the pit in which high negative effect can be sensed, especially for long term air quality monitoring. One of the definite adverse effects, causing by the altering of air quality during increasing of the pit depth is the atmospheric inversion. This phenomenon occurred over the basin, the particles suspend in the air underneath its layer and traps of contaminants at the ground surface causing negative effects to the operators. The results of spatial concentrations of air pollutants indicate that area of C2, which is the location of the deepest pit level, contains the highest potential risk in causing the negative effect to the mine-operators as can be followed in Table 1. Moreover, the high-risk area can be sensed at area of SE and SW-pit where dense hauling and burden removal activities were detected. The SMDMC integrated simulation using CALMET can be applicable for identifying the serious location from air pollutions and precaution of avoiding the exposure.

Table 1: Summarized of the potential risk from atmospheric inversion over the operating pit of the Mae Moh mine.

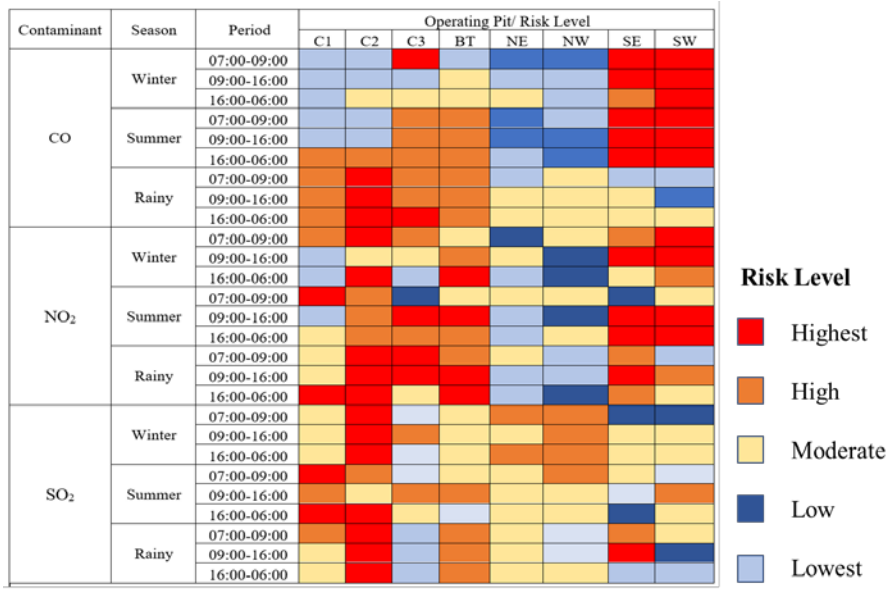

**SAFETY AND HEALTH MANAGEMENT**

**Keywords:** Spatial Risk Assessment; Combustion Gas; Deep Open Pit Coal Mine; SMCDM; CALMET; Mixing Hight.

## References

[1] Lee, T., et al., Respirable size-selective sampler for end-of-shift quartz measurement: Development and performance. Journal of occupational and environmental hygiene, 2017. **14**(5): p. 335-342.
[2] Li, Z., et al., Aerosol and boundary-layer interactions and impact on air quality. National Science Review, 2017. **4**(6): p. 810-833.
[3] Böhme, K. and P. Schön, From Leipzig to Leipzig. disP - The Planning Review, 2006. **42**(165): p. 61-70.
[4] Herrmann, S. and E. Osinski, Planning sustainable land use in rural areas at different spatial levels using GIS and modelling tools. Landscape and Urban Planning, 1999. **46**(1): p. 93-101.
[5] Domingo-Santos, J.M., et al., The visual exposure in forest and rural landscapes: An algorithm and a GIS tool. Landscape and Urban Planning, 2011. **101**(1): p. 52-58.
[6] Tassinari, P.T., D., Visual Impact Assessment Methodologies for Rural Building Design. The International Commission of Agricultural Engineering, 2006. **8**.
[7] Hernández, J., L. García, and F. Ayuga, Integration Methodologies for Visual Impact Assessment of Rural Buildings by Geographic Information Systems. Biosystems Engineering, 2004. **88**(2): p. 255-263.
[8] Hwang, C.-L. and K. Yoon, Methods for Multiple Attribute Decision Making, in Multiple Attribute Decision Making: Methods and Applications A State-of-the-Art Survey, C.-L. Hwang and K. Yoon, Editors., Springer Berlin Heidelberg: Berlin, Heidelberg, 1981 :p. 58-191.
[9] Malczewski, J., Visualization in multicriteria spatial decision support systems. GEOMATICA, 1999. **53**(2): p. 139-147.
[10] Roy, S., Spatial variation of soil physico-chemical properties influenced by spatial and temporal variation of litter in a dry tropical forest floor. Oecologia Montana, 1996. **5**(1): p. 21-26.
[11] Somprasong, K. and M. Assawadithalerd, Integrated spatial approaches for long-term monitoring of cadmium contamination caused by rainfall erosion: A case study of overland sediment in Mae Sot, Thailand. Physics and Chemistry of the Earth, Parts A/B/C, 2021. **121**: p. 102961.
[12] Park, J. and H.-Y. Jeong, The QoS-based MCDM system for SaaS ERP applications with Social Network. The Journal of Supercomputing, 2013. **66**(2): p. 614-632.
[13] Ayalew, L., Yamagishi, H., & Ugawa, N., Landslide susceptibility mapping using GIS-based weighted linear combination, the case in Tsugawa area of Agano River, Niigata Prefecture, Japan. Landslides, 2004. **1**(1): p. 73-81.
[14] Rashed, T. and J. Weeks, Assessing vulnerability to earthquake hazards through spatial multicriteria analysis of urban areas. International Journal of Geographical Information Science, 2003. **17**(6): p. 547-576.
[15] Pece V. Gorsevski, P.J. and a.P.E. Gessler, An heuristic approach for mapping landslide hazard byintegrating fuzzy logic with analytic hierarchy process. Control and Cybernetics, 2006. **35**(1): p. 121-146.

**SEPARATION TECHNOLOGY**

**Paper ID: ESCE013**

# ZIRCONIUM DIOXIDE NANO-HYBRIDS FOR ADSORPTION OF PALLADIUM AND GOLD

**Q. A. Trieu[1]*, T. H. Bui[2]**

[1] *Faculty of Environmental and Food Engineering, Nguyen Tat Thanh University, Ho Chi Minh, Vietnam.*
[2] *Faculty of Chemical and Food Technology, Ho Chi Minh City University of Technology and Education, Ho Chi Minh, Vietnam.*
*Corresponding author: tqan@ntt.edu.vn

## Extended Abstract

Management and recycling of e-waste closely relate to many sustainable development goals, including decent work & economic growth, good health & well-being, clean water & sanitation, and life below water. Hydrometallurgical techniques, particularly adsorption processes, have drawn significant attention due to their capabilities to recover a trace amount of noble metals in the effluents from recycling plants. In this study, the syntheses of surface-modified $ZrO_2$ nano-hybrids to capture efficiently and selectively Au (III) and Pd (II) ions were investigated. The resultant materials including thioctic acid (TOA), dioctyldiglycoamide (DODGA), (N, N)-bis (2- ethylhexyl) carbamoylmethylphosphonic acid (DEHCMPA), (N, N)-dioctylcarbamoylmethylphosphonic acid (DOCMPA), phosphonomethylimino diacetic acid (PMIDAA) surface-modified $ZrO_2$ nano-hybrids were extensively characterized using ATR-FTIR, TGA, $^{31}P$ solid-state NMR, BET, and elemental analysis (ICP-OES). Batch-mode adsorption experiments combined with the ICP-OES method conducted for Pd (II) and Au (III) adsorption on the fabricated materials showed that the thioctic acid-modified $ZrO_2$ nano-hybrid ($ZrO_2$-TOA) exhibited superior adsorption properties toward both Pd (II) and Au (III) among the hybrid adsorbents. It was found that the adsorption data of $ZrO_2$-TOA were well fitted to the Langmuir adsorption model. The adsorption kinetics of $ZrO_2$-TOA was described by the pseudo-second model in which chemical interaction between active sites of materials and target metals is the rate-limiting step. The $ZrO_2$-TOA nano-hybrid has demonstrated promising adsorption capabilities in the recovery of Pd and Au from industrial effluents.

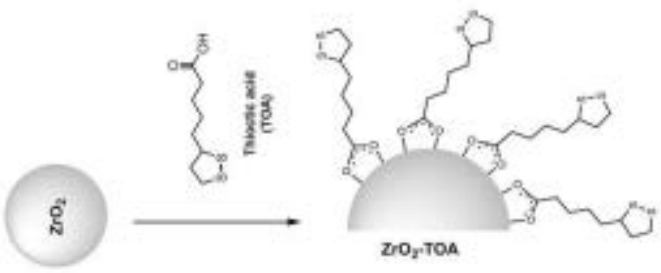


Fig. 1: Schematic representation of surface modification of nano-$ZrO_2$ with thioctic acid.

**Keywords:** Thioctic acid; Phosphonic acid; Hybrid nanomaterial; Surface-modified zirconia; Palladium and gold adsorption.

### Acknowledgment

This research was funded by Nguyen Tat Thanh University, Ho Chi Minh city, Vietnam.

### References

[1] Abd Razak, N. F., M. Shamsuddin & S. L. Lee (2018) Adsorption kinetics and thermodynamics studies of gold (III) ions using thioctic acid functionalized silica coated magnetite nanoparticles. Chemical Engineering Research and Design, 130, 18- 28.

## SEPARATION TECHNOLOGY

[2] Forti V., B. C. P., Kuehr R., Bel G. 2020. The Global E-waste Monitor 2020: Quantities, flows and the circular economy potential. ed. I. T. U. I. I. S. W. A. I. United Nations University (UNU)/United Nations Institute for Training and Research (UNITAR) – co-hosted SCYCLE Programme.

[3] Sánchez, J. M., M. Hidalgo & V. Salvadó (2001) The selective adsorption of gold (III) and palladium (II) on new phosphine sulphide-type chelating polymers bearing different spacer arms: Equilibrium and kinetic characterisation. Reactive and Functional Polymers, 46, 283-291.

[4] Aghaei, E., D. R. Alorro, N. A. Encila & K. Yoo (2017) Magnetic Adsorbents for the Recovery of Precious Metals from Leach Solutions and Wastewater. Metals, 7.

[5] Hancock, R. D. & A. E. Martell (1996) Hard and Soft Acid-Base Behavior in Aqueous Solution: Steric Effects Make Some Metal Ions Hard: A Quantitative Scale of Hardness-Softness for Acids and Bases. Journal of Chemical Education, 73, 654.

**SEPARATION TECHNOLOGY**

**Paper ID: ESCE020**

# SEPARATION OF STABLE OIL/WATER EMULSION BY USING COMMERCIAL MICROFILTRATION POLYVINYLIDENE FLUORIDE MEMBRANES

**C. K. Chiam[1,3]*, A. Darmarajoo[2], Z. Kamin[1,3], N. M. Ismail[2,3], R. Sarbatly[2,3]**

[1] *Oil & Gas Engineering,* [2] *Chemical Engineering,* [3] *Membrane Technology Research Group, Material and Mineral Research Unit, Universiti Malaysia Sabah, Jalan UMS 88400 Kota Kinabalu, Sabah, Malaysia.*
*Corresponding author: chiamchelken@ums.edu.my

## Extended Abstract

Oily wastewaters generated by various industries such as oil and gas, metal working, textile and paper, food processing, and pharmaceuticals are hazardous to the environment if discharging without treatment. Membrane filtration has been attractive in treating the oily wastewaters since few decades ago [1-3]. This work attempts to separate the oil from the water by coalescing the oil droplets by using two types of commercial polyvinylidene fluoride membranes: PVDF-Westran and PVDF-Synder membranes. Distilled water and a synthesised oily water are tested as the feed solutions. The permeate of each experiment is collected in a floatation vessel and three- layer fractions are visible after left for 1 day of settling. The oil droplet size distribution in the permeate is analysed by using a dynamic light scattering instrument. The membranes are characterised in terms of the pore size distribution and distilled water permeation flux. The permeability of the PVDF-Westran membrane was relatively higher than that of the PVDF-Synder membrane. The fibrous polypropylene layer that supported the PVDF-Synder membrane has significantly reduced the average membrane pore size and slightly increased the membrane thickness which essentially decreased the membrane permeability. Similar findings have been reported by Lohokare et al. [4] and Wei et al. [5] in their ultrafiltration and osmotic membrane systems, respectively. Compared with the oil droplet radius in the feed solution (20 – 180 nm), Fig. 1 shows the PVDF- Westran membrane can coalesce the oil droplets up to 0.55 µm while the PVDF-Synder membrane can enlarge the oil droplets to approximately 2.8 µm as presented in Fig. 2. The PVDF-Synder membrane with narrower pore sizes exhibited better performance than the PVDF-Westran membrane in the separation of oil-water.

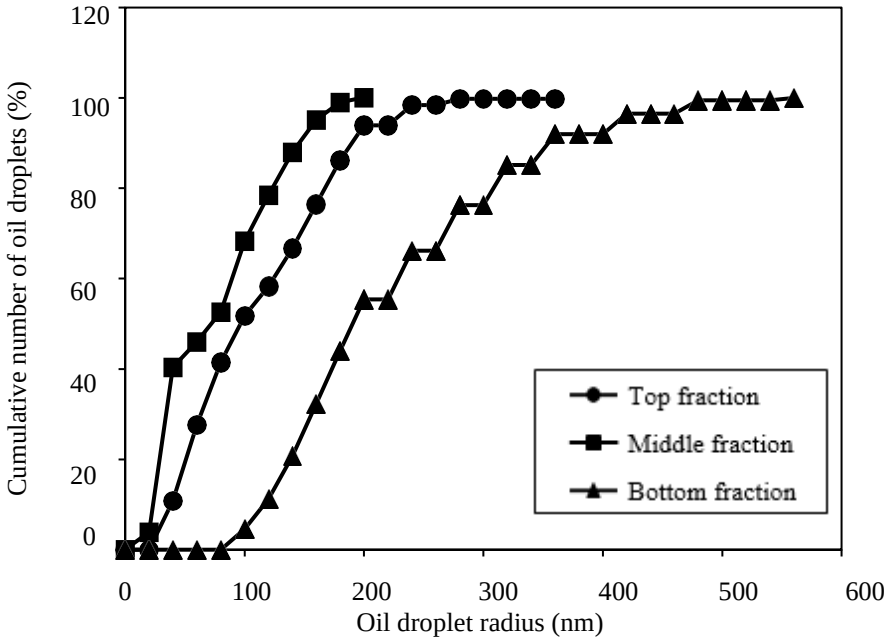


Fig. 1: Distribution of oil droplet radius in the permeate by using the PVDF-Westran microfiltration membrane.

**SEPARATION TECHNOLOGY**

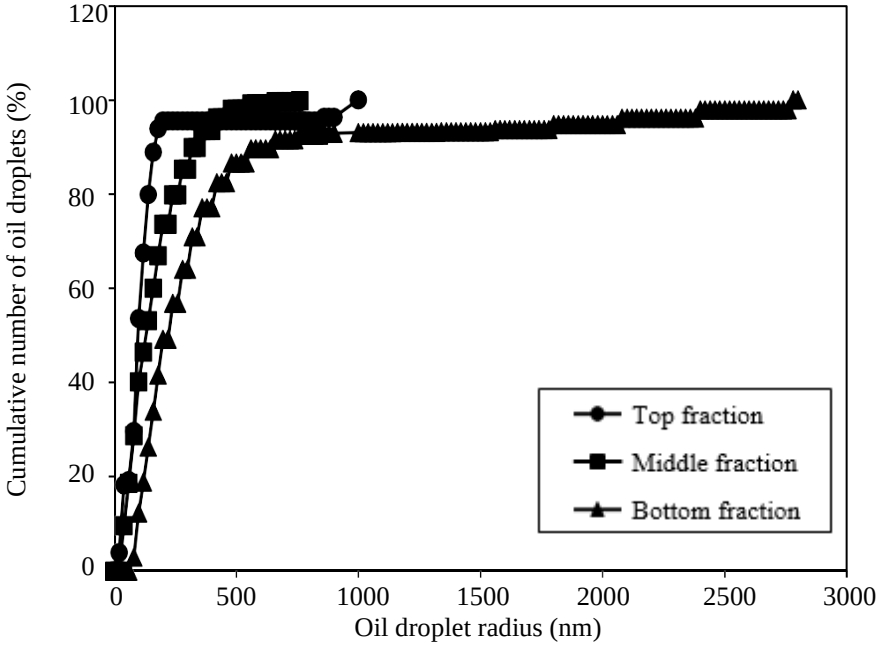


Fig. 2: Distribution of oil droplet radius in the permeate by using the PVDF-Synder microfiltration membrane.

**Keywords:** Oily water; Microfiltration; Coalescence; PVDF commercial membranes; Oil droplet.

**Acknowledgement**

The authors gratefully acknowledge the financial support from the Ministry of Higher Education Malaysia under the Fundamental Research Grant Scheme (FRG0418-TK-1/2015). The authors also wish to thank the research facilities provided by the Universiti Malaysia Sabah.

**References**

[1] Hong, A., Fane, A. G., & Burford, R. (2003). Factors Affecting Membrane Coalescence Of Stable Oil-In-Water Emulsions. J. Membr. Sci. 222: 19–39.
[2] Kumar, S., Nandi, B.K., Guria, C., & Mandal, A. (2017). Oil Removal From Produced Water By Ultrafiltration Using Polysulfone Membrane. Brazilian J. Chem. Eng. 34: 583–596.
[3] Rahimpour, A., Rajaeian, B., Hosienzadeh, A., Madaeni, S. S., & Ghoreishi, F. (2011). Treatment Of Oily Wastewater Produced By Washing Of Gasoline Reserving Tanks Using Self-Made And Commercial Nanofiltration Membranes. Des. 265: 190–198.
[4] Lohokare, H.R., Bhole, Y.S., Kharul, U.K. (2006). Effect of Support Material on Ultrafiltration Membrane Performance. J. Appl. Polym. Sci. 99: 3389 – 3395.
[5] Wei, J., She, Q., Liu, X. (2021). Insight Into The Influence of Membrane Permeability and Structure On Osmotically-driven Membrane Processes. Membranes. 11: 153 – 173.

**SEPARATION TECHNOLOGY**

**Paper ID: ESCE031**

# VISIBLE-LIGHT RESPONSIVE PVDF-ZnO/$Ag_2CO_3$/$Ag_2O$ MIXED MATRIX MEMBRANE WITH ENHANCED UF ANTIFOULING PROPERTIES AND PHOTOCATALYTIC-FILTRATION PERFORMANCE OF PHARMACEUTICAL REMOVAL

**Nurafiqah Rosman[1,2], Wan Norharyati Wan Salleh[1,2]*, Juhana Jaafar[1,2], Zawati Harun[3], Ahmad Fauzi Ismail[1,2], Nor Hafiza Ismail[1,2], Siti Zu Nurain Ahmad[1,2], Nur Aqilah Mohd Razali [1,2], Nor Asikin Awang[1,2]**

[1] *Advanced Membrane Technology Research Centre (AMTEC),* [2] *School of Chemical and Energy Engineering, Faculty of Engineering, Universiti Teknologi Malaysia, 81310 Skudai, Johor, Malaysia.*
[3] *Integrated Material and Process, Advanced Materials and Manufacturing Centre (AMMC), Faculty of Mechanical and Manufacturing Engineering, Universiti Tun Hussein Onn Malaysia, 86400 Parit Raja, Batu Pahat, Johor Darul Takzim, Malaysia.*
*Corresponding author: hayati@petroleum.utm.my

## Extended Abstract

Reports of pharmaceuticals exist in surface water and drinking water around the world, indicate they are ineffectively removed from water and wastewater using conventional treatment technologies. These pharmaceuticals can have adverse effects on public health and aquatic life, which has prompted the development of water treatment technology [1]. It is likely that membrane filtration and advances in oxidation can provide effective means for simultaneous degradation and separation in hybrid treatment processes [2]. The introduction of hybrid photocatalytic membrane for instance brings a new perspective and has a good potential in the field of pharmaceutical residue treatment.

Based on the integration concept of membrane and photocatalytic, the photocatalytic membrane is developed via incorporation of ZnO/$Ag_2CO_3$/$Ag_2O$ in polyvinylidene fluoride (PVDF) polymeric matrix membrane. These photocatalytic membranes were fabricated via phase inversion technique in flat sheet form. The PVDF membrane was incorporated with 0.5–3 wt% ZnO/$Ag_2CO_3$/$Ag_2O$ were produced in the UF range using PVP and lithium chloride as an additive altered its morphological and physicochemical properties. Characterization techniques, such as XRD, FTIR, SEM-EDX, and AFM were used to characterize the blended membranes as to analyze their structural and functional attributes. Further, the membranes were analyzed by using permeation techniques to analyze their flux profiles. Similarly, antifouling nature and hydrophilicity of the membranes were studied by permeating aqueous BSA solutions and measuring the dynamic water contact angle (DWCA), respectively.

Results showed that the modified membrane exhibited high BSA rejection of 98% and an improved anti-fouling property due to membrane's hydrophilicity and charge repulsion effect. Also, a significant improvement in UF performance in terms of membrane flux recovery was observed, signifying that the effect of protein fouling on membrane filtration was further reduced due to a lower degree of BSA fragment deposition in the membrane pores. Moreover, these composite membranes were also evaluated for pharmaceutical removal studies with ibuprofen (IBF) using a lab-scale photofiltration system. As the effluent circulates through the photo-filter system, the presence of light improved the composite membranes performance. The 2wt% of photocatalyst loading attributes highest IBF removal of 49.96% after 3 h reaction under the IBF flux of 21.51 $Lm^{-2}h^{-1}$ (as seen in Figure 1(a)). Also, the IBF removal and flux increased up to 92.38% and 61.76%, respectively. Results indicate that the introduction of ZnO/$Ag_2CO_3$/$Ag_2O$ in the PVDF hybrid photocatalytic membrane demonstrated a great potential for photocatalytic activities and stable reusability during IBF degradation. The photo-induced hydrophilicity phenomenon via ZnO/$Ag_2CO_3$/$Ag_2O$ photocatalyst was attributed to the increase in membrane hydrophilicity. As a result, when filtration of IBF was performed under light irradiation (photo-filtration), an increase of permeate flux could be obtained. An innovative photocatalytic membrane comprised of a ZnO/$Ag_2CO_3$/$Ag_2O$ composite was found to have bright prospect for continuous wastewater treatment.

**SEPARATION TECHNOLOGY**

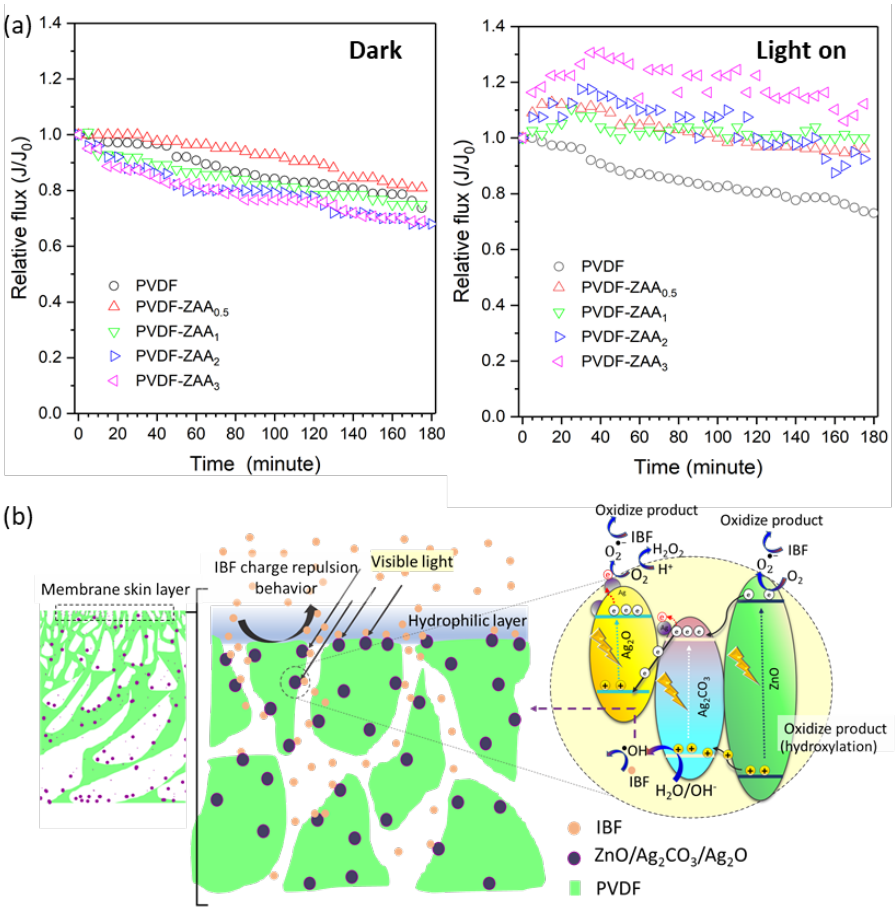


Fig. 1: (a) IBF permeation in the darkness and under visible light irradiation for prepared membranes; (b) Schematic illustration of IBF photodegradation with PVDF composite membrane. Enlarge is the photocatalytic mechanism over $ZnO/Ag_2CO_3/Ag_2O$

**Keywords:** Photocatalytic membrane; Ibuprofen; Photocatalyst; Antifouling; Multiple heterojunction.

## Acknowledgment

The authors gratefully acknowledge the financial support from the Ministry of Education and Universiti Teknologi Malaysia under Higher Institution Centre of Excellence Scheme (Project Number: R. J090301.7851.4J423) and UTM High Impact Research (Project Number: Q.J130000.2451.08G36). The authors would also like to acknowledge technical and management support from Research Management Centre (RMC), Universiti Teknologi Malaysia.

## References

[1] Nurafiqah Rosman, W.N.W. Salleh, Mohamad Azuwa Mohamed, J. Jaafar, A.F. Ismail, Z. Harun Hybrid membrane filtration-advanced oxidation processes for removal of pharmaceutical residue, Journal of Colloid and Interface Science 532 (2018) 236–260.
[2] Yahui Shi, Jinhui Huang, Guangming Zeng, Wenjian Cheng, Jianglin Hu; Photocatalytic membrane in water purification: is it stepping closer to be driven by visible light? Journal of Membrane Science 584 (2019) 364–392.

**SEPARATION TECHNOLOGY**

**Paper ID: ESCE065**

# PVDF/HMO MIXED MATRIX MEMBRANE COATED WITH L-DOPA/APTES VIA SPRAY COATING METHOD

**Nor Hafiza Ismail[1,2], Wan Norharyati Wan Salleh[1,2]*, Nurafiqah Rosman[1,2], Siti Zu Nur Ahmad[1,2], Ahmad Fauzi Ismail[1,2], Farhana Aziz[1,2], Norhaniza Yusof[1,2]**

[1] *Advanced Membrane Technology Research Centre (AMTEC),* [2] *School of Chemical and Energy Engineering, Faculty of Engineering, Universiti Teknologi Malaysia, Skudai, Johor Bahru, Malaysia.*
*Corresponding author: hayati@petroleum.utm.my

## Extended Abstract

Finding efficient, cost-effective, and environmentally friendly treatments to treat oily wastewater from industrial effluents is a challenging task. Untreated oily wastewater discharge negatively affects the aquatic ecosystem, the environment, and living organisms [1]. Membrane technology was utilized in this work to overcome these issues. The issue regarding membrane application in oil/water emulsion treatment is fouling [2]. Polymeric membrane is one of the promising candidates for membrane technology. However, polymeric membrane has some drawbacks that need to be overcome.

Polyvinylidene fluoride (PVDF)/ hydrous manganese dioxide (HMO) mixed matrix membrane (MMM) from previous study [3], after few hours of operation the water flux decline and resulted to membrane fouling when 1000 ppm oil emulsion was used as feed. Thus, this research is going to focus on the fouling issue. Where the MMM surface was altered using levodopa (L-DOPA) to improve the membrane's hydrophilicity and oleophobicity via spray coating (MMM LA).

First, the Tris-HCl solution was generated by stirring tris (hydroxymethyl)aminomethane (Tris) in 800 mL deionized water. Then, hydrochloric acid (HCl) was added gradually ~35m*l* until the solution reached to pH 8.5. The volume of the solution was adjusted to 1 L with deionized water. L-DOPA was first stirred in 100 mL Tris-HCl. After that, the obtained L-DOPA solution was sprayed directly to the PVDF/HMO surface with pressure of 0.5 bar and distance between the membrane and spray nozzle was approximately 20 cm. Low pressure was utilized to avoid the membrane from damaged. The sprayed membrane was left for 24 h before rinsed with deionized water. Then, the membrane was further immersed in deionized water to remove impurities before dried.

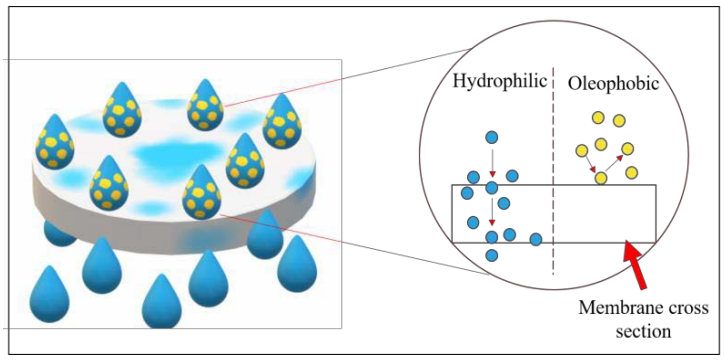


Fig. 1: The mechanism of fabricated L -DOPA/APTES layer on PVDF/HMO.

Fig. 1 illustrates the mechanism that occurred during the separation of synthetic oil/water emulsion separation. The presence of L-DOPA layer increase the affinity of the membrane surface and water molecule [4]. The oil droplets was repelled when it contact on the membrane surface. On the other hand, water droplets immmediately penetrated into the membrane. This was proved by the water contact angle value, as the water droplets completely penetrated into the membrane in short time (less 2 min). Meanwhile, the oil droplets of the coated MMM has greater value contact angle as the L-DOPA layer can reduce and weakend the interaction of the oil from membrane

surface [5]. These wetting properties is excellent for membrane to be applied in oily wastewater treatment. The water flux performance of the MMM LA greater than PVDF/HMO MMM when 1000 ppm oil emulsion was used.

**Keywords:** Oil/water separation; Oily wastewater; Hydrophilic membrane; Oil emulsion; Coating method.

## Acknowledgment

The authors would like to thank the Ministry of Education and Universiti Teknologi Malaysia for the financial support provided under Fundamental Research Grant Scheme Fundamental Research Grant Scheme (FRGS/1/2020/STG05/UTM/02/1, VOT NO. 5F369) and UTM High Impact Research Grant (Project Number: Q.J130000.2451.08G36) in completing this work. N.H. Ismail would like to acknowledge the support from Universiti Teknologi Malaysia for ZAMALAH scholarship.

## References

[1] Zhao, C, Zhou, J., Yan, Y., Yang, L., Xing, G., Li, H., Wu, P., Wang, M., Zheng, H. (2020) Application of coagulation/flocculation in oily wastewater treatment: A review. Sci. Total Environ. 142795.
[2] Ikhsan, S.N.W., Yusof, N., Aziz, F., Misdan, N., Ismail, A.F., Lau, W.J., Jaafar, J., Salleh, W.N.W., Hairom, N.H.H. (2018) Efficient separation of oily wastewater using polyethersulfone mixed matrix membrane incorporated with halloysite nanotube-hydrous ferric oxide nanoparticle. Sep. Purif. Technol. 199: 161-169.
[3] Ismail, N. H., Salleh, W. N. W., Awang, N. A., Ahmad, S. Z. N., Rosman, N., Sazali, N., Ismail, A. F. (2019) PVDF/HMO ultrafiltration membrane for efficient oil/water separation. Chem. Eng. Comms. 208:463-473.
[4] Mu, K., Zhang, D., Shao, Z., Qin, D., Wang, Y., Wang, S. (2017) Enhanced permeability and antifouling performance of cellulose acetate ultrafiltration membrane assisted by L-DOPA functionalized halloysite nanotubes. Carbohydr. Polym. 174:688-696.
[5] Vatanpour, V., Esmaeili, M., Farahani, M. (2014). Fouling reduction and retention increment of polyethersulfon nanofiltration membranes embedded byamine-functionalized multi-walled carbon nanotubes. J. Membr. Sci. 466: 70–81.

**SEPARATION TECHNOLOGY**

**Paper ID: ESCE072**

# EFFECTS OF DIFFERENT SOLVENTS ON THE PREPARATION OF ZEOLITIC IMIDAZOLATE FRAMEWORK-8 (ZIF-8) FOR THE REMOVAL OF LEAD AND CADMIUM

**S. Z. N. Ahmad[1,2], W. N. W. Salleh[1,2]*, N. H. Ismail[1,2], N. Rosman[1,2], M. Z. M. Yusop[1,3], R. Hamdan[4], A. F. Ismail[1,2]**

[1] *Advanced Membrane Technology Research Centre (AMTEC),* [2] *School of Chemical and Energy Engineering,* [3] *School of Mechanical Engineering, Faculty of Engineering, Universiti Teknologi Malaysia, 81310 Skudai, Johor Bahru, Malaysia.*
[4] *Micro-pollutant Research Centre (MPRC), Faculty of Civil Engineering and Built Environment, Universiti Tun Hussein Onn Malaysia, 86400 Parit Raja, Batu Pahat, Johor, Malaysia.*
*Corresponding author: hayati@petroleum.utm.my

## Extended Abstract

The harmful effects of heavy metals on human and environment have been widely discussed and more efforts could be seen on the removal of heavy metals from the ecosystem. Lead (Pb) and cadmium (Cd) are common heavy metals associated with different industries such as batteries, paints and electroplating industries [1]. These industrial wastewaters introduced lead and cadmium onto the water bodies which caused water pollution. Adsorption is one of the most frequently used method in the treatment of wastewater due to its simplicity, low-cost, and varieties of potential sorbents [2]. Potential adsorbents should have high porosity, high specific surface area, as well as suitable functional groups for heavy metals removal. Zeolitic imidazolate framework-8 (ZIF-8) is one type of metal organic framework and has large specific surface area and highly porous, which makes it a good option in heavy metals removal [3]. The purity of ZIF-8 particles is mainly influenced by the crystallization temperature, type of solvents, and content of linkers. Besides that, the synthesis conditions such as zinc source, ratio of zinc and 2-methylimidazole, temperature, and solvents affect the properties of the prepared ZIF-8, including the morphology, particle size, and pore distribution. The different solvents used have thermodynamic and kinetic impacts on coordinating the self-assembly process of the prepared ZIF-8 thus affecting their performance in removing heavy metals.

Therefore, this study utilizes ZIF-8 synthesized using different solvent, which are aqueous water (ZIF-8 (H), methanol (ZIF-8) (M)), and aqueous ammonia (ZIF-8 (N)) as the adsorbents to remove Pb and Cd from the synthetic wastewater. The effects of solvents on the morphology and particle sizes were explored. The adsorbents were characterized using X-ray Diffractometer (XRD), Scanning Electron Microscopy with Energy Dispersive X-ray (SEM-EDX), and Fourier Transform Infrared Spectrometer (FTIR). Figure 1 shows the SEM image of ZIF-8 (N) which confirmed that the ZIF-8 formed had cubic shapes, similar with previous studies [4]. ZIF-8(N) obtained the biggest average size of 573.4 nm, followed by ZIF-8 (H) and ZIF-8 (M) which produced smaller average size of ZIF-8 cubes, with 108.92 and 61.86 nm, respectively.

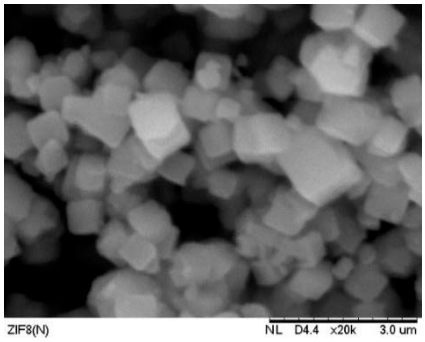


Fig. 1: SEM image of ZIF-8 (N).

For the performance studies of adsorbents in removing Pb and Cd, the effects of operating parameters such as pH, dosage, contact time, and initial concentration were studied for all adsorbents. Generally, ZIF-8 (N) had the greatest performance in removing Pb, whereas ZIF-8 (H) performed the best in removing Cd. Although ZIF-8 (N) have the biggest size, its surface charge and higher tendency to not agglomerate had caused the increase in specific surface area for adsorption. The optimum operating parameters obtained were at neutral pH and 100 ppm initial concentration for both Pb and Cd, and optimum dose of 20 mg for Pb and 5 mg for Cd. ZIF-8 (N) showed rapid equilibrium time for Pb and Cd adsorption, which was within 15 min, whereas ZIF-8(H) took 240 min and ZIF-8 (M) took 300 min to reach equilibrium. The Pb and Cd adsorption isotherm using ZIF-8s follows Langmuir isotherm which indicated the monolayer sorption. Meanwhile, the adsorption kinetic follows pseudo-second order kinetic model which suggested that chemisorption occurred during the adsorption of Pb and Cd on the surface of ZIF-8s. The Langmuir maximum adsorption capacity for Pb was 454.54, 434.78, and 476.19 mg/g, and 312.50, 277.78, and 263.16 mg/g for Cd while using ZIF-8 (H), ZIF-8 (M), and ZIF-8 (N) adsorbents, respectively. Therefore, all ZIF-8 adsorbents synthesized using different solvent showed excellent performance in removing Pb and Cd, which can be potential adsorbents for wastewater remediation.

**Keywords:** Adsorption; Heavy metals; Solvent; Wastewater treatment; ZIF.

## Acknowledgment

The authors would like to thank the Ministry of Education and Universiti Teknologi Malaysia for the financial support provided under Fundamental Research Grant Scheme Fundamental Research Grant Scheme (FRGS/1/2020/STG05/UTM/02/1, VOT NO. 5F369) and UTM High Impact Research Grant (Project Number: Q.J130000.2451.08G36) in completing this work. S. Z. N. Ahmad would like to acknowledge the support from Universiti Teknologi Malaysia for ZAMALAH scholarship.

## References

[1] Boskabady M., Marefati N., Farkhondeh T., Shakeri F., Farshbaf A. (2018) Environ Int. 120:404–20.
[2] Ahmad S. Z. N., Salleh W. N. W., Ismail N. H., Rosman N., Razali N. A. M., Hamdan R., et al. (2021) Mater. Today Proc. 42:8–14.
[3] Wang J., Li Y., Lv Z., Xie Y., Shu J., Alsaedi A., et al. (2019) J. Colloid Interface Sci. 542:410–20.
[4] Chi W. S., Hwang S., Lee S. J., Park S., Bae Y. S., Ryu D. Y., et al. (2015) J. Memb. Sci. 2015;495:479–88.

**SEPARATION TECHNOLOGY**

**Paper ID: ESCE099**

# EVIDENCE OF LOSS OF $N_2/O_2$ ADSORPTION SELECTIVITY OF LILSX DUE TO ION EXCHANGE BETWEEN SODIUM AEROSOL AND LITHIUM CATIONS

**N. Ardhan[1,2], S. Tontisirin[1], S. Nuchdang[3], A. Kongnoo[4], C. Phalakornkule[1,2]***

[1] *Department of Chemical Engineering, Faculty of Chemical Engineering,*
[2] *Research Center for Circular Products and Energy, King Mongkut's University of Technology North Bangkok, 1518 Pracharat 1 Rd., Bangkok, 10800, Thailand.*
[3] *Research and Development Division, Thailand Institute of Nuclear Technology, Pathumtani, 12120, Thailand.*
[4] *Faculty of Environmental Management, Prince Songkla University, Hat Yai, Songkhla, 90110, Thailand.*
*Corresponding author: chantaraporn.p@eng.kmutnb.ac.th

## Extended Abstract

**Objective**
Generation of oxygen using pressure swing adsorption (PSA) has been commercialized for a few decades. However, the efficiency of the adsorption process in purifying $O_2$ has typically dropped with operating times. A main drawback of the PSA process for $O_2$ production is the loss of the selective $N_2$ adsorption capacity of the zeolite adsorbent over time. A well-known cause of the loss of $N_2$ adsorption capacity of the zeolite in the PSA process is the adsorption of water molecules on the active sites of zeolite X [1]. However, it has been shown that conventional heating and ultrasound-assisted heating can effectively desorb water molecules from the adsorption sites of zeolite 13X [2]. It has been reported that an amount of $Li^+$ in the zeolite of greater than 70% occupancy is very important for maintaining the effectiveness of the zeolite for adsorbing $N_2$ [3]. However, as far as the authors are aware, neither studies of $Li^+$ loss from the zeolite structure nor $Li^+$ transport mechanism in zeolite pores has been reported in the literature.

In this study, the reasons for the loss of adsorption capacity of zeolite adsorbent were investigated by carrying out physical and chemical characterizations of zeolite samples collected from a commercial PSA-based $O_2$ generator, which were identified as LiLSX zeolite. As will be illustrated later, adsorption of water molecules in this commercial zeolite as well as the replacement of $Li^+$ with $Na^+$ were two major causes for the loss of $N_2$ adsorption capacity of the zeolite samples.

**Materials and methods**
Three adsorbent samples of zeolite obtained from a commercial oxygen generator were used in this study: (1) an active sample of zeolite which has a capability of producing ca. 94% $O_2$ (v/v); (2) an inactive sample of zeolite from a commercial oxygen generator which had lost its ability to produce high purity $O_2$; (3) a regenerated sample obtained by drying an inactive sample at 200 °C and pressure of 90 kPa for 12 h. Characterizations of the zeolite samples were performed using the methods and equipment described in [4].

A PSA process was set up to evaluate the efficiency of the zeolite samples in producing enriched $O_2$ from air. The PSA unit consisted of two carbon steel columns, each had a diameter and height of 6 cm and 40 cm, respectively. The columns were packed with about 0.9 kg of each zeolite sample per column. The PSA was operated automatically by smart relays in a four step-cyclic mode: (1) pressurization 25 s, (2) adsorption 25 s, (3) blow down 25 s, (4) purge 25 s.

Ion exchange experiments
Liquid-phase ion exchange: 1 g of each adsorbent sample was immersed in 100 mL of 1 M NaCl. The suspension was agitated at 50 °C for 24 h. After that, the suspension was filtered and the filtrate was collected for the measurement of $Li^+$ cation concentration.

## SEPARATION TECHNOLOGY

Gas-phase ion exchange: an experimental unit was set up to prepare sodium aerosol. The wet air was allowed to flow through an adsorption column containing an active zeolite sample for 122 h. After the wet air flow, the zeolite sample, referred to as an exposed sample, was collected for the analysis of elemental compositions.

**Results and discussion**

After being employed for purifying $O_2$ from humid air in an adsorption process for a certain period, the degree of crystallinity of LiLSX zeolite dropped only slightly, while the surface area dropped remarkably from > 700 to 400 $m^2/g$. Vacuum heating of the LiLSX zeolite could bring the BET surface area back up to ca. 700 $m^2/g$. However, the efficiency of the LiLSX zeolite in separating $N_2/O_2$from humid air could not be recovered due to the replacement of $Li^+$ with $Na^+$ ions. It was found that the substitution of $Na^+$ for $Li^+$ in the zeolite structure also caused deformation of the initial zeolite structure. The results from this study showed that both water molecules and airborne salinity in a working environment were detrimental to LiLSX zeolite.

Table 1: BET surface areas and pore volumes of active, inactive and regenerated zeolite samples.

| Sample | BET surface area ($m^2/g$) | $V_{pore}$ ($cm^3/g$) | $V_{micro}$ ($cm^3/g$) | $V_{meso}$ ($cm^3/g$) |
|---|---|---|---|---|
| Active zeolite | 711 | 0.343 | 0.259 | 0.084 |
| Inactive zeolite | 400 | 0.271 | 0.142 | 0.129 |
| Regenerated zeolite | 696 | 0.343 | 0.251 | 0.092 |
| Exposed zeolite (122 h) | 262 | 0.169 | 0.090 | 0.079 |

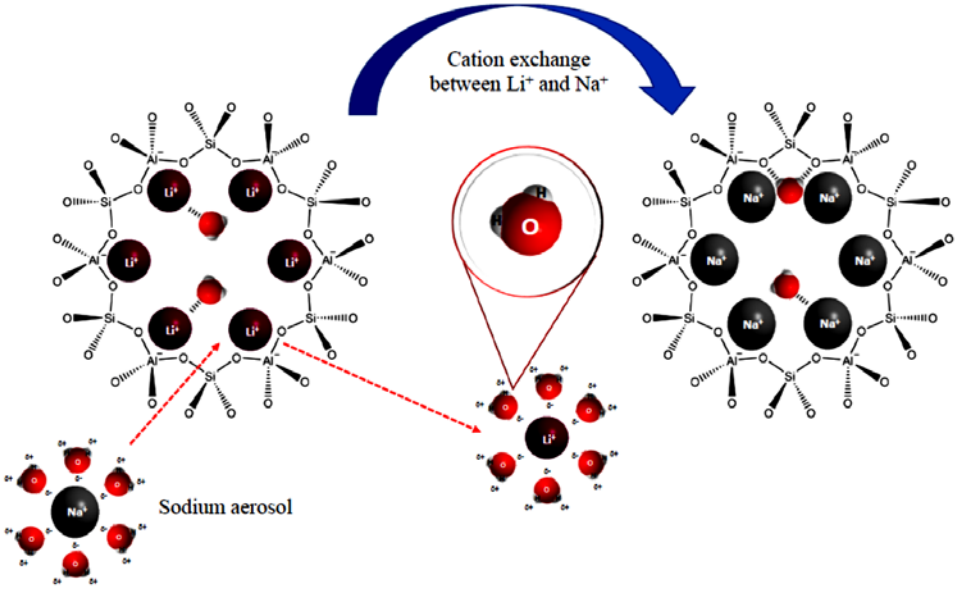


Fig 1: A proposed mechanism for the replacement of $Li^+$ with $Na^+$ ions in LiLSX zeolite.

**Conclusion**

It was illustrated that the adsorption of water molecules on a lithium-exchanged low silica X (LiLSX*)* zeolite and the replacement of $Li^+$ with $Na^+$ in the zeolite structure were major causes for the loss of selective adsorption of the zeolite. While the water molecules could be desorbed and the surface area of the adsorbent could be regained by vacuum heating at 200 °C and 90 kPa, the $N_2/O_2$ separation efficiency of the adsorbent could not be recovered. An elemental composition analysis showed that when an active LiLSX was placed in a high salinity, wet air flow, there occurred gas-phase ion exchange between $Na^+$ and $Li^+$ cations. The results from this study showed that airborne salinity in a working environment was detrimental to adsorption processes with LiLSX zeolite as the adsorbent.

**Keywords:** Adsorption; LiX zeolite; LiLSX; Oxygen; Regeneration.

**SEPARATION TECHNOLOGY**

## Acknowledgment

The authors are grateful for the research funding from the National Science and Technology Development Agency (NSTDA) of Thailand (Grant No. FDA-CO-2560-4809-TH; Project No. P-16-50237) and King Mongkut's University of Technology North Bangkok under grant No. KMUTNB-BasicR-64-28-16.

## References

[1] Oh H.T., Lim S.J., Kim J.H., Lee C.H. (2017) Adsorption equilibria of water vapor on an alumina/zeolite 13X composite and silica gel. J. Chem. Eng. Data 62: 804-811.
[2] Sayilgan Ş.Ç., Mobedi M., Ülkü S. (2016) Effect of regeneration temperature on adsorption equilibria and mass diffusivity of zeolite 13x-water pair. Microporous Mesoporous Mater. 224: 9-16.
[3] Chao C.C. (1989) Process for separating nitrogen from mixtures thereof with less polar substances, U.S. Patent No. 4 859 (1989) 217.
[4] Kongnoo A., Tontisirin S., Worathanakul P., Phalakornkule C. (2017) Surface characteristics and $CO_2$ adsorption capacities of acid-activated zeolite 13X prepared from palm oil mill fly ash. Fuel 193: 385-394.

**SEPARATION TECHNOLOGY**

**Paper ID: ESCE135**

# COMPARATIVE BETWEEN VERTICAL AND HORIZONTAL PANEL ORIENTATION FOR OPTIMUM SURFACE PATTERNING EFFECT

**Wan Nur Aisyah Wan Osman[1,2] *, Normi Izati Mat Nawi[1], Shafirah Samsuri[1,2], Suzana Yusup[1,2], Muhammad Roil Bilad[3]**

[1] *Chemical Engineering Department,* [2] *HICoE Centre for Biofuel and Biochemical Research, Institute of Self-Sustainable Building, Universiti Teknologi PETRONAS, 32610, Seri Iskandar, Perak, Malaysia.*
[3] *Department of Chemistry Education, Universitas Pendidikan Mandalika (UNDIKMA), Jl. Pemuda No. 59A, Mataram 83126, Indonesia.*
*Corresponding author: wan_19001650@utp.edu.my

## Extended Abstract

It is well-known that aeration is an efficient method to reduce fouling formation for the membrane-based system. In recent years, membrane surface patterning has come forward as an innovation that would increase the efficiency of aeration by enhancing the scouring action of air bubbles. Many studies reported that the combination of aeration and membrane surface patterning showed excellent membrane-based system performance for various applications. In this study, another method known as membrane panel orientation was evaluated to observe the performance of membrane-based microalgae harvesting to apply *Chlorella vulgaris* filtration. The aim is to determine the most optimum panel orientation that would maximize the surface patterning effect, as well as an improvement for a combined method of aeration and membrane surface patterning as membrane fouling control technique. Hence, the main focus is to select the best panel orientation that would give higher permeability increment in terms of surface patterning effect.

Two types of membrane were fabricated in this study: flat membrane (FM) and corrugated membrane (CM). FM has a flat and smooth surface (without surface patterning method) while CM has hills and valleys topography (with surface patterning method). For the preparation of CM, an additional step was added, which was known as the imprinting step (spacer was placed and pushed on top of the cast film) to create a membrane with surface corrugation. This additional step was excluded for the fabrication of FM. The membrane filtration performance for this study was assessed in a crossflow filtration system. The membrane performance was evaluated in terms of membrane panel orientation. Both FM and CM would be tested under different panel orientation (tilting angle), and different operating transmembrane (TMP) applied. The main purpose of this study was to determine the optimum panel orientation that would maximize the surface patterning effect. Hence, this study investigated the effect of surface patterning on the improvement of membrane performance via permeability increment. The permeability increment due to surface patterning was calculated using Eq. 1.

$$Permeability\ increment = \frac{(L_{CM} - L_{FM})}{L_{CM}}\ x\ 100\% \quad (1)$$

where $L_{CM}$ is the permeability for CM (L/(m$^2$hrbar)) and $L_{FM}$ is the permeability for FM (L/(m$^2$hrbar)).

First of all, the effect of panel orientation was measured to find out the most optimum tilting angle that could have higher membrane permeability. The tilting angle measured were 0º (vertical), 15º, 30º, 45º, 60º, 75º and 90º (horizontal) in an aerated membrane system under constant TMP (10 kPa). Results showed that permeability increases as the tilting angle increases from 0º to 90º, with a permeability of CM is higher than FM under all applied tilted angles (refer to Figure 1). The highest permeability increment observed was at 0º (vertical) with a value of 20.5 %.

Even though the highest permeability increment was reported at the membrane in vertical panel orientation, the highest permeability shown for both CM and FM in previous Figure 1 was at horizontal panel orientation with 746 and 623 L/(m$^2$hrbar), respectively. Hence, panel orientation effects specifically at 0º (vertical) and 90º (horizontal) were further evaluated under various operating TMP applied (2.5, 5, 7.5, 10, 12.5, 15, 17.5 and 19

**SEPARATION TECHNOLOGY**

kPa) for both FM and CM. Based on Figure 2, it was found that the trend for permeability increment was inconsistent. For the horizontal panel, the highest found was 17.30 % at operating TMP of 5 kPa. Meanwhile, the highest permeability increment found for the vertical panel was 21.65 % at an operating TMP of 2.5 kPa. Even at most operating TMPs value (from 2.5 kPa till 12.5 kPa), vertical panel showed higher permeability increment than the horizontal membrane.

On the other hand, by referring to Figure 2, it was observed that at higher operating TMP (15 kPa till 19 kPa), the permeability increment for both vertical and horizontal panel orientation was similar. This is where the membrane compaction phenomenon was discovered. Membrane compaction is defined as physical compression on the membrane due to either high operating pressure or high operating pressure. A higher rate of membrane compaction would negatively affect membrane performance (high compaction lead to low permeability).

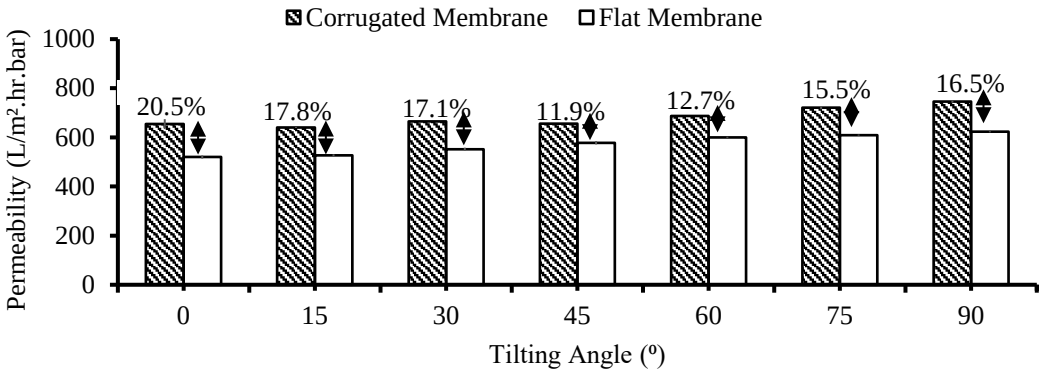


Fig. 1: Permeability versus tilting angle for flat and corrugated membrane.

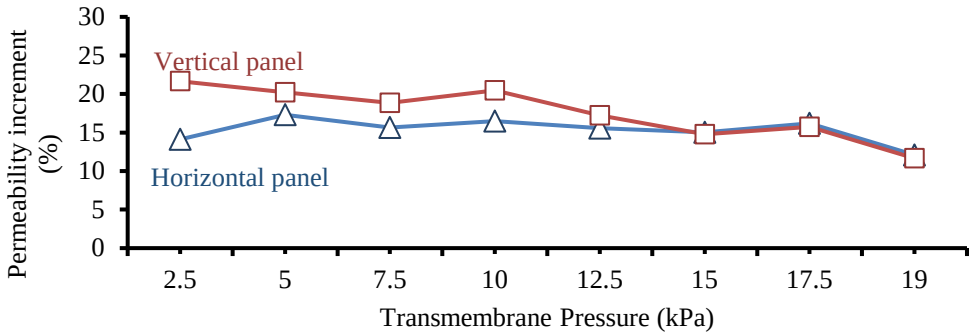


Fig. 2: Permeability increment due to surface patterning for vertical and horizontal panel orientation.

This study proved that the highest TMP would negatively affect membrane performance due to the membrane compaction phenomenon. The compaction phenomenon was difficult to be removed, even by the presence of aeration. Hence, this study recommended an operated membrane system in low TMP applied coupled with aeration as a fouling control technique for applying membrane-based microalgae harvesting. In addition, a new finding highlighted in this study was the panel orientation that maximizes the surface patterning effect for aerated membrane system. It was found that membrane in vertical panel orientation showed a higher permeability increment than horizontal panel orientation at most of the operating TMP applied (from 2.5 to 12.5 kPa). Hence, a new suggestion from this study was to use vertical CM at the lowest operating TMP (2.5 kPa) under an aerated membrane system that could overcome the limitations of both fouling formation and membrane compaction phenomenon.

**Keywords:** Fouling control; Membrane compaction; Microalgae filtration; Surface patterning; Panel orientation.

**Acknowledgement**

This study was supported by PETRONAS via YUTP-FRG (Cost Centre: 015LC0-079).

## References

[1] I. Barros, A. L. Gonçalves, M. Simões, and J. C. M. Pires, "Harvesting techniques applied to microalgae: A review," *Renewable and Sustainable Energy Reviews*, vol. 41, pp. 1489–1500, Jan. 2015, doi: 10.1016/j.rser.2014.09.037.

[2] A. Gonçalves, M. Alvim-Ferraz, F. Martins, M. Simões, and J. Pires, "Integration of Microalgae-Based Bioenergy Production into a Petrochemical Complex: Techno-Economic Assessment," *Energies*, vol. 9, no. 4, p. 224, Mar. 2016, doi: 10.3390/en9040224.

[3] N. Uduman, Y. Qi, M. K. Danquah, G. M. Forde, and A. Hoadley, "Dewatering of microalgal cultures: A major bottleneck to algae-based fuels," *Journal of Renewable and Sustainable Energy*, vol. 2, no. 1, p. 012701, Jan. 2010, doi: 10.1063/1.3294480.

[4] L. Brennan and P. Owende, "Biofuels from microalgae—A review of technologies for production, processing, and extractions of biofuels and co-products," *Renewable and Sustainable Energy Reviews*, vol. 14, no. 2, pp. 557–577, Feb. 2010, doi: 10.1016/j.rser.2009.10.009.

[5] Y. Chisti, "Biodiesel from microalgae," *Biotechnology Advances*, vol. 25, no. 3, pp. 294–306, May 2007, doi: 10.1016/j.biotechadv.2007.02.001.

[6] I.-S. Chang, P. Le Clech, B. Jefferson, and S. Judd, "Membrane Fouling in Membrane Bioreactors for Wastewater Treatment," *Journal of Environmental Engineering*, vol. 128, no. 11, pp. 1018–1029, Nov. 2002, doi: 10.1061/(ASCE)0733-9372(2002)128:11(1018).

[7] C. Visvanathan, R. B. Aim, and K. Parameshwaran, "Membrane Separation Bioreactors for Wastewater Treatment," *Critical Reviews in Environmental Science and Technology*, vol. 30, no. 1, pp. 1–48, Jan. 2000, doi: 10.1080/10643380091184165.

[8] W. Guo, H.-H. Ngo, and J. Li, "A mini-review on membrane fouling," *Bioresource Technology*, vol. 122, pp. 27–34, Oct. 2012, doi: 10.1016/j.biortech.2012.04.089.

[9] X. Shi, G. Tal, N. P. Hankins, and V. Gitis, "Fouling and cleaning of ultrafiltration membranes: A review," *Journal of Water Process Engineering*, vol. 1, pp. 121–138, Apr. 2014, doi: 10.1016/j.jwpe.2014.04.003.

[10] A. Eliseus, M. R. Bilad, N. A. H. M. Nordin, Z. A. Putra, and M. D. H. Wirzal, "Tilted membrane panel: A new module concept to maximize the impact of air bubbles for membrane fouling control in microalgae harvesting," *Bioresource Technology*, vol. 241, pp. 661–668, Oct. 2017, doi: 10.1016/j.biortech.2017.05.175.

[11] A. Eliseus and M. R. Bilad, "Improving membrane fouling control by maximizing the impact of air bubbles shear in a submerged plate-and-frame membrane module," Kedah, Malaysia, 2017, p. 020039. doi: 10.1063/1.5005372.

[12] N. U. Barambu, M. R. Bilad, Y. Wibisono, J. Jaafar, T. M. I. Mahlia, and A. L. Khan, "Membrane Surface Patterning as a Fouling Mitigation Strategy in Liquid Filtration: A Review," *Polymers*, vol. 11, no. 10, p. 1687, Oct. 2019, doi: 10.3390/polym11101687.

[13] I. G. Rácz, J. G. Wassink, and R. Klaassen, "Mass transfer, fluid flow and membrane properties in flat and corrugated plate hyperfiltration modules," *Desalination*, vol. 60, no. 3, pp. 213–222, Jan. 1986, doi: 10.1016/0011-9164(86)85001-9.

[14] K. Scott, A. J. Mahmood, R. J. Jachuck, and B. Hu, "Intensified membrane filtration with corrugated membranes," *Journal of Membrane Science*, vol. 173, no. 1, pp. 1–16, Jul. 2000, doi: 10.1016/S0376-7388(00)00327-6.

[15] A. Osman *et al.*, "Patterned Membrane in an Energy-Efficient Tilted Panel Filtration System for Fouling Control in Activated Sludge Filtration," *Polymers*, vol. 12, no. 2, p. 432, Feb. 2020, doi: 10.3390/polym12020432.

[16] W. Nur Aisyah Wan Osman, M. Bilad, and S. Samsuri, "Assessment of patterned membrane in a tilted panel filtration system for fouling control in activated sludge filtration," *IOP Conference Series: Materials Science and Engineering*, vol. 778, p. 012174, May 2020, doi: 10.1088/1757-899X/778/1/012174.

[17] Y. K. Dasan *et al.*, "Cultivation of Chlorella vulgaris using sequential-flow bubble column photobioreactor: A stress-inducing strategy for lipid accumulation and carbon dioxide fixation," *Journal of CO2 Utilization*, vol. 41, p. 101226, Oct. 2020, doi: 10.1016/j.jcou.2020.101226.

[18] J. A. Kharraz, M. R. Bilad, and H. A. Arafat, "Simple and effective corrugation of PVDF membranes for enhanced MBR performance," *Journal of Membrane Science*, vol. 475, pp. 91–100, Feb. 2015, doi: 10.1016/j.memsci.2014.10.018.

[19] J. Blazheska, "Insight in the thin-film polyamide membrane structure after compaction Doctoral Thesis," p. 118, 2016.

[20] K. W. Lawson, M. S. Hall, and D. R. Lloyd, "Compaction of microporous membranes used in membrane distillation. I. Effect on gas permeability," *Journal of Membrane Science*, vol. 101, no. 1–2, pp. 99–108, May 1995, doi: 10.1016/0376-7388(94)00289-B.

[21] J. L. Bert, "Membrane compaction: A theoretical and experimental explanation," *Journal of Polymer Science Part B: Polymer Letters*, vol. 7, no. 9, pp. 685–691, Sep. 1969, doi: 10.1002/pol.1969.110070909.

[22] D. Nitto, "Design Parameters Affecting Performance," p. 5, 2001.

[23] S. Stade, M. Kallioinen, A. Mikkola, T. Tuuva, and M. Mänttäri, "Reversible and irreversible compaction of ultrafiltration membranes," *Separation and Purification Technology*, vol. 118, pp. 127–134, Oct. 2013, doi: 10.1016/j.seppur.2013.06.039.

[24] M. R. Bilad *et al.*, "Low-pressure submerged membrane filtration for potential reuse of detergent and water from laundry wastewater," *Journal of Water Process Engineering*, vol. 36, p. 101264, Aug. 2020, doi: 10.1016/j.jwpe.2020.101264.

2ND ENERGY SECURITY AND CHEMICAL ENGINEERING CONGRESS 2021
*"Sustainable Technological Solution for a Better World"*
VIRTUAL CONFERENCE | 3-5 NOVEMBER 2021

**SEPARATION TECHNOLOGY**

**Paper ID: ESCE173**

# AN IN-DEPTH INVESTIGATION INTO ADSORPTION EQUILIBRIUM, KINETICS, AND THERMODYNAMICS OF SPENT COFFEE GROUNDS FOR METHYLENE BLUE REMOVAL

**Q. A. Trieu[1]*, D. H. Nguyen[1], H. T. Bui[2]**

[1] *Faculty of Environmental and Food Engineering, Nguyen Tat Thanh University, Ho Chi Minh, Vietnam.*
[2] *Faculty of Chemical and Food Technology, Ho Chi Minh City University of Technology and Education, Ho Chi Minh, Vietnam.*
*Corresponding author: tqan@ntt.edu.vn

## Extended Abstract

The adsorption performance, thermodynamics, and kinetics of spent coffee grounds (SCG) in the removal of Methylene Blue (MB) from an aqueous solution were extensively investigated in this study. Unmodified SCG were characterized using scanning electron microscopy, Fourier transform infrared spectroscopy, BET specific surface area analyzer, and the point of zero charge ($pH_{pzc}$) determination to identify surface chemistry, morphology, and textural properties. The batch adsorption experiment, and the nonlinear optimization method, combined with the chi-squared test, were utilized in modeling adsorption equilibrium and kinetics. The results demonstrated that the nonlinear Langmuir adsorption isotherm well fitted to adsorption equilibrium data, which indicated a maximum monolayer adsorption capacity of 73.38 mg/g (Fig. 1). Adsorption kinetics exhibited a better description of the nonlinear pseudo-second-order kinetic model. The values obtained from the thermodynamics study showed the adsorption process is spontaneous at increased temperatures ($\Delta G°<0$, $\Delta S°>0$), and endothermic ($\Delta H°>0$). Additionally, the magnitude of MB adsorption enthalpy change ($\Delta H° = 4.18$ kJ/mol) can assist in predicting the MB adsorption of SCG is physisorption and probably driven by hydrogen bondings combined with π-π interactions. This study demonstrates the potential of adsorbents derived from spent coffee grounds in textile wastewater treatment and reveals the nature of the interaction between MB and SCG.

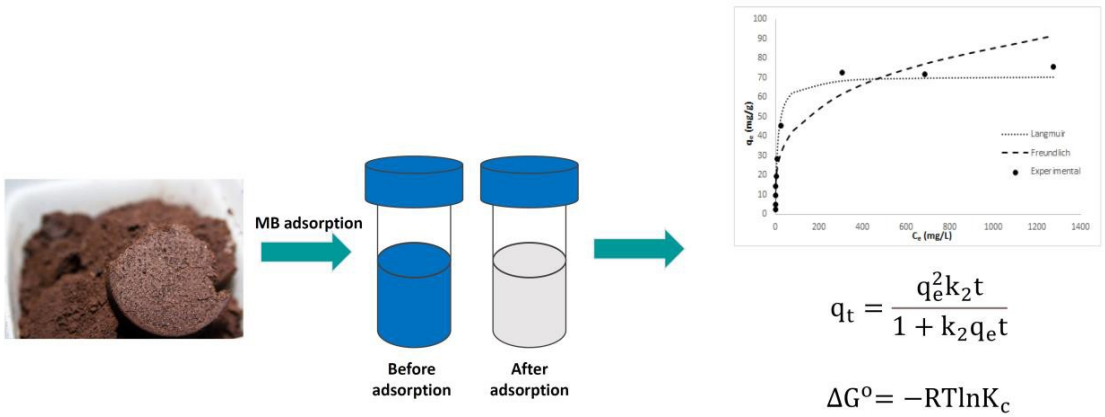


Fig. 1: Schematic representation of the study of MB adsorption on SCG's surface.

**Keywords:** Methylene blue; Spent coffee grounds; Equilibrium; Kinetics; Adsorption thermodynamics.

**Acknowledgment**

This research was funded by Nguyen Tat Thanh University, Ho Chi Minh City, Vietnam.

**SEPARATION TECHNOLOGY**

## References

[1] Shiklomanov, I. (1993). World fresh water resources. In P. H. Gleick (Ed.), Water in Crisis: A Guide to the World's Fresh Water Resources: Oxford University Press, New York.
[2] Franca, A. S., Oliveira, L. S., & Ferreira, M. E. (2009). Kinetics and equilibrium studies of methylene blue adsorption by spent coffee grounds. Desalination, 249(1), 267-272.
[3] Tran, H. N., You, S.-J., Hosseini-Bandegharaei, A., & Chao, H.-P. (2017). Mistakes and inconsistencies regarding adsorption of contaminants from aqueous solutions: A critical review. Water Research, 120, 88-116.
[4] Rafatullah, M., Sulaiman, O., Hashim, R., & Ahmad, A. (2010). Adsorption of methylene blue on low-cost adsorbents: A review. J Hazard Mater, 177(1), 70-80.
[5] Singh, R., Singh, T. S., Odiyo, J. O., Smith, J. A., & Edokpayi, J. N. (2020). Evaluation of Methylene Blue Sorption onto Low-Cost Biosorbents: Equilibrium, Kinetics, and Thermodynamics. Journal of Chemistry, 2020.

**SEPARATION TECHNOLOGY**

**Paper ID: ESCE185**

# EXTRACTION OF CELLULOSE FROM SUGARCANE BAGASSE VIA ULTRASONIC-ASSISTED ALKALINE TECHNOLOGY

**K. S. Phuang[1], P. Y. Toh[1,2], L. M. Chng[1,2]***

[1] *Department of Petrochemical Engineering, Faculty of Engineering and Green Technology,*
[2] *Centre of Environment and Green Technology Research (CEGT), Universiti Tunku Abdul Rahman, 31900 Kampar, Perak, Malaysia.*
*Corresponding author: chnglm@utar.edu.my

## Extended Abstract

Cellulose is a kind of biopolymer that possess outstanding properties and abundantly available in nature. It is sturdy, hydrophobic, and versatile leading to wide application such as carboxymethycellulose (CMC). Current cellulose production process is considered conventional that mainly depends on mechanical-chemical technology which is strongly not environmental friendly due to the high chemical usage. The technology required extreme conditions such as high temperature and long process time when the feedstock is lignocellulose biomass that consists of complex and firm plant structure made by cellulose, hemicellulose and lignin [1,2]. The lignocellulose biomass is a potential feedstock for cellulose due to its high cellulose content, and it is widely available as agriculture waste including sugarcane bagasse (SCB) in this study [3,4]. Ultrasonic-assisted alkaline (UAA) technology is a type of extraction method that apply sonication waves in alkaline solution to create and collapse tiny bubbles, with alternate pressure changes that able to rupture the bonding in lignocellulose structure thus release the cellulose and isolate it's from lignin and hemicellulose [5]. Therefore, ultrasonic-assisted alkaline technology to effectively produce cellulose from sugarcane bagasse is essential to be studied here to obtain more details of the extraction process via UAA technology.

The sugarcane bagasse powder with mesh size of 4 mm is prepared by grinding and drying. For the study, SCB is pretreated via autoclave process before undergo ultrasonic extraction in alkali medium. About 5 g of SCB powder is immersed in 150 mL of distilled water and autoclaved at 121 C for 30 mins. The powder is stirred for another 30 mins after autoclaved and further washed for few times. The washed powder is dried and 5 g is mixed with 150 ml of potassium hydroxide (KOH) solution. The mixed solution is treated with ultrasonic homogenizer equipped with probe under various treatment temperature. The extracted product is washed for few times and dried for subsequent characterization. Including functional group identification using Fourier Transform Infrared spectroscopy (FTIR) and cellulose content determination using High Performance Liquid Chromatography (HPLC) that estimated using glucose as reference. The extracted products under optimum condition is further carboxymethylated with two steps reaction. It is firstly alkalized with 17.5%(w/v) of sodium hydroxide followed with carboxymethylation with sodium monochloroacetate. The resulted product is CMC which is analyzed by FTIR and potentiometric titration.

The functional groups show by Fourier Transform Infrared analysis indicate the successful of extraction process where there is absence of lignin peaks, the carbonyl ester at wavenumbers of 1723 $cm^{-1}$ for extracted product as illustrated in Fig. 1 [6]. It is observed that peaks in the finger print region (1000 – 1600 $cm^{-1}$) is more predominant when purer cellulose is attained [6]. Based on the HPLC analysis, there is about 41 %(w/w) cellulose content in the sugarcane bagasse. Figure 2 shows the effect of three process parameters to yield of cellulose in weight basis based on HPLC analysis. The bar length that represented cellulose yield increases to its maximum at amplitude of 30% and reduce afterwards. The pattern indicates ultrasonic amplitude need proper manipulation to achieve higher yield of cellulose. Similar outcome was reported by Ramadoss and Muthukumar [7], revealed that bigger sonication waves could bring adverse effects to extraction process. The generated cavitation bubbles under high amplitude could block the transfer of energy to the solution thus reduce its chances to break the plant structure. Effect of ultrasonic under various treatment temperature are illustrated in second group of Fig. 2. The cellulose yield is increasing from 63.75 %(w/w) to 73.59 %(w/w) with increases of treatment temperature from 70 – 90 °C when the ultrasonic amplitude is maintained at 30% with KOH of 0.75 M. The results depicted bonding between hemicellulose and lignin were broken down under heated alkaline solution [7]. While the KOH concentration is

significant to increase the cellulose yield, reach its maximum of 83.22 %(w/w) at 1.25 M. The outcome is closely agree with other studies as lignin is soluble in alkaline solution thus remove from solid cellulose in the washing process [8,9].

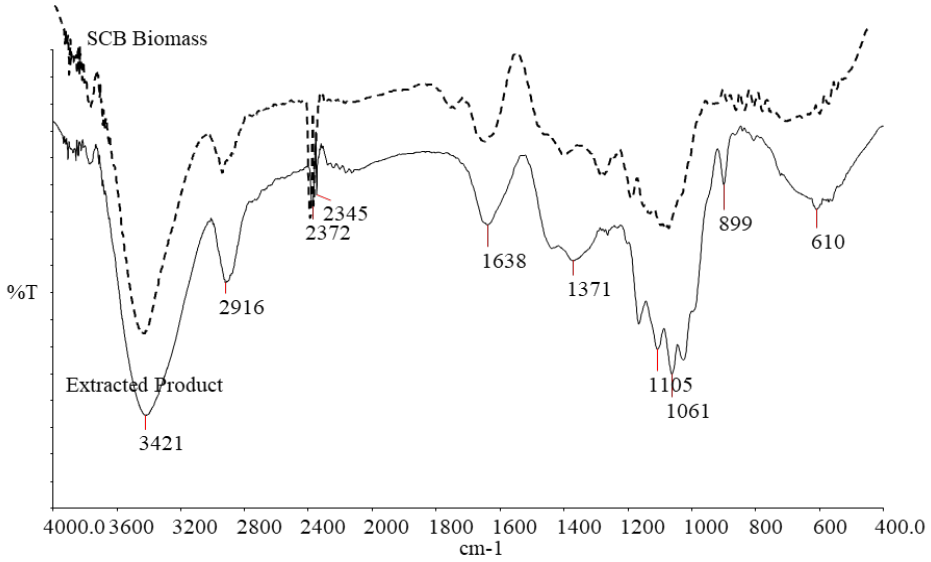


Fig. 1: Functional group profile of SCB biomass (dash line) and extracted product (solid line).

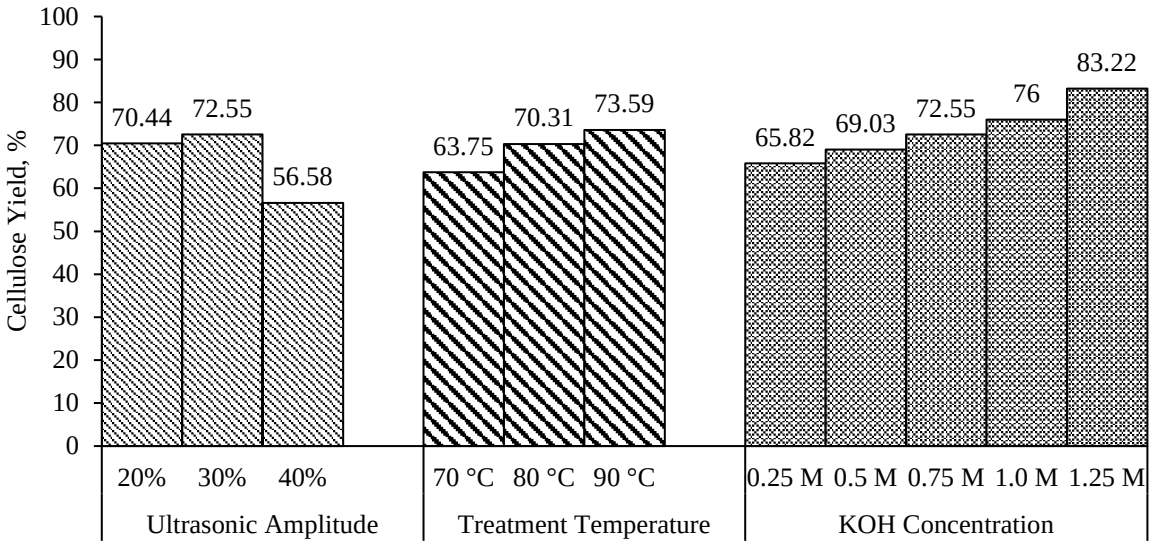


Fig. 2: Effect of ultrasonic amplitude, treatment temperature and potassium hydroxide (KOH) concentrations on cellulose production via ultrasonic-assisted alkaline technology.

As conclusion, the cellulose is successfully extracted from sugarcane bagasse with highest yield, 83.22 % (w/w) at KOH concentration of 1.25 M, ultrasonic temperature of 80 °C and ultrasonic amplitude of 30%. It is successfully carboxymethylated to produce soluble CMC with DS value of 0.3456 which is able to form film.

**Keywords:** Carboxymethylcellulose; Cellulose; Extraction; Sugarcane Bagasse; Ultrasonic-assisted Alkaline.

**Acknowledgment**

This study was supported by Universiti Tunku Abdul Rahman grant, IPSR/RMC/UTARRF/2019-C2/C04.

**SEPARATION TECHNOLOGY**

## References

[1] Lee H. V., Hamid S. B. A., Zain S. K. (2014) Conversion of Lignocellulosic Biomass to Nanocellulose: Structure and Chemical Process. Sci. World J. 2014.
[2] Ranganagowda R. P. G, Kamath S. S, Bennehalli B. (2019) Extraction and Characterization of Cellulose from Natural Areca Fiber. Mat. Sci. Res. 16-1.
[3] Teboho, M., Mochane, M., Tshwafo, M., Linganiso, L., Thekisoe, O., and Songca, S. (2018) Sugarcane Bagasse and Cellulose Polymer Composites.
[4] Qi, G., Peng, F., Xiong, L., Lin, X., Huang, C., Li, H., Chen, X. and Chen, X. (2016) Extraction and Characterization of Wax from Sugarcane Bagasse and the Enzymatic Hydrolysis of Dewaxed Sugarcane Bagasse. Prep. Biochem. Biotechnol 47(3):276-281.
[5] Liu J. H., Wang K. Y. (2016) Study on Technology Optimization of Lignin Removalin Cellulose Extraction from Wheat Bran by Combination of Ultrasound and Hydrogen Peroxide. Biotechnology 15:135-140.
[6] Md Salim, R., Asik, J., Sarjadi, M.S. (2021) Chemical Functional Groups of Extractives, Cellulose and Lignin Extracted From Native *Leucaena Leucocephala* Bark. Wood Sci Technol 55: 295-313.
[7] Ramadoss, G. and Muthukumar, K. (2014) Ultrasound Assisted Ammonia Pretreatment of Sugarcane Bagasse for Fermentable Sugar Production. Biochem. Eng. J. 83:33-41.
[8] Liu, C.F., Ren, J.L., Xu, F., Liu, J.J., Sun, J.X. and Sun, R.C. (2006) Isolation and Characterization of Cellulose Obtained from Ultrasonic Irradiated Sugarcane Bagasse. J. Agric. Food Chem. 54(16):5742-5748.
[9] Vu, N., Tran, H., Nhi, B., Vu, C., and Nguyen, H. (2017) Lignin and Cellulose Extraction from Vietnam's Rice Straw using Ultrasound-Assisted Alkaline Treatment Method. Int. J. Polym. Sci. 2017: 1-8.

**WASTE WATER**

**Paper ID: ESCE012**

# CHARACTERIZATION OF β-CYCLODEXTRIN FUNCTIONALIZED RICE HUSK BIOCHAR

**P. Rajandran[1], N. Masngut[1,2]***

[1] *Department of Chemical Engineering, College of Engineering,* [2] *Centre for Research in Advanced Fluid & Process, University Malaysia Pahang, 26300 Gambang, Pahang, Malaysia.*
*Corresponding author: nasratun@ump.edu.my

## Extended Abstract

Because of its unfavorable effects on human health, organic and inorganic pollution has gotten a lot of attention. The pollutant formation mainly originates from anthropogenic activities such as the combustion of carbon-containing fuels and the accidental disposal of industrial materials. Pollutants, once produced, enter the water body via wastewater, surface runoff, and atmospheric deposition [1]. Therefore, water sectors around the world are looking for water treatment that could provide an efficient solution. Adsorption is a current trend in water treatment because of its simplicity and affordable cost [2]. Numerous types of adsorbents for the removal of contaminants have been studied extensively on the laboratory scale. However, β-cyclodextrin functionalized rice husk biochar (CD-RHB) as an adsorbent for pollutants removal is rarely reported. The study aimed to look into the best crosslinker for CD-RHB preparation and the surface characteristics of CD-RHB. In this study, two different crosslinkers participated in preparing CD-RHB, namely epichlorohydrin and phosphoric acid. Then, the surface characteristics of the developed adsorbents were analyzed using scanning electron microscopy (SEM), Fourier-transform infrared (FTIR) spectroscopy, and a thermal analyzer [3, 4]. As observed, β-cyclodextrin was successfully decorated and grafted on both CD-RHBs. However, epichlorohydrin-based CD-RHB shows higher β-cyclodextrin content than phosphoric acid-based CD-RHB on its surface. In conclusion, epichlorohydrin is the appropriate crosslinker for the preparation of CD-RHB.

**Keywords:** β-cyclodextrin; Epichlorohydrin; Phosphoric acid; SEM; FTIR; Thermal analyzer.

### Acknowledgment

The authors would like to thank University Malaysia Pahang for providing financial support under Post Graduate Research Scheme (PGRS 210372) and laboratory facilities.

### References

[1] Costa, J.A.S., et al., Efficient adsorption of a mixture of polycyclic aromatic hydrocarbons (PAHs) by Si–MCM–41 mesoporous molecular sieve. Powder Technology, 2017. **308**: p. 434-441.
[2] Solano, R.A., et al., Polycyclic aromatic hydrocarbons (PAHs) adsorption from aqueous solution using chitosan beads modified with thiourea, TiO2 and Fe3O4 nanoparticles. Environmental Technology & Innovation, 2021. **21**: p. 101378.
[3] Qu, J., et al., Microwave-assisted one pot synthesis of β-cyclodextrin modified biochar for concurrent removal of Pb(II) and bisphenol a in water. Carbohydrate Polymers, 2020. **250**: p. 117003.
[4] Qu, J., et al., Microwave-assisted synthesis of β-cyclodextrin functionalized celluloses for enhanced removal of Pb(II) from water: Adsorptive performance and mechanism exploration. Science of The Total Environment, 2021. **752**: p. 141854.

**WASTE WATER**

**Paper ID: ESCE027**

# INTERFERING IONS AND CONTROLLING THEIR EFFECTS ON THE DIRECT ANALYSIS OF TOTAL DISSOLVED AMMONIA IN AQUACULTURAL WASTEWATER USING MOLECULAR ABSORPTION SPECTROMETRY

**Nguyen Thanh-Nho[1]*, Le Thi Anh-Dao[1], Le Thi Huynh-Mai[2], and Nguyen Cong-Hau[1]***

[1] *Faculty of Environmental and Food Engineering, Nguyen Tat Thanh University (NTTU).*
[2] *Department of Analytical Chemistry, Faculty of Chemistry, University of Science, Vietnam National University Ho Chi Minh City (US-VNUHCMC).*
*Corresponding author: ntnho@ntt.edu.vn and nchau@ntt.edu.vn

## Extended Abstract

Ammonia, soluble in water, exists in equilibrium as both molecular ammonia ($NH_3$) and ammonia in the form of the ammonium ion ($NH_4^+$). Temperature and pH are considered important factors that directly affect the equilibrium between $NH_4^+$ and $NH_3$ in water (i.e., the rising of temperature leads to more discharge of $NH_3$ from the aqueous phase). The ammonium ion is not highly toxic to organisms and the human body, less harmful than molecular ammonia ($NH_3$) [1]. However, ammonium in water could be converted into nitrite and nitrate, known as carcinogens, particularly when the ammonium content is over the permitted levels. Several published studies showed that the excess ammonia level is among the common reasons causing the death of fish and other aquatic living organisms [2-4]. Moreover, high ammonia is favorable for various water microorganisms, especially algae, to grow rapidly, affecting water quality, especially its clarity, smell, and beneficial microorganisms. Therefore, total dissolved ammonia is considered an important parameter for the assessment of water quality. In the present study, our aim was to determine directly total dissolved ammonia in shrimp farming effluents. To reach our goals, the influence of several major ions e.g., $Cl^-$, $Ca^{2+}$, $Mg^{2+}$, etc., on the quantifying total dissolved ammonia were evaluated using the artificial samples via Salicylate and Indophenol methods [5, 6]. For ion interferences, chloride is known as one of the most popular ion species in shrimp farming effluent which affects differently the absorbance signals measured between both those procedures (Figure 1).

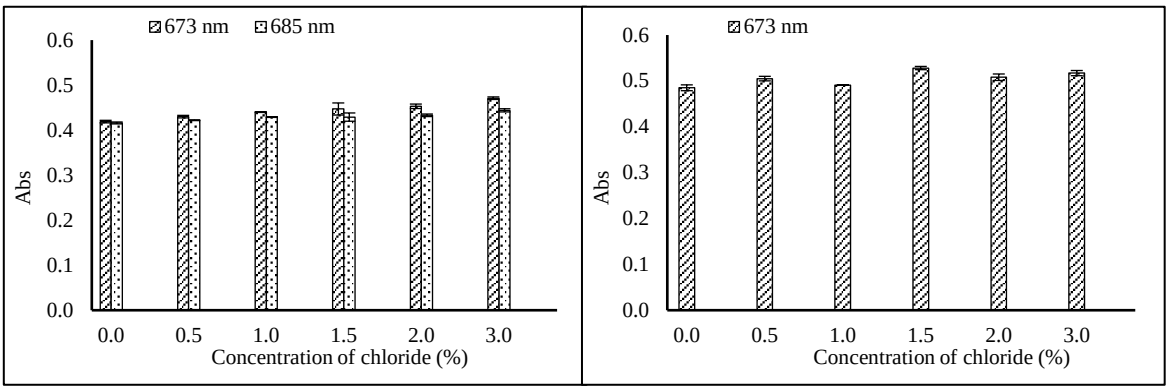


Fig. 1: Effects of chloride ion at different concentrations on the absorbance recorded from salicylate (left) and indophenol (right) procedures.

For the salicylate method, the increase of chloride contents would shift the maximum wavelength towards higher values (from 673 to 685 nm). However, when chloride concentration got higher, the absorbance obtained at 685 nm varied in smaller ranges than 673 nm (Figure 1). In addition, the results showed that solutions containing 1.0%, 1.5%, 2.0%, and 3.0% of $Cl^-$, respectively, the recovery at 0.5 µg $L^{-1}$ ammonia in these solutions increased when measured at 673 nm and their values were 103.2%, 103.2%, 104.3%, and 106.9%, respectively. However, at 685nm, the recoveries were about 97 ÷ 98%. For the indophenol procedure, the rising of chloride contents also

created the fluctuation in the absorbance values recorded; however, the maximum wavelength did not perform any shift and the absorbance did not show any typical trend. For each concentration of $Cl^-$ investigated, the measured signal was repeated, but compared to the absorbance of a solution without $Cl^-$ present, these solutions exhibited a higher absorbance but did not show any tendency. At concentrations of 0.5%, 1.0%, 1.5%, 2.0%, and 3.0% of $Cl^-$, the deviations of the absorption from the artificial samples were 4.1%, 5.4%, 8.9%, 10.0%, and 11.9%, respectively. Therefore, the salicylate method could be a more favorable choice for determining total dissolved ammonia in water containing a certain amount of chloride. Then, wavelength of 685 nm was utilized for total dissolved ammonia quantification during the salicylate approach, and 673 nm was chosen for indophenol one.

The salicylate procedure was validated and applied to determine total dissolved ammonia in shrimp farming effluent collected in Can Gio District, Ho Chi Minh City, Vietnam, exhibiting the total dissolved ammonia ranging from 0.09 to 1.22 mg $L^{-1}$. Besides, several physical-chemical parameters and common elements were measured, including pH (7.0-8.0), salinity (7.9-24.1), total organic carbon (0.165-1.63%), $Mg^{2+}$ (312-996 mg $L^{-1}$), $Ca^{2+}$ (132-368 mg $L^{-1}$), and $Fe^{3+}$ (0.050-1.275 mg $L^{-1}$). These results were in accordance with the national regulation for shrimp farming activities.

**Keywords:** Shrimp activity; Effluent; Ammonia; Salicylate; Indophenol.

## Acknowledgment

This study was supported by Nguyen Tat Thanh University and University of Science, Vietnam National University, Ho Chi Minh City, Vietnam.

## References

[1] Cho Y. B., Jeong S. H., Chun H., and Kim Y. S. (2018) Selective colorimetric detection of dissolved ammonia in water via modified Berthelot's reaction on porous paper. Sensors and Actuators B: Chemical 256:167-175.
[2] Kagaya S., Nakada S., Inoue Y., Kamichatani W., Yanai H., Saito M., Yamamoto T., Takamura Y., and Tohda K. (2010) Determination of cadmium in water samples by liquid electrode plasma atomic emission spectrometry after solid phase extraction using a mini cartridge packed with chelate resin immobilizing carboxymethylated pentaethylenehexamine. Anal. Sci 26:515-518.
[3] Randall D. J. and Tsui T. (2002) Ammonia toxicity in fish. Mar. Pollut. Bull 45:17-23.
[4] Bhatnagar A. and Devi P. (2013) Water quality guidelines for the management of pond fish culture. Int. J. of Envir. Sci 3:1980.
[5] Kempers A. and Kok C. (1989) Re-examination of the determination of ammonium as the indophenol blue complex using salicylate. Anal. Chim. Acta 221:147-155.
[6] Verdouw H., Van Echteld C., and Dekkers E. (1978) Ammonia determination based on indophenol formation with sodium salicylate. Water Res 12:399-402.

**WASTE WATER**

**Paper ID: ESCE070**

# STRUCTURAL CHARACTERIZATION OF DIFFERENT CONCENTRATION OF ACID AND ALKALI TREATED-CORNCOB WASTE: A POTENTIAL RESOURCES BIOSORBENT

**N. A. Awang[1,2], W. N. Wan Salleh[1,2], I. Ahmad Fauzi[1,2], A. Farhana[1,2], Y. Norhaniza[1,2]**

[1,2] *Advanced Membrane Technology Research Centre (AMTEC),* [1,2] *School of Chemical & Energy Engineering,*
[1,2] *Faculty of Engineering ,Universiti Teknologi Malaysia, 81310 Skudai, Johor, Malaysia.*
*Corresponding author: hayati@petroleum.utm.my

## Extended Abstract

Preferred scientific name of corn is *Zea mays* known as the third largest agricultural crop after rice and wheat in the world. Till 2020, In Malaysia, the production of corn was 28,000 tonnes compared to 5,000 tonnes in 1971. The increment was growing up to with average annual rate of 13.97%. Most of the corncob which covered almost quarter of the corn's quantity is directly combusted which creating waste and serious atmospheric solution. The corncob can be a good material to act as the adsorbent in heavy metal removal. In this context, corn cob is viewed as a waste material with no commercial value, discarded or burned in open spaces without energetic utility. On the other hand, corn cob is a good alternative to produce activated carbon since it is renewable, available, and low-cost precursor [1]. In addition, the corn cob contains 40–45% cellulose, 30–35% hemicellulose, and 10–20% lignin, with a high carbon content and low ash content compared to other biomasses [2]. Therefore, the objective of this study is to highlight a structural and surface characterization of raw corncob, H3PO4-pretreated corncob, and KOH-pretreated corncob. The biomass samples were characterized via Fourier transforminfrared spectroscopy (FTIR) and Brunauer–Emmett–Teller (BET) analysis. The FTIR result shows that the major functional groups of corncob such as –OH, C–O, C–H, and C=C experienced a slight shift due to the presence of KOH and H3PO4. Treatments with KOH and $H_3PO_4$ improved the BET surface area with the values of 8.8920 and 6.7894 $m^2/g$, respectively, compared with raw corncob (0.5011 $m^2/g$). The results indicate that the pretreatment of corncob influenced the functional groups and surface area of the raw corncob.

FTIR spectra of CC, 2M-KOH–CC, and 2M-H3PO4–CC are presented in Figure 1. The FTIR spectra demonstrated an indistinguishable adsorption band with a slight shift. The broad stretching vibration was observed at 3334 cm−1, which is ascribed to the presence of the hydroxyl group, O–H [3], [4]. The structure of cellulose, having intramolecular and intermolecular hydro gen bonds, contributed to the broadening of the absorption band. The peak at 2922 cm−1 represents the asymmetric C–H groups of the alkyl group, such as methyl and methylene. The absorption peak is observed in all the samples as all the carbon is present with different intensities. The difference in the carbon intensities was due to the different pretreatment processes, leading to different rates of the C–H3 group being removed.

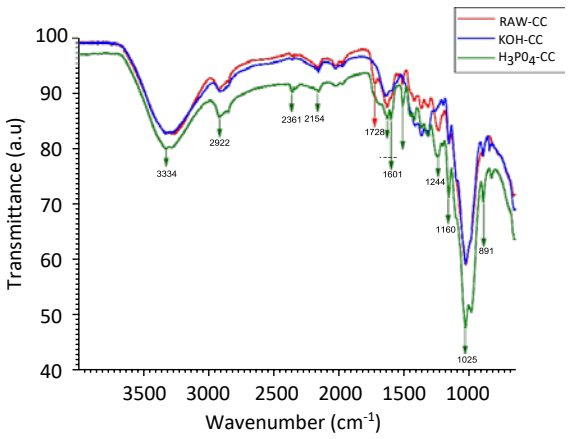


Fig. 1: FTIR images for three different samples of raw-CC, KOH-CC and $H_3PO_4$-CC.

**Keywords:** Corncob waste; Modification; Acid treatment; Base treatment.

## Acknowledgment

The authors gratefully acknowledge the financial support from the Ministry of Education and Universiti Teknologi Malaysia under Higher Institution Centre of Excellence Scheme (Project Number: R. J090301.7851.4J423) and UTM High Impact Research (Project Number: Q.J130000.2451.08G36). The authors would also like to acknowledge technical and management support from Research Management Centre (RMC), Universiti Teknologi Malaysia.

## References

[1] S. T. Neeli, H. Ramsurn, C. Y. Ng, Y. Wang, and J. Lu, *J. Environ. Chem. Eng.*, 8, 103886 (2020).
[2] D. Yang *et al.*, *Sci. Total Environ.*, 708, 134823 (2020).
[3] N. K. Berber-Villamar, A. R. Netzahuatl-Muñoz, L. Morales-Barrera, G. M. Chávez-Camarillo, C. M. Flores-Ortiz, and E. Cristiani-Urbina, *PLoS One*, 13, pp. 1–30 (2018).
[4] M. Luo, H. Lin, B. Li, Y. Dong, Y. He, and L. Wang, *Bioresour. Technol.*, 259, 312–318 (2018).

**WASTE WATER**

**Paper ID: ESCE110**

# COMPARATIVE RATES AND YIELDS OF ELECTRONS RELEASED FROM ZVI POWDER IN BATCH REACTORS WITH AND WITHOUT INOCULATED HYDROGENOTROPHIC METHANOGENS

**N. Paepatung[1], W. Songkasiri[1,2,3], H. Yasui[4], C. Phalakornkule[1,5]***

[1] *The Joint Graduate School of Energy and Environment,* [2] *Excellence Center of Waste Utilization and Management, Pilot Plant Development and Training Institute, King Mongkut's University of Technology Thonburi, Bangkok, 10150 Thailand.*
[3] *National Center for Genetic Engineering and Biotechnology, National Science and Technology Development Agency, Pathumtani, 12120 Thailand.*
[4] *Faculty of Environmental Engineering, The University of Kitakyushu, 1-1 Hibikino, Wakamatsu, Kitakyushu, Fukuoka 808-0135, Japan.*
[5] *Department of Chemical Engineering, Research Center for Circular Products and Energy, King Mongkut's University of Technology North Bangkok, Bangkok 10800, Thailand.*
*Corresponding author: chantaraporn.p@eng.kmutb.ac.th and cphalak21@gmail.com

## Extended Abstract

### Objectives

In recent years, zero valent iron (ZVI) has received increasing attention from the research community as it can enhance methane ($CH_4$) production from organic matters via anaerobic process. There are two roles of ZVI in enhancing the $CH_4$ production: direct and indirect electron donor. In its first role, ZVI donates electrons directly to the working microorganisms, and serves as a biotic factor for stimulating the metabolic activities of the microorganisms [1]. In its second role, ZVI oxidation causes the release of electrons, which are transferred to protons that are dissociated from water molecules [2]. The indirect electron transfer from ZVI to the microorganisms might be difficult to occur due to the accumulation of hydrogen ($H_2$) makes the reaction thermodynamically unfavorable [3]. Hydrogenotrophic methanogens plays an important role in continuously removing the $H_2$ and makes the reaction thermodynamically favorable [2]. As rates and yields of electrons released from ZVI surface are important parameters for the ZVI application, in this study, rates and yields of electrons released from ZVI powder in batch reactors were investigated with and without inoculated hydrogenotrophic methanogens. In addition, the effects of ZVI surface area on the amounts of released electrons and on the rates of electron release were also investigated.

### Methodology

Two set of batch experiments were conducted in parallel in the bottles with 1 L working volume. In the first experimental set, the reactors were inoculated with the sludge that had been fed with HCOOH and HCOONa for four months. $NaHCO_3$ and $NH_4HCO_3$ were added to the reactors to serve as the source of $CO_2$ with a total concentration of 89.28 mM. ZVI powder with 99% Fe purity, <45 µm in length and 2.8 g/cm$^3$ in apparent density was added to three reactors at a dosage of 5.25, 26.66 and 105.04 g/reactor, giving the ZVI surface area of 0.5, 2.5 and 10 m$^2$/L, respectively. The culture pH was controlled in the range of 7-7.5 throughout the experiments. In the second experimental set, the reactors were set up in a similar way as in the first experimental set except that no sludge was inoculated. Gas productions from the reactors and compositions of $CH_4$ and $H_2$ in the biogas were continuously measured using a water displacement method and gas chromatograph, respectively. The molar amounts of electrons released from ZVI were estimated based on the following stoichiometry: 1 mole of $CH_4$: 8 moles of electrons, 1 mole of $H_2$: 2 moles of electrons, and 4 moles of $Fe^0$: 1 mole of $CH_4$.

### Results and discussion

In the inoculated culture, the $CH_4$ production increased with the increasing ZVI surface area with the maximum methane production of 20, 108 and 491 mL for the ZVI surface area of 0.5, 2.5 and 10 m$^2$/L, respectively. In the uninoculated culture, the maximum $H_2$ production was 15, 327 and 1,285 mL for the surface area of 0.5, 2.5 and 10 m$^2$/L, respectively. Fig. 1 compares the amounts of released electrons equivalent to the produced $CH_4$ and $H_2$ in the first and second set of batch experiments, respectively. On day 50 in which the amounts of electrons released

**WASTE WATER**

in the uninoculated culture stopped, the amounts of electrons released from ZVI in the inoculated culture was greater than the uninoculated culture about 3.7, 1 and 1 times for the ZVI surface area of 0.5, 2.5 and 10 $m^2$/L, respectively. While the electron release in the uninoculated culture stopped within 50 days, the electron release in the inoculated culture continued to day 100. The $H_2$ production ceased on day 20, 40 and 60 while the $CH_4$ production ceased on day 65, 100 and 120 for the ZVI surface area of 0.5, 2.5 and 10 $m^2$/L, respectively. The results showed that the inoculum enriched with hydrogenotrophic methanogens drove the extents of electron release.

Table 1 reports the maximum rates of electron release with varying ZVI surface area. The results showed that the rates of electron release were a function of ZVI surface area. That is, the maximum electron release rates increased with increasing ZVI surface area. The rates of electron release in the uninoculated culture were 1.6 times and 2.1 times faster than those in the inoculated culture with ZVI surface area of 2.5 $m^2$/L and 10 $m^2$/L, respectively. The specific rate of electron release per surface area of the inoculated and uninoculated culture were 2 x $10^{-4}$ mole $e^-/m^2$ day and 5 x $10^{-4}$ mole $e^-/m^2$ day, respectively. The specific rate of electron release in the uninoculated culture was in the same order as those reported in the literature (ca. 5 x $10^{-4}$ mole $e^-/m^2$ day).

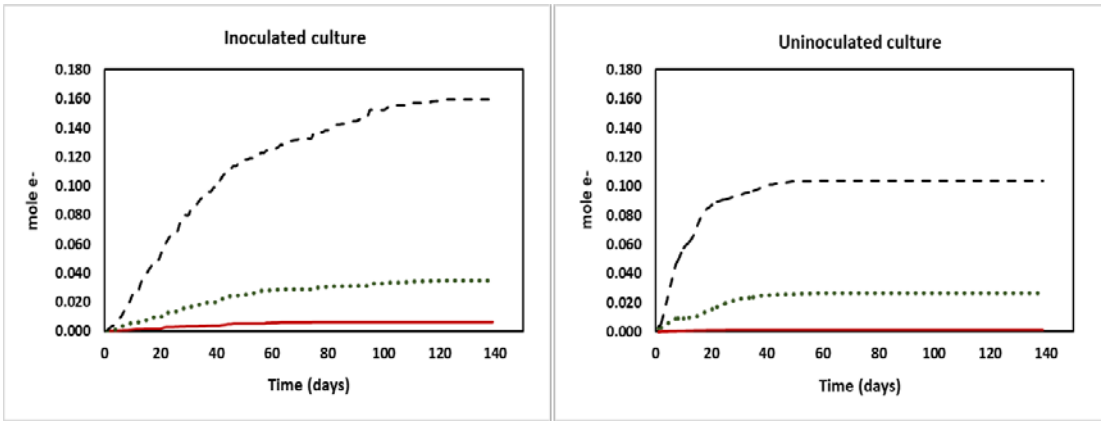


Fig. 1: Cumulative amounts of released electrons: (–) ZVI surface area of 0.5 $m^2$/L, (⋯) ZVI surface area of 2.5 $m^2$/L and (---) ZVI surface area of 10 $m^2$/L.

Table 1: Maximum rates of electron release, total amount of released electrons and specific rates of electron release with varying ZVI surface area.

| Surface area ($m^2$/L) | Maximum rates of electron release (mole $e^-$/day) | | Total amount of electron released (mole $e^-$) | | Specific rates of electron release (mole $e^-/m^2$ day) | |
|---|---|---|---|---|---|---|
| | Inoculated[a] | Uninoculated[b] | Inoculated[a] | Uninoculated[b] | Inoculated[a] | Uninoculated[b] |
| 0.5 | 0.00014 | 0.00011 | 0.00649 | 0.00141 | 2.80 x $10^{-4}$ | 2.20 x $10^{-4}$ |
| 2.5 | 0.00054 | 0.00086 | 0.03499 | 0.02648 | 2.13 x $10^{-4}$ | 3.39 x $10^{-4}$ |
| 10 | 0.00246 | 0.00522 | 0.15925 | 0.10401 | 2.46 x $10^{-4}$ | 5.22 x $10^{-4}$ |

Note: [a] moles of electrons equivalent to moles of $CH_4$ produced in the inoculated culture; [b] moles of electrons equivalent to moles of $H_2$ produced in the uninoculated culture.

**Conclusion**

The results showed that the inoculum enriched with hydrogenotrophic methanogens drove both rates and extents of the electron release from ZVI. There was a linear relationship between the maximum specific rates of electron release and ZVI surface area in both inoculated and uninoculated culture.

**Keywords:** Anaerobic digestion; Zero valent iron; Methane; Hydrogen; Electron donor.

**Acknowledgment**

We acknowledge the Joint Graduate School of Energy and Environment for the financial support and the research facility of the Excellent Center of Waste Utilization and Management (EcoWaste) at KMUTT. We also thank the research grants from King Mongkut's University of Technology North Bangkok (Grant No.: KMUTNB-BasicR-64-28-06) and Japan International Cooperation Agency (Collaborative Education Program Fiscal Year 2021).

**WASTE WATER**

## References

[1] Dinh HT, Kuever J, Mussmann M, Hassel AW, Stratmann M, Widdel F. (2004) Iron corrosion by novel anaerobic microorganisms. Nature 427:829–832.
[2] Daniels L, Belay N, Rajagopal BS, Weimer PJ. (1987) Bacterial methanogenesis and growth from CO2 with elemental iron as the sole source of electrons. Science 237:509–511.
[3] Karri S., Sierra-Alvarez R., Field J.A. (2005) Zero valent iron as an electron-donor for methanogenesis and sulfate reduction in anaerobic sludge. Biotechnology and Bioengineering 92:810–819.


**Centre for Research in Advanced Fluid and Processes**

Pusat Penyelidikan Bendalir dan Proses Termaju

Centre for Research in Advanced Fluid & Processes
Universiti Malaysia Pahang
26300 Gambang, Kuantan
Pahang, Malaysia


+609 549 3232


esche@ump.edu.my